

NATIONAL LIBRARY

BIBLIOTHÈQUE NATIONALE

OTTAWA

OTTAWA



6229

NAME OF AUTHOR.....WILFRID BERNARD O'CALLACHAN  
TITLE OF THESIS.....REACTIONS OF GROUND-STATE  
.....SULFUR ATOMS  
.....  
UNIVERSITY.....OF ALBERTA  
DEGREE.....Ph.D.....YEAR GRANTED.....1970

Permission is hereby granted to THE NATIONAL  
LIBRARY OF CANADA to microfilm this thesis and to  
lend or sell copies of the film.

The author reserves other publication rights,  
and neither the thesis nor extensive extracts from  
it may be printed or otherwise reproduced without  
the author's written permission.

(Signed).....W.B. Callaghan

PERMANENT ADDRESS:

.....Apt #2  
.....168, RADIN RD.  
.....ARVIDA, QUEBEC

DATED.....Dec 5th.....1969

NL-91

THE UNIVERSITY OF ALBERTA  
REACTIONS OF GROUND-STATE SULFUR ATOMS

by



WILFRID BERNARD O'CALLAGHAN

A THESIS  
SUBMITTED TO THE FACULTY OF GRADUATE STUDIES  
IN PARTIAL FULFILMENT OF THE REQUIREMENTS  
FOR THE DEGREE OF DOCTOR OF PHILOSOPHY

DEPARTMENT OF CHEMISTRY

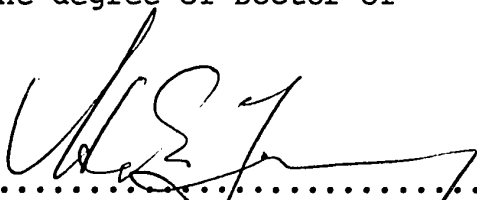
EDMONTON, ALBERTA

SPRING, 1970

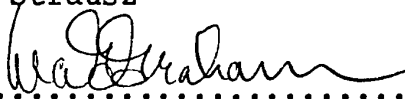
UNIVERSITY OF ALBERTA  
FACULTY OF GRADUATE STUDIES


The undersigned certify that they have read, and  
recommend to the Faculty of Graduate Studies for acceptance,  
a thesis entitled


"REACTIONS OF GROUND-STATE SULFUR ATOMS"  
submitted by Wilfrid Bernard O'Callaghan in partial fulfil-  
ment of the requirements for the degree of Doctor of  
Philosophy.

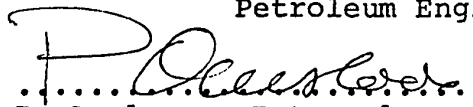
  
.....  
H.E. Gunning Supervisor

  
.....  
O.P. Strausz

  
.....  
W.A.G. Graham

  
.....  
G.R. Freeman

  
.....  
F.D. Otto - Chemical and  
Petroleum Engineering

  
.....  
P. Ausloos - External Examiner

Dated....*Dec 4th/69*.....

## ABSTRACT

Relative rates and Arrhenius parameters are measured for the addition of  $S(^3P)$  atoms to the following alkenes and alkynes: ethylene, propylene, isobutylene, trimethylethylene, tetramethylethylene, 1,3-butadiene, vinyl chloride, cis- and trans-difluoroethylene, tetrafluoroethylene, 2-fluoropropene, 3,3,3-trifluoropropene, 2-trifluoromethylpropene, 3,3-4,4,4-pentafluorobutene-1, vinyl-trifluorosilane, acetylene, methylacetylene and dimethylacetylene. The trend in reactivity is mainly due to activation energy differences and demonstrates clearly the electrophilic behaviour of  $S(^3P)$  atoms.

The rate parameters are compared and contrasted with those of other atomic and free radical species, and their variation with molecular structure are explained in terms of substituent effects such as the inductive effect, hyperconjugation, resonance and steric effects. The relationships of the activation energies with molecular properties such as localization energies, ionization potentials, singlet-triplet excitation energies, free valences and bond orders are examined.

A detailed mechanism is proposed in terms of a Potential Energy - Reaction Co-ordinate Diagram for the



addition of  $S(^3P)$  atoms to ethylene.

The fragmentation of "hot" episulfides formed by the addition of  $S(^3P)$  atoms to ethylene and propylene at low pressures is investigated.

Relative rates and Arrhenius parameters are measured for the abstractive reactions of  $S(^3P)$  atoms with ethylene episulfide and propylene episulfide to give  $S_2$  and the corresponding olefin.

The secondary  $\alpha$ -deuterium isotope effect is measured for the addition of  $S(^3P)$  atoms to ethylene- $d_4$ , ethylene-1,1- $d_2$  and cis- and trans-ethylene- $d_2$  over a temperature range from 27°C to 150°C. The  $k_D/k_H$  ratio for each of the deuterated ethylenes was constant over the temperature range and the results are consistent with a transition state in which the sulfur atom is partially bonded to both carbon atoms and to two hydrogen atoms.

### ACKNOWLEDGEMENTS

The author wishes to express his sincere appreciation and gratitude to Dr. H. E. Gunning and to Dr. O. P. Strausz for their guidance and assistance throughout the course of this study.

Special thanks go to the members and ex-members of the Photochemistry group, particularly to Mr. W. Duholke who performed the flash photolysis - kinetic mass spectrometry experiment, Mr. R. E. Berkley, Drs. E. M. Lown, E. L. Dedio, H. A. Wiebe, H. S. Sandhu, B. T. Woods and E. N. Jakubowski for many interesting and helpful discussions.

The invaluable assistance of the entire technical staff of the Chemistry Department is also appreciated.

The conscientious efforts of Mrs. R. Tarnowski in the typing of this thesis are gratefully acknowledged.

The author would like to express his gratitude to his wife, Geraldine, whose devotion and unceasing co-operation have made this work possible.

Finally, the financial assistance of the University of Alberta and the National Research Council is gratefully acknowledged.

## TABLE OF CONTENTS

TITLE	<u>Page</u>
ABSTRACT.....	i
ACKNOWLEDGEMENTS.....	iii
LIST OF TABLES.....	vii
LIST OF ILLUSTRATIONS.....	xv
CHAPTER I      INTRODUCTION.....	1
A)    Reactions of S( <sup>3</sup> P) Atoms with Alkenes and Alkynes	
B)    Additions of Atoms and Radicals to Multiple Bonds	
C)    The Secondary Kinetic Isotope Effect	
D)    The Present Investigation	
CHAPTER II    EXPERIMENTAL.....	25
1)    High-Vacuum System	
2)    Photolytic Assembly	
3)    Analytical System	
4)    Operating Procedures	
5)    Materials	
6)    Further Analysis	

	<u>Page</u>
CHAPTER III	
RELATIVE RATES AND ARRHENIUS	
PARAMETERS FOR THE ADDITION OF	
$S(^1P)$ ATOMS TO OLEFINIC AND	
ACETYLENIC BONDS.....	43
A) Relative Rates	
Results	
B) Arrhenius Parameters	
Results	
C) Discussion	
(a) Activation Energy	
(b) A-Factors	
(c) The Transition State for	
$S(^3P)$ Atom Addition to	
Olefins	
CHAPTER IV	
INVESTIGATION OF $S(^3P)$ - OLEFIN	
SYSTEMS AT LOW PRESSURES.....	201
A) Preliminary Experiments	
B) Steady-State Treatment	
C) Fragmentation of 'Hot'	
Episulfides	
Discussion	
D) The Reaction of $S(^3P)$ Atoms with	
Episulfides	
Results	
Discussion	

	<u>Page</u>
CHAPTER V      ADDITION OF S( <sup>3</sup> P) ATOMS TO	
DEUTERIO-ETHYLENES.....	233
Results	
Discussion	
CHAPTER VI      SUMMARY AND CONCLUSIONS.....	252
BIBLIOGRAPHY    .....	256
APPENDIX        MASS SPECTRAL DATA.....	264

## LIST OF TABLES

<u>TABLE</u>	<u>Page</u>
I Relative Rates of Addition of Atoms and Radicals to Olefins.....	6
II G.L.C. Operating Conditions and Elution Times for Episulfides.....	33
III Distillation Temperatures for Separation of Products.....	37
IV Materials Used.....	39
V Addition of S( <sup>3</sup> P) Atoms to Ethylene and Propylene. Product Formation as a Function of Exposure Time for $[C_2H_4]/[C_3H_6] = 1.50$ .....	48
VI Addition of S( <sup>3</sup> P) Atoms to Ethylene and Propylene. Product Formation as a Function of Exposure Time for $[C_2H_4]/[C_3H_6] = 2.98$ .....	51
VII Addition of S( <sup>3</sup> P) Atoms to Ethylene and Propylene. Product Formation as a Function of Exposure Time for $[C_2H_4]/[C_3H_6] = 6.06$ .....	54
VIII Addition of S( <sup>3</sup> P) Atoms to Isobutene and Propene. Product Formation as a Function of Exposure Time for $[C_3H_6]/[C_4H_8] = 6.86$	59

TABLE		<u>Page</u>
IX	Addition of S( <sup>3</sup> P) Atoms to Trimethyl- ethylene and Isobutene. Product Formation as a Function of Exposure Time for $[C_4H_8]/[C_5H_{10}] = 2.45$ .....	62
X	Addition of S( <sup>3</sup> P) Atoms to Tetramethyl- ethylene and Trimethylethylene. Tetra- methylethylene Episulfide Formation as a Function of Added Trimethylethylene.....	64
XI	Addition of S( <sup>3</sup> P) Atoms to 1,3-Butadiene and Isobutene. Isobutene Episulfide Formation as a Function of Added Butadiene.....	67
XII	Addition of S( <sup>3</sup> P) Atoms to 2-Trifluoro- methylpropene and Propene. Product Formation as a Function of Exposure Time for $[C_3H_6]/[C_4F_3H_5] = 0.47$ .....	69
XIII	Addition of S( <sup>3</sup> P) Atoms to 2-Fluoropro- pane and Ethylene. Product Formation as a Function of Exposure Time for $[C_2H_4]/[C_3FH_5] = 1.79$ .....	71
XIV	Addition of S( <sup>3</sup> P) Atoms to 3,3-4,4,4- Pentafluorobutene-1 and 2-Fluoropropene. Product Formation as a Function of Exposure Time for $[C_3FH_5]/[C_4F_5H_3] =$ 0.070 .....	74

TABLE		<u>Page</u>
XV	Addition of S( <sup>3</sup> P) Atoms to 3,3-4,4,4-Pentafluorobutene-1 and 2-Fluoropropene. Product Formation as a Function of Exposure Time for $[C_3FH_5]/[C_4F_5H_3] = 0.056$ .....	75
XVI	Addition of S( <sup>3</sup> P) Atoms to 3,3-4,4,4-Pentafluorobutene-1 and Propene. Product Formation as a Function of Exposure Time for $[C_3H_6]/[C_4F_5H_3] = 0.120$ .....	78
XVII	Addition of S( <sup>3</sup> P) Atoms to Acetylene and Ethylene. Ethylene Episulfide Formation as a Function of Added Acetylene.....	80
XVIII	Addition of S( <sup>3</sup> P) Atoms to Methylacetylene and Ethylene. Ethylene Episulfide Formation as a Function of Added Methylacetylene.....	83
XIX	Addition of S( <sup>3</sup> P) Atoms to Dimethylacetylene and Cyclopentene. Cyclopentene Episulfide Formation as a Function of Added Dimethylacetylene.....	86
XX	Addition of S( <sup>3</sup> P) Atoms to Propene and Isobutene. Product Formation as a Function of Temperature for $[C_3H_6]/[C_4H_8] = 8.08$ .....	95



TABLE		<u>Page</u>
XXI	Addition of S( <sup>3</sup> P) Atoms to Trimethyl- ethylene and Isobutene. Product Forma- tion as a Function of Temperature for [C <sub>4</sub> H <sub>8</sub> ]/[C <sub>5</sub> H <sub>10</sub> ] = 1.69.....	98
XXII	Addition of S( <sup>3</sup> P) Atoms to Tetramethyl- ethylene and Cyclopentene. Cyclopentene Episulfide as a Function of Temperature for [C <sub>5</sub> H <sub>8</sub> ]/[C <sub>6</sub> H <sub>12</sub> ] = 2.90.....	100
XXIII	Addition of S( <sup>3</sup> P) Atoms to 1,3-Butadiene and Propene. Propene Episulfide as a Function of Temperature for [C <sub>3</sub> H <sub>6</sub> ]/[C <sub>4</sub> H <sub>6</sub> ] = 8.03.....	103
XXIV	Addition of S( <sup>3</sup> P) Atoms to Vinyl Chloride and Propene. Product Formation as a Function of Temperature for [C <sub>3</sub> H <sub>6</sub> ]/[C <sub>2</sub> H <sub>3</sub> Cl] = 0.201.....	105
XXV	Addition of S( <sup>3</sup> P) Atoms to <u>Cis</u> -1,2- Difluoroethylene and Ethylene. <u>Cis</u> - Difluoroethylene Episulfide Formation as a Function of Temperature for [C <sub>2</sub> H <sub>4</sub> ]/[C <sub>2</sub> F <sub>2</sub> H <sub>2</sub> ] = 0.259.....	108
XXVI	Addition of S( <sup>3</sup> P) Atoms to Trans-1,2- Difluoroethylene and Ethylene. Product Formation as a Function of Temperature for [C <sub>2</sub> H <sub>4</sub> ]/[C <sub>2</sub> F <sub>2</sub> H <sub>2</sub> ] = 0.181.....	111

TABLE		<u>Page</u>
XXVII	Addition of S( <sup>3</sup> P) Atoms to Tetrafluoro- ethylene and Ethylene. Ethylene Epi- sulfide Formation as a Function of Temperature for $[C_2H_4]/[C_2F_2] = 0.49....$	114
XXVIII	Addition of 3,3,3-Trifluoropropene and Ethylene. Product Formation as a Function of Temperature for $[C_2H_4]/[C_3F_3H_3] =$ 0.170.....	116
XXIX	Addition of S( <sup>3</sup> P) Atoms to Acetylene and Propylene. Propylene Episulfide as a Function of Temperature for $[C_3H_6]/[C_2H_2]$ $= 0.080.....$	119
XXX	Addition of S( <sup>3</sup> P) Atoms to Methylacetylene and Propylene. Propylene Episulfide as a Function of Temperature for $[C_3H_6]/[C_3H_4]$ $= 0.897.....$	122
XXXI	Addition of S( <sup>3</sup> P) Atoms to Dimethylacety- lene and Cyclopentene. Cyclopentene Episulfide Formation as a Function of Temperature for $[C_5H_8]/[C_4H_6] = 2.16....$	125
XXXII	Relative Rates and Arrhenius Parameters for S( <sup>3</sup> P) Addition Reactions.....	128
XXXIII	Relative Activation Energies for Additions to Hydrocarbon Olefins.....	133

TABLE	<u>Page</u>
XXXIV Relative Reactivities of Singlet and Triplet Species with Olefins.....	139
XXXV Relative Rates for Additions to Halogenated Olefins.....	156
XXXVI Relative Activation Energies for Additions to Halogenated Olefins.....	158
XXXVII Comparison of Activation Energies for $\text{CCl}_3$ and $\text{S}(^3\text{P})$ Additions to Fluoroethylenes..	162
XXXVIII Relative Rates and Activation Energies for Additions to Acetylenes.....	169
XXXIX Relative A-factors for Additions to Olefins and Acetylenes.....	171
XL Rate Constants and Arrhenius Parameters for Group VI Atom Additions to Ethylene.	180
XLI Calculated A-factors for S and O Atom Addition to Ethylene.....	183
XLII Photolysis of $\text{COS-CO}_2\text{-C}_2\text{H}_4$ . Variation of EES/CO with Pressure and Exposure Time.....	203
XLIII Photolysis of $\text{COS-CO}_2\text{-C}_2\text{H}_4$ . Variation of EES Yield with CO Yield at Constant Pressure.....	206
XLIV Photolysis of $\text{COS-CO}_2\text{-C}_2\text{H}_4$ . Variation of $[\text{C}_2\text{H}_4]/[\text{EES}]$ with Total Pressure.....	211

TABLE		<u>Page</u>
XLV	Photolysis of COS-CO <sub>2</sub> -C <sub>3</sub> H <sub>6</sub> . Variation of [C <sub>3</sub> H <sub>6</sub> ]/[EES] as a Function of Pressure.....	218
XLVI	Photolysis of COS-CO <sub>2</sub> -C <sub>2</sub> H <sub>4</sub> . Steady-State EES Pressure as a Function of P(C <sub>2</sub> H <sub>4</sub> )...	220
XLVII	Photolysis of COS-CO <sub>2</sub> -C <sub>2</sub> H <sub>4</sub> . Variation of k <sub>3</sub> /k <sub>6</sub> as a Function of Temperature.....	222
XLVIII	Photolysis of COS-CO <sub>2</sub> -C <sub>3</sub> H <sub>6</sub> . Variation of k <sub>9</sub> /k <sub>10</sub> as a Function of Temperature.....	225
XLIXa	Mass Spectrometric Calibrations of Binary Episulfide Mixtures.....	235
XLIXb	Isotope Effect as a Function of Temperature for Ethylene-d <sub>4</sub> .....	235
La	Mass Spectrometric Calibrations of Binary Episulfide Mixtures.....	238
Lb	Isotope Effect as a Function of Temperature for 1,1-Ethylene-d <sub>2</sub> .....	238
LIa	Mass Spectrometric Calibrations of Binary Episulfide Mixtures.....	239
LIb	Isotope Effect as a Function of Temperature for <u>cis</u> -1,2-Ethylene-d <sub>2</sub> .....	239
LI Ia	Mass Spectrometric Calibration of Binary Episulfide Mixtures.....	241
LI Ib	Isotope Effect as a Function of Temperature for <u>trans</u> -1,2-Ethylene-d <sub>2</sub> .....	241

TABLE	<u>Page</u>
LIII Secondary Isotope Effects for Addition of S( <sup>3</sup> P) to Ethylene.....	242
LIV Secondary Isotope Effects for Additions of Atoms and Radicals to Olefins.....	242

## LIST OF ILLUSTRATIONS

NUMBER		<u>Page</u>
1)	High-Vacuum System.....	26
2)	Hg-Photosensitization Assembly.....	28
3)	G.L.C. Unit.....	30
4a)	Addition of S( <sup>3</sup> P) Atoms to Ethylene and Propylene. Episulfide vs CO yields for [C <sub>2</sub> H <sub>4</sub> ]/[C <sub>3</sub> H <sub>6</sub> ] = 1.50.....	49
4b)	Addition of S( <sup>3</sup> P) Atoms to Ethylene and Propylene. Relative Rate vs CO yield for [C <sub>2</sub> H <sub>4</sub> ]/[C <sub>3</sub> H <sub>6</sub> ] = 1.50.....	50
5a)	Addition of S( <sup>3</sup> P) Atoms to Ethylene and Propylene. Episulfide vs CO yields for [C <sub>2</sub> H <sub>4</sub> ]/[C <sub>3</sub> H <sub>6</sub> ] = 2.98.....	52
5b)	Addition of S( <sup>3</sup> P) Atoms to Ethylene and Propylene. Relative Rate vs CO yield for [C <sub>2</sub> H <sub>4</sub> ]/[C <sub>3</sub> H <sub>6</sub> ] = 2.98.....	53
6a)	Addition of S( <sup>3</sup> P) Atoms to Ethylene and Propylene. Episulfide vs CO yields for [C <sub>2</sub> H <sub>4</sub> ]/[C <sub>3</sub> H <sub>6</sub> ] = 6.06.....	55
6b)	Addition of S( <sup>3</sup> P) Atoms to Ethylene and Propylene. Relative Rate vs CO yield for [C <sub>2</sub> H <sub>4</sub> ]/[C <sub>3</sub> H <sub>6</sub> ] = 6.06.....	56
7)	Addition of S( <sup>3</sup> P) Atoms to Isobutene and Propene. Episulfide vs CO yield.....	60

NUMBER		<u>Page</u>
8)	Addition of $S(^3P)$ Atoms to Trimethyl- ethylene and Isobutene. Episulfide vs CO yield.....	63
9)	Addition of $S(^3P)$ Atoms to Tetramethyl- ethylene and Trimethylethylene. $(A_O-A)/A$ vs $P(C_5H_{10})/P(C_6H_{12})$ .....	65
10)	Addition of $S(^3P)$ Atoms to 2-Trifluorome- thylpropene and Propene. Episulfide vs CO yield.....	70
11)	Addition of $S(^3P)$ Atoms to 2-Fluoropro- pene and Ethylene. Episulfide vs CO yield	72
12)	Addition of $S(^3P)$ Atoms to 3,3-4,4,4- Pentafluorolutene-1 and 2-Fluoropropene. Relative Rate vs CO yield.....	76
13)	Addition of $S(^3P)$ Atoms to 3,3-4,4,4- Pentafluorobutene-1 and Propene. Episul- fide vs CO yield.....	79
14)	Addition of $S(^3P)$ Atoms to Acetylene and Ethylene. $(A_O-A)/A$ vs $P(C_2H_2)/P(C_2H_4)$ ....	81
15)	Addition of $S(^3P)$ Atoms to Methylacetylene and Ethylene. $(A_O-A)/A$ vs $P(C_3H_4)/P(C_2H_4)$	84
16)	Addition of $S(^3P)$ Atoms to Dimethylacety- lene and Cyclopentene. $(A_O-A)/A$ vs $P(C_4H_6)/P(C_5H_8)$ .....	87
17)	Oscillogram; Mass 144, $SiF_3C_2H_3S$ .....	90

NUMBER		<u>Page</u>
18)	Oscillogram; Mass 144, $\text{SiF}_3\text{C}_2\text{H}_3\text{S}$ . Corrected for Bleed-out.....	90
19)	Addition of $\text{S}(^3\text{P})$ Atoms to Isobutene. Episulfide/CO yield as a function of Temperature.....	92
20)	Addition of $\text{S}(^3\text{P})$ Atoms to Isobutene and Propene. Arrhenius Plot.....	96
21)	Addition of $\text{S}(^3\text{P})$ Atoms to Trimethyl- ethylene and Isobutene. Arrhenius Plot...	99
22)	Addition of $\text{S}(^3\text{P})$ Atoms to Tetramethyl- ethylene and Cyclopentene. Arrhenius Plot	101
23)	Addition of $\text{S}(^3\text{P})$ Atoms to 1,3-Butadiene and Propylene. Arrhenius Plot.....	104
24)	Addition of $\text{S}(^3\text{P})$ Atoms to Vinyl Chloride and Propylene. Arrhenius Plot.....	106
25)	Addition of $\text{S}(^3\text{P})$ Atoms to <u>cis</u> -1,2-difluoro- ethylene and Ethylene. Arrhenius Plot....	109
26)	Addition of $\text{S}(^3\text{P})$ Atoms to <u>trans</u> -1,2-di- fluoroethylene and Ethylene. Arrhenius Plot	112
27)	Addition of $\text{S}(^3\text{P})$ Atoms to Tetrafluoro- ethylene and Ethylene. Arrhenius Plot....	115
28)	Addition of $\text{S}(^3\text{P})$ Atoms to 3,3,3-Trifluoro- propene and Ethylene. Arrhenius Plot.....	117
29)	Addition of $\text{S}(^3\text{P})$ Atoms to Acetylene and Propylene. Arrhenius Plot .....	120



NUMBER		<u>Page</u>
30)	Addition of S( <sup>3</sup> P) Atoms to Methylacetylene and Propylene. Arrhenius Plot.....	123
31)	Addition of S( <sup>3</sup> P) Atoms to Dimethylacetylene and Cyclopentene. Arrhenius Plot....	126
32)	Potential Energy - Reaction Co-ordinate Diagram for Addition of Radicals to Unsaturated Compounds.....	131
33)	Plot of Ionization Potentials vs Activation Energies for S( <sup>3</sup> P) Atom Addition to Olefins	134
34)	Potential Energy - Reaction Co-ordinate Diagram for Addition of Radicals to Unsaturated Compounds.....	145
35)	Plot of Activation Energies for S( <sup>3</sup> P) Atom Addition to Olefins vs Excitation Energies	151
36)	Plot of Activation Energies for S( <sup>3</sup> P) Atom Addition to Olefins vs Bond Orders.....	152
37)	Plot of Average Atom Localization Energies of Both Carbon Atoms vs Activation Energies for S( <sup>3</sup> P) Atom Addition to Olefins.....	163
38)	Plot of Activation Energies for S( <sup>3</sup> P) Atom Addition to Halogenated Alkenes and Alkynes	165
39)	Potential Energy - Reaction Co-ordinate Diagram for Addition of S( <sup>3</sup> P) Atoms to Ethylene.....	187
40)	Potential Energy - Reaction Co-ordinate Diagram for Addition of S( <sup>3</sup> P) Atoms to Ethylene	190

NUMBER		<u>Page</u>
41)	Potential Energy - Reaction Co-ordinate Diagram for Addition of S( <sup>3</sup> P) Atoms to Ethylene	199
42)	Photolysis of COS-CO <sub>2</sub> -C <sub>2</sub> H <sub>4</sub> ; EES/CO yield vs Total Pressure.....	204
43)	Photolysis of COS-CO <sub>2</sub> -C <sub>2</sub> H <sub>4</sub> ; EES yield vs CO yield.....	207
44)	Photolysis of COS-CO <sub>2</sub> -C <sub>2</sub> H <sub>4</sub> ; [C <sub>2</sub> H <sub>4</sub> ]/[EES] vs Reciprocal-Pressure.....	212
45)	Potential Energy - Reaction Co-ordinate Diagram for Addition of S( <sup>3</sup> P) Atoms to Ethylene	215
46)	Photolysis of COS-CO <sub>2</sub> -C <sub>2</sub> H <sub>4</sub> ; Plot of P(EES) at Steady State vs P(C <sub>2</sub> H <sub>4</sub> ).....	221
47)	Photolysis of COS-CO <sub>2</sub> -C <sub>2</sub> H <sub>4</sub> ; Arrhenius Plot for k <sub>3</sub> /k <sub>6</sub> .....	223
48)	Photolysis of COS-CO <sub>2</sub> -C <sub>3</sub> H <sub>6</sub> ; Arrhenius Plot for k <sub>9</sub> /k <sub>10</sub> .....	226

## CHAPTER I

INTRODUCTION

The sulfur atom, having two unpaired electrons, is a divalent species. As such it can be classified chemically with other Group VI atoms and with divalent radicals such as :NH, :C<sub>2</sub>O, :CH<sub>2</sub>, substituted methylenes, etc. In each of these species the spin vectors of the two valence electrons can be parallel or anti-parallel, thus giving rise to triplet or singlet electronic states respectively. An upper electronic state has a long natural lifetime with respect to radiative decay to a lower one of different multiplicity since the transition is spin forbidden; thus under the proper conditions, the chemical behaviour of either spin state can be studied. From the large body of data accumulated for the reactivities of these divalent species it is now clear that both the reactivity and the type of chemical reaction are profoundly affected by the spin state of the biradical.

The atoms in Group VI of the Periodic Table have two degenerate p-orbitals available for the two valence electrons thus giving rise to the following three electronic states:  $^3P$ ,  $^1D_2$  and  $^1S_0$ . The  $^3P$  state in accordance with Hund's rule is the ground state and consists of three components  $^3P_2$ ,  $^3P_1$  and  $^3P_0$  depending on the spin-orbit

coupling. In the case of the sulfur atom the  $^3P_1$  and  $^3P_0$  components are respectively 1.14 and 1.64 kcal mole<sup>-1</sup> above the  $^3P_2$  state (1), so that for practical purposes the ground state will be labeled  $^3P$ . The  $^1D_2$  and  $^1S_0$  states of sulfur are respectively 26.4 and 63.4 kcal mole<sup>-1</sup> above the ground state.

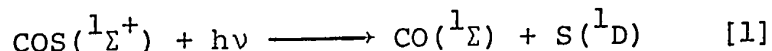
Since the present study is concerned with the addition reactions of  $S(^3P)$  atoms with olefinic and acetylenic bonds, it seems desirable first of all to give a brief description of the current status of our knowledge of these reactions. This will be followed by a general review of the pertinent features of the addition reactions of monovalent and divalent atoms and free radicals with multiple bonds.

#### A) Reactions of $S(^3P)$ Atoms With Alkenes and Alkynes

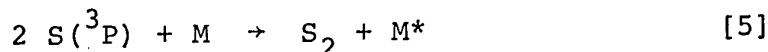
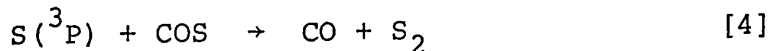
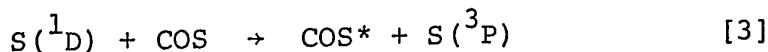
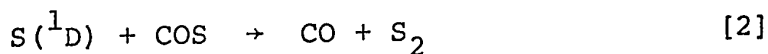
##### i) Sources of $S(^3P)$ Atoms

Extensive studies of the reactions of both  $S(^3P)$  and  $S(^1D)$  atoms with a large number of hydrocarbons and halides have been carried out over the past several years and have recently been reviewed by Strausz and Gunning (2). The source of sulfur atoms in these systems was the photolysis of carbonyl sulfide in the wavelength region 2550 - 2290 Å. The u.v. spectrum of COS consists of a banded spectrum extending from about 2600 Å to 1800 Å, with a maximum at

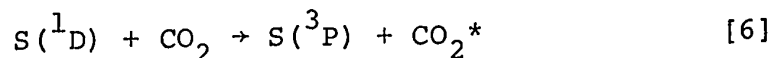
2235 $\text{\AA}$ . Semi-empirical M.O. calculations (3) indicate that the transition is a  $\Pi \rightarrow \Pi^*$ , and the radiative lifetime of the upper state has been estimated to be  $3.7 \times 10^{-7}$  sec. (4). It has been shown that the quantum yield of the primary step at both wavelengths 2537 $\text{\AA}$  and 2288 $\text{\AA}$  is



0.9, the slight inefficiency being due to radiative or non-radiative transitions to the ground state. Reaction [1] requires a minimum energy of 98.8 kcal mole $^{-1}$  corresponding to 2895 $\text{\AA}$ ; to produce  $\text{S}({}^1\text{S}_0)$  atoms a minimum energy of 135.8 kcal mole $^{-1}$  would be required corresponding to  $\lambda = 2105\text{\AA}$ . Other reactions occurring in the photolysis of COS are the following:

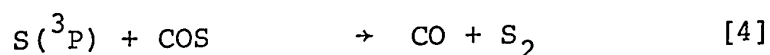
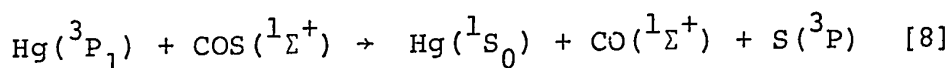
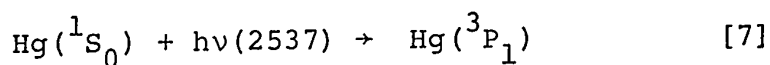


Reactions [3], [4] and [5] are of minor importance. Carbon dioxide has been shown to be a very efficient deactivator of  $\text{S}({}^1\text{D})$  atoms to the ground state (5). In the presence of a large excess of this inert gas reactions [2] and [3] are replaced by the reaction



thus affording a useful source of ground state sulfur atoms.

Sidhu et al (3) have shown that the Hg-photosensitization of COS also provides a clean source of  $S(^3P)$  atoms. At a COS pressure of 200 torr it has been shown that the quantum yield of CO formation is 1.79, almost the same as for the photolysis of COS. The following reaction sequence may be written:



Although the exothermicity of reaction [8] is sufficient to promote the sulfur atoms to the  $(^1D_2)$  state, it has been shown that only  $(^3P)$  atoms are produced, in accordance with the spin conservation rule.

## ii) Addition of $S(^3P)$ to Alkenes

The only reaction occurring between  $S(^3P)$  atoms and alkenes is addition across the double bond to form the corresponding episulfide. Investigations of the reactions of  $S(^3P)$  atoms to many olefins, including cyclic and halogenated olefins have been carried out (6, 7, 8). The reactions with internal olefins were stereospecific to a high degree. The addition reaction with ethylene is so rapid that a fairly low ethylene to COS ratio is sufficient to suppress reactions [4] and [5].

iii) Addition of S(<sup>3</sup>P) to Alkynes

The products of sulfur atom addition to alkynes are unstable entities. By utilizing the technique of flash photolysis with kinetic mass spectrometry, Strausz et al (9) have shown that the products of sulfur addition to acetylene, propyne, butyne-2 and hexafluorobutyne-2 were the corresponding thiirenes with decay half-lives of 2, 5, 7 and 0.1 seconds, respectively.

B) Additions of Atoms and Radicals to Multiple Bonds

In this section it is desired only to point out those studies in which the relative addition rates to unsaturated compounds were measured, and to describe briefly the nature of the reactions and the methods employed in the measurements. The relative rates of addition of several monovalent and divalent reagents to a series of olefins are summarized in Table I, where it can be seen that the variation in addition rate with olefin structure is markedly dependent on the reagent involved. Two general trends of rate variation are discernible, due to (a) "electrophilic" additions and (b) "free radical" type additions. The former type are tabulated in the left-hand side of Table I and the free radical type reagents are to the right.

TABLE I

COMPARISON OF THE RELATIVE RATE CONSTANTS OF ADDITION TO OLEFINS OF SEVERAL REAGENTS

Olefin	$O(^3P)^a$ (25°)	$Se(^3P)^b$ (25°)	$C_2O(^3\Sigma)^c$ (29°)	$CF_3^d$ (65°)	$CH_2(^3\Sigma)^e$ (24°)	$CH_2(^1A_1)^e$ (24°)	$H^f$ (25°)	$CH_3^g$ (65°)	$N^h$ (27°)
$CH_2=CH_2$	1	1	1	1	1	1	1	1	1
$CH_3 \cdot CH=CH_2$	5.8	3.5	6.0	1.2	1.0	1.3	1.8	0.6	2.15
$C_2H_5 \cdot CH=CH_2$	5.8	7.1	6.9	1.2	1.6	1.6	1.9	0.8	2.3
$(CH_3)_2C=CH_2$	25	45	57	3.7	2.9	2.0	4.4	1.1	4.1
$cis-CH_3 \cdot CH=CH \cdot CH_3$	24	24	9.7	0.9	0.94	1.4	0.8	0.10	1.1
$trans-CH_3 \cdot CH=CH \cdot CH_3$	28	56	11.7	1.0	0.89	1.4	1.1	0.20	1.3
$(CH_3)_2C=CH \cdot CH_3$	79	-	96	-	1.8	2.1	-	0.16	2.9
$(CH_3)_2C=C \cdot (CH_3)_2$	102	-	245	1.3	2.7	2.2	8.7	-	2.3
$CH_2=CH-CH=CH_2$	24	98	210	8.7	19.0	3.9	2.0	59	-

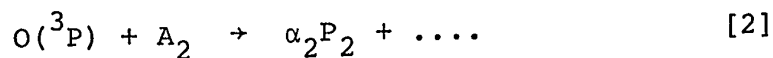
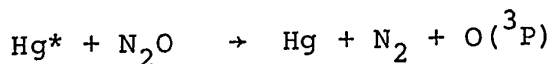
(a) Reference 10 (b) Reference 14 (c) Reference 21

(d) Reference 29, 114 (e) Reference 16 (f) Reference 33

(g) Reference 26 (h) Reference 126



The addition reactions of  $O(^3P)$  atoms with olefins have been reviewed by Cvetanovic (10). Since these addition reactions are exothermic by about 100 kcal mole<sup>-1</sup> the initially formed adduct undergoes various secondary reactions such as isomerizations, "pressure independent" fragmentations, and "pressure dependent" fragmentations before stable products are produced. At limiting high pressures however, the products are formed in a constant ratio, e.g. the addition of  $O(^3P)$  to cis-2-pentene yields cis- $\beta$ -pentene oxide (23%), trans  $\beta$ -pentene oxide (31%), methyl-n-propyl ketone and diethyl ketone (25%) and 2-methyl butanal (21%) so that the number of oxygen atoms that have reacted can be determined by monitoring a single product. Thus with the use of the nitrous oxide technique, Cvetanovic and co-workers obtained accurate values of the relative addition rate constants at various temperatures by carrying out competitive reactions of oxygen atoms with two olefins at a time. The rate constant measurements were based on the following scheme:



$$\text{Thus } \frac{k_1}{k_2} = \frac{\alpha_2}{\alpha_1} \left( \frac{\Delta P_1}{\Delta P_2} \right) \frac{(A_2)}{(A_1)},$$

where  $\alpha$  is the fraction of the total products constituted by P,  $\Delta P$  is the yield of product P and (A) is the olefin concentration. Since

$$\left(\frac{1}{\alpha_1}\right) \Delta P_1 + \left(\frac{1}{\alpha_2}\right) \Delta P_2 = \Delta N_2 ,$$

then

$$\frac{k_1}{k_2} = \frac{(A_2)}{(A_1)} \cdot \left[ \frac{\alpha_1 \Delta N_2}{\Delta P_1} - 1 \right]^{-1} ,$$

so that the relative rate constants of two olefins can be calculated by measuring the yield of  $N_2$  and a single product. The same method was used by Moss and Jennings (11) to measure the relative addition rates of  $O(^3P)$  atoms to a number of fluorinated olefins. Saunders and Heicklen (12) measured the rate constants for addition of  $O(^3P)$  atoms to some saturated and unsaturated hydrocarbons by means of competition between the hydrocarbon and  $C_2F_4$  for oxygen atoms produced by the  $N_2O$  technique.  $O(^3P)$  atoms react with  $C_2F_4$  to give  $CF_2O$  as the sole oxygen-containing product so that relative rates could be measured by observing the quantum yield of  $CF_2O$  in the presence of various concentrations of hydrocarbons, and applying the following equation:

$$\frac{k(\text{hydrocarbon})}{k(C_2F_4)} = \frac{[C_2F_4]}{[\text{hydrocarbon}]} \cdot \frac{1 - \phi_{CF_2O}}{\phi_{CF_2O}}$$

The same technique was employed by Tyerman (13) to measure relative rates for addition of  $O(^3P)$  atoms to several

halogenated ethylenes, employing flash photolysis of  $\text{NO}_2$  as a source of ground state oxygen atoms.

The Arrhenius parameters for addition of  $\text{Se}(^3\text{P})$  atoms to a series of olefins have been measured by Callear and Tyerman (14), who used the flash photolysis of  $\text{CSe}_2$  as a source of selenium atoms. The technique was to record the intensities of the olefin-selenide spectra produced in flashed mixtures of  $\text{CSe}_2$  and two olefins. Relative addition rates were then evaluated for olefins X and Y from the equation

$$\frac{k_x}{k_y} = \frac{[Y]}{[X]} \cdot \frac{h_0 - h}{h}$$

where  $h_0$  is the peak height in the presence of olefin Y alone and  $h$  is that due to the mixture.

A similar technique has recently been employed by Connor, Greig and Strausz (15) to measure the rate constants for  $\text{Te}(^3\text{P})$  atom addition to olefins. Te atoms were produced by flash photolysis of dimethyltelluride which in the presence of an olefin gives rise to a band system due to the epitelluride.

By means of competitive studies, Kryzanowski and Cvetanovic (16) have measured the relative rates of reaction with olefins at room temperature of  $^1\text{CH}_2$  and  $^3\text{CH}_2$  produced respectively by the photolysis and mercury-photosensitization of ketene. One of the two competing olefins was always isobutene and the relative rates were

evaluated from the variation in yield of a singlet product, dimethylcyclopropane.

Relative addition rates to olefins of  $\text{:CBr}_2$  were obtained in t-butyl alcohol solution by Skell and Garner (17) by measuring the yields of the corresponding dibromocyclopropanes produced from two olefins in competition.

Closs and Coyle (18) have measured the relative reactivities of  $\text{:CHCl}$  and  $\text{:CHBr}$  with olefins in solution at  $-30^\circ\text{C}$ . The carbenes were produced from the thermolysis of chloro- and bromo-diazomethane and were found to add stereospecifically across the double bond of the olefins to yield the corresponding cyclopropanes. Wherever two epimers were possible, these were formed in a 1:1 ratio. Tritium-labeled monofluorocarbene has been shown to react with olefins in a similar manner and the relative reactivities have been measured by Tang and Rowland (19).

The photolysis of  $\text{C}_3\text{O}_2$  at  $3000\text{\AA}$  has been postulated to yield  $\text{:C}_2\text{O}$  ( $X^3\Sigma$ ) and  $\text{CO}$ , (20). The  $\text{C}_2\text{O}$  reacts with ethylene by insertion into the double bond to give allene and  $\text{CO}$ . From competitive studies between ethylene and another olefin, at different temperatures, Williamson and Bayes (21) have obtained the Arrhenius parameters for the reaction of  $\text{C}_2\text{O}$  with a series of olefins by measuring the allene yield in the presence of a second olefin.

Since the primary products of the addition reactions

of monovalent atoms and radicals with unsaturated compounds are themselves free radicals which undergo various secondary reactions, the final products are difficult to determine quantitatively. Thus relative addition rates for these monovalent species are usually determined by competition between the addition reaction and an abstraction reaction with a paraffin which may be present as a solvent. Such a technique has been employed by Szwarc and co-workers to obtain relative reactivities of  $\text{CH}_3$ ,  $\text{C}_2\text{H}_5$  and  $\text{CF}_3$  radicals with both aliphatic and aromatic unsaturates using iso-octane or 2,3-dimethylbutane as liquid solvent or gaseous diluent (22-29). As a source of methyl radicals Szwarc and co-workers used the pyrolysis of acetyl peroxide which yields an equal number of  $\text{CO}_2$  molecules as an internal monitor of  $\text{CH}_3$  radicals. The photolysis of perfluoroazomethane was employed as a source of  $\text{CF}_3$  radicals. In the case of the methyl radical addition the ratio of the addition rate constant to that of the abstraction reaction is

$$\text{given by } \frac{k_{\text{add}}}{k_{\text{abs}}} = \frac{\left( \frac{R_{\text{CH}_4}}{R_{\text{CO}}} \right)_X - \left( \frac{R_{\text{CH}_4}}{R_{\text{CO}}} \right)_Y}{\left( \frac{R_{\text{CH}_4}}{R_{\text{CO}}} \right)_Y} \cdot \frac{[\text{Solvent}]}{[\text{Olefin}]}$$

where the subscripts X and Y represent yields in the absence and presence of the olefin respectively. Cvetanovic and Irwin (30) have determined the Arrhenius parameters for  $\text{CH}_3$  addition to olefins in the gas phase by allowing competition

between addition to the olefin and abstraction from isobutane. The results are in good agreement with those of Feld and Szwarc (26).

By measuring the yields of final products, Tedder and Walton (31) have been able to determine Arrhenius parameters for the addition of  $\text{CCl}_3$  radicals to either carbon atom in some fluorinated ethylenes.

Recently Cvetanovic and Doyle (32) have re-determined the relative rates of reaction of H atoms with olefins and found good agreement with previously measured values (33). H atoms were produced by Hg-photosensitization of  $\text{H}_2$  and relative reaction rates with olefins compared with ethylene were determined by measuring the yield of n-butane in the absence and presence of the second olefin.

### C) The Secondary Kinetic Isotope Effect

When a deuterated or partially deuterated molecule is involved in a chemical equilibrium or a chemical reaction, the ratio of the corresponding equilibrium constant or rate constant to that of the non-deuterated analogue differs from unity. This deviation from unity in  $K_{\text{H}}/K_{\text{D}}$ , or  $k_{\text{H}}/k_{\text{D}}$  is a manifestation of the isotope effect and in the latter case is known as the kinetic isotope effect. Prior to 1952 it was believed that an isotope effect only occurred in those reactions where

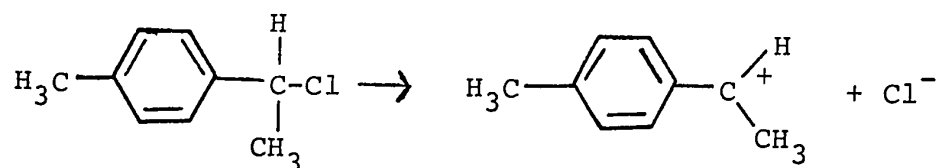
isotopic substitution was effected on the bond to be broken or formed in the reaction; such a case is now described as the primary isotope effect.

Secondary isotope effects occur in reactions where no bonds to isotopic atoms are broken, and are divided into two classes, depending on the position of isotopic substitution relative to the reaction site. These two classes are defined by Halevi (34) as (a) "secondary isotope effects of the first kind", in which bonds to isotopic atoms have undergone spatial reorientation and (b) "secondary isotope effects of the second kind" in which no such reorientation takes place.

Solvolysis reactions account for the vast majority of secondary kinetic isotope effects which have been measured, the other reactions including thermal decompositions, radical additions to olefins and Diels-Alder reactions. The first secondary effect of the first kind ( $\alpha$ -effect) reported was by Streitweiser and Fahey (35) in 1957 for an  $S_N1$  solvolysis reaction where the effect measured was  $k_H/k_D = 1.16$ . Since then, the secondary  $\alpha$ -effects measured in numerous reactions show a remarkable constancy, averaging a 10 - 12% effect per  $\alpha$ -deuterium atom (36) for  $S_N1$  solvolysis reactions. Effects of the second kind vary greatly depending on molecular structure and solvent effects (37,38). All of the solvolysis reactions involve charged species and their isotope effects have usually

been explained in terms of currently accepted theories of substituent effects such as the inductive effect, conjugation, hyperconjugation, steric effects and hybridization. One of the earliest and strongest pieces of evidence that secondary isotope effects are related to the usual electronic substituent effects was Lewis and Coppinger's (39) demonstration that the hyperconjugative retardation of solvolysis by deuterium is transmitted through an aromatic ring.

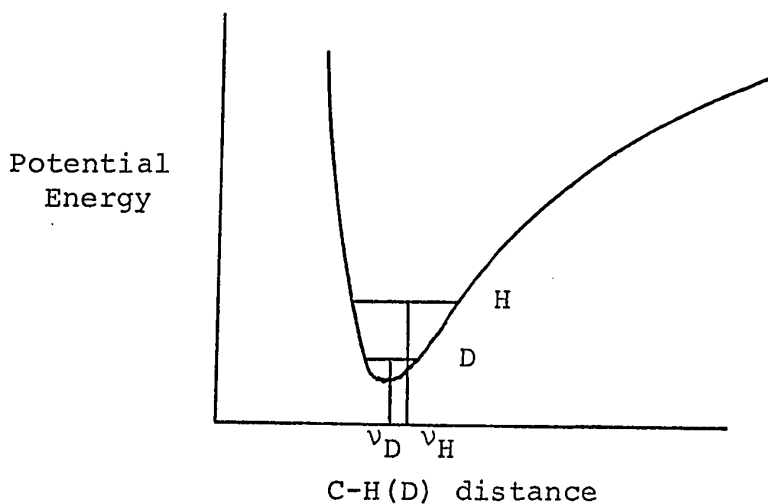
Working with methyl-paratolylcarbiny chloride:



they showed that acetolysis at 50°C of the β-deuterated compound had an isotope effect of  $k_H/k_D = 1.11$ , per deuterium atom while deuteration at the para-methyl position resulted in the smaller but still substantial effect of  $k_H/k_D = 1.05$  per deuterium atom. Similar effects of transmission from the para position of the benzene ring have been reported by Shiner and Verbanic (40). Effects of γ-deuteration have also been reported (41). Some authors, on the other hand, such as Bartell (42) and Brown et al (43) believe that the secondary isotope effect is entirely due to non-bonded interactions and arises because of the smaller steric requirements of the deuterium atom compared with hydrogen.



While the precise cause of secondary effects is not fully understood, it is certain that they do originate from changes in force constants which in turn may be caused by hyperconjugative, inductive, steric and hybridizational effects. These electronic effects are themselves vibrational in origin and their different magnitudes in deuterated and normal molecules are due to the anharmonicity of the vibrations involving motion of the hydrogen atoms resulting in different average bond lengths and bond angles in the deuterated and normal molecules, as shown in the diagram below:



A consequence of this is the greater Inductive Effect of C-D compared with C-H.

The evidence from physical properties such as dipole moments, NMR and nuclear quadrupole coupling constants, molecular refraction and optical activity is consistent with the view that deuterium bonded to carbon is more electro-positive, but less polarizable, than protium (34).

Since we are concerned here with the reaction of a sulfur atom with ethylene, a reaction involving a small molecule and devoid of complications due to solvent effects or hyperconjugation etc., it is best to stick to the formal framework of isotope effect theory and try to interpret the isotope effect in terms of the force constant changes and the geometry of the transition state. Thus, the secondary isotope effect is used as a probe to gain information about the transition state and therein lies its main usefulness. We shall therefore briefly review the formal theory and its application to simple gas phase reactions.

The complete expression of Bigeleisen (44) is based on absolute reaction rate theory and is given as follows:

$$\frac{k_H}{k_D} = \frac{\kappa_H}{\kappa_D} \cdot \frac{\frac{v_H^\ddagger}{v_D^\ddagger} \prod_{i=1}^{3N-7} \frac{U_i^\ddagger(H)}{U_i^\ddagger(D)} \cdot \frac{[1 - \exp\{-U_i^\ddagger(D)\}]}{[1 - \exp\{-U_i^\ddagger(H)\}]} \cdot \frac{\exp\{-\frac{1}{2}U_i^\ddagger(H)\}}{\exp\{-\frac{1}{2}U_i^\ddagger(D)\}}}{\prod_{j=1}^{3N-6} \frac{U_j(H)}{U_j(D)} \cdot \frac{[1 - \exp\{-U_j(D)\}]}{[1 - \exp\{-U_j(H)\}]} \cdot \frac{\exp\{-\frac{1}{2}U_j(H)\}}{\exp\{-\frac{1}{2}U_j(D)\}}}$$

$v_H^\ddagger$  and  $v_D^\ddagger$  represent respectively the imaginary frequency along the reaction co-ordinate in the normal and deuterated molecules and their ratio gives the temperature independent factor.  $U_i = hc\omega_i/kT$ , and the product in the numerator is over all of the  $i$  normal modes of the transition state while

that in the denominator is over all the  $j$  normal modes in the reactants. The calculation of this equation requires a complete vibrational analysis of the reactants and transition state. Schachtschneider has written a computer program which is used to calculate vibrational frequencies from a complete set of force constants, atomic masses and geometry of the molecule (45). Wolfsberg and Stern have modified the program to calculate the isotope effect directly, and have used it on a series of model reactions (46,47) in order to test the variation of the secondary isotope effect with small changes in force constants. Exact calculations have also been made by Seltzer and Mylonakis (15) for the thermal decompositions of three aralkyl azo compounds. The force fields chosen for the reactants were obtained from reported force constants of analogous groupings, while those for the transition states were constructed in such a way as to be consistent with detailed mechanisms suggested by previous work. In this way they were able to reproduce the experimentally measured isotope effects. Undoubtedly there are many ways in which the force field of the transition state could be altered which would lead to the same isotope effects, but the changes in force constants might not be internally self-consistent. Thus, the major contribution of Seltzer and Mylonakis was that they were able to show, by isotopic substitution of both the leaving group and an  $\alpha$ -hydrogen, that for small normal or inverse secondary

isotope effects the relative change in the H-C-X (where X is the leaving group or atom) bending force constant from reactant to transition state reflects the same change in the C-X stretching force constant. If numerical agreement between a calculated isotope effect and experiment does not constitute proof of the correctness of the model, nevertheless, a model which yields an isotope effect in sharp disagreement with experiment can be excluded as being in all probability unrealistic.

Streitweiser et al (36) have simplified Bigeleison's isotope effect equation by applying the following approximations:

- (i) Deuterium substitution will change significantly only those frequencies primarily associated with the motion of the isotopically substituted hydrogen atoms.
  - (ii) The C-H and C-D stretching and bending modes are of sufficiently high frequency that only the zero point energy differences need be considered.
  - (iii) The ratio of C-D frequencies to C-H frequencies is 1/1.35.
  - (iv) The ratio  $\nu_H^\ddagger/\nu_D^\ddagger$  ( $= m_D^\ddagger/m_H^\ddagger$ ) equals unity.
- The resulting equation is

$$\frac{k_H}{k_D} \approx \exp \left\{ \frac{0.187}{T} \sum_i (\omega_{H_i} - \omega_{H_i}^\ddagger) \right\}$$

where  $\omega_{H_i}$  and  $\omega_{H_i}^\ddagger$  represent respectively the frequencies in wave numbers of the bending and stretching modes of the C-H bonds in the nondeuterated reactant and transition state. This equation clearly interprets the secondary isotope effect as being mainly due to the difference in zero-point energy between the normal and deuterated molecules in the reactant and transition state. If the X-C-H bending frequencies increase in going from the reactant to transition state e.g. going from  $sp^2$  to  $sp^3$  hybridization,  $k_D$  will be greater than  $k_H$  i.e. an inverse isotope effect.

Streitweiser (36) measured the secondary  $\alpha$ -effect in the acetolysis of cyclopentyl tosylate-1-d obtaining a value of  $k_H/k_D = 1.15$ . If the transition state is considered to be a carbonium ion with the positively charged carbon atom having  $sp^2$  hybridization, then the frequency change  $\omega_{H_i} - \omega_{H_i}^\ddagger = 550 \text{ cm}^{-1}$  leading to a calculated value of  $k_H/k_D = 1.38$ . To account for the discrepancy between the observed and the calculated, Streitweiser proposed that the loose C-H wagging motion is impeded by the proximity of the leaving tosylate group. A frequency change of about  $300 \text{ cm}^{-1}$  in going from reactant to transition state would be consistent with the measured effect.

Additions to double bonds result in a change of hybridization in either one or two carbon atoms from  $sp^2$  to  $sp^3$ , which should result in an inverse secondary  $\alpha$ -isotope effect. The first evidence that this is so was

provided by Denny and Tunkel (16) who compared the relative reactivity of trans-stilbene- $d_2$  and the parent trans-stilbene towards a variety of reagents in solvents of varying polarity. The average value of  $k_H/k_D$  for seven such reactions was  $0.88 \pm 0.02$ .  $k_H/k_D$  for epoxidation was 0.90. The constancy of the effect seems to bear out Streitweiser's suggestion that it is due to the increased frequency of the out-of-plane CH bending mode as the molecule leaves the planar configuration. Since it is not known in all of these reactions whether the reagent is attacking one or both ends of the double bond in the rate determining step, it is not certain whether all of the 10 - 15% acceleration should be referred to bending one or two C-D bonds out of the nodal plane.

Matsuoka and Szwarc (17) measured an inverse isotope effect of 1.09 for the addition of  $\cdot CH_3$  to styrene-1,1,2 $d_3$  in isooctane solution. This value is very much less than the value of 1.82 which would be predicted on Streitweiser's model and the authors conclude that the transition state resembles the reactant in that the C-H bonds are only slightly bent, and the new bond being formed perpendicular to the nodal plane is still long. The quantitative conclusion is doubtful since a  $\beta$ -effect in the opposite direction would be expected in this molecule due to hyperconjugative stabilization of the newly forming radical. Similar considerations might apply to the small

rate enhancement ( $k_D/k_H = 1.08$ ) observed by Takahasi and Cvetanovic (18) on the addition of hydrogen atoms to propylene- $d_6$  at 25°C.

Szwarc et al (19) also measured the secondary isotope effect for addition of both  $CF_3$  and  $CH_3$  radicals to perdeuterated ethylene and propylene, obtaining a value of about 1.08 for  $k_D/k_H$ . His conclusion, again based on the Streitweiser model, was that the trigonal hybridization is hardly disturbed in the transition state and the incipient C-C  $\sigma$ -bond is very long.

Simons and Rabinowitch (20) measured a normal isotope effect of 1.07 at 25°C and 1.09 at -30°C for addition of singlet methylene to per-deuterated cis-2-butene.

The secondary  $\alpha$ -deuterium isotope effect was measured by Seltzer (21) for the  $SCN^-$  catalyzed isomerization of maleic acid -2,3- $d_2$  over the temperature range 15 - 80°. Using the Streitweiser model, the net change in the C-H vibrational frequencies in going from the ground state has been evaluated and it appears as if the transition state lies a little more than half way between a trigonal and tetrahedral carbon atom. From the Arrhenius plot intercept a value of  $\nu_H^\ddagger/\nu_D^\ddagger = 1.00 \pm 0.05$  was calculated for the ratio of the imaginary frequencies along the reaction co-ordinate. Zavitsas and Seltzer determined the secondary  $\alpha$ -deuterium effect for the unimolecular formation of  $\cdot CH_3$  and  $\cdot CD_3$  radicals from the cumyloxy radical

$\phi - C(CH_3)(CD_3)O\cdot$  as a function of temperature (22).  $k_H/k_D$  varied from 1.17 at  $-9^\circ$  to 1.12 at  $75^\circ C$ . From the temperature dependence of the effect it was concluded that the transition state is more akin to products than to the reactant oxy radical i.e. the  $sp^2$  configuration is favoured in the transition state. A pre-exponential factor of 0.93 was found.

#### The Present Investigation

In the study of atomic reactions with alkenes and alkynes it is desirable, as a long term objective, to seek the following information in each case: (1) the type of products formed and their relative abundance, (2) the role played by the vibrationally excited products and their lifetimes, (3) the type of fragmentation or rearrangement of the hot products, (4) the existence or lack of "pressure-independent" rearrangement and fragmentation processes, (5) accurate relative rates for each series of substrates, and their temperature dependence, and (6) reasonably accurate absolute values of the rate constants.

It is the aim of the present investigation to extend the knowledge and understanding of ground state sulfur atoms within the above framework. Relative rates and Arrhenius parameters are measured for the addition



of  $S(^3P)$  atoms to alkenes, alkynes and halogenated alkenes. It is expected that sulfur atoms, like the other Group VI atoms, should exhibit distinct electrophilic behaviour in their reactions as contrasted, for example, with the electro-neutral hydrogen atoms and methyl radicals. Systematic studies of reactions of atoms and radicals with unsaturated compounds in the gas phase may contribute significantly to the understanding of the factors determining rates of attack and the dependence of activation energy and A-factor on molecular structure. The results of the present study are compared with those of the additions of other atoms and radicals and also with molecular properties such as ionization potentials, localization energies, free valences and bond orders. Thus they should contribute to a better fundamental understanding of the detailed reaction path and the intermediate complexes involved.

In order to gain further information about the nature and structure of the transition state involved in the addition of  $S(^3P)$  atoms to ethylene, the secondary deuterium isotope effect is measured for addition to ethylene-1,1- $d_2$ , cis-ethylene- $d_2$ , trans-ethylene- $d_2$  and ethylene- $d_4$ .

To determine the role played by the initially-formed "hot" products, the addition reactions of  $S(^3P)$  atoms with ethylene and propylene are studied at low pressures and the lifetimes of the vibrationally excited

products are estimated.

Relative rates and Arrhenius parameters are also measured for the abstractive reactions of  $S(^3P)$  atoms with ethylene episulfide and propylene episulfide.

## CHAPTER II

EXPERIMENTAL1) High-vacuum System

A conventional high-vacuum system, constructed of pyrex tubing and evacuated to  $10^{-6}$  torr, was used throughout the present investigation. Evacuation was achieved by means of a two-stage mercury diffusion pump backed by a Welch duoseal Model 1402 oil pump. The system, which consisted of two distillation trains (one for purification of substrates, the other for separation of products), a photolytic assembly, a gas storage system and Toepler pump-gas burette, is illustrated in Fig. 1. In order to prevent loss of products by dissolution in stopcock grease, Delmar float valves, Hoke and Springham valves were used exclusively. Four conveniently located Pirani gauge tubes (Consolidated Vacuum Corporation Catalogue No. GP-001) were used to monitor gas pressures below one torr. The Pirani vacuum gauge (Type GP-140) was calibrated by means of a McLeod gauge. The G.L.C. inlet system was connected directly to both the gas burette and the distillation train, thus enabling the condensable products to by-pass the Toepler pump and gas burette.

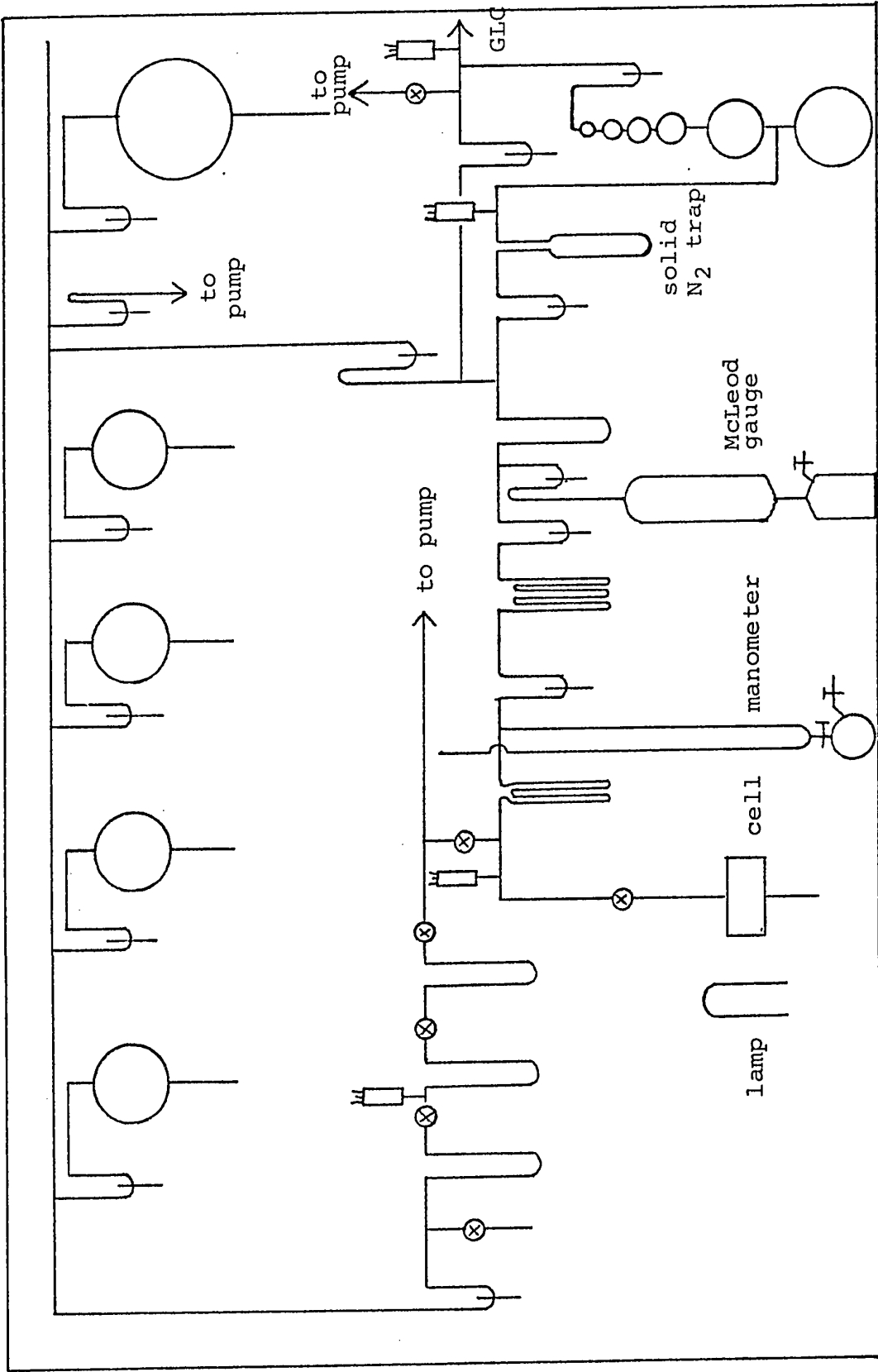


Figure 1: High-Vacuum System

## 2) Photolytic Assembly

The Hg-photosensitization runs were carried out in a circulating system (Fig. 2). The quartz reaction cell which was 60 mm. in length and 50 mm. in diameter was sealed to the rest of the system with quartz-to-pyrex graded seals. The circulating pump consisted of stainless steel rotor blades mounted on a central shaft set in Rulon bearings. A cylindrical magnet mounted at right-angles to the shaft was driven externally by a magnetic motor. The mercury reservoir was heated to boiling from time to time to remove the surface film of HgS.

For the direct photolysis runs a static system was used, the reaction vessel being a quartz cell 100 mm. in length and 50 mm. in diameter which was connected to a Hoke valve via a quartz-to-pyrex graded seal as shown in Fig. 1. For the temperature studies the same quartz cell was placed in a hollowed-out cylindrical aluminum block furnace measuring 28 cm. in length, 12 cm. in external diameter and 5½ cm. in internal diameter. The two open ends of the furnace were covered with quartz plates to prevent cooling of the cell-face by air currents. Surrounding the aluminum block was a thick covering of glass wool insulating material. The furnace was heated by means of two 300 watt chromalox pencil heaters, 20 cm. in length, inserted axially into the block. Temperatures were measured with a mercury thermometer which was calibrated

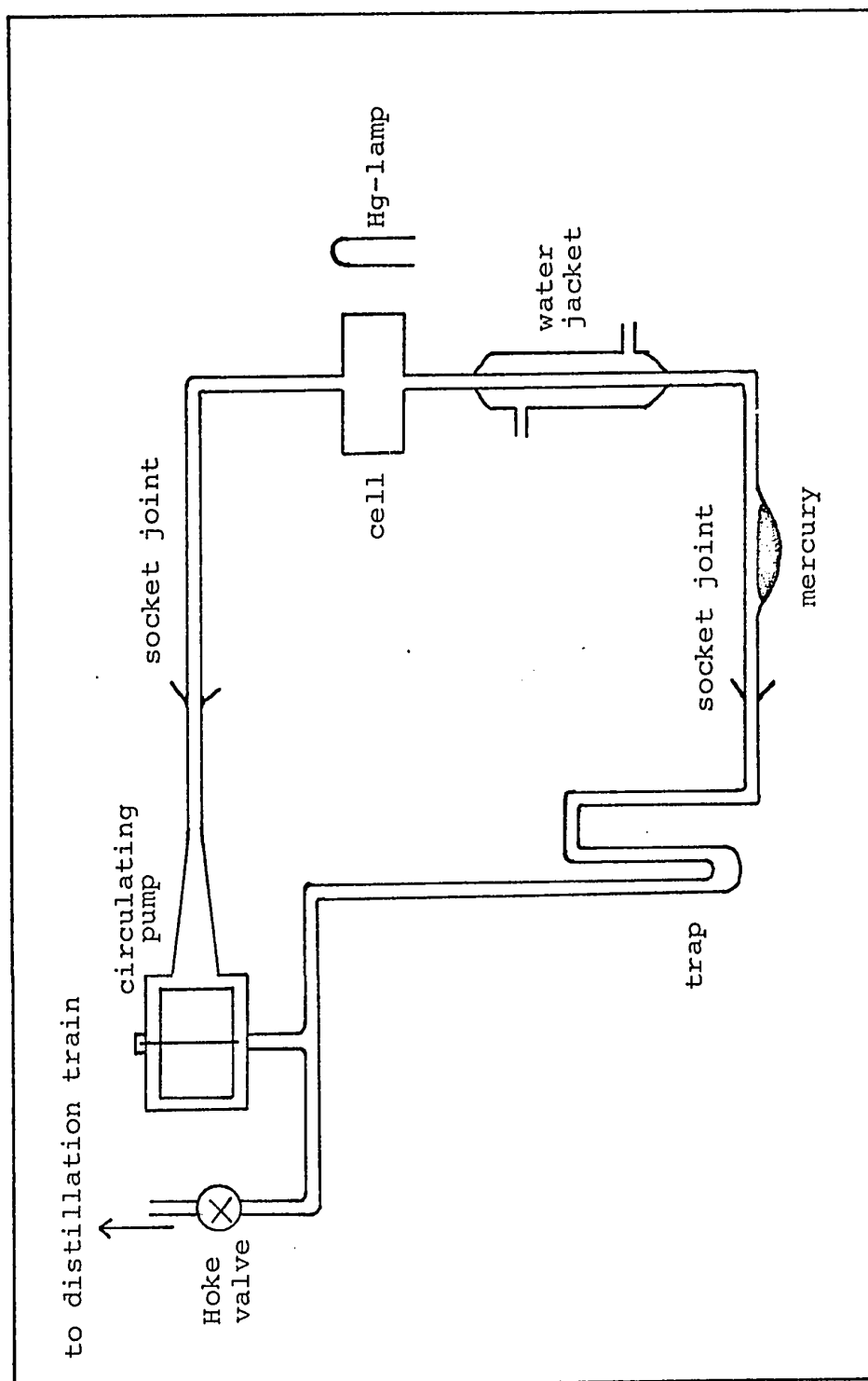


Figure 2: Mercury-photosensitization Assembly

against an iron-constantin thermocouple.

The radiation sources were a Hanovia medium pressure mercury arc (Model 30620) and an Osram cadmium spectral lamp for the direct photolysis runs, while a mercury resonance lamp was used for the mercury sensitization. Three vycor 7910 filters, (2 mm. in thickness) provided a cut-off for the mercury lamps below  $2290\text{\AA}$  so that the effective radiation for the medium pressure mercury arc in the photolysis of COS was limited to  $2290\text{\AA}$ - $2550\text{\AA}$  with the most intense region centered around  $2490\text{\AA}$  (56). The effective emission of the mercury and cadmium resonance lamps were the broadened resonance lines centred at  $2537\text{\AA}$  and  $2288\text{\AA}$  respectively.

Due to fluctuations in the intensity output of the lamps and sulfur deposition on the cell-face along with changes in the COS absorbtivity with temperature, the amount of conversion was measured by the yield of CO rather than by the actual exposure time.

### 3) Analytical System

Gas-liquid chromatography was used for quantitative analysis of the stable products and also for the purification of some of the substrate materials. The G.L.C. unit is illustrated in Fig. 3. The Gow-Mac hot wire detector Model TRIIB was powered by a Gow-Mac power supply Model 9999-C. The signals, produced by cooling of

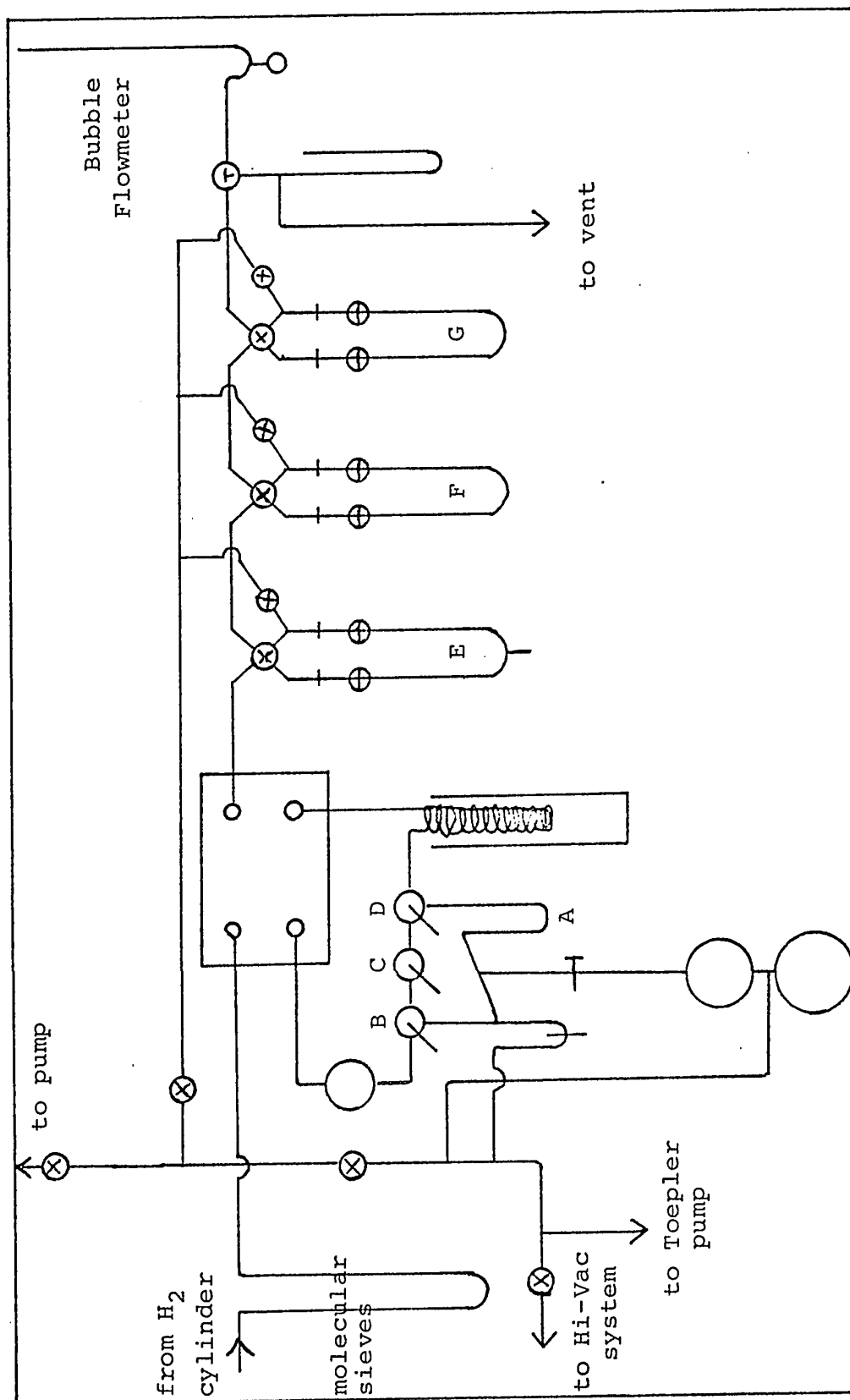


Figure 3: G.L.C. Unit



the hot filament by the separated components of the injected sample, were fed into a Sargent Model S-72180 recorder which was operated at a chart speed of one inch per minute. The filament current was kept constant at 250 mA while the detector chamber was thermostated at 200°F. Hydrogen (Canadian Liquid Air Ltd.), which was used as carrier gas, was dried by passage through a column of Molecular Sieves 13X. Its flow rate was measured on an open-end oil manometer which was calibrated against a bubble flowmeter. The spiral pyrex column (6 mm. in diameter) used for separating the products was enclosed in an insulated metal heating jacket.

The technique for analyzing a mixture of products will now be briefly described by referring to Fig. 3.

A typical condensible sample was distilled through the open float valve into the sample loop A where it was frozen at -196°C. Non-condensable gases were pumped into the sample loop via the Toepler pump. After raising the mercury in the float valve and Toepler pump the loop was filled with carrier gas by rapidly opening and closing the cam-operated Hoke valve B. The sample was then allowed to warm up by surrounding the sample with a water bath at 50°C, following which valves B and D were opened and C closed thus changing the carrier gas flow from BCD to BAD and sweeping the gaseous sample onto the column. Individual products could be trapped quantitatively by turning the four-way stopcocks to direct the flow through

the detachable traps E, F and G which were immersed in liquid nitrogen at  $-196^{\circ}\text{C}$ , as soon as the recorder pen indicated the elution of a specific product. The traps, following evacuation of the hydrogen, could then be removed for further analysis. In the case of substrate purification the pure compound was frozen down in the cold finger in Trap E and then transferred to the reaction system.

The column packings, lengths, operating conditions and retention times are given in Table II. The peak areas recorded on the chart paper were measured with an Ott Planimeter. Each compound was calibrated for detector response by measuring out samples in the gas burette and plotting the number of micro-moles against the corresponding peak areas recorded. For samples from 0.5 - 5.0  $\mu\text{moles}$ , in which range the products occurred, the relationship was linear.

#### 4) Operating Procedures

All experiments were carried out in the gas phase. Gas pressures were measured on a mercury manometer while they occupied the reaction cell, coil trap and manometer arm. After the measurement, which was carried out visually or, in the case of substrate pressures below 30 torr, with the aid of a cathetometer (Griffin and

TABLE II

G.L.C. OPERATING CONDITIONS AND ELUTION TIMES FOR EPISULFIDES

Episulfide	Column <sup>a</sup>	Column Temperature (°C)	Retention Time (mins)
Ethylene	I	40	9.4
Propylene	I	40	15.6
Isobutene	I	60	11.0
Trimethylethylene	I	60	21.1
Tetramethylethylene	II	70	5.6
Cyclopentene	II	70	12.4
Trans-1,2-difluoroethylene	I	40	5.3
Cis-1,2-difluoroethylene	I	40	25.4
Vinyl chloride	I	60	25.8
2-Trifluoromethyl-propene	I	40	12.3
2-Fluoropropene	I	40	12.6
3,3-4,4-Pentafluoro-butene-1	I	40	10.1

TABLE II (continued)

Episulfide	Column <sup>a</sup>	Column Temperature (°C)	Retention Time (mins)
3,3,3-trifluoro-propene	I	40	10.6

<sup>a</sup>

Column I: 8 ft. tricresyl-phosphate (10%) on Diatoport W.A.W. 60 - 80 mesh.

Column II: 2½ ft. tricresyl-phosphate (10%) on Diatoport W.A.W. 60 - 80 mesh.

<sup>b</sup>. The carrier gas flow in each case was 85 cc/min. hydrogen.

George Ltd., No. 3416) the Hoke valve connected to the cell was closed leaving the measured pressure of gas in the cell. The cell was then evacuated and each component of the reaction mixture was measured in the same way, following which the whole mixture was then distilled back into the cell through the coil trap (Fig. 1), which was in a slush bath at  $-23^{\circ}\text{C}$  whenever it was desired to keep mercury from the cell. The reactants, which were usually at a pressure of over 1,000 torr, were allowed to equilibrate for at least a few hours and if possible overnight. The lamp was operated for about an hour before irradiation. Periodically, to remove deposited sulfur, the cell-face was flamed with the oxygen torch while the cell was filled with air. From time to time, more frequently with the Hg-photosensitization runs, the cell was cut off, rinsed with dilute HF and baked at  $200^{\circ}\text{C}$ .

After irradiation the cell contents were frozen in the cold finger and the non-condensable gas, carbon monoxide, was transferred through a series of spiral traps at  $-196^{\circ}\text{C}$  to the gas burette via the Toepler pump. The complete mixture was warmed and frozen from trap to trap to ensure removal of all of the CO. Whenever ethylene was present the CO was passed through a solid nitrogen trap ( $-212^{\circ}\text{C}$ ) which retained the ethylene. All the condensibles were then frozen over the large surface volume in the cold finger A in order to facilitate

distillation of the solid  $\text{CO}_2$  by providing thermal contact with the walls. From this cold finger the reactants were then distilled at appropriate low temperatures, as indicated in Table III, through the triple vertical spiral trap B and the double spiral C at the same low temperatures and back into the cell cold finger for further photolysis. The products which were retained in the traps A, B and C were then thawed and frozen into the G.L.C. sampler for analysis.

#### 5) Materials

The materials used, along with their source and method of purification, are given in Table IV. All compounds used in the gas phase were degassed at  $-196^\circ\text{C}$ .

#### 6) Further Analysis

Samples, separated and collected on the G.L.C. unit, were subjected to mass spectrometric analysis on Associated Electrical Industries Model MS2 and MS9 instruments. Mixtures of deuterated and non-deuterated ethyleneepisulfide were analyzed quantitatively on an Associated Electronics MS10 mass spectrometer. Unstable short-lived products, whose formation had not previously been known, were detected on a flash photolysis - kinetic mass spectrometry unit. This instrument has been described elsewhere (57).

TABLE III  
DISTILLATION TEMPERATURES FOR REACTANTS FROM CORRESPONDING EPISULFIDES

Compound	Temperature (°C)	Slush-bath
Ethylenes	-160	Isopentane
Carbonyl sulfide	-139	Ethyl-chloride
Carbon dioxide	-139	Ethyl-chloride
Propylene	-139	Ethyl-chloride
Acetylene	-139	Ethyl-chloride
Methyl-acetylene	-139	Ethyl-chloride
Tetrafluoro-ethylene	-139	Ethyl-chloride
3-trifluoro-propene	-130	n-pentane
2-fluoro-propene	-130	n-pentane
trans-1,2-difluoro-ethylene	-130	n-pentane
1,3-butadiene	-117	2-chloro-propane
Vinyl-trifluoro-silane	-117	2-chloro-propane

TABLE III (continued)

Compound	Temperature (°C)	Slush-bath
cis-1,2-difluoro-ethylene	-117	2-chloro-propane
Vinyl-chloride	-117	2-chloropropane
Isobutene	-107	2,2,4-trimethylpentane
Trimethyl-ethylene	-107	2,2,4-trimethylpentane
2-trifluoromethyl-propene	-107	2,2,4-trimethylpentane
3,3-4,4,4-pentafluoro-butene-1	-107	2,2,4-trimethylpentane
Cyclopentene	-87	Trichloroethylene
Dimethyl acetylene	-87	Trichloroethylene
Tetramethyl-ethylene	-78	Dry Ice/Trichloroethylene
Trans-1,2-dichloro-ethylene	-78	Dry Ice/Trichloroethylene



TABLE IV

## MATERIALS USED

Material	Source	Grade and Purity	Purification
Ethylene	Phillips	Research grade >99.5%	distilled at -160°C
Propylene	Phillips	Research Grade >99.5%	distilled at -130°C
Isobutene	Phillips	Research Grade >99.5%	distilled at -107°C
Trimethyl-Ethylene	Matheson, Coleman and Bell	Reagent	distilled at -78°C
Tetramethyl-Ethylene	A.P.I.	A.P.I. certified	None
Cyclopentene	A.P.I.	A.P.I. certified	None
1,3-Butadiene	Phillips	Research Grade >99.5%	distilled at -107°C
Trans-1,2-difluoro- ethylene	Peninsular Chem. Research	Technical (mixture of cis and trans)	g.c. 16 ft. di- isodecylphthalate on 60/80 ultrasorb AW at 0°C

TABLE IV (continued)

Material	Source	Grade and Purity	Purification
Cis-1,2-difluoro-ethylene	Peninsular Chem. Research	Technical (mixture of cis and trans)	g.c. 16 ft. diisodecylphthalate on 60/80 ultrasorb AW at 0°C
Trans-1,2-dichloro-ethylene	Matheson, Coleman and Bell	Reagent (90%)	g.c. 20 ft. silicone gum rubber
Tetrafluoro-ethylene	Peninsular	Inhibited	distilled at -130°C
Vinyl Chloride	Matheson	C.P. Grade (99%)	distilled at -117°C
2-trifluoromethyl-propene	Peninsular	Reagent	distilled at -107°C g.c. 40 ft. dimethyl-sulfolane (10%) at 0°C
3,3,3-trifluoro-propene	Pierce Chemical	Reagent (~98%)	distilled at -117°C + g.c. 15 ft. med. activity silica gel @ 45°C
3,3-4,4,4-pentafluoro-butene-1	Peninsular	Technical (~50%)	distilled at -107°C g.c. 40 ft. dimethyl-sulfolane at 0°C
Vinyl-trifluoro-silane	Peninsular	Technical	distilled at -117°C g.c. 40 ft. dimethyl-sulfolane at 0°C

TABLE IV (continued)

Material	Source	Grade and Purity	Purification
2-fluoro-propene	Columbia	Technical	distilled at -130°C g.c. 40 ft. dimethyl- sulfolane at 0°C
Acetylene	Matheson	contained acetone	distilled at -139°C
Methyl acetylene	Matheson	Technical (97%)	distilled at -117°C
Dimethyl acetylene	Farchan Res. Lab.	Reagent (99%)	distilled at -78°C
Ethylene-d <sub>4</sub>	Merck, Sharp and Dohme	Reagent	distilled at -160°C
cis-ethylene-d <sub>2</sub>	Merck, Sharp and Dohme	Reagent	distilled at -160°C
trans-ethylene-d <sub>2</sub>	Merck, Sharp and Dohme	Reagent	distilled at -160°C
1,1-ethylene-d <sub>2</sub>	Merck, Sharp and Dohme	Reagent	distilled at -160°C
Ethylene-episulfide	Prepared (3)	small trace of water	degassed at -139° distilled at -78°C
KSCN	Fisher	Reagent (99.99%)	None
Ethylene carbonate	Eastman Organic	Reagent	None

TABLE IV (continued)

Material	Source	Grade and Purity	Purification
Carbonyl sulfide	Matheson	contained H <sub>2</sub> S	Bubbled through sat. solution of NaOH, dried, and distilled at -130°C. Degassed at -160°C
Carbon dioxide	Airco	High Purity	None

## CHAPTER III

RELATIVE RATES AND ARRHENIUS PARAMETERS FOR THE  
ADDITION OF S(<sup>3</sup>P) ATOMS TO OLEFINIC AND ACETYLENIC BONDS

Rate constants, Arrhenius pre-exponential factors and activation energies were measured for the addition of S(<sup>3</sup>P) atoms to a series of alkenes, alkynes and substituted alkenes relative to an arbitrary rate constant and pre-exponential factor of 1.0 for the addition to ethylene.

A) Relative Rates

The relative rate of addition for a given substrate was measured by competition between it and another substrate (whose relative addition rate was known) for S(<sup>3</sup>P) atoms produced in situ. The relative yields of the episulfides, which are the only reaction products in this system could then be taken as a measure of the relative reactivity of these substrates towards ground state sulfur atoms. Substrate pairs having similar vapour pressures were chosen so that the episulfides could be recovered by low temperature distillation of the reactants. Wherever feasible, the reactant concentrations were fixed such that equimolar amounts of episulfides were produced. In some cases a relative rate was cross-checked by competition with a different reactant partner whose relative rate had been

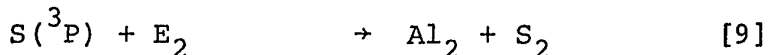
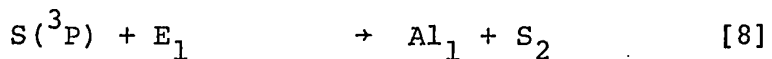
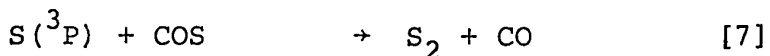
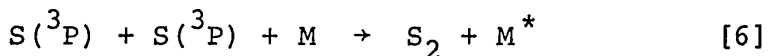
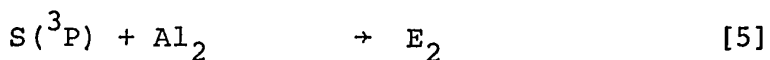
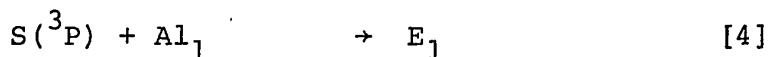
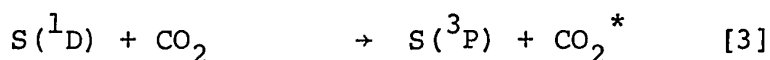
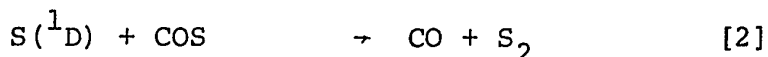
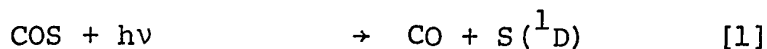
previously measured. Invariably, both measured rates were identical within experimental error.

In those cases where one of the two competing substrates produced an unstable adduct with  $S(^3P)$  atoms its relative rate was determined by gradually increasing the relative concentration of that substrate and measuring the consequent decrease in yield of the stable episulfide.

The  $S(^3P)$  atoms were produced by two methods:

(i) electronic deactivation of  $S(^1D)$  atoms produced by photolysis of COS and (ii) Hg-photosensitization of COS.

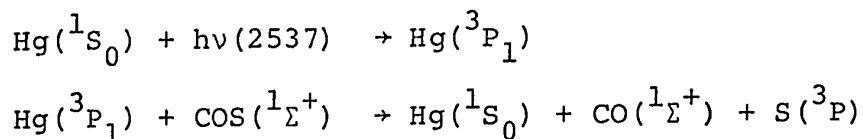
For the photolysis system the following scheme can be written:



where  $\text{Al}_1$  and  $\text{Al}_2$  are the reacting substrates (alkene or alkyne) and  $E_1$  and  $E_2$  the respective episulfides.

It has been demonstrated (6) that when the  $\text{CO}_2$  to ethylene ratio is sufficiently large in the system no mercaptan is formed; thus, all  $\text{S}(^1\text{D})$  atoms are deactivated to  $\text{S}(^3\text{P})$  and reaction [2] is eliminated since  $\text{S}(^1\text{D})$  atoms react somewhat faster with ethylene than with COS (59). Reaction [6] is of very minor importance and can be neglected in low-intensity photolysis. Since the yield of episulfide relative to the CO produced is unchanged by a drastic increase in the COS to ethylene ratio, in the presence of a large excess of  $\text{CO}_2$ , it is clear that reaction [7] is very slow. The secondary reactions [8] and [9] can be essentially eliminated by using fairly high reactant concentrations and low conversions, since under these conditions the rate of production of episulfides remains constant. The scheme therefore reduces to reactions [1], [3], [4] and [5].

In the Hg-photosensitization system, the first three reactions in the above scheme are replaced by the following two:



The ratio of the rate constants for the addition reactions can then be calculated from the simple relation

$$\frac{k_4}{k_5} = \frac{R(E_1)}{R(E_2)} \times \frac{[A]_2}{[A]_1} \quad \text{I}$$

where  $R(E_1)$  and  $R(E_2)$  are the rates of formation of the episulfides.

In the case where  $Al_1$  forms an unstable sulfide, its relative addition rate is obtained from the relation

$$\frac{k_4}{k_5} = \frac{A_0 - A}{A} \times \frac{[Al_2]}{[Al_1]} \quad \text{II}$$

where  $A_0$  = yield of  $E_2$  per  $\mu\text{mole CO}$  in the absence of  $Al_1$ , assuming complete scavenging of  $S(^3P)$  atoms by  $Al_2$  and  $A$  = yield of  $E_2$  per  $\mu\text{mole CO}$  with  $Al_1$  present in the system. (Chromatographic Peak Area/ $\mu\text{CO}$ )

For Equation I the yields of each episulfide were plotted against the CO yields, since the lamp intensity was not always constant, yielding two straight lines through the origin. The ratio of the slopes of these lines was equal to  $R(E_1)/R(E_2)$ . For Equation II, the concentration of  $Al_1$  was increased gradually and a plot was made of  $\frac{A_0 - A}{A}$  versus  $[Al_1]/[Al_2]$  yielding a straight line through the origin. The slope of this line, obtained by least mean squares treatment of the points, gave  $\frac{k_3}{k_4}$ . With some reactants, at longer conversions, the plot of episulfide against CO yields gave a curve with decreasing slope indicating removal of episulfide by secondary reactions. Thus  $R(E_1)/R(E_2)$  was a function of CO yield (or time) and the ratio was therefore extrapolated to zero conversion.

A medium pressure mercury arc was used for all the photolysis runs. In order to decrease the possibility



of secondary photolysis of sulfides three vycor 7910 filters were employed to cut off light below about  $2200\text{\AA}$ .

The reaction products could be recovered and measured with a precision generally in the range  $\pm 10\%$ . Due to averaging of the points, the precision in the relative rate constants was somewhat better than this.

The rates of addition of  $S(^3P)$  atoms to the following compounds relative to ethylene were studied: propylene, isobutylene, trimethylethylene, tetramethylethylene, 1,3-butadiene, 2-trifluoromethyl-propene, 2-fluoropropene, 3,3-4,4,4-pentafluoro-butene-1, acetylene, methylacetylene, dimethylacetylene, vinyl-trifluorosilane and trans-1,2-dichloroethylene.

#### Ethylene - Propylene System

In this system the validity of the method was tested by varying the amount of conversion and changing the relative concentrations of the reactants.

$S(^3P)$  atoms were produced by the Hg-photosensitization of COS. Relative rates were measured using three different gas mixtures:

(a) Mixture consisted of 300 torr COS, 30.0 torr  $C_2H_4$  and 20.0 torr  $C_3H_6$ . Product yields are given in Table V as a function of exposure time. Episulfides are plotted as a function of CO yield in Fig. 4a, where it is seen that propylene episulfide is being consumed in a secondary

TABLE V  
ADDITION OF S(<sup>3</sup>P) ATOMS TO ETHYLENE AND PROPYLENE<sup>a</sup>

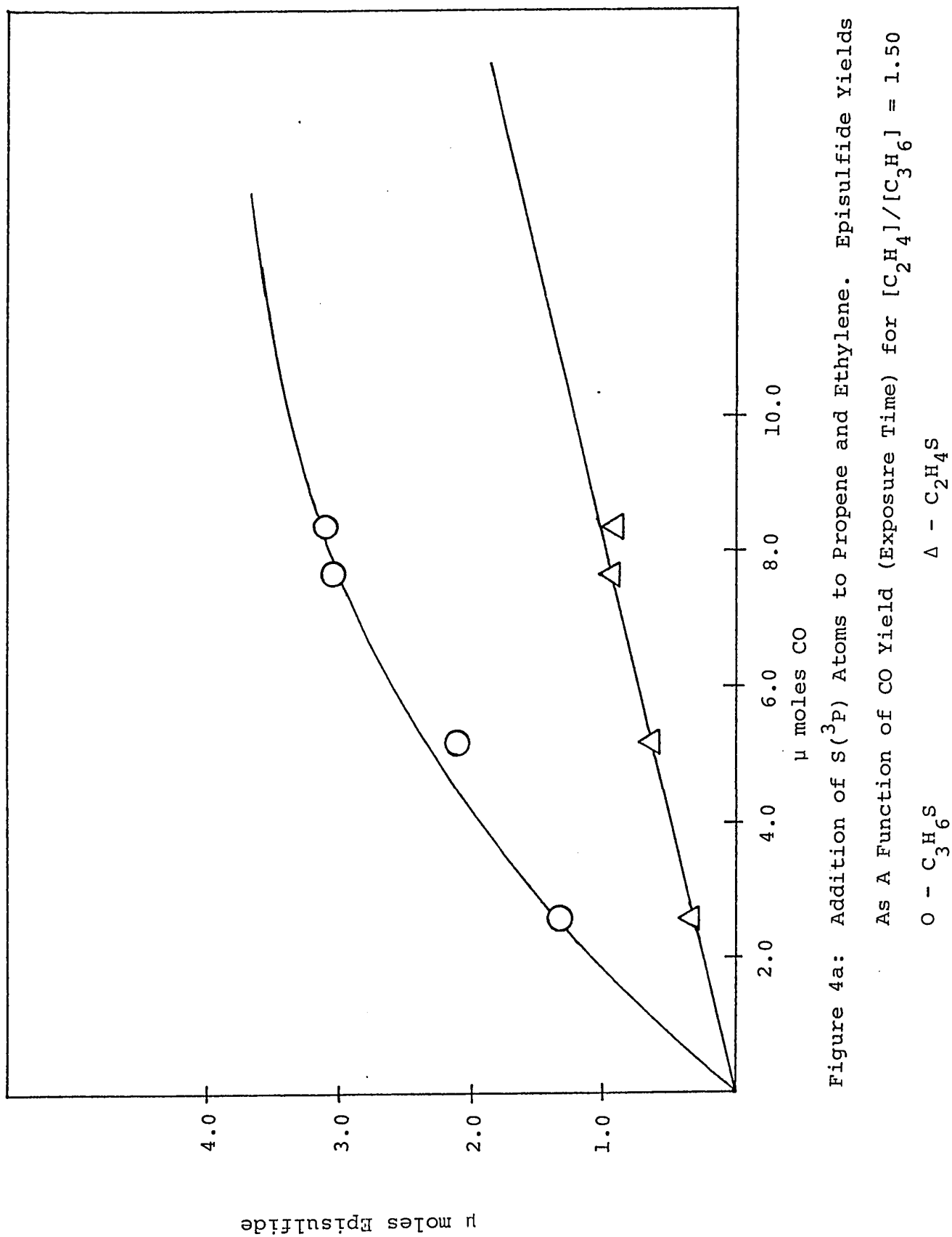
PRODUCT FORMATION AS A FUNCTION OF EXPOSURE TIME FOR $[C_2H_4]/[C_3H_6] = 1.50$					
Exposure Time (minutes)	Yields, $\mu$ moles		$\frac{C_3H_6S}{C_2H_4S}$	$\frac{k_{C_3H_6}}{k_{C_2H_4}}$	% yield d
	CO	$\frac{C_2H_4S^b}{C_3H_6S^b}$			
31	2.6	0.32	1.32	4.13	63
60	5.2	0.62	2.10	3.39	52
93	7.7	0.92	3.04	3.30	51
90	8.4	0.90	3.11	3.46	48

a.  $P(COS) = 300$ ,  $P(C_2H_4) = 30.0$ ,  $P(C_3H_6) = 20.0$  torr

b. Episulfides

c.  $\frac{C_3H_6S}{C_2H_4S} \times 1.50$

d.  $\frac{\Sigma(\text{episulfides})}{CO} \times 100$



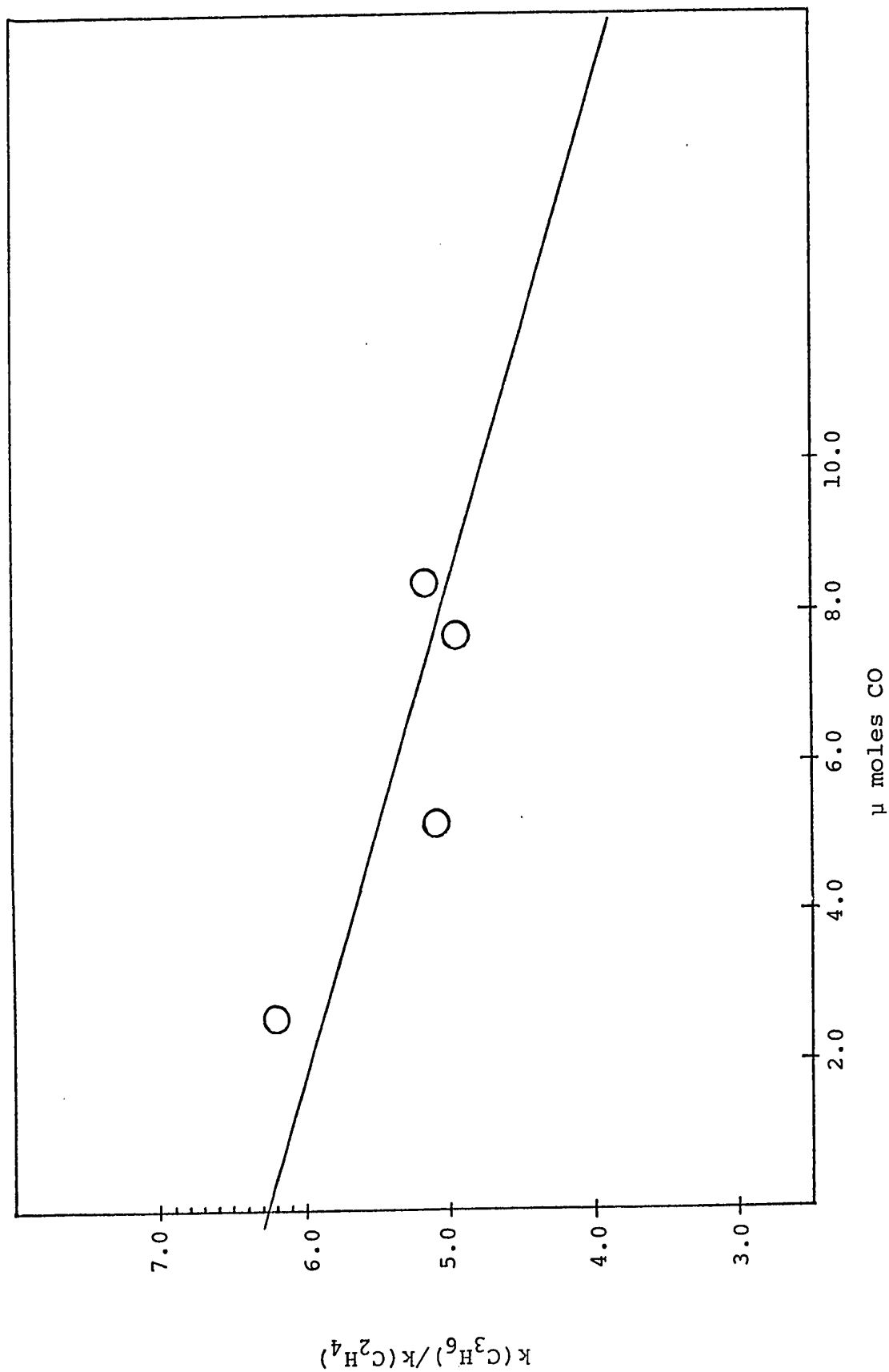


Figure 4b: Addition of  $\text{s}(\text{}^3\text{P})$  Atoms to Propene and Ethylene. Relative Rate As A  
Function of CO yield for  $[\text{C}_2\text{H}_4]/[\text{C}_3\text{H}_6] = 1.50$ .

TABLE VI  
 ADDITION OF  $S(^3P)$  ATOMS TO ETHYLENE AND PROPYLENE<sup>a</sup>  
 PRODUCT FORMATION AS A FUNCTION OF EXPOSURE TIME FOR  $[C_2H_4]/[C_3H_6] = 2.98$

Exposure Time (minutes)	Yields, $\mu$ moles		$\frac{C_3H_6S}{C_2H_4S}$	$\frac{k_{C_3H_6}}{k_{C_2H_4}}$	% Yield
	CO	$C_2H_4S^b$			
15	1.7	0.29	0.66	2.28	56
30	3.5	0.44	1.20	2.73	47
60	6.4	0.95	2.00	2.11	46
90	9.1	1.26	2.65	2.10	43
120	10.3	1.65	2.95	1.79	45

a.  $P(COS) = 640$ ,  $P(C_2H_4) = 37.5$ ,  $P(C_3H_6) = 12.6$  torr

b. Episulfides

c.  $\frac{C_3H_6S}{C_2H_4S} \times 2.98$

d.  $\frac{\Sigma(\text{episulfides})}{CO} \times 100$

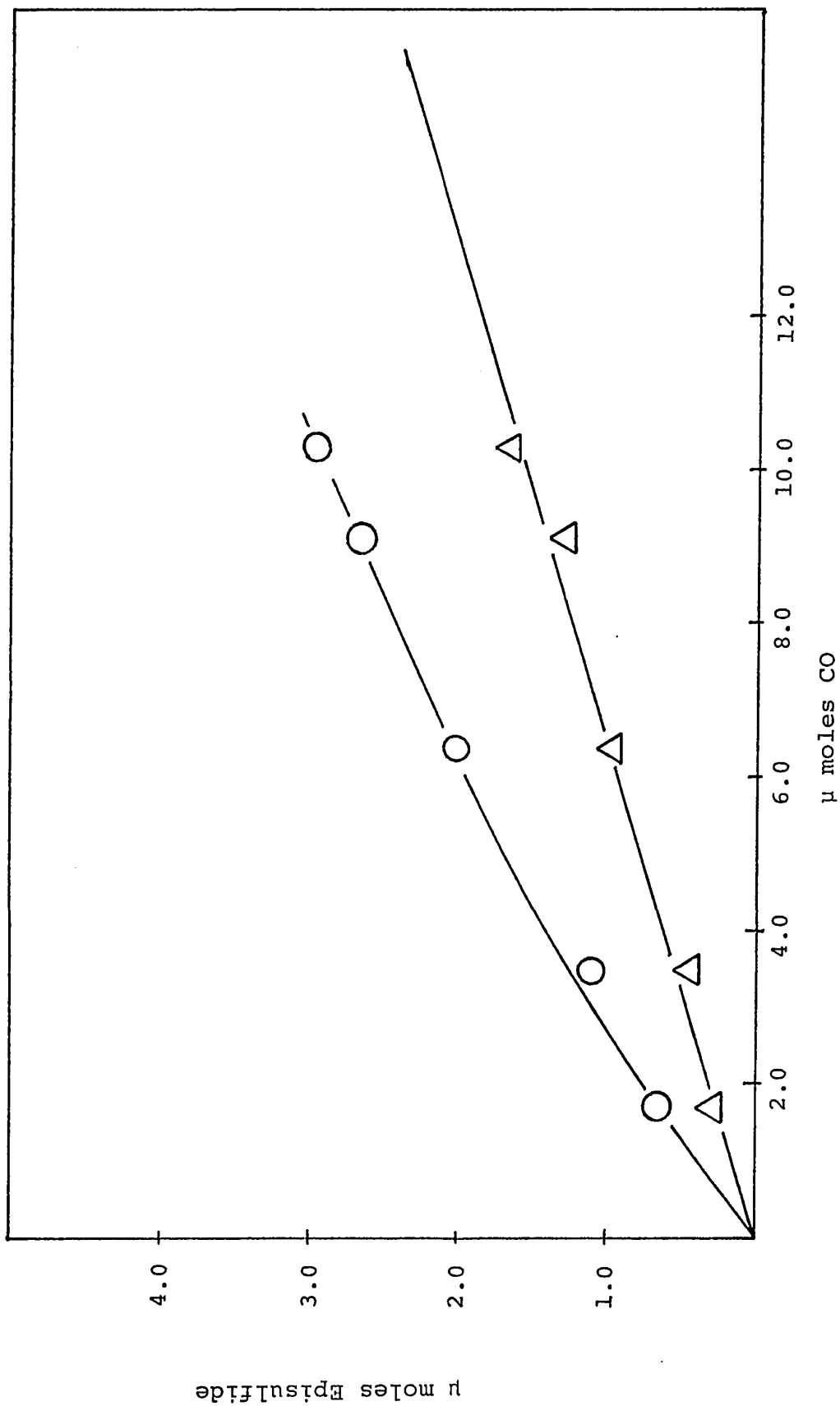


Figure 5a: Addition of  $S(^3P)$  Atoms to Propene and Ethylene. Episulfide Yields

As A Function of CO Yield for  $[C_2H_4]/[C_3H_6] = 2.98$ .

O -  $C_3H_6S$

$\Delta$  -  $C_2H_4S$

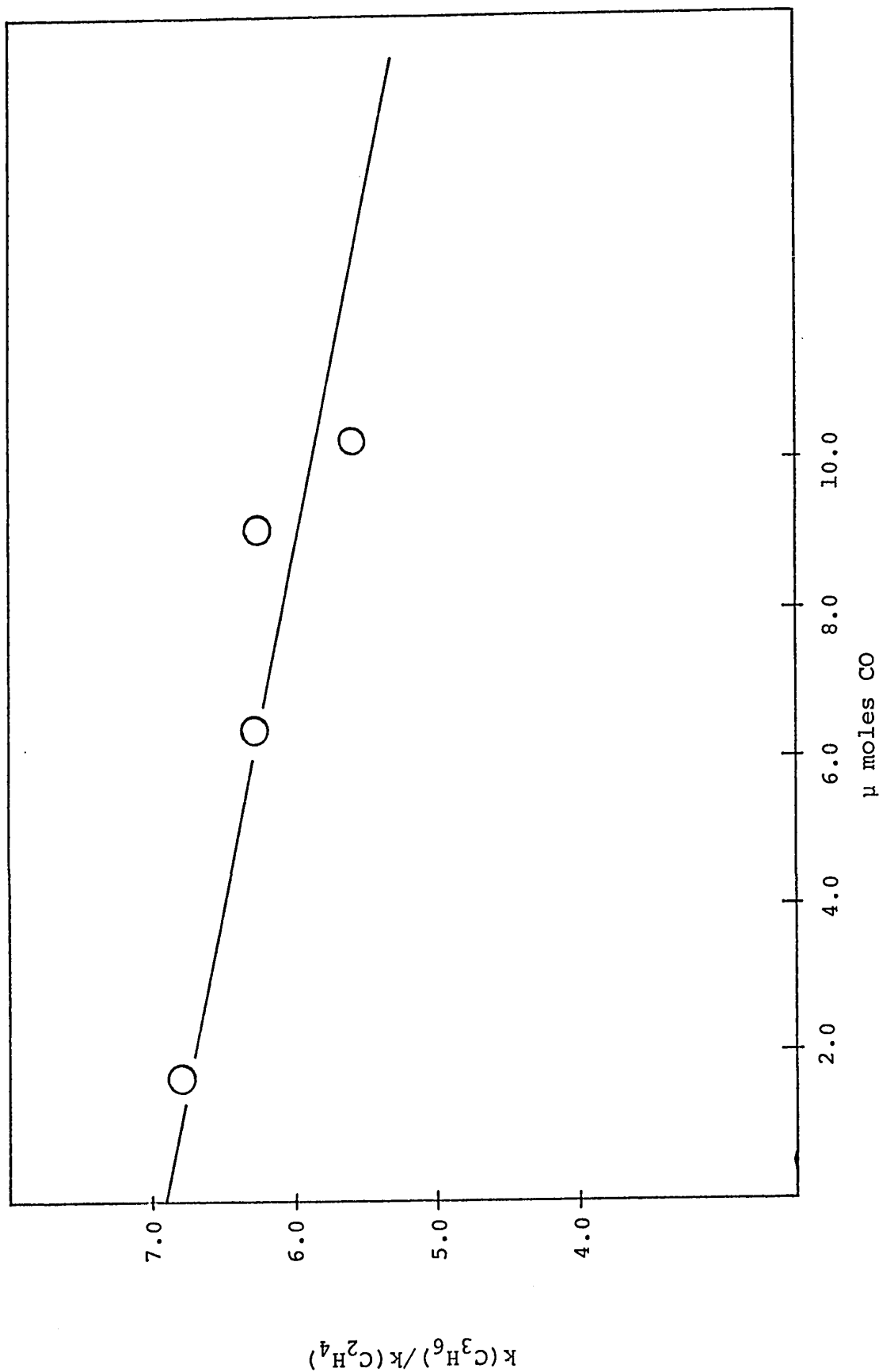


Figure 5b: Addition of  $S(^3P)$  Atoms to Propene and Ethylene. Relative Rate As A  
Function of CO Yield for  $[C_2H_4]/[C_3H_6] = 2.98$

TABLE VII  
 ADDITION OF  $S(^3P)$  ATOMS TO ETHYLENE AND PROPYLENE<sup>a</sup>  
 PRODUCT FORMATION AS A FUNCTION OF EXPOSURE TIME FOR  $[C_2H_4]/[C_3H_6] = 6.06$

Exposure Time (minutes)	Yields, $\mu$ moles		$\frac{C_3H_6S}{C_2H_4S}$	$\frac{k_{C_3H_6}}{k_{C_2H_4}}$ <sup>c</sup>	% Yield <sup>d</sup>
	CO	$\frac{C_2H_4S^b}{C_3H_6S^b}$			
15	1.7	0.47	1.00	6.06	55
60	6.0	1.45	0.91	5.51	46
90	8.2	1.86	0.84	5.09	42
150	12.3	2.39	0.90	5.45	37
290	19.6	3.61	0.78	4.73	33

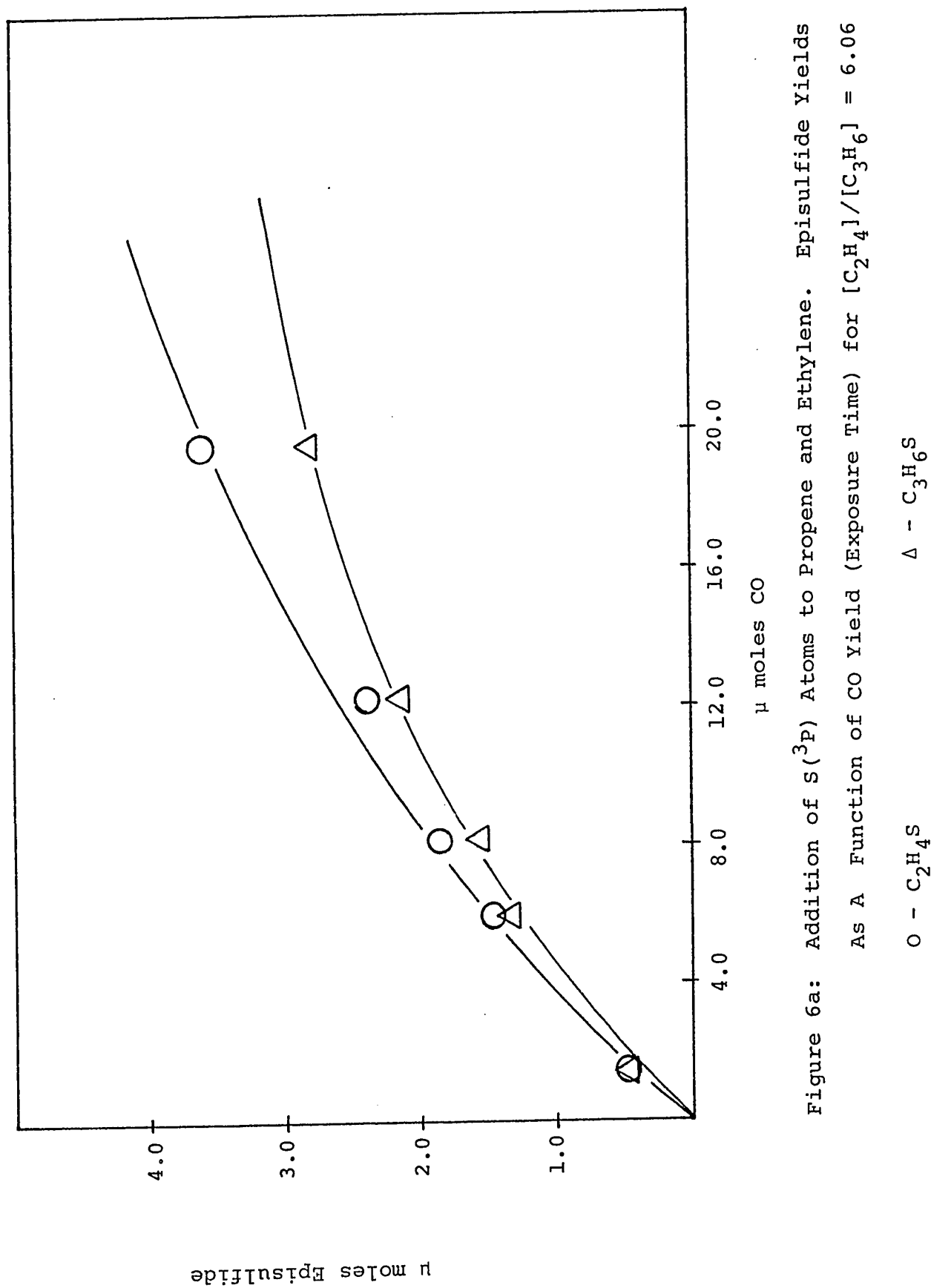
a.  $P(COS) = 582$ ,  $P(C_2H_4) = 43.0$ ,  $P(C_3H_6) = 7.1$  torr

b. Episulfides

c.  $\frac{C_3H_6S}{C_2H_4S} \times 6.06$

d.  $\frac{\Sigma(\text{episulfides})}{CO} \times 100$





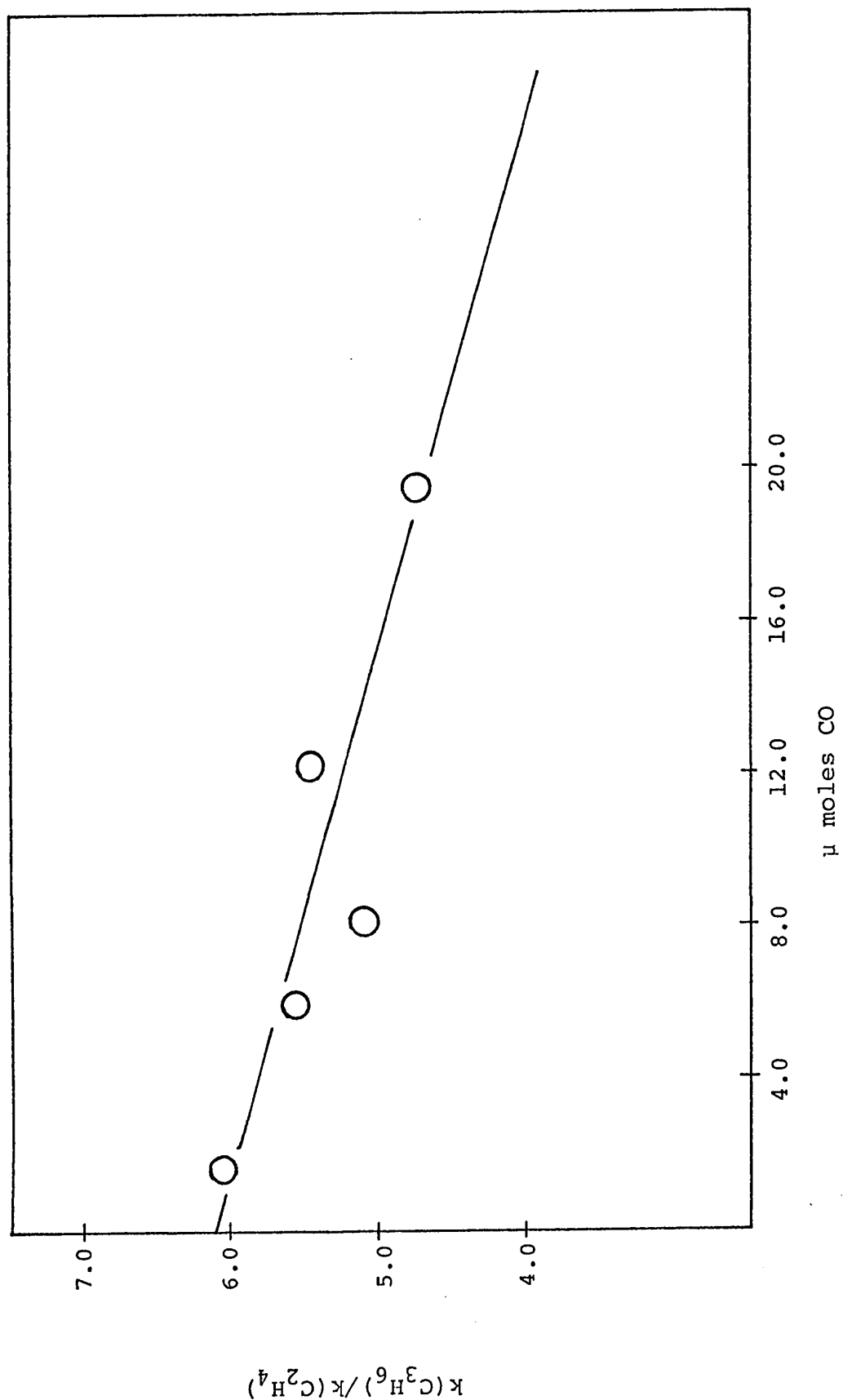


Figure 6b: Addition of  $\text{S}(\text{}^3\text{P})$  Atoms to Propene and Ethylene. Relative Rate As A

Function of CO Yield For  $[\text{C}_2\text{H}_4]/[\text{C}_3\text{H}_6] = 6.06$

reaction, while the decrease in ethylene episulfide is hardly noticeable. The % yield in terms of CO decreases with exposure time so that the propylene episulfide being consumed is not yielding ethylene episulfide. In Fig. 4b the relative rate is extrapolated to zero conversion and a least mean squares treatment of the line gives

$k_{\text{C}_3\text{H}_6}/k_{\text{C}_2\text{H}_4} = 6.43$ . While this line is theoretically not a straight line but one whose curvature will depend on the relative reactant concentrations, the data are not sufficiently accurate to draw the curve and a least mean squares line will be a reasonably good approximation and will allow for consistency in the three mixtures.

(b) The mixture consisted of 640 torr COS, 37.5 torr  $\text{C}_2\text{H}_4$  and 12.6 torr  $\text{C}_3\text{H}_6$  so that the ratio of ethylene to propylene was now approximately 3.0 compared with 1.5 in mixture (a). Product yields are given in Table VI. Again the % yield of episulfide decreases with exposure time with the propylene episulfide being consumed more rapidly than the ethylene episulfide as shown in Fig. 5a. The extrapolation of the relative rate to zero CO yield, shown in Fig. 5b leads to  $k_{\text{C}_3\text{H}_6}/k_{\text{C}_4\text{H}_4} = 7.88$  with the least mean squares line having a slope approximately the same as in Fig. 4b.

(c) Here, the ratio of ethylene to propylene was increased to about 6 to 1 with the mixture consisting of 582 torr COS, 43.0 torr  $\text{C}_2\text{H}_4$  and 7.1 torr  $\text{C}_3\text{H}_6$ . Product yields are given in Table VII where again the decrease in % yield with exposure time is obvious. In this mixture the yields

of both episulfides were about the same and, as can be seen in Fig. 6a, the secondary depletion of  $C_2H_4S$  is much more pronounced than previously. The least mean squares plot of the rate constant ratio against CO yield, shown in Fig. 6b, gives an intercept for  $k_{C_3H_6}/k_{C_2H_4} = 5.98$ . The slope of the line, though much less than those from mixtures (a) and (b) is still negative indicating greater depletion of  $C_3H_6S$  than of  $C_2H_4S$ .

Taking the average of the three relative rate values above we then have  $k(S + C_3H_6)/k(S + C_2H_4) = 6.8$ .

#### Isobutene - Propylene System

As a result of the previous experiments it was decided to keep the amount of conversion as low as possible.  $S(^3P)$  atoms were produced in this system by Hg-photosensitization of COS. The mixture consisted of 605 torr COS, 71.4 torr  $C_3H_6$  and 10.4 torr  $C_4H_8$ . Product yields are shown in Table VIII and plotted in Fig. 7. At these low conversions, removal of episulfides by secondary reactions does not occur and the ratio of the episulfides is independent of the CO yield. The ratio of the slopes is 1.15 giving a value of  $k(S + C_4H_8)/k(S + C_3H_6) = 7.9$ , in good agreement with the value of 7.2 measured in the COS/ $CO_2$  photolysis system, where the ratio of propylene to isobutylene was 1.4 (60). Therefore,  $k(S + C_4H_8)/k(S + C_2H_4) = 7.9 \times 6.8 = 54$ .

TABLE VIII  
 ADDITION OF S(<sup>3</sup>P) ATOMS TO ISOBUTENE AND PROPENE<sup>a</sup>

PRODUCT FORMATION AS A FUNCTION OF EXPOSURE TIME FOR [C <sub>3</sub> H <sub>6</sub> ]/[C <sub>4</sub> H <sub>8</sub> ] = 6.86						
Exposure Time (minutes)	Yields, μmoles		$\frac{C_4H_8S}{C_3H_6S}$	$\frac{C_4H_8S}{C_3H_6S}$	$\frac{k_{C_4H_8}}{k_{C_3H_6}}$	% Yield <sup>d</sup>
	CO	C <sub>3</sub> H <sub>6</sub> S <sup>b</sup>				
15	2.31	0.76	0.86	1.13	7.75	70
30	4.30	1.36	1.63	1.20	8.23	70
15	1.50	0.56	0.63	1.13	7.75	79
25	2.46	0.78	0.92	1.18	8.09	70
10	1.32	0.33	0.37	1.12	7.68	53
6	0.62	0.18	0.21	1.16	7.96	63
35	3.30	1.13	1.23	1.09	7.48	72
35	1.56	0.43	0.52	1.21	8.30	61
20	1.91	0.66	0.75	1.14	7.82	64

a. P(COS) = 605, P(C<sub>3</sub>H<sub>6</sub>) = 71.4, P(C<sub>4</sub>H<sub>8</sub>) = 10.4 torr

b. Episulfides

c.  $\frac{C_4H_8S}{C_3H_6S} \times 6.86$

d.  $\frac{\Sigma(\text{episulfides})}{CO} \times 100$

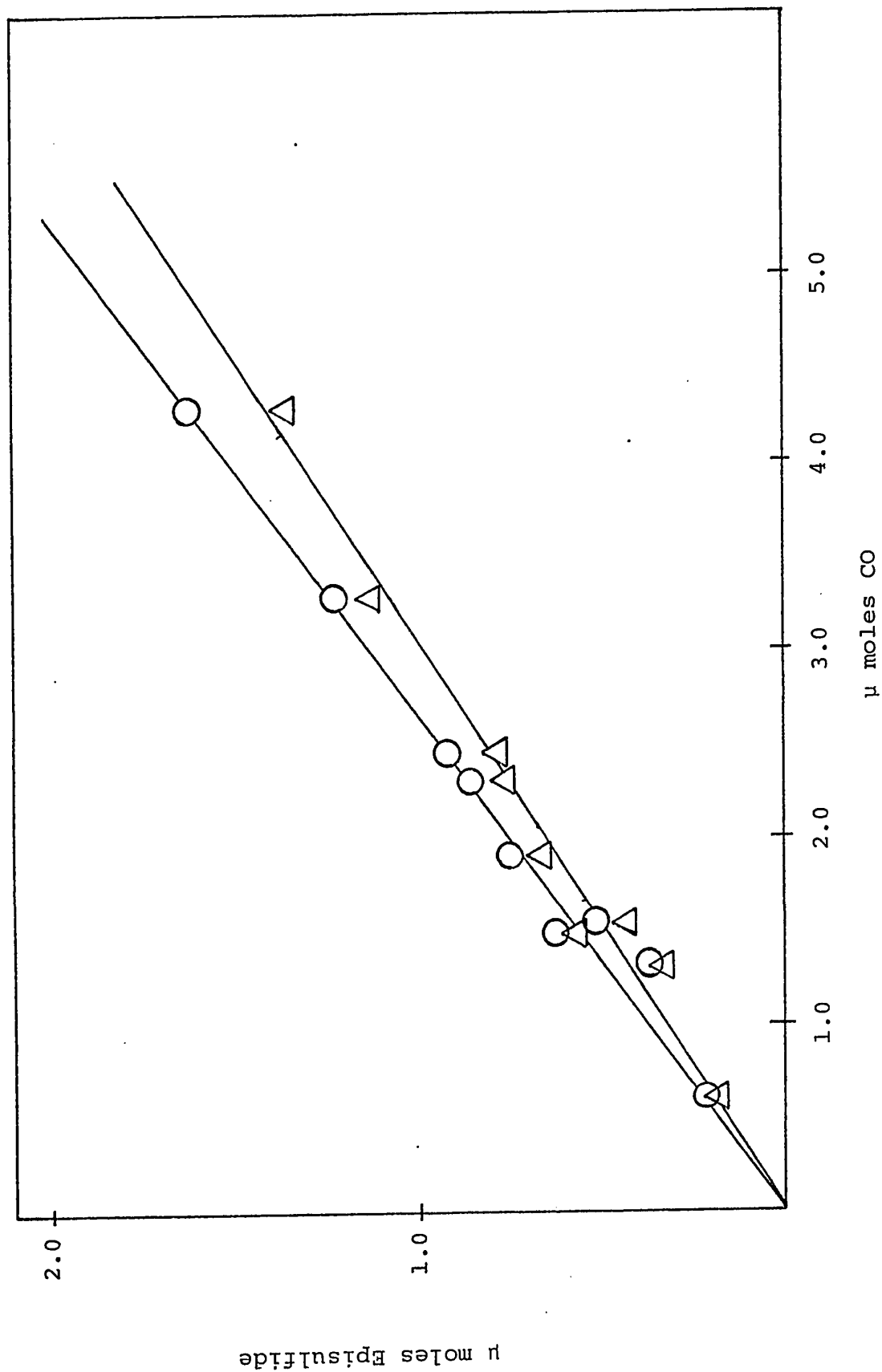


Figure 7: Addition of  $S(^3P)$  Atoms to Isobutene and Propene. Episulfide Yield  
As A Function of CO Yield.

O -  $C_4H_8S$

$\Delta$  -  $C_3H_6S$

### Trimethylethylene - Isobutylene System

Hg-photosensitization of COS was carried out in a mixture consisting of 561 torr COS, 27.0 torr  $C_4H_8$  and 11.0 torr  $C_5H_{10}$ . Product yields are given in Table IX. Conversions were kept below 3  $\mu$ moles of CO and it is seen that the % yield is roughly constant within this range. The straight line plots in Fig. 8 indicate no depletion of episulfides. It would seem likely that those olefins, having a higher reactivity with  $S(^3P)$  atoms, prevent the removal of episulfides and that the mode of episulfide depletion is, therefore, via reaction with sulfur atoms. Also the % yield is somewhat higher in this system than in the previous two indicating the possibility of some abstraction from COS by  $S(^3P)$  atoms in the presence of less reactive olefins. From the ratio of the slopes in Fig. 8,  $k_{C_5H_{10}}/k_{C_4H_8} = 1.63$ . Therefore

$$\frac{k(S + C_5H_{10})}{k(S + C_2H_4)} = 54 \times 1.63 = 88.$$

### Tetramethylethylene - Trimethylethylene System

The  $S(^3P)$  atoms were produced in this system by photolyzing COS and deactivating the  $S(^1D)$  atoms to the ground state with a large concentration of  $CO_2$ . The mixture consisted of 31.0 torr COS, 1,362 torr  $CO_2$  and 20.2 torr  $C_6H_{12}$ . It was found that at the temperature required

TABLE IX

ADDITION OF S(<sup>3</sup>P) ATOMS TO TRIMETHYLETHYLENE AND ISOBUTENE<sup>a</sup>PRODUCT FORMATION AS A FUNCTION OF EXPOSURE TIME FOR  $[C_4H_8]/[C_5H_{10}] = 2.45$ 

Exposure Time (minutes)	Yields, $\mu$ moles		$\frac{C_5H_{10}S}{C_4H_8S}$		$\frac{k_{C_5H_{10}}}{k_{C_4H_8}}$		% yield d
	CO	$C_4H_8S^b$	$C_5H_{10}S^b$				
20	1.71	0.86	0.59	0.69	1.69	85	
30	2.36	1.22	0.79	0.65	1.59	85	
15	1.37	0.72	0.45	0.63	1.54	85	
20	1.65	0.85	0.54	0.64	1.57	84	
25	1.86	0.95	0.65	0.68	1.67	86	
30	2.40	1.22	0.85	0.69	1.69	86	
35	3.00	1.51	1.00	0.66	1.62	84	

a.  $P(COS) = 561$ ,  $P(C_4H_8) = 27.0$ ,  $P(C_5H_{10}) = 11.0$  torr

b. Episulfides

c.  $\frac{C_5H_{10}S}{C_4H_8S} \times 2.45$ d.  $\frac{\Sigma(\text{episulfides})}{CO} \times 100$



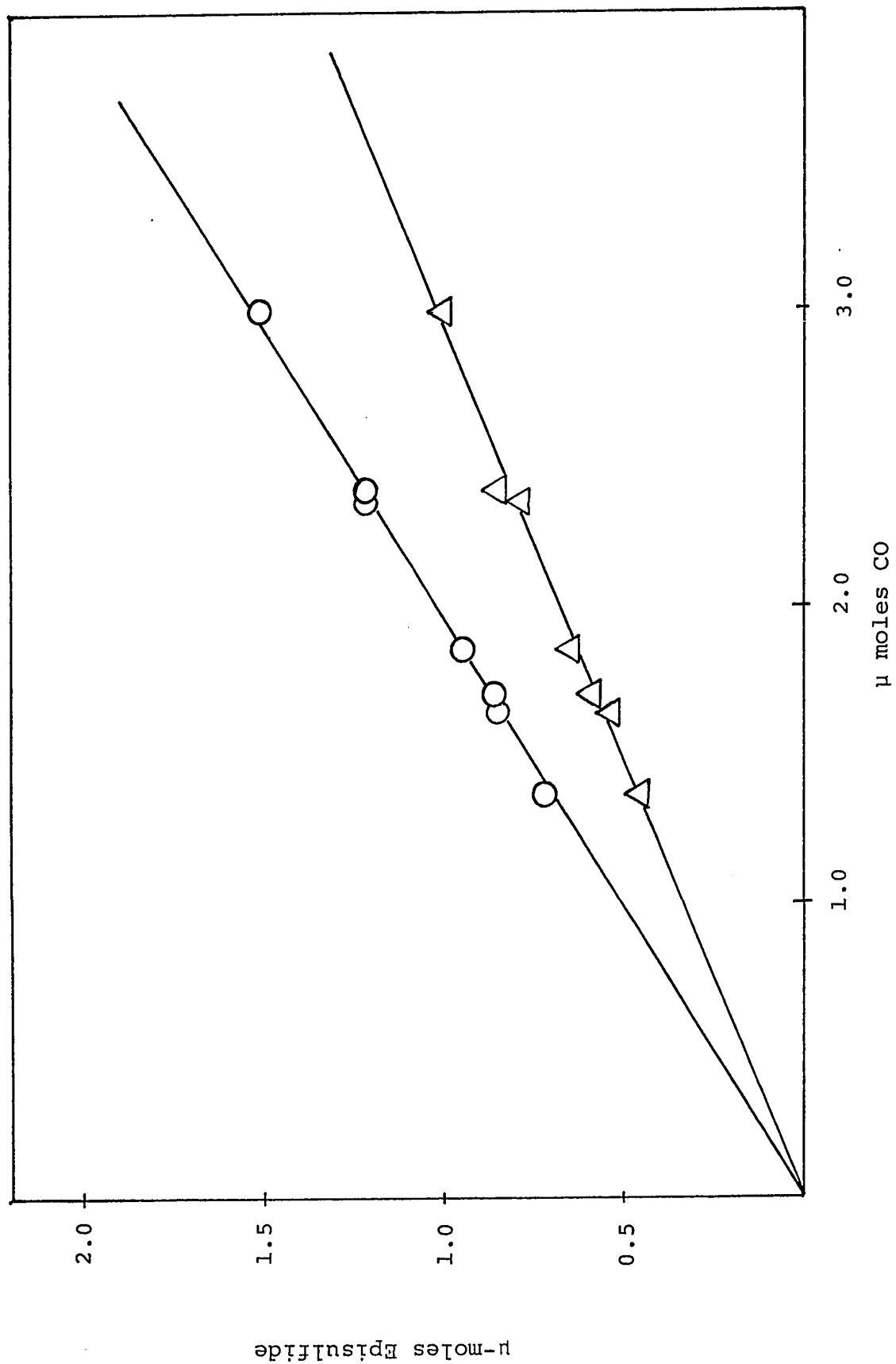


Figure 8: Addition of  $S(^3P)$  Atoms to Trimethylethylene and Isobutene.

O -  $C_4H_8$

Δ -  $C_5H_{10}S$

TABLE X

ADDITION OF S(<sup>3</sup>P) ATOMS TO TETRAMETHYLETHYLENE AND TRIMETHYLETHYLENE<sup>a</sup>

$C_6H_{12}S^b$  FORMATION AS A FUNCTION OF ADDED TRIMETHYLETHYLENE

Exposure Time (minutes)	P( $C_5H_{10}$ ) (torr)	$\frac{[C_5H_{10}]}{[C_6H_{12}]}$	CO ( $\mu$ moles)	$\frac{C_6H_{12}S^c}{CO}$	$\frac{A - A_o}{A}$ <sup>d</sup>	$\frac{k_{C_6H_{12}}}{k_{C_5H_{10}}}$ <sup>e</sup>
20	0	0	1.44	253	-	-
25	14.5	0.72	1.73	171	0.48	1.50
20	7.6	0.38	1.40	206	0.23	1.65
24	14.3	0.71	1.67	163	0.55	1.29
28	22.1	1.09	1.87	140	0.81	1.35
29	28.5	1.41	1.96	129	0.96	1.47
30	35.7	1.77	1.95	111	1.28	1.38
32	43.2	2.14	2.15	107	1.36	1.57

a.  $P(COS) = 31.0$ ,  $P(CO_2) = 1,362$ ,  $P(C_6H_{12}) = 20.2$  torr

b. Tetramethylethylene episulfide

c. Arbitrary Units (= A)

d.  $A_o = \frac{C_6H_{12}S}{CO}$  in the absence of  $C_5H_{12} = 253$

$A = \frac{C_6H_{12}S}{CO}$  in the presence of  $C_5H_{12}$

e.  $\frac{[C_5H_{10}]}{[C_5H_{12}]} \div \frac{A - A_o}{A}$

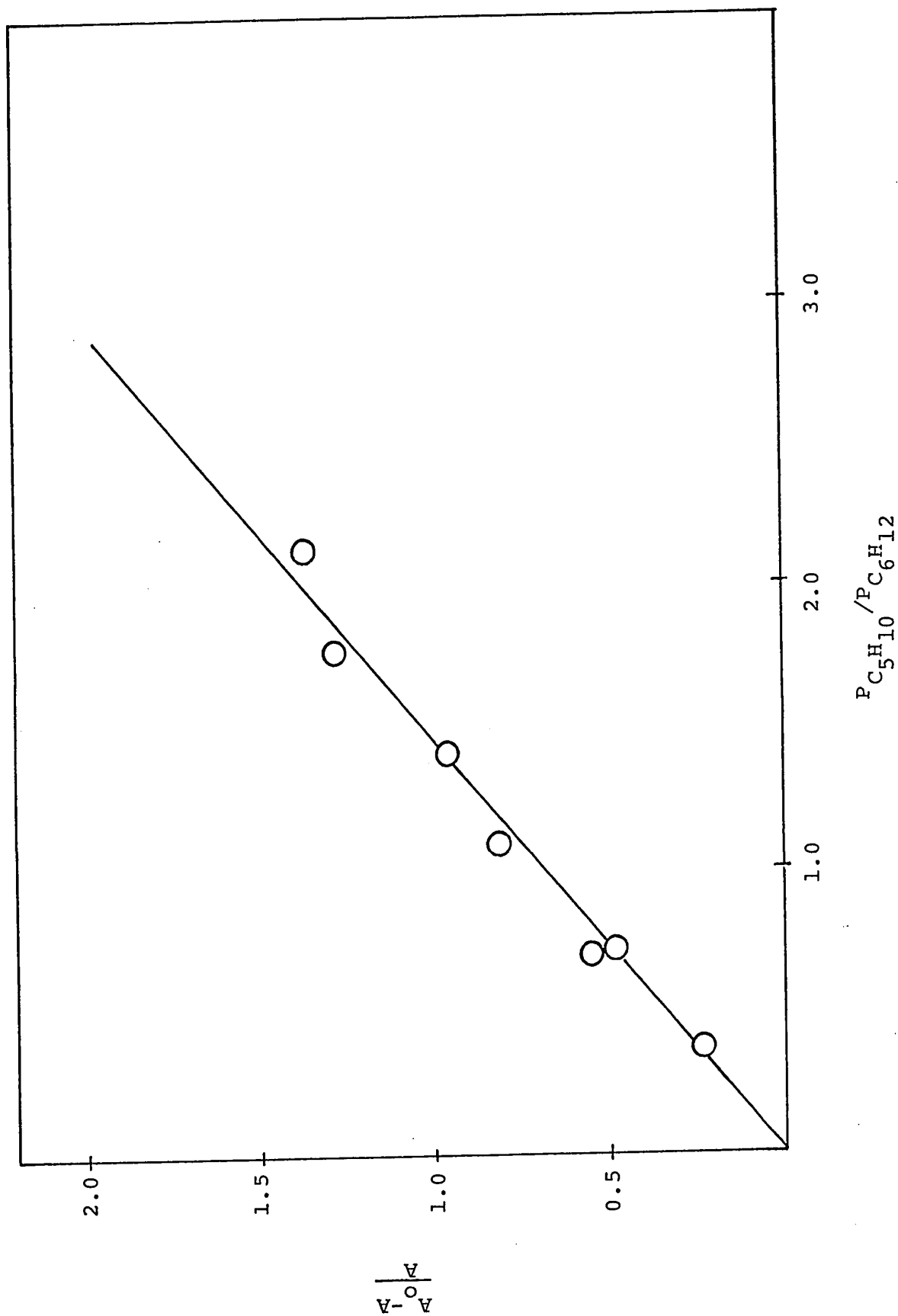


Figure 9: Addition of  $S(^3P)$  Atoms to Tetramethylethylene and Trimethylethylene.

for distillation of tetramethylethylene, the trimethylethylene-episulfide could not be recovered quantitatively so the relative rate was determined by measuring the decreased yield of tetramethylethylene episulfide resulting from an increase in the relative concentration of trimethylethylene. Table X shows the  $C_6H_{12}S$  yield as a function of the ratio  $[C_5H_{10}]/[C_6H_{12}]$ . This ratio is plotted against  $(A_0 - A)/A$  in Fig. 9 giving a straight line through the origin. The slope of this line, determined by least mean squares treatment of the points including the origin, equalled  $0.67 \pm .06$ . Thus  $k_{C_5H_{10}}/k_{C_6H_{12}} = 0.67 \pm 0.05$  and  $k(S + C_6H_{12})/k(S + C_2H_4) = 88 \div 0.67 = 131$ .

#### 1,3-Butadiene - Isobutene System

Addition of  $S(^3P)$  atoms to butadiene gives vinylthiacyclopropane as the main product (60). However since this product polymerizes rapidly with other olefins, its yield is strongly dependent on olefin pressure and cannot be taken as a measure of sulfur atom addition to butadiene. The relative rate for this compound was therefore measured by observing the decrease in isobutene-episulfide yield upon addition of butadiene to a mixture of 604 torr COS and 10.8 torr isobutene. Taking an average of the three runs shown in Table XI one obtains  $k_{C_4H_6}/k_{C_4H_8} = 1.43$ . Therefore,

$$k(S + C_4H_6)/k(S + C_2H_4) = 1.43 \times 54 = 77$$

TABLE XI  
ADDITION OF S(<sup>3</sup>P) ATOMS TO 1,3-BUTADIENE AND ISOBUTENE<sup>a</sup>

C <sub>4</sub> H <sub>8</sub> S <sup>b</sup> FORMATION AS A FUNCTION OF ADDED BUTADIENE						
Exposure Time (minutes)	P(C <sub>4</sub> H <sub>6</sub> ) (torr)	$\frac{[C_4H_8]}{[C_4H_6]}$	CO	$\frac{C_4H_8S^c}{CO}$	$\frac{A - A^d}{A}$	$\frac{k_{C_4H_6}^e}{k_{C_4H_8}}$
20	0	∞	2.06	170 <sup>f</sup>		
20	7.8	1.38	1.95	79	1.15	1.59
20	7.8	1.38	1.94	86	0.98	1.35
20	7.8	1.38	2.22	86	0.98	1.35

a. P(COS) = 604, P(C<sub>4</sub>H<sub>8</sub>) = 10.8 torr

b. Isobutene - episulfide

c. Arbitrary units (= A)

d. A<sub>O</sub> = 170

e.  $\frac{A_{O-A}}{A} \times \frac{[C_4H_8]}{[C_4H_6]}$

f. Average of 6 runs

### 2-Trifluoromethylpropene - Propene System

Since the addition reactions of sulfur atoms with 2-trifluoromethylpropene had not previously been studied, a mixture of 500 torr COS and 50 torr  $\text{CF}_3(\text{CH}_3)\text{C}=\text{CH}_2$  was Hg-photosensitized resulting in one major product. Its mass spectrum, which is given in the appendix, indicated a molecular weight of 142 so it was taken to be the episulfide since there are no  $\text{S}(^1\text{D})$  atoms in the system to produce mercaptans. A mixture was then made up consisting of 511 torr COS, 10.3 torr  $\text{C}_3\text{H}_6$  and 22.0 torr  $\text{C}_4\text{F}_3\text{H}_5$ . The product yields from the Hg-photosensitization of this mixture are shown in Table XII. The episulfides are plotted against CO yield in Fig. 10. The ratio of the slopes, determined by least mean squares treatment of the data, is 0.36.

Thus,  $k_{\text{C}_4\text{F}_3\text{H}_5}/k_{\text{C}_3\text{H}_6} = 0.17$  giving

$$k(\text{S} + \text{C}_4\text{F}_3\text{H}_5)/k(\text{S} + \text{C}_2\text{H}_4) = 0.17 \times 6.8 = 1.16$$

### 2-Fluoropropene - Ethylene System

The reactions of sulfur atoms with 2-fluoropropene had not previously been studied; therefore a mixture of 500 torr COS and 50 torr  $\text{C}_3\text{FH}_5$  was Hg-sensitized. The only resulting product was shown by its mass spectrum, which is given in the appendix, to have a molecular weight of 92 and was therefore taken to be the episulfide.

Hg-photosensitization was then carried out on a mixture

TABLE XII

ADDITION OF S(<sup>3</sup>P) ATOMS TO 2-TRIFLUOROMETHYLPROPENE AND PROPENE<sup>a</sup>PRODUCT FORMATION AS A FUNCTION OF EXPOSURE TIME FOR [C<sub>3</sub>H<sub>6</sub>]/[C<sub>4</sub>F<sub>3</sub>H<sub>5</sub>] = 0.47

Exposure Time (minutes)	Yields, $\mu$ moles		$\frac{C_4F_3H_5S}{C_3H_6S}$		$\frac{k_{C_4F_3H_5S}}{k_{C_3H_6}}$		% Yield <sup>d</sup>
	CO	C <sub>3</sub> H <sub>6</sub> S <sup>b</sup>	C <sub>4</sub> F <sub>3</sub> H <sub>5</sub> S <sup>b</sup>				
20	1.85	0.51	0.24	0.47	0.22		45
25	2.30	0.77	0.32	0.42	0.20		47
30	3.01	1.08	0.33	0.31	0.15		47
35	3.46	1.21	0.38	0.31	0.15		46

a. P(COS) = 511, P(C<sub>3</sub>H<sub>6</sub>) = 10.3, P(C<sub>4</sub>F<sub>3</sub>H<sub>5</sub>) = 22.0 torr

b. Episulfides

c.  $\frac{C_4F_3H_5S}{C_3H_6S} \times 0.47$ d.  $\frac{\Sigma(\text{episulfides})}{CO} \times 100$

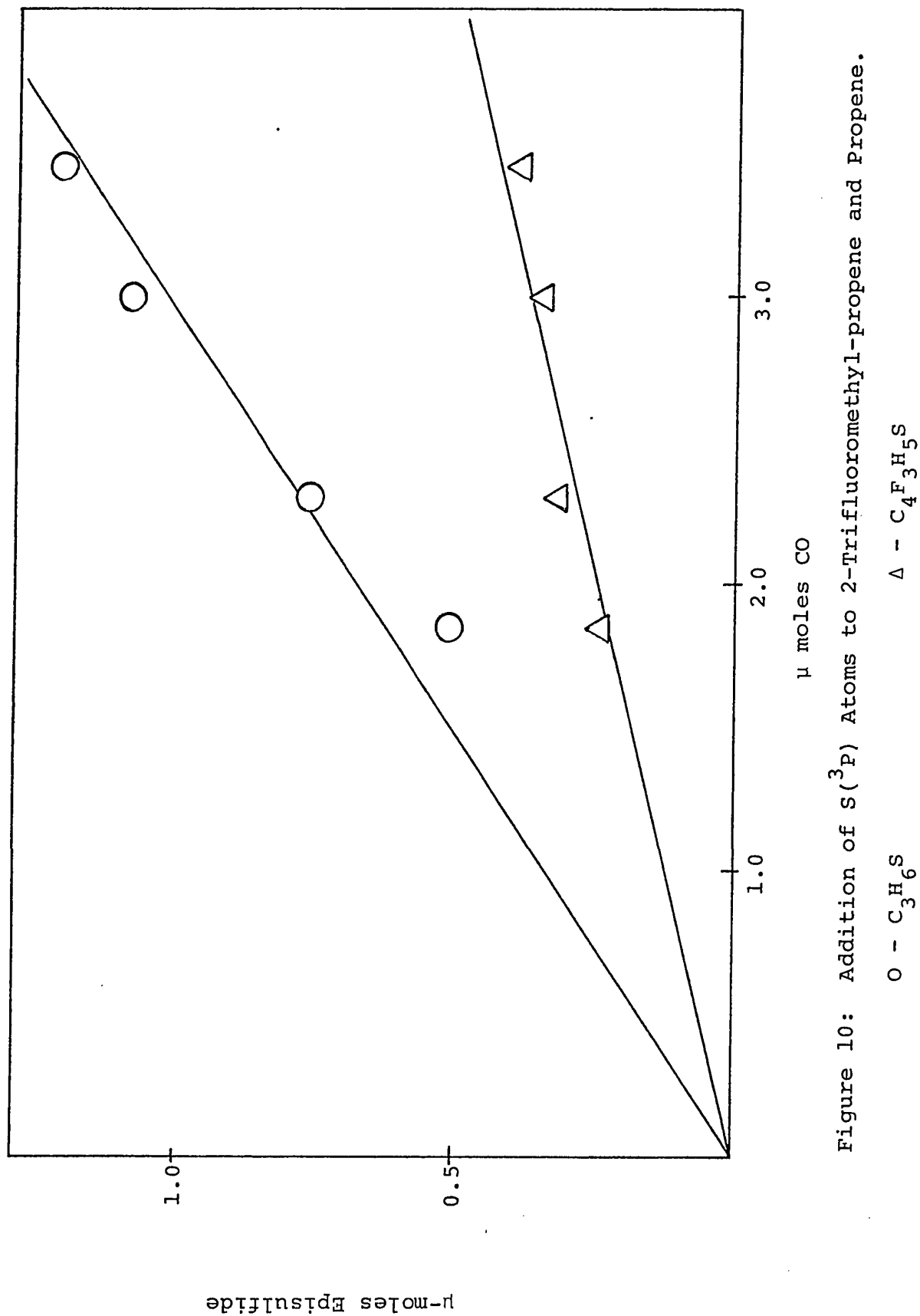


Figure 10: Addition of  $\text{S}(^3\text{P})$  Atoms to 2-Trifluoromethyl-propene and Propene.



TABLE XIII

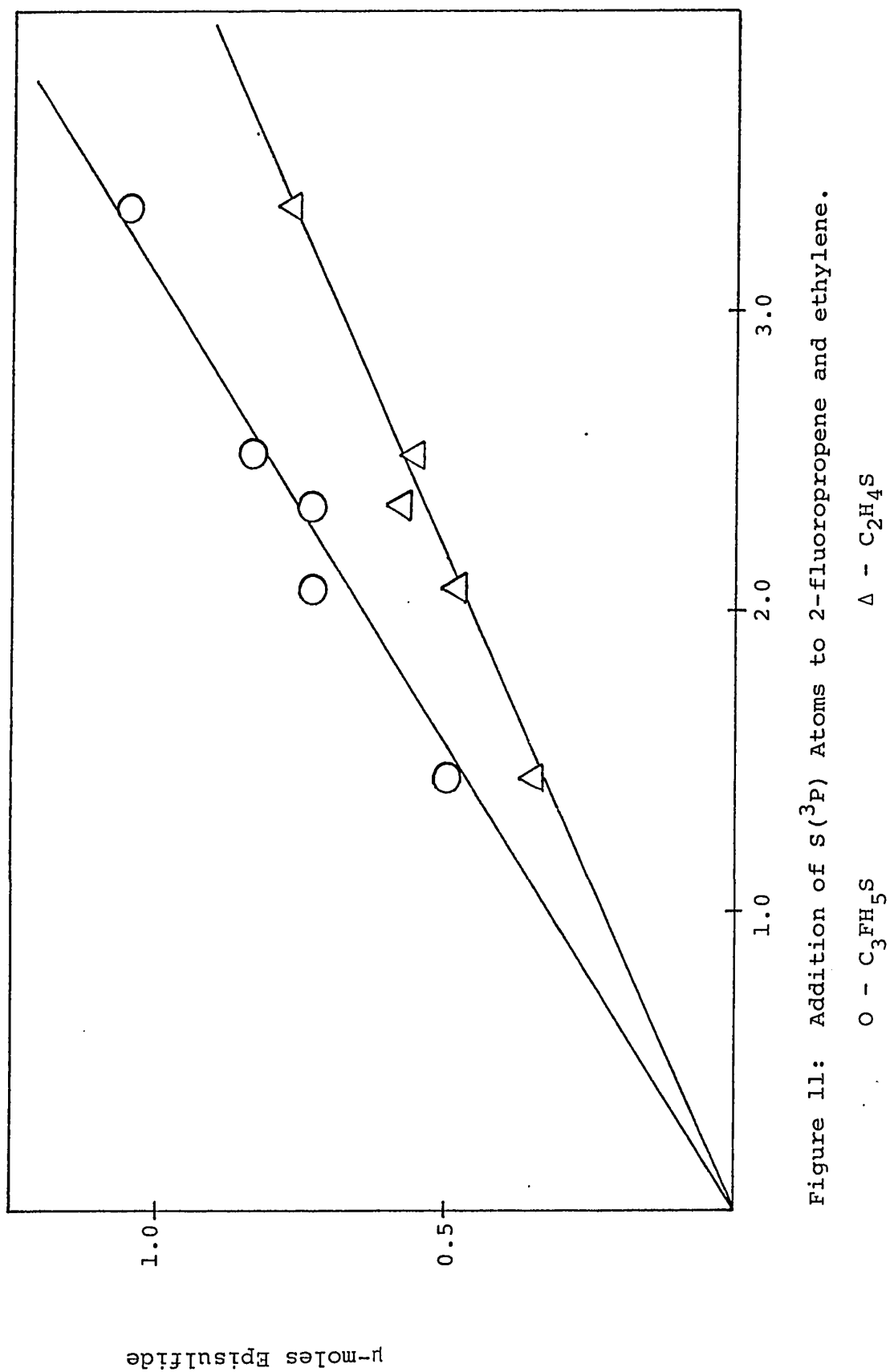
ADDITION OF S(<sup>3</sup>P) ATOMS TO 2-FLUORO-PROPENE AND ETHYLENE<sup>a</sup>PRODUCT FORMATION AS A FUNCTION OF EXPOSURE TIME FOR  $[C_2H_4]/[C_3FH_5] = 1.79$ 

Exposure Time (minutes)	Yields, $\mu$ moles		$\frac{C_3FH_5}{C_2H_4}$ <sup>c</sup>		% Yield <sup>d</sup>
	CO	$C_3FH_5$ <sup>b</sup>	$C_2H_4$ <sup>b</sup>	$\frac{C_3FH_5}{C_2H_4}$	
35	3.35	1.05	0.77	1.36	54
25	2.34	0.73	0.58	1.26	56
30	2.53	0.84	0.55	1.53	55
20	1.44	0.50	0.35	1.43	59
25	2.07	0.73	0.48	1.52	58

a.  $P(COS) = 532$ ,  $P(C_2H_4) = 23.5$ ,  $P(C_3FH_5) = 13.1$  torr.

b. Episulfides

c.  $\frac{C_3FH_5}{C_2H_4} \times 1.79$ d.  $\frac{\Sigma(\text{episulfides})}{CO} \times 100$



of 532 torr COS, 23.5 torr  $C_2H_4$  and 13.1 torr  $C_3FH_5$ . The product yields are shown in Table XIII and plotted in Fig. 11. The ratio of the slopes obtained by least mean squares treatment of the data is 1.45 leading to

$$k(S + C_3FH_5)/k(S + C_2H_4) = 2.60$$

### 3,3-4,4,4-Pentafluoro-1-butene - 2-Fluoropropene System

Since the addition of sulfur atoms to 3,3-4,4,4-pentafluoro-1-butene had not previously been investigated, Hg-photosensitization was carried out on a mixture of 500 torr COS and 50 torr  $C_4F_5H_3$ . The mass spectrum of the only resulting product is shown in the appendix. Due to the strong parent peak at  $m/e = 178$  and an appropriate cracking pattern, this compound was taken to be the episulfide. Table XIV and XV respectively show the product yields obtained by Hg-sensitization of two separate mixtures, the first one consisting of 549 torr COS, 98.0 torr  $C_4F_5H_3$  and 6.9 torr  $C_3FH_5$  and the second consisting of 550 torr COS, 82.5 torr  $C_4F_5H_3$  and 4.6 torr  $C_3FH_5$ . In both cases the % yield decreases with increasing CO yield. The relative rate was therefore extrapolated to zero CO yield. A least mean squares treatment of the points shown in Fig. 12 gives a line with a slope of 0.002 and an intercept of 0.036. (This treatment always assumes that the abscissae are correct and the error is in the ordinates.) From the extrapolated relative rate we have then

TABLE XIV

ADDITION OF  $S(^3P)$  ATOMS TO 3,3-4,4,4-PENTAFLUORO-1-BUTENE AND 2-FLUOROPROPENE<sup>a</sup>PRODUCT FORMATION AS A FUNCTION OF EXPOSURE TIME FOR  $[C_3FH_5]/[C_4F_5H_3] = 0.070$ 

Exposure Time (minutes)	Yields, $\mu$ moles		$\frac{C_4F_5H_3S}{C_3FH_5S}$	$\frac{k_{C_4F_5H_3}^c}{k_{C_3FH_5}^c}$	% yield <sup>d</sup>
	CO	$C_4F_5H_3S^b$	$C_3FH_5S^b$		
20	1.83	0.35	0.65	0.54	54
25	2.27	0.40	0.70	0.57	48
30	2.70	0.50	0.77	0.65	47
35	3.13	0.50	0.87	0.57	44

a.  $P(COS) = 549$ ,  $P(C_4F_5H_3) = 98.0$ ,  $P(C_3FH_5) = 6.9$  torr

b. Episulfides

c.  $\frac{C_4F_5H_3S}{C_3FH_5S} \times 0.07$ d.  $\frac{\Sigma(\text{episulfides})}{CO} \times 100$

TABLE XV

ADDITION OF S(<sup>3</sup>P) ATOMS TO 3,3-4,4,4-PENTAFLUORO-1-BUTENE AND 2-FLUOROPROPENEPRODUCT FORMATION AS A FUNCTION OF EXPOSURE TIME FOR  $[C_3FH_5]/[C_4F_5H_3] = 0.056$ 

Exposure Time (Minutes)	Yields, $\mu$ moles		$\frac{C_4F_5H_3S}{C_3FH_5S}$	$\frac{k_{C_4F_5H_3}}{k_{C_3FH_5}}$ <sup>c</sup>	% Yield <sup>d</sup>
	CO	$C_4F_5H_3S$ <sup>b</sup>	$C_3FH_5S$ <sup>b</sup>		
7	0.62	0.15	0.23	0.65	61
20	1.72	0.32	0.41	0.78	42
35	3.16	0.53	0.68	0.78	38

a.  $P(COS) = 550$ ,  $P(C_4F_5H_3) = 82.5$ ,  $P(C_3FH_5) = 4.6$  torr

b. Episulfides

c.  $\frac{C_4F_5H_3S}{C_3FH_5S} \times 0.056$ d.  $\frac{\Sigma(\text{episulfides})}{CO} \times 100$

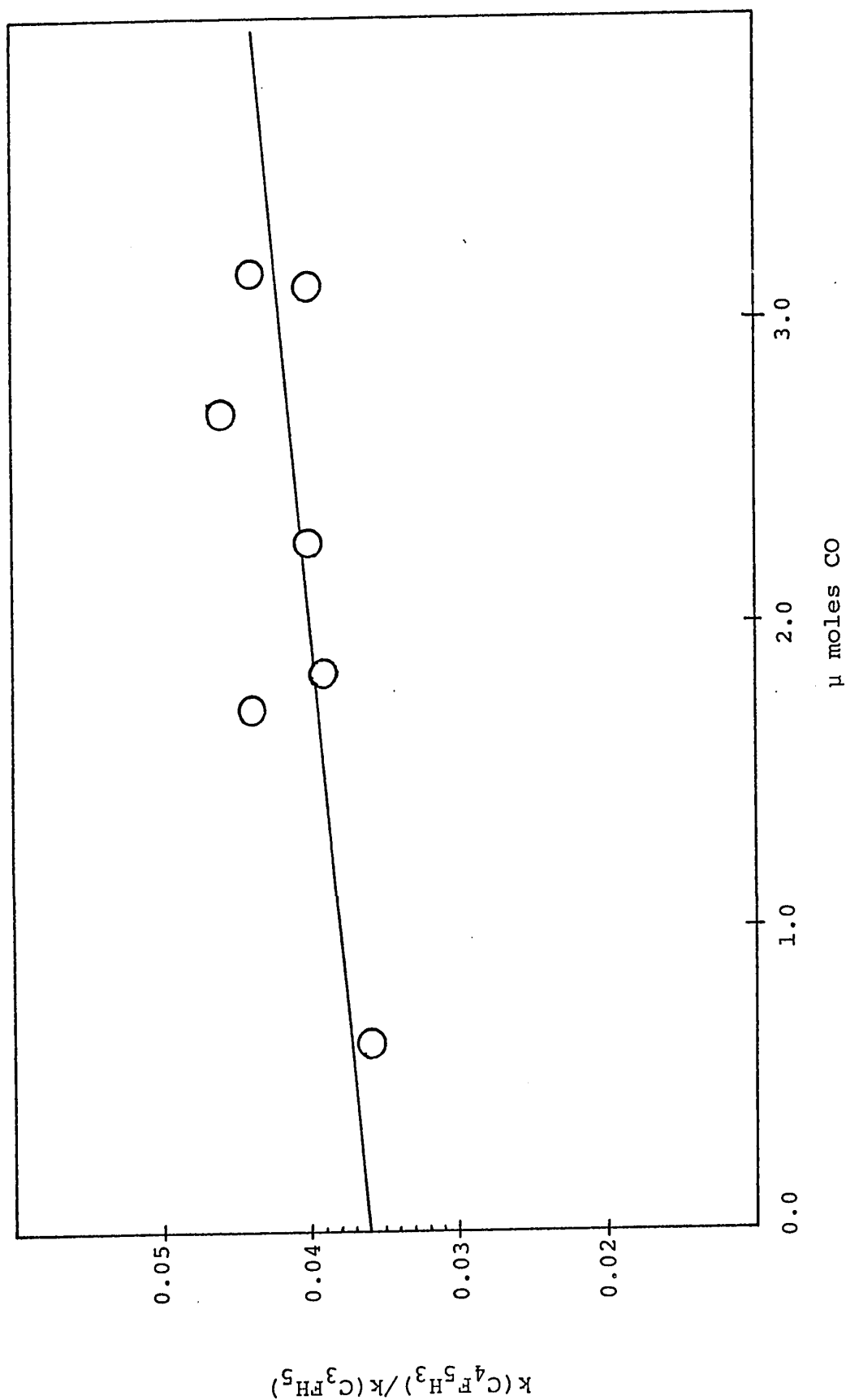


Figure 12: Addition of S(<sup>3</sup>P) Atoms to 3,3-4,4,4-pentafluoro-1-butene and 2-fluoropropene. Relative Rate as a Function of CO Yield.

$$k(S + C_4F_5H_3)/k(S + C_2H_4) = 0.036 \times 2.60 = 0.094$$

### 3,3-4,4,4-Pentafluoro-1-butene - Propene System

As a check on the relative rate for 3,3-4,4,4-pentafluoro-1-butene, Hg-photosensitization was carried out on a mixture of 540 torr COS, 8.70 torr  $C_3H_6$  and 70.8 torr  $C_4F_5H_3$ . The yields from the two runs are shown in Table XVI. Since two points are insufficient for an extrapolation to zero CO yield, the relative rate is taken from the ratio of the slopes in Fig. 13, giving

$$k(S + C_4F_5H_3)/k(S + C_3H_6) = 0.015.$$

Therefore,

$$k(S + C_4F_5H_3)/k(S + C_2H_4) = 0.015 \times 6.8 = 0.102,$$

in excellent agreement with the previously measured value of 0.094, thus confirming the relative rates for both propylene and 2-fluoropropylene.

### Acetylene - Ethylene System

Since the addition of sulfur atoms to acetylenes produces the corresponding unstable thiirenes (9), relative rates for these additions could only be measured by observing the decrease in episulfide yield from a second reactant upon adding increasing amounts of the alkyne. As shown in Table XVII the concentration of acetylene was gradually increased in a mixture of 31.0 torr COS, 1,330 torr  $CO_2$  and 20.3 torr  $C_2H_4$ .  $(A_0 - A)/A$  is plotted against

TABLE XVI

ADDITION OF  $S(^3P)$  ATOMS TO 3,3-4,4,4-PENTAFLUORO-1-BUTENE AND PROPENE<sup>a</sup>

PRODUCT FORMATION AS A FUNCTION OF EXPOSURE TIME FOR  $[C_3H_6]/[C_4F_5H_3] = 0.120$

Exposure Time (minutes)	Yields, $\mu$ moles		$\frac{C_4F_5H_3S}{C_3H_6S}$	$\frac{k_{C_4F_5H_3C}}{k_{C_3H_6}}$	% Yield <sup>d</sup>
	CO	$C_4F_5H_3S^b$	$C_3H_6S^b$		
15	1.28	0.10	0.85	0.12	0.014
25	2.01	0.18	1.13	0.16	0.019

a.  $P(COS) = 540$ ,  $P(C_3H_6) = 8.70$ ,  $P(C_4F_5H_3) = 70.8$  torr

b. Episulfides

c.  $\frac{C_4F_5H_3S}{C_3H_6S} \times 0.12$

d.  $\frac{\Sigma(\text{episulfides})}{CO} \times 100$



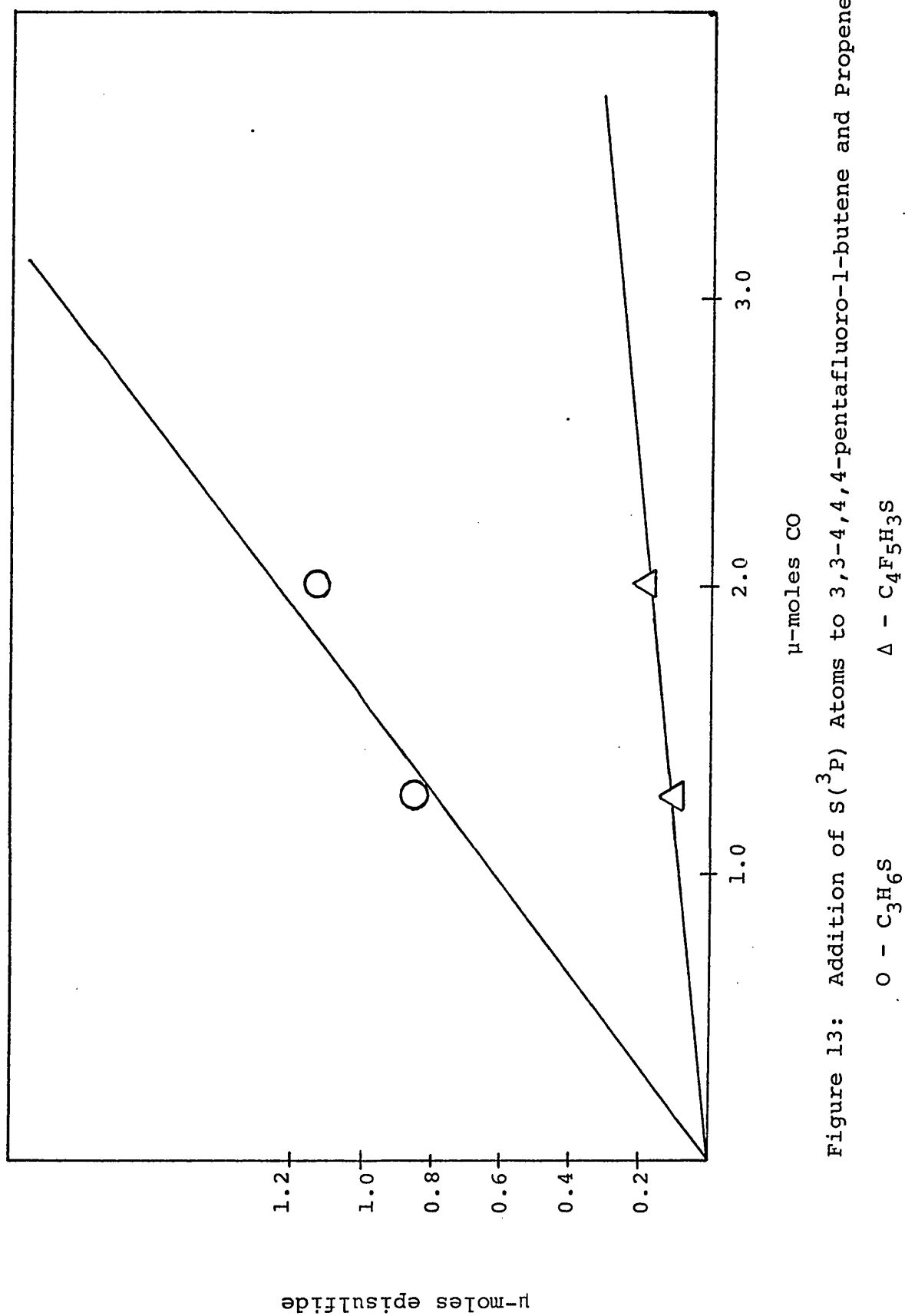


Figure 13: Addition of  $S(^3P)$  Atoms to 3,3-4,4,4-pentafluoro-1-butene and Propene

TABLE XVII  
ADDITION OF S(<sup>3</sup>P) ATOMS TO ACETYLENE AND ETHYLENE<sup>a</sup>  
C<sub>2</sub>H<sub>4</sub>S<sup>b</sup> FORMATION AS A FUNCTION OF ADDED ACETYLENE

Exposure Time (minutes)	P(C <sub>2</sub> H <sub>2</sub> )	$\frac{[C_2H_2]}{[C_2H_4]}$	CO (μmoles)	$\frac{C_2H_4S^c}{CO}$	$\frac{A - A^d}{A}$	$\frac{k_{C_2H_2}^e}{k_{C_2H_4}}$
20	0	0	1.71	109		
20	0	0	1.60	96		
20	0	0	1.93	106		
20	20.9	1.03	1.87	83	0.24	0.23
20	41.7	2.05	1.89	56	0.84	0.41
20	81.8	4.03	1.86	44	1.34	0.33
20	101.8	5.01	1.65	42	1.45	0.29
60	121.1	5.97	4.35	32	2.22	0.38
60	141.8	6.99	4.62	29	2.55	0.36

a. P(COS) = 31.0, P(CO<sub>2</sub>) = 1,330, P(C<sub>2</sub>H<sub>4</sub>) = 20.3 torr.

b. Ethylene episulfide

c. Arbitrary units (= A)

d.  $A_O = \frac{C_2H_4S}{CO}$  in the absence of C<sub>2</sub>H<sub>2</sub> = 103 (average of first 3 runs)

$A = \frac{C_2H_4S}{CO}$  in the presence of C<sub>2</sub>H<sub>2</sub>

e.  $\frac{A_O - A}{A} \times \frac{[C_2H_4]}{[C_2H_2]}$

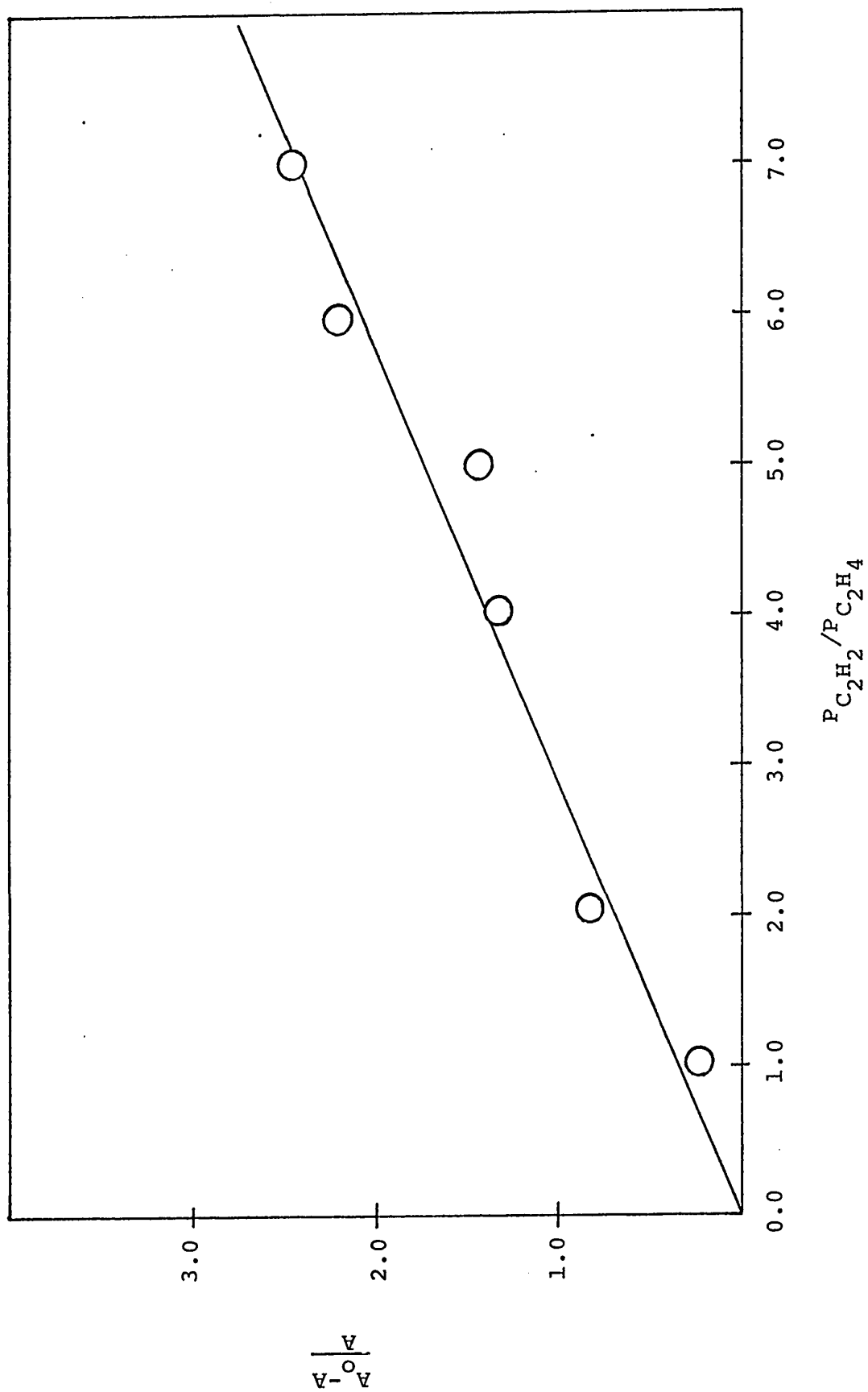


Figure 14: Addition of  $S(^3P)$  Atoms to Acetylene and Ethylene.

$[C_2H_2]/[C_2H_4]$  in Fig. 14, giving a reasonably good straight line. Least mean squares treatment of the points including the origin gives a slope of  $0.35 \pm 0.04$ . Therefore

$$k(S + C_2H_2)/k(S + C_2H_4) = 0.35.$$

If, because of the fairly low ethylene concentration, secondary reactions such as the reaction of  $S(^3P)$  atoms with ethylene episulfide are important in this system, the true relative rate for acetylene would be higher than the measured one. The lower the yield of ethylene episulfide, the less depletion by secondary reactions. Therefore as the acetylene concentration is increased the measured  $A$  values will be relatively high compared with the measured  $A_0$  and thus the  $\frac{A_0-A}{A}$  values will be low leading to a low value for the relative reactivity of acetylene. Thus in the last two runs in Table XVII the amount of conversion was increased in order to keep the episulfide yield approximately the same. Since the line in Fig. 14 does not show any marked departure from linearity it is probable that the measured relative rate is very close to the true one.

#### Methylacetylene - Ethylene System

As in the previous system the concentration of methylacetylene was increased gradually in a mixture which consisted of 32.0 torr COS, 1,313 torr  $CO_2$  and 22.1 torr  $C_2H_4$ . The data are shown in Table XVIII;  $\frac{A_0-A}{A}$  is plotted against  $[C_3H_4]/[C_2H_4]$  in Fig. 15. Least mean squares

TABLE XVIII

ADDITION OF S(<sup>3</sup>P) ATOMS TO METHYLACETYLENE AND ETHYLENE<sup>a</sup>C<sub>2</sub>H<sub>4</sub>S<sup>b</sup> FORMATION AS A FUNCTION OF ADDED METHYLACETYLENE

Exposure Time (minutes)	P(C <sub>3</sub> H <sub>4</sub> )	$\frac{[C_3H_4]}{[C_2H_4]}$	CO (μmoles)	$\frac{C_2H_4S^c}{CO}$	$\frac{A - A^d}{A}$	$\frac{k_{C_3H_4}^e}{k_{C_2H_4}}$
30	0	0	2.44	100	-	-
30	10.5	0.48	2.42	55	0.82	1.72
30	21.5	0.96	2.24	30	2.30	2.39
35	32.3	1.46	2.33	25	3.00	2.04
45	38.7	1.75	2.97	21	3.8	2.17
45	46.0	2.08	2.85	17	4.9	2.35

a. P(COS) = 32.0, P(CO<sub>2</sub>) = 1,313, P(C<sub>2</sub>H<sub>4</sub>) = 22.1 torr

b. Ethylene Episulfide

c. Arbitrary units (= A)

d.  $A_O = \frac{C_2H_4S}{CO}$  in the absence of C<sub>3</sub>H<sub>4</sub> = 100 $A = \frac{C_2H_4S}{CO}$  in the presence of C<sub>3</sub>H<sub>4</sub>e.  $\frac{A - A}{A} \times \frac{[C_2H_4]}{[C_3H_4]}$

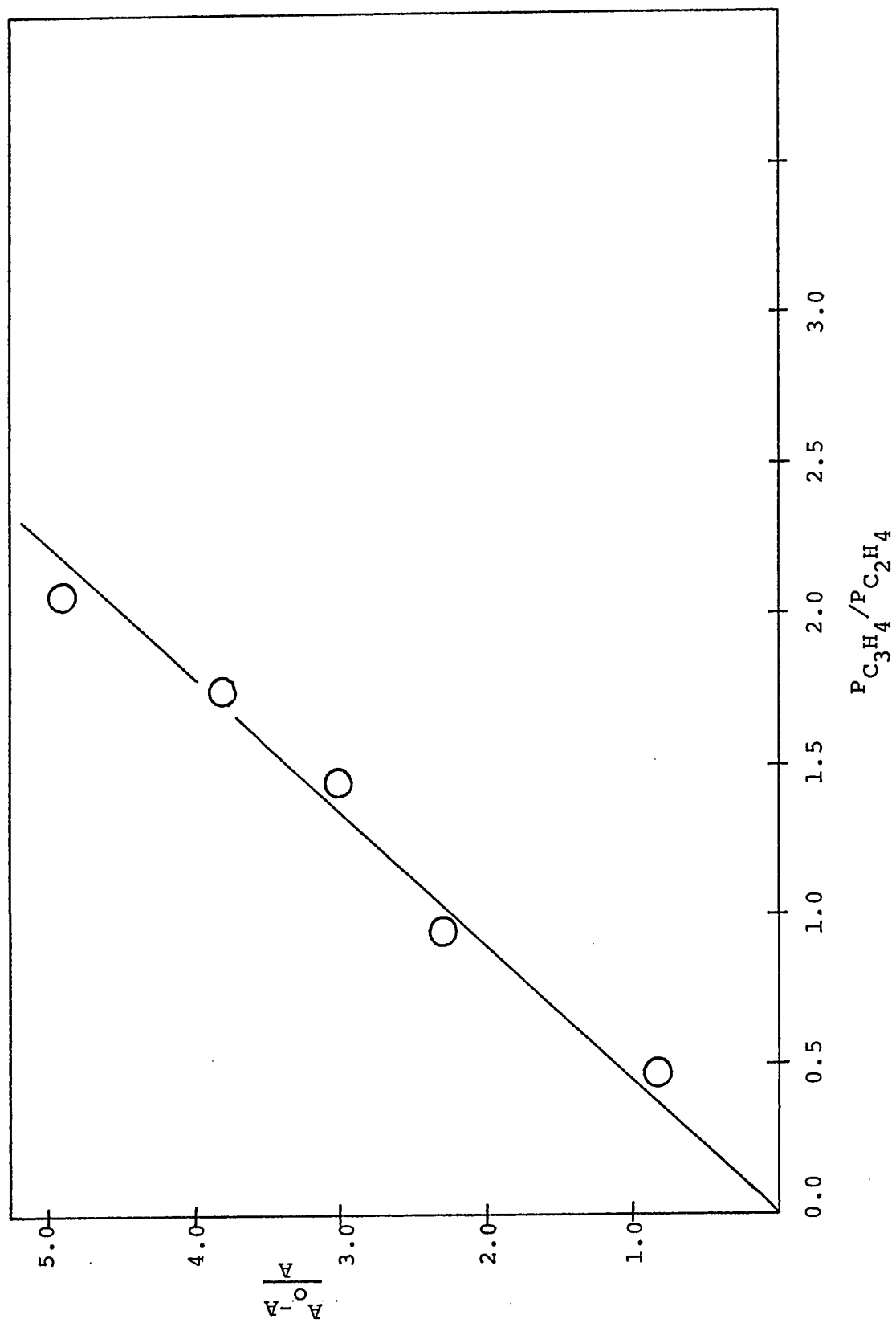


Figure 15: Addition of  $s(3p)$  Atoms to Methylacetylene and Ethylene.

treatment of the points, including the origin, gives a slope of  $2.30 \pm 0.27$ . Therefore  $k(S + C_3H_4)/k(S + C_2H_4) = 2.30$ . If depletion of ethylene episulfide by secondary reactions occurs in this system its effect would be similar to that in the previous system in that the measured relative rate would be too low. It is shown in Chapter IV that with 20 torr ethylene present in the system the ethylene episulfide concentration reaches a steady state value of over 400 peak area units on the gas chromatograph. The peak area in the present system for  $A_0$  was 244 units. Thus since the episulfide yield reached only about half its maximum value, its removal by secondary reactions would be very slight. This argument is supported by the lack of curvature in the plot in Fig. 15. Thus the measured value is very close to the true one.

#### Dimethylacetylene - Cyclopentene System

The relative rate for addition to dimethylacetylene was determined by measuring the decrease in yield of cyclopentene episulfide per  $\mu$ mole CO upon increasing the concentration of dimethylacetylene in a reaction mixture of 31.0 torr COS, 1,357 torr  $CO_2$  and 20.0 torr  $C_5H_8$ . The data are shown in TableXIX. Least mean squares treatment of the points in Fig. 16, including the origin gives a slope of 1.37. The intercept is -0.05, which is very close to the origin. Therefore  $k(S + C_4H_6)/k(S + C_5H_8) = 1.37$ .

TABLE XIX

ADDITION OF  $S(^3P)$  ATOMS TO DIMETHYLACETYLENE AND CYCLOPENTENE<sup>a</sup> $C_5H_8$ <sup>b</sup> FORMATION AS A FUNCTION OF ADDED DIMETHYLACETYLENE

Exposure Time (minutes)	$P(C_4H_6)$	$\frac{[C_4H_6]}{[C_5H_8]}$	CO ( $\mu$ moles)	$\frac{C_5H_8S^c}{CO}$	$\frac{A_{O-A}^d}{A}$	$\frac{k_{C_4H_6}^e}{k_{C_5H_8}}$
20	0	0	1.70	200	-	-
20	0	0	1.75	174	-	-
20	9.0	0.45	1.65	110	0.70	1.55
35	16.5	0.83	2.84	92	1.03	1.25
40	23.2	1.16	3.01	78	1.40	1.20
43	28.2	1.41	2.90	73	1.56	1.11
51	38.7	1.93	3.09	50	2.74	1.42
52	38.7	1.93	3.08	50	2.74	1.42

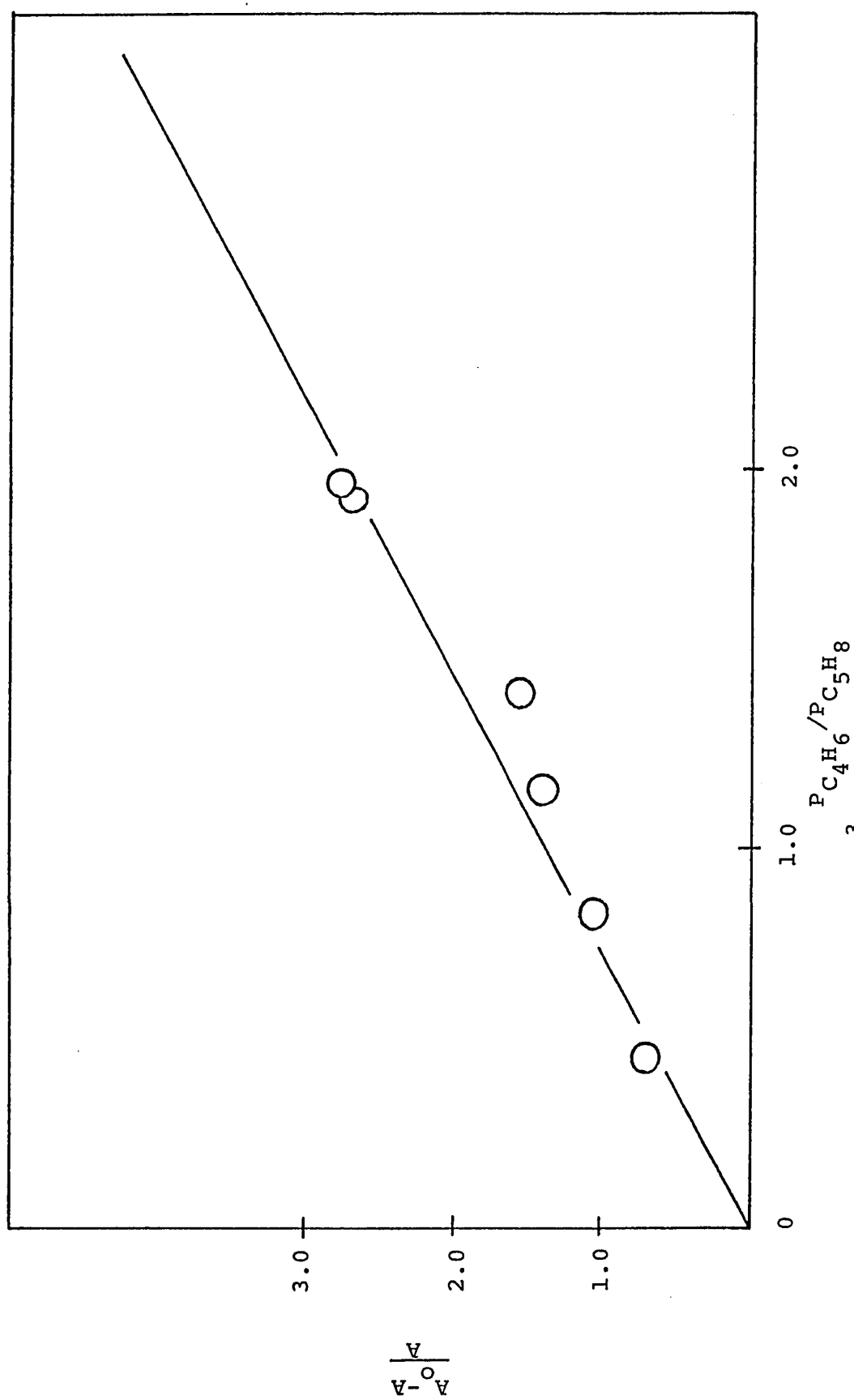
a.  $P(COS) = 31.0$ ,  $P(CO_2) = 1,357$ ,  $P(C_5H_8) = 20.0$  torr

b. Cyclopentene - episulfide

c. Arbitrary units

d.  $A_O = \frac{C_5H_8S}{CO}$  in the absence of  $C_4H_6 = 187$  (average of first 2 runs) $A = \frac{C_5H_8S}{CO}$  in the presence of  $C_4H_6$ e.  $\frac{A_{O-A}}{A} \times \frac{[C_5H_8]}{[C_4H_6]}$





The relative rate of addition of  $S(^3P)$  atoms to cyclopentene was determined to be 21 (60). Thus

$$k(S + C_4H_6)/k(S + C_2H_4) = 29.$$

Since cyclopentene is highly reactive compared with ethylene it is unlikely that there are any secondary reactions in this system. Thus the errors in the points are random errors in recovery of cyclopentene episulfide which has a very low vapour pressure. The standard error in the slope in Fig. 16, calculated by least mean squares treatment for a 90% confidence level, is 0.22 which is about  $\pm 16\%$ . This is somewhat higher than the error in the other acetylenes measured.

#### Vinyltrifluorosilane-3,3,4,4-Pentafluoro-1-butene System

The reactions of sulfur atoms with vinyltrifluorosilane (VTFS) had not previously been studied. When a mixture of 500 torr COS and 30 torr VTFS was Hg-photosensitized, no major product was obtained. Mass spectral analysis of the fraction condensable at  $-118^\circ C$  showed peaks up to  $m/e = 200$ . This indicated fragmentation and polymerization of the addition product. It was therefore decided to study the system by means of flash photolysis-kinetic mass spectrometry.

A mixture of COS (226 microns), VTFS (650 microns) and 14 torr He was flash photolyzed and a peak was observed at mass 144. This would correspond to the episulfide of

VTFS. By monitoring this peak a time-resolved oscillogram (Fig. 17) was obtained. This trace was corrected for bleed-out through the leak giving the dotted curve in Fig. 18 which indicates that the adduct decays with a half-life of several seconds.

As a preliminary experiment, 65 torr VTFS was added to the mixture of COS, pentafluorobutene and fluoropropene in Table XV. Hg-photosensitization of this mixture gave 0.32  $\mu$ moles  $C_4F_5H_3S$ , 0.39  $\mu$ moles  $C_3FH_5S$  and 4.41  $\mu$ moles CO. From Table XV, the yield of  $C_3FH_5S$  and  $C_4F_5H_3S$  would be 1.54  $\mu$ moles ( $\sim 35\%$  of CO yield) in the absence of VTFS, and thus the amount of VTFS-episulfide formed was 0.83  $\mu$ moles. Therefore  $k(S + VTFS)/k(S + C_4F_5H_3) = \frac{0.83}{0.32} \times \frac{82.5}{65} \sim 3.7$  giving  $k(S + VTFS)/k(S + C_2H_4) \sim 0.4$ . This value is probably only correct within  $\pm 30\%$ .

#### Trans-1,2-dichloroethene - Cyclopentene System

$S(^3P)$  atoms add to trans-1,2-dichloroethene to form 90% trans-episulfide and 10% cis episulfide(57). The product yields were found to depend on the total pressure in the system. Because of the low vapour pressure of trans-dichloroethene the only competing reactant which was suitable was cyclopentene. Photolysis of a mixture of 12.3 torr COS, 863 torr  $CO_2$  and 12.1 torr cyclopentene gave a peak area for cyclopentene episulfide of 251 units per  $\mu$ mole CO. Addition of 121.3 torr of trans- $C_2H_2Cl_2$  to the

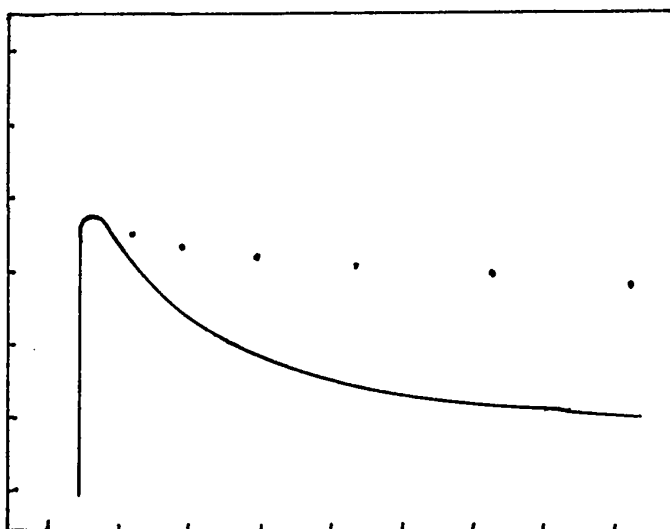
2.0 volts  
per div.



0.5 seconds per div.

Figure 17: Mass 144;  $\text{SiF}_3\text{C}_2\text{H}_3\text{S}$  from Flash  
Photolysis of 226 microns COS  
650 microns  $\text{SiF}_3\text{C}_2\text{H}_3$  and 14 torr  
He.

2.0 volts  
per div.



0.5 seconds per div.

Figure 18: Mass 144;  $\text{SiF}_3\text{C}_2\text{H}_3\text{S}$

Dotted line corrected for bleed-out.

system decreased the peak area to 78 units per  $\mu\text{mole CO}$ . As the temperature was increased new products were formed, which were not identified. When a mixture of 16 torr COS, 840 torr  $\text{CO}_2$  and 52 torr trans- $\text{C}_2\text{H}_2\text{Cl}_2$  was photolyzed three products were obtained in very small yield. The ratio of these to each other varied drastically with the temperature. One of these products had the same G.L.C. retention time as cyclopentene episulfide and thus the decrease in peak area of 173 units/ $\mu\text{mole CO}$  mentioned above represents a minimum value. We can therefore calculate a minimum value for the relative addition rate of trans- $\text{C}_2\text{H}_2\text{Cl}_2$ . Thus

$$k(\text{S} + \text{C}_2\text{H}_2\text{Cl}_2)/k(\text{S} + \text{C}_5\text{H}_8) > \frac{173}{78} \times \frac{12.1}{121} \sim 0.22.$$

leading to  $k(\text{S} + \text{trans } \text{C}_2\text{H}_2\text{Cl}_2)/k(\text{S} + \text{C}_2\text{H}_4) > 4.6$ .

#### B) Arrhenius Parameters

Thermolytic studies (61) have shown that ethylene episulfide will start to undergo decomposition at  $180^\circ\text{C}$  and that for episulfides in general the activation energy for decomposition decreases as the molecular weight increases. To test the influence of temperature on the stability of newly formed episulfides produced by the addition of  $\text{S}(^3\text{P})$  atoms, photolysis was carried out on a gaseous mixture consisting of 20.3 torr COS, 808 torr  $\text{CO}_2$  and 6.1 torr isobutene. The yields of isobutene episulfide per  $\mu\text{mole CO}$  are shown in Fig. 19 as a function of temperature. The yield starts to fall off above  $175^\circ\text{C}$ ; it was therefore

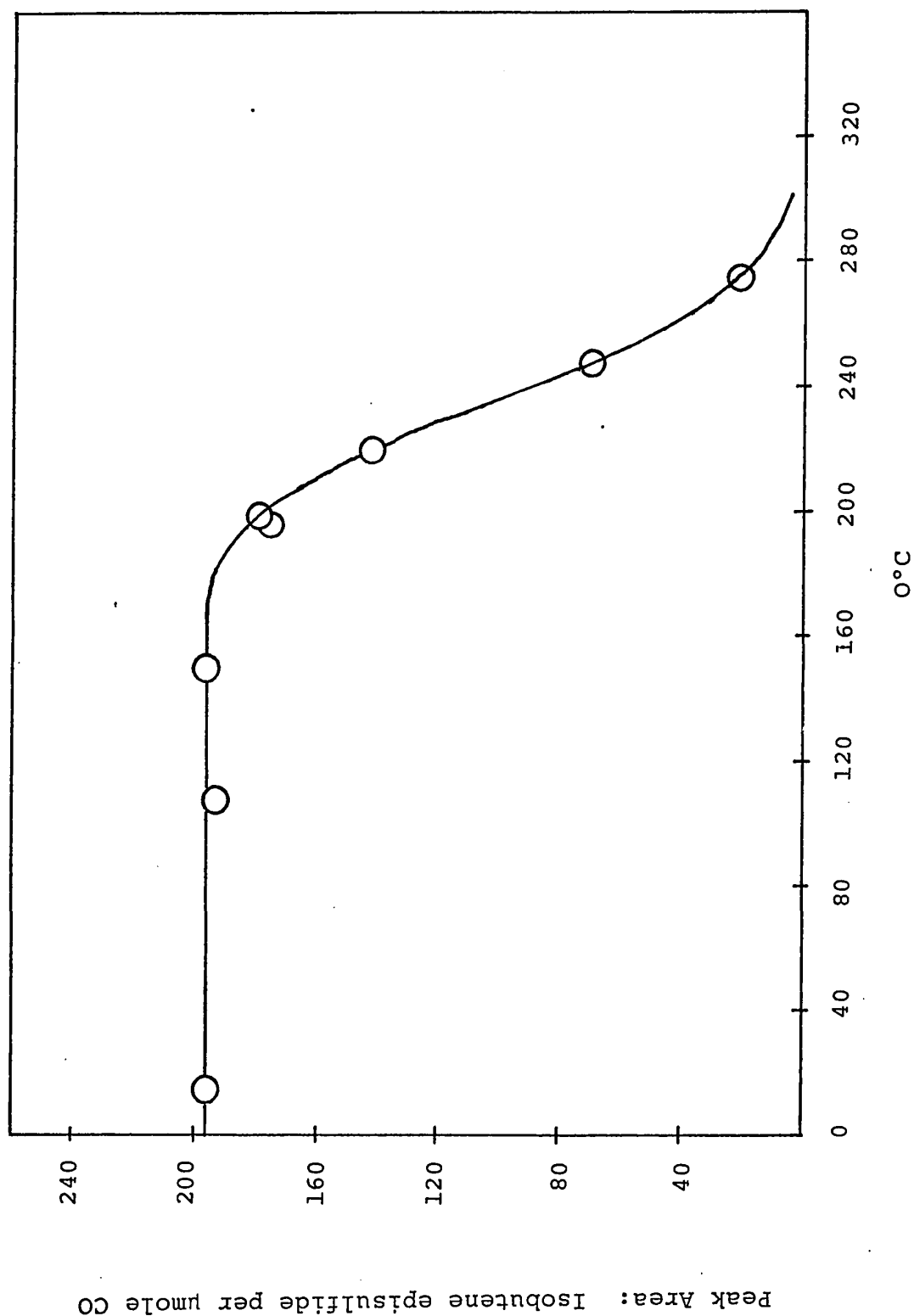


Figure 19: Yield of isobutene episulfide per  $\mu\text{mole CO}$  as a function of temperature from photolysis of 20 torr COS, 6 torr isobutene and 800 torr  $\text{CO}_2$ .

decided to measure the Arrhenius parameters within the temperature range of 25° - 160°C. The slopes and intercepts of the Arrhenius plots were obtained by least mean squares treatment of the points, assuming the temperature reading to be correct and a random error in the relative rate constants. Standard deviations in the slopes and intercepts are given assuming a 90% confidence level.

Since the COS absorption increases with temperature, it was attempted to keep the amount of conversion approximately constant by decreasing the photolysis time as the temperature was increased, in order to eliminate possible errors due to secondary reactions involving the episulfides.

Arrhenius parameters were measured for the following compounds: isobutene, trimethylethylene, tetramethylethylene, 1,3-butadiene, vinyl chloride, cis-difluoroethylene, trans-difluoroethylene, tetrafluoroethylene, 3,3,3-trifluoropropene, acetylene, methylacetylene and dimethylacetylene.

#### Isobutene - Propene System

In this system, as in all the following systems,  $S(^3P)$  atoms were produced by electronic deactivation of  $S(^1D)$  atoms resulting from the photolysis of COS. A mixture of 19.6 torr COS, 916 torr  $CO_2$ , 4.9 torr  $C_4H_8$  and 39.6 torr  $C_3H_6$  was photolyzed at various temperatures up to 188°C. The episulfide yields are given in Table XX as a function

of temperature. In Fig. 20 the natural logarithm of the relative rate ratio is plotted against  $\frac{1}{T} \times 10^3$ . The point at 188°C is seen to be low due to decomposition of isobutene episulfide and is therefore not included in the least mean squares calculation. The % yield is constant throughout the temperature range indicating the lack of reactions of  $S(^3P)$  atoms with the episulfides; this reaction becomes less favorable for the sulfur atoms compared with addition to the olefins, as the temperature is increased (see Chapter IV). From the first six points then, the calculated slope is  $0.615 \pm 0.06$  and the intercept is  $0.036 \pm 0.18$ . Thus  $E(C_3H_6) - E(C_4H_8) = 1.22 \pm 0.11 \text{ kcal mole}^{-1}$  and  $A(C_3H_6)/A(C_4H_8) = 0.97$  within a factor of 1.2. The Arrhenius parameters for  $C_3H_6$  relative to  $C_2H_4$  have previously been measured (62) as  $E(C_2H_4) - E(C_3H_6) = 1.14$  and  $A(C_3H_6)/A(C_2H_4) = 1.0$ . Thus  $E(C_2H_4) - E(C_4H_8) = 2.36$  and  $A(C_4H_8)/A(C_2H_4) = 0.97$ .

#### Trimethylethylene - Isobutene System

Quantitative recovery of isobutene episulfide from a mixture containing trimethylethylene is difficult to achieve by low temperature distillation; therefore, in this system only the trimethylethylene episulfide was measured. When a mixture consisting of 20.4 torr COS, 933 torr  $CO_2$  and 12.1 torr  $C_5H_{10}$  was photolyzed the peak area of trimethylethylene episulfide per  $\mu\text{mole CO}$  was 285. 20.5 torr



TABLE XX

ADDITION OF  $S(^3P)$  ATOMS TO PROPENE AND ISOBUTENE<sup>a</sup>PRODUCT FORMATION AS A FUNCTION OF TEMPERATURE FOR  $[C_3H_6]/[C_4H_8] = 8.08$ 

Exposure Time	$\frac{1}{T^{\circ}K} \times 10^3$	Yields, $\mu$ moles		$\frac{k_{C_4H_8}}{k_{C_3H_6}}$	$\frac{k_{C_4H_8}}{\ln k_{C_3H_6}}$	% Yield	d
		CO	$C_4H_8S^b$	$C_3H_6S^b$			
200	3.356	2.88	0.93	0.93	8.08	2.09	65
175	3.058	2.72	0.83	0.98	6.84	1.92	67
153	2.882	2.63	0.76	1.03	5.96	1.79	68
125	2.618	2.53	0.67	1.00	5.41	1.69	66
121	2.410	2.89	0.67	1.20	4.51	1.52	65
91	2.262	2.62	0.58	1.15	4.07	1.40	66
78	2.169	2.62	0.52	1.17	3.59	1.29	65

a.  $P(COS) = 19.6$ ;  $P(CO_2) = 916$ ;  $P(C_4H_8) = 4.9$ ;  $P(C_3H_6) = 39.6$  torr

b. Episulfides

c.  $\frac{C_4H_8S}{C_3H_6S} \times 8.08$ d.  $\frac{\Sigma(\text{episulfides})}{CO} \times 100$

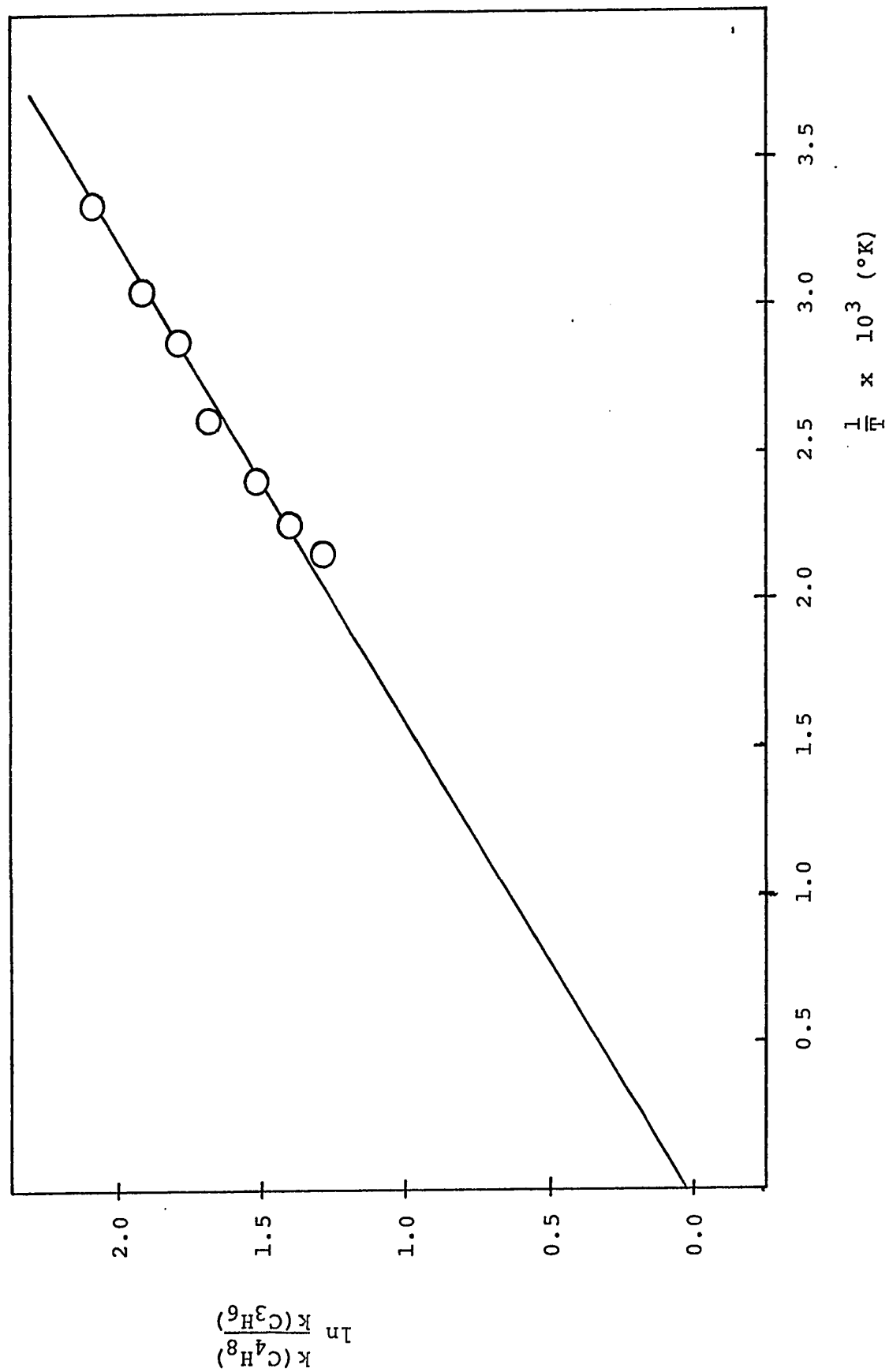


Figure 20: Addition of S(<sup>3</sup>P) Atoms to Isobutene and Propene.  
Arrhenius Plot.

isobutene was then added to the system; the yields of  $C_5H_{10}S$  are shown in Table XXI for the various temperatures. Least mean squares treatment of the Arrhenius plot in Fig. 21 give an activation energy difference.  $E(C_5H_{10}) - E(C_4H_8) = -0.65 \pm 0.20 \text{ kcal mole}^{-1}$  and an A-factor ratio of  $A(C_5H_{10})/A(C_4H_8) = 0.53$  within a factor of 1.34.

#### Tetramethylethylene - Cyclopentene System

Photolysis was carried out on a mixture of 37.3 torr COS, 943 torr  $CO_2$  and 19.7 torr  $C_5H_8$ ; the G.L.C. peak area of cyclopentene episulfide per  $\mu\text{mole CO}$  obtained was 245. Table XXII gives the  $C_5H_8S$  yields at different temperatures after addition of 6.81 torr  $C_6H_{12}$ . Least mean squares treatment of the Arrhenius plot in Fig. 22 gives an activation energy difference  $E(C_5H_8) - E(C_6H_{12}) = 1.21 \pm 0.25 \text{ kcal mole}^{-1}$  and an A-factor ratio of  $A(C_6H_{12})/A(C_5H_8) = 0.75$  within a factor of 1.45. The Arrhenius parameters for  $S(^3P)$  addition to cyclopentene relative to those for ethylene have been measured previously (11) as  $E(C_2H_4) - E(C_5H_8) = 2.15 \text{ kcal mole}^{-1}$  and  $A(C_5H_8)/A(C_2H_4) = 0.67$ . Therefore we get  $E(C_2H_4) - E(C_6H_{12}) = 3.36$  and  $A(C_6H_{12})/A(C_2H_4) = 0.50$ .

#### 1,3-Butadiene - Propene System

The relative addition rates of these compounds as a function of temperature are given in Table XXIII.

TABLE XXI

ADDITION OF S(<sup>3</sup>P) ATOMS TO TRIMETHYLETHYLENE AND ISOBUTENE<sup>a</sup> $C_5H_{10}S^b$  FORMATION AS A FUNCTION OF TEMPERATURE FOR  $[C_4H_8]/[C_5H_{10}] = 1.69$ 

Exposure Time (minutes)	$\frac{1}{T^\circ K} \times 10^3$	CO	$\frac{C_5H_{10}S^e}{CO}$	$\frac{A}{A_0 - A}$	$\frac{k_{C_5H_{10}}}{k_{C_4H_8}}$	$\frac{k_{C_5H_{10}}}{\ln k_{C_4H_8}}$
205	3.322	2.15	138	0.939	1.586	0.457
192	2.994	2.36	130	0.838	1.416	0.351
181	2.740	2.66	128	0.815	1.377	0.314
126	2.532	2.23	122	0.748	1.264	0.231
113	2.353	3.01	114	0.666	1.125	0.113

a.  $P(COS) = 20.4$ ;  $P(CO_2) = 933$ ;  $P(C_4H_8) = 20.5$ ;  $P(C_5H_{10}) = 12.1$  torr

b. Trimethylethylene - episulfide

c.  $A_0 = \frac{C_5H_{10}S}{CO}$  in the absence of  $C_4H_8 = 285$  $A = \frac{C_5H_{10}S}{CO}$  in the presence of  $C_4H_8$ d.  $\frac{A}{A_0 - A} \times 1.69$ 

e. Arbitrary units

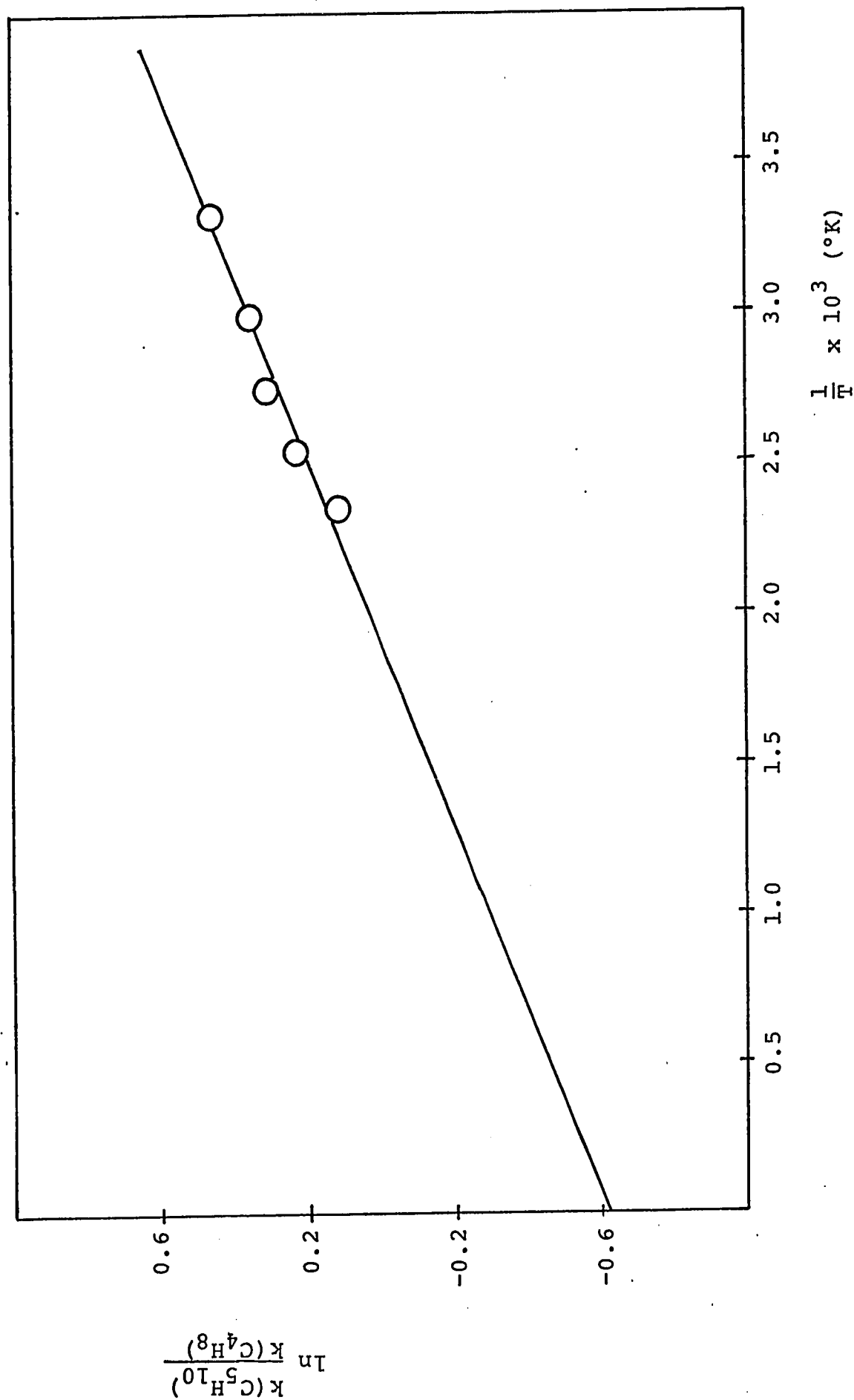


Figure 21: Addition of  $S(^3P)$  Atoms to Trimethylethylene and Isobutene.  
Arrhenius plot.

TABLE XXII

ADDITION OF  $S(^3P)$  ATOMS TO TETRAMETHYLETHENE AND CYCLOPENTENE<sup>a</sup> $C_5H_8$ <sup>b</sup> FORMATION AS A FUNCTION OF TEMPERATURE FOR  $[C_5H_8]/[C_6H_{12}] = 2.90$ 

Exposure Time	$\frac{1}{T^\circ K} \times 10^3$	CO	$\frac{C_5H_8 S^e}{CO}$	$\frac{A_O - A}{A}$ <sup>c</sup>	$\frac{k_{C_6H_{12}}}{k_{C_5H_8}}$ <sup>d</sup>	$\ln \frac{k_{C_6H_{12}}}{k_{C_5H_8}}$
250	3.289	1.66	81	2.02	5.86	1.77
255	2.958	1.87	98	1.50	4.35	1.47
250	2.958	2.04	100	1.45	4.21	1.44
200	2.532	2.20	112	1.19	3.45	1.24
222	2.364	2.60	115	1.13	3.28	1.19
90	2.369	2.17	118	1.08	3.13	1.14

a.  $P(COS) = 37.3$ ;  $P(CO_2) = 943$ ;  $P(C_5H_8) = 19.7$ ;  $P(C_6H_{12}) = 6.81$  torr

b. Cyclopentene - episulfide

c.  $A_O = \frac{C_5H_8 S}{CO}$  in the absence of added  $C_6H_{12} = 245$  $A = \frac{C_5H_8 S}{CO}$  in the presence of added  $C_6H_{12}$ d.  $\frac{A_O - A}{A} \times 2.90$ 

e. Arbitrary units

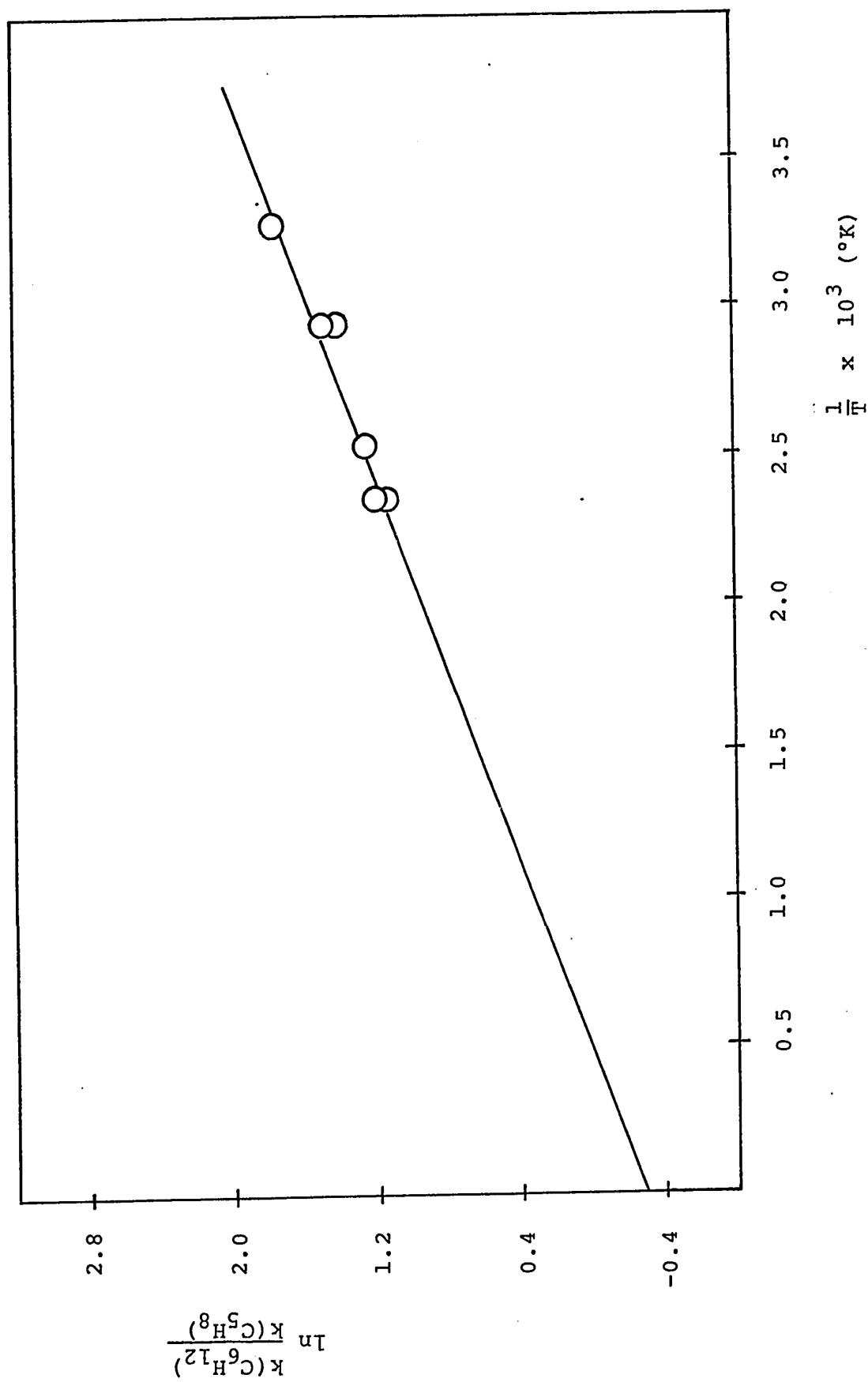


Figure 22: Addition of  $S(^3P)$  Atoms to Tetramethylethylene and Cyclopentene.  
Arrhenius plot.

They were determined by measuring the yield of  $C_3H_6S$  per  $\mu$ mole CO resulting from the photolysis of a mixture consisting of 32.0 torr COS, 887 torr  $CO_2$ , 53.1 torr  $C_3H_6$  and 6.8 torr  $C_4H_6$  as shown in the Table. Least mean squares treatment of the corresponding Arrhenius plot in Fig. 23 gives an activation energy difference  $E(C_3H_6) - E(C_4H_6) = 0.90 \pm 0.23 \text{ kcal mole}^{-1}$  and an A-factor ratio  $A(C_4H_6)/A(C_3H_6) = 2.41$  within a factor of 1.43. Thus, from the previously measured parameters for  $C_3H_6$ , we get  $E(C_2H_4) - E(C_4H_6) = 2.04 \text{ kcal mole}^{-1}$  and  $A(C_4H_6)/A(C_2H_4) = 2.4$ .

#### Vinyl Chloride - Propene System

Photolysis was carried out on a mixture of 21 torr COS 927 torr  $CO_2$  and 31.5 torr  $C_3H_6$  and 157 torr  $C_2H_3Cl$ . The yields of the two episulfides produced are given in Table XXIV as a function of temperature. Fig. 24 shows the corresponding Arrhenius plot. Calculation of the slope and intercept by the least mean squares method gives  $E(C_2H_3Cl) - E(C_3H_6) = 1.66 \pm 0.12 \text{ kcal mole}^{-1}$  and  $A(C_2H_3Cl)/A(C_3H_6) = 3.38$  within a factor of 1.19. Thus  $E(C_2H_4) - E(C_2H_3Cl) = -0.52 \text{ kcal mole}^{-1}$  and  $A(C_2H_3Cl)/A(C_2H_4) = 3.4$ .



TABLE XXIII

ADDITION OF  $S(^3P)$  ATOMS TO 1,3-BUTADIENE AND PROPYLENE<sup>a</sup> $C_3H_6S^b$  FORMATION AS A FUNCTION OF TEMPERATURE FOR  $[C_3H_6]/[C_4H_6] = 8.03$ 

Exposure Time (minutes)	$\frac{1}{T^{\circ}K} \times 10^3$	CO	$\frac{C_3H_6S^e}{CO}$	$\frac{A - A^c}{A}$	$\frac{k_{C_4H_6}^d}{k_{C_3H_6}}$	$\frac{k_{C_4H_6}}{\ln k_{C_3H_6}}$
25	3.333	2.96	92	1.39	10.84	2.38
22	2.967	2.84	99	1.22	9.81	2.28
24	2.785	3.26	109	1.02	8.17	2.10
19	2.538	2.91	113	0.95	7.60	2.03
19.5	2.381	3.33	116	0.90	7.19	1.97

a.  $P(COS) = 32.0$ ;  $P(CO_2) = 887$ ;  $P(C_3H_6) = 53.1$ ;  $P(C_4H_6) = 6.8$  torr

b. Propylene - episulfide

c.  $A_O = \frac{C_3H_6S}{CO}$  in the absence of  $C_4H_6 = 220$  $A = \frac{C_3H_6S}{CO}$  in the presence of  $C_4H_6$ d.  $\frac{A - A_O}{A} \times 8.03$ 

e. Arbitrary units

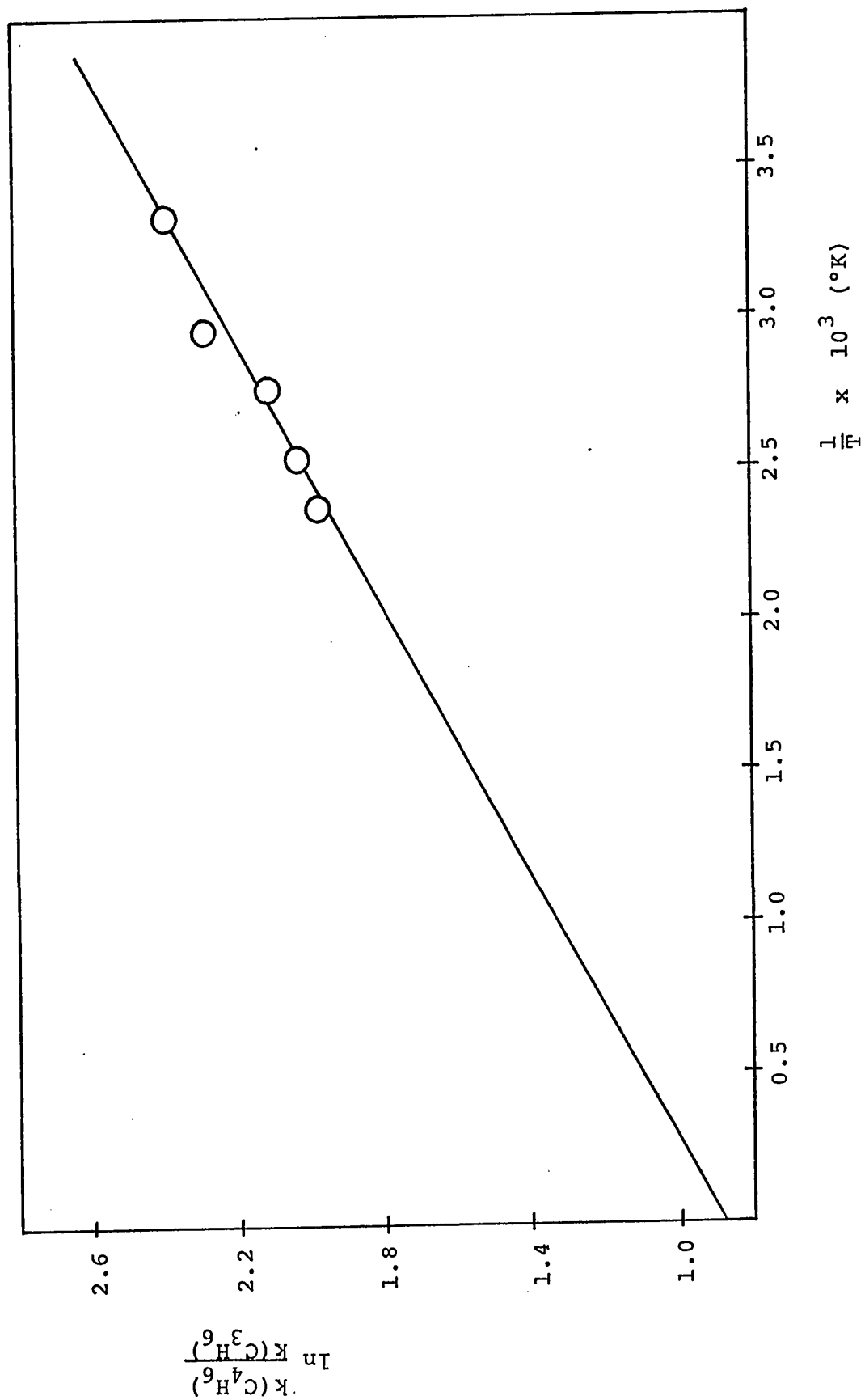


Figure 23: Addition of  $S(^3P)$  Atoms to 1,3-Butadiene and Propylene.

Arrhenius plot.

TABLE XXIV

ADDITION OF S(<sup>3</sup>P) ATOMS TO VINYL CHLORIDE AND PROPYLENE<sup>a</sup>PRODUCT FORMATION AS A FUNCTION OF TEMPERATURE FOR  $[C_3H_6]/[C_2H_3Cl] = 0.201$ 

Exposure Time (minutes)	$\frac{1}{T^{\circ}K} \times 10^3$	Yields, $\mu$ moles		$\frac{k_{C_2H_3Cl}^c}{k_{C_3H_6}}$	$\frac{k_{C_2H_3Cl}}{\ln k_{C_3H_6}}$	% Yield <sup>d</sup>
		CO	$C_2H_3ClS^b$	$C_3H_6S^b$		
25	3.333	3.37	1.086	1.029	0.212	-1.55
23	2.950	3.45	1.352	0.968	0.281	-1.27
21	2.736	3.35	1.328	0.779	0.343	-1.07
20	2.597	3.24	1.307	0.697	0.377	-0.97
20	2.481	3.70	1.537	0.738	0.419	-0.87
20	2.331	3.71	1.598	0.647	0.496	-0.70

a.  $P(COS) = 21.0$ ;  $P(CO_2) = 927$ ;  $P(C_3H_6) = 31.5$ ;  $P(C_2H_3Cl) = 157.0$  torr

b. Episulfides

c.  $\frac{C_2H_3ClS}{C_3H_6S} \times 0.201$ d.  $\frac{\Sigma(\text{episulfides})}{CO} \times 100$

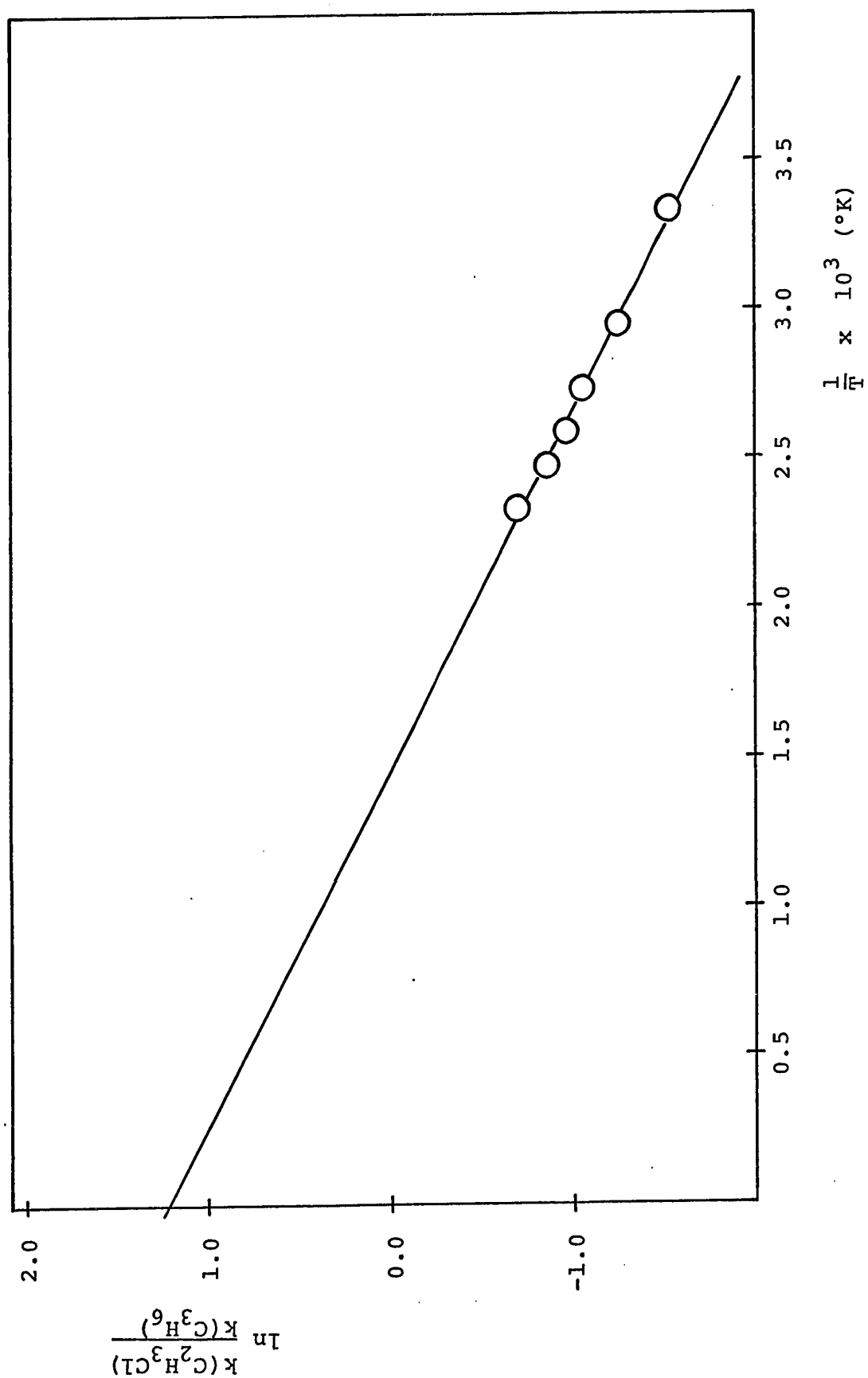


Figure 24: Addition of  $S(^3P)$  Atoms to Vinyl Chloride and Propylene.

Arrhenius plot.

### Cis-1,2-Difluoroethylene - Ethylene System

The addition of  $S(^3P)$  atoms to cis-1,2-difluoroethylene has been shown (59) to produce the isomeric episulfides. The cis configuration is retained in the episulfide to the extent of >99%, making this the most stereospecific olefin in its reaction with  $S(^3P)$  atoms at room temperature. In the present study none of the trans episulfide was found even at the highest temperature used. The yields of cis-difluoroethylene episulfide obtained from the photolysis of a mixture consisting of 20 torr COS, 920 torr  $CO_2$ , 36.1 torr  $C_2H_4$  and 139.2 torr cis- $C_2F_2H_2$  are shown in Table XXV as a function of temperature. The relative rate at each temperature is calculated in the Table from a knowledge of the cis-difluoroethylene yield in the absence of ethylene. The corresponding Arrhenius plot is shown in Fig. 25; the slope and intercept, calculated by the least mean squares method, yield the following Arrhenius parameters:  $E(\text{cis-}C_2F_2H_2) - E(C_2H_4) = 2.71 \pm 0.40 \text{ kcal mole}^{-1}$  and  $A(\text{cis-}C_2F_2H_2)/A(C_2H_4) = 1.66$  within a factor of 1.76.

### Trans-1,2-Difluoroethylene - Ethylene System

$S(^3P)$  atoms have been shown to add to trans-1,2-difluoroethylene to give both episulfide isomers with retention of configuration to the extent of about 80%.

TABLE XXV

ADDITION OF  $S(^3P)$  ATOMS TO CIS-1,2-DIFLUOROETHYLENE AND ETHYLENE<sup>a</sup>

$C_2F_2H_2S^b$  FORMATION AS A FUNCTION OF TEMPERATURE FOR  $[C_2H_4]/[C_2F_2H_2] = 0.259$

Exposure Time (minutes)	$\frac{1}{T^\circ K} \times 10^3$	CO	$\frac{C_2F_2H_2S^b}{CO}$	$\frac{A}{A_0 - A}$	$\frac{k_{C_2F_2H_2}^d}{k_{C_2H_4}}$	$\frac{k_{C_2F_2H_2}}{\ln k_{C_2H_4}}$
34	3.355	3.10	7	0.065	0.017	-4.07
30	2.985	3.07	11	0.107	0.028	-3.58
25	2.736	2.93	15	0.152	0.040	-3.22
23	2.509	3.22	18	0.188	0.049	-3.02
20	2.336	3.31	25	0.281	0.073	-2.62

a.  $P(COS) = 20.0$  torr;  $P(CO_2) = 920$ ;  $P(C_2H_4) = 36.1$ ;  $P(C_2F_2H_2) = 139.2$  torr

b. cis-1,2-Difluoroethylene - episulfide

c.  $A_0 = \frac{C_2F_2H_2S}{CO}$  in the absence of ethylene = 114

$A = \frac{C_2F_2H_2S}{CO}$  in the presence of ethylene

d.  $\frac{A}{A_0 - A} \times 0.259$

e. Arbitrary units

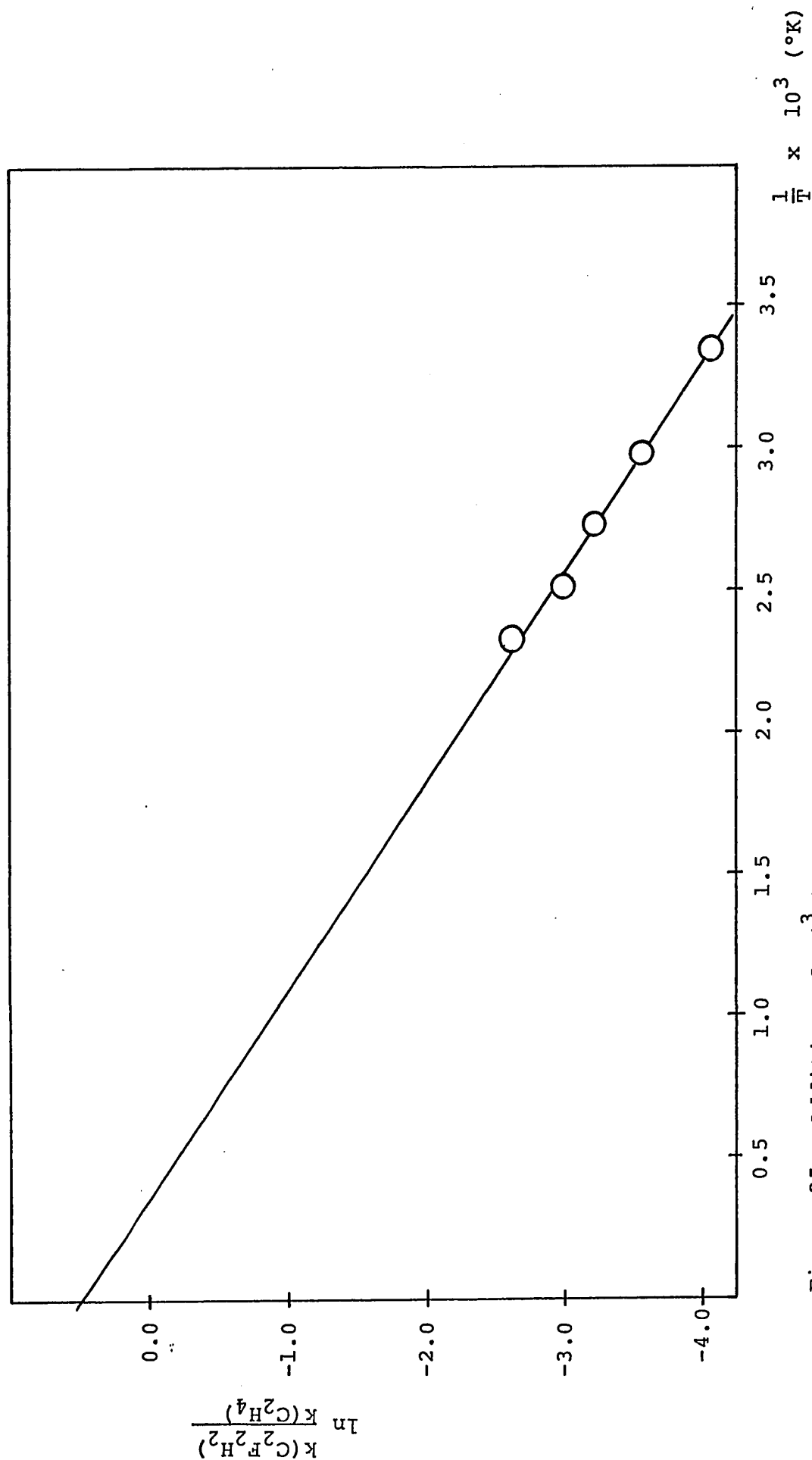


Figure 25: Addition of  $\text{S}(\text{}^3\text{P})$  Atoms to cis-1,2-difluoroethylene and ethylene.

Thus, the 1,2-difluoroethylenes are in contrast with the 2-butenes and the 1,2 dichloroethylenes, where stereospecificity is highest with the trans isomer. In the present study the stereospecificity of this addition reaction was temperature dependent, decreasing from ~84% at room temperature to about ~73% at 150°C. Table XXVI gives the episulfide yields resulting from the photolysis of a mixture of 20 torr COS, 952 torr CO<sub>2</sub>, 33.8 torr C<sub>2</sub>H<sub>4</sub> and 186.5 torr trans-C<sub>2</sub>F<sub>2</sub>H<sub>2</sub> at different temperatures. Unlike the previous system, the ethylene episulfide was recoverable due to the higher volatility of trans-1,2-difluoroethylene as compared to the cis isomer. Least mean squares treatment of the Arrhenius plot in Fig. 26 gives  $E(\text{trans-C}_2\text{F}_2\text{H}_2) - E(\text{C}_2\text{H}_4) = 2.62 \pm 0.23 \text{ kcal mole}^{-1}$  and  $A(\text{trans-C}_2\text{F}_2\text{H}_2)/A(\text{C}_2\text{H}_4) = 3.36$  within a factor of 1.38.

#### Tetrafluoroethylene - Ethylene System

S(<sup>3</sup>P) atoms have been shown (59) to react with tetrafluoroethylene although no stable product has been recovered. A C<sub>2</sub>F<sub>4</sub>S adduct has been observed from the C<sub>2</sub>F<sub>4</sub> - S(<sup>1</sup>D) reaction by the method of flash photolysis - kinetic mass spectrometry. The oscillogram indicated a half-life of ca. 10 seconds for the adduct which probably was tetrafluoroethylene episulfide.

In the present study, photolysis was carried out on a mixture consisting of 21 torr COS, 814 torr CO<sub>2</sub> and



TABLE XXVI

ADDITION OF  $S(^3P)$  ATOMS TO TRANS-1,2-DIFLUOROETHYLENE AND ETHYLENE<sup>a</sup>PRODUCT FORMATION AS A FUNCTION OF TEMPERATURE FOR  $[C_2H_4]/[C_2F_2H_2] = 0.181$ 

Exposure Time (minutes)	$\frac{1}{T^{\circ}K} \times 10^3$	Yields, $\mu$ moles			$\frac{k_{C_2F_2H_2}}{k_{C_2H_4}}$	$\ln \frac{k_{C_2F_2H_2}}{k_{C_2H_4}}$	% yield	
		CO	$C_2H_4S^b$	$\frac{trans-C_2F_2H_2S^b}{cis-C_2F_2H_2S^b}$				
25	3.322	1.60	0.342	0.064	0.012	0.040	-3.19	26
28	2.967	1.65	0.335	0.115	0.015	0.071	-2.65	28
21	2.736	1.63	0.335	0.115	0.055	0.092	-2.39	31
26	2.755	1.67	0.324	0.133	0.028	0.091	-2.41	29
22	2.500	1.65	0.313	0.167	0.054	0.129	-2.04	32
20	2.375	1.79	0.265	0.142	0.055	0.134	-2.00	26
20	2.331	1.69	0.217	0.148	0.046	0.161	-1.82	24

a.  $P(COS) = 20.0$ ;  $P(CO_2) = 952$ ;  $P(C_2H_4) = 33.8$ ;  $P(C_2F_2H_2) = 186.5$  torr

b. Episulfides

c.  $\frac{cis-C_2F_2H_2S + trans-C_2F_2H_2S}{C_2H_4S} \times 0.181$ d.  $\frac{\Sigma(episulfides)}{CO} \times 100$

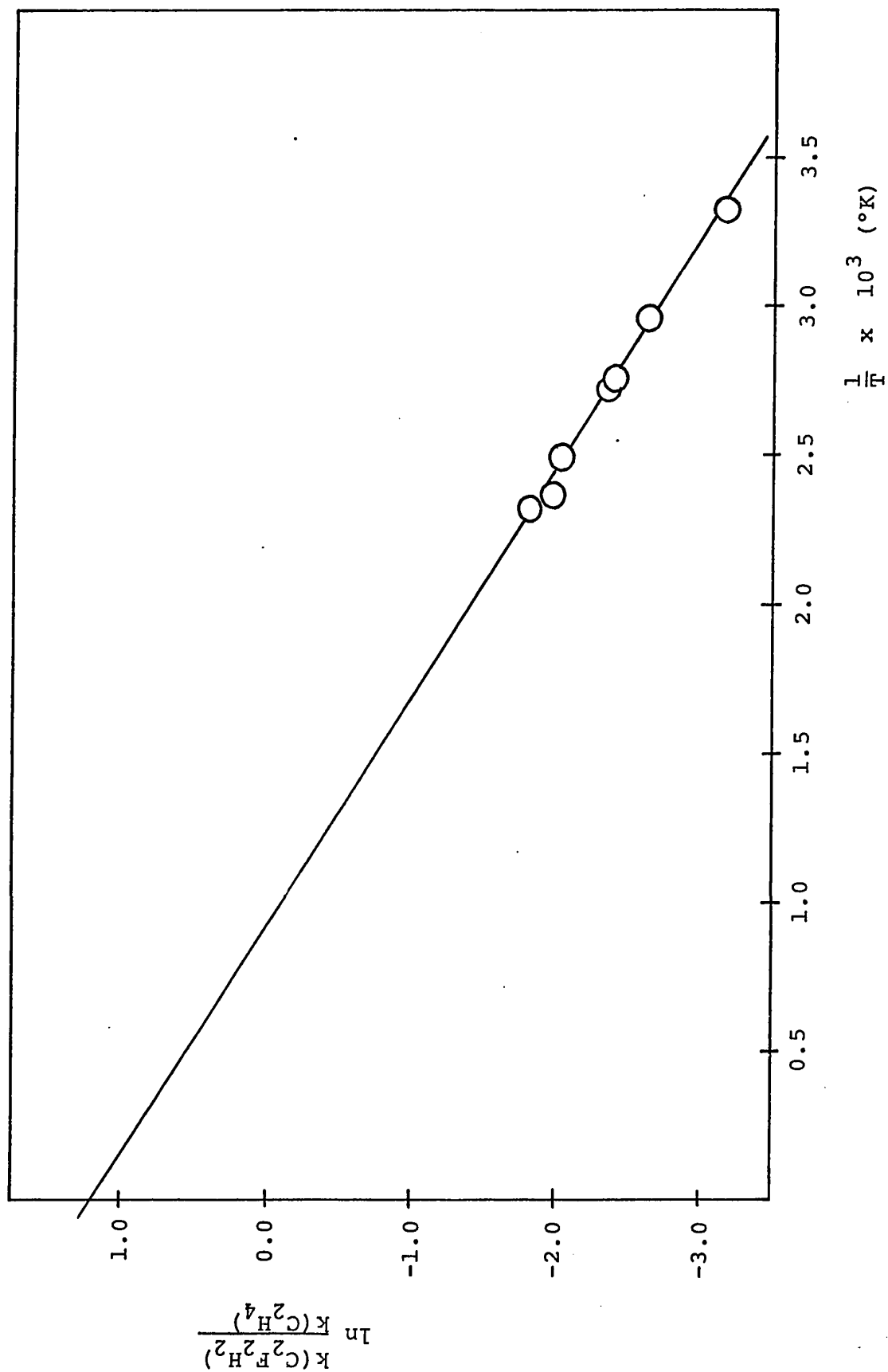


Figure 26: Addition of  $S(^3P)$  Atoms to trans-1,2-difluoroethylene and Ethylene.  
Arrhenius Plot.

49.5 torr  $C_2H_4$ . An average G.L.C. peak area of 162 units per  $\mu$ mole CO was obtained for the ethylene episulfide. A pressure of 101.5 torr  $C_2F_4$  was then added and the resulting ethylene episulfide yields are shown in Table XXVII as a function of temperature. Calculation, by the least mean squares method, of the slope and intercept of the corresponding Arrhenius plot, which is shown in Fig. 27, leads to the following values for the activation energy difference and relative A-factor:  $E(C_2F_4) - E(C_2H_4) = 1.38 \pm 0.16$  kcal mole<sup>-1</sup> and  $A(C_2F_4)/A(C_2H_4) = 1.35$  within a factor of 1.25.

### 3,3,3-Trifluoropropene - Ethylene System

The reactions of sulfur atoms with 3,3,3-trifluoropropene have not previously been studied; thus as a preliminary experiment a mixture of 20 torr COS, 1,000 torr  $CO_2$  and 50 torr  $C_3F_3H_3$  was photolyzed. G.L.C. analysis showed only one major product. The mass spectrum of this product, given in the Appendix, indicated a molecular weight of 128. It was therefore assumed to be the episulfide.

Photolysis of a mixture of 14.1 torr COS, 926 torr  $CO_2$ , 30.6 torr  $C_2H_4$  and 180 torr  $C_3F_3H_3$  at different temperatures gave the product distributions shown in Table XXVIII. Fig. 28 shows the corresponding Arrhenius plot with the slope and intercept calculated by least mean squares treatment of the data. The Arrhenius parameters

TABLE XXVII

ADDITION OF  $S(^3P)$  ATOMS TO TETRAFLUOROETHYLENE AND ETHYLENE<sup>a</sup> $C_2H_4S^b$  FORMATION AS A FUNCTION OF TEMPERATURE FOR  $[C_2H_4]/[C_2F_4] = 0.49$ 

Exposure Time (Minutes)	$\frac{1}{T^{\circ}K} \times 10^3$	CO	$\frac{C_2H_4S^e}{CO}$	$\frac{A_O - A^c}{A}$	$\frac{k_{C_2F_4}^d}{k_{C_2H_4}}$	$\ln \frac{k_{C_2F_4}}{k_{C_2H_4}}$
10	3.322	1.27	164 <sup>f</sup>	-	-	-
10	3.322	1.25	160	-	-	-
15	3.322	1.79	127	0.276	0.135	-2.00
20	2.946	2.79	121	0.339	0.170	-1.77
18	2.740	2.81	116	0.396	0.194	-1.64
11	2.288	2.20	103	0.573	0.281	-1.27
11	2.500	1.89	110	0.473	0.232	-1.46

a.  $P(COS) = 21.0$ ;  $P(CO_2) = 814$ ;  $P(C_2H_4) = 49.5$ ;  $P(C_2F_4) = 101.5$  torr

b. Ethylene - episulfide

c.  $A_O = \frac{C_2H_4S}{CO}$  in the absence of  $C_2F_4 = 162$  $A = \frac{C_2H_4S}{CO}$  in the presence of  $C_2F_4$ d.  $\frac{A_O - A}{A} \times 0.49$ 

e. Arbitrary units

f. No  $C_2F_4$  present

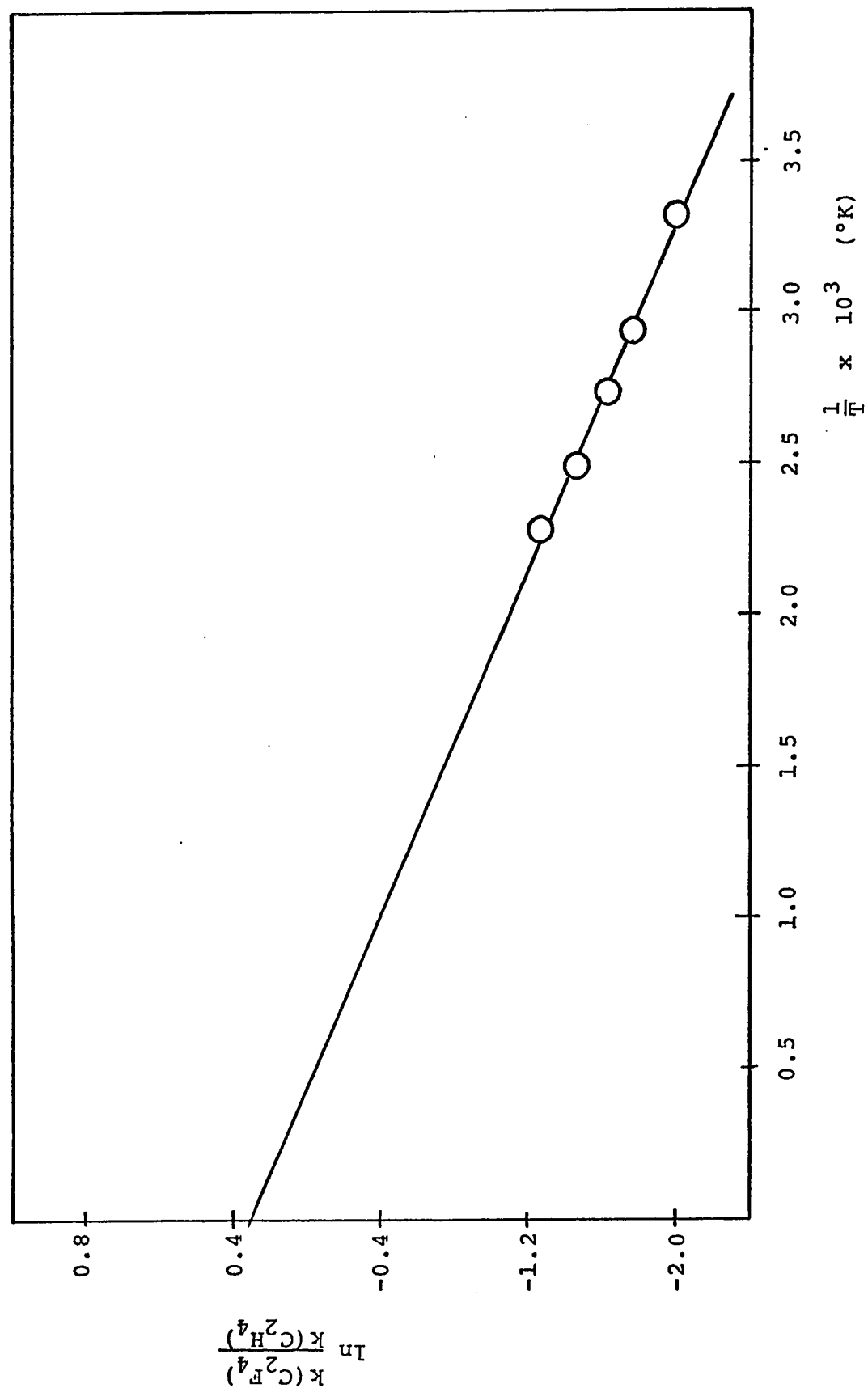


Figure 27: Addition of  $S(^3P)$  Atoms to Tetrafluoroethylene and Ethylene  
Arrhenius Plot.

TABLE XXVIII

ADDITION OF  $S(^3P)$  ATOMS TO 3,3,3-TRIFLUOROPROPENE AND ETHYLENE<sup>a</sup>

PRODUCT FORMATION AS A FUNCTION OF TEMPERATURE FOR  $[C_2H_4]/[C_3F_3H_3] = 0.170$

Exposure Time (minutes)	$\frac{1}{T^\circ K} \times 10^3$	Yields, $\mu\text{moles}$		$\frac{k_{C_3F_3H_3}^c}{k_{C_2H_4}}$	$\ln \frac{k_{C_3F_3H_3}}{k_{C_2H_4}}$	% Yield <sup>d</sup>
		CO	$C_2H_4S^b$			
25	3.322	2.14	0.783	0.484	-2.25	60
20	2.972	2.18	0.743	0.557	-2.06	60
20	2.732	2.42	0.750	0.696	-1.83	60
16	2.724	1.74	0.529	0.516	-1.80	60
18	2.513	2.21	0.695	0.739	-1.70	65
15.5	2.304	2.36	0.632	0.820	-1.51	61

a.  $P(COS) = 14.1$ ;  $P(CO_2) = 926$ ;  $P(C_2H_4) = 30.6$ ;  $P(C_3F_3H_3) = 180$  torr

b. Episulfides

c.  $\frac{C_3F_3H_3S}{C_2H_4S} \times 0.170$

d.  $\frac{\Sigma(\text{episulfides})}{CO} \times 100$

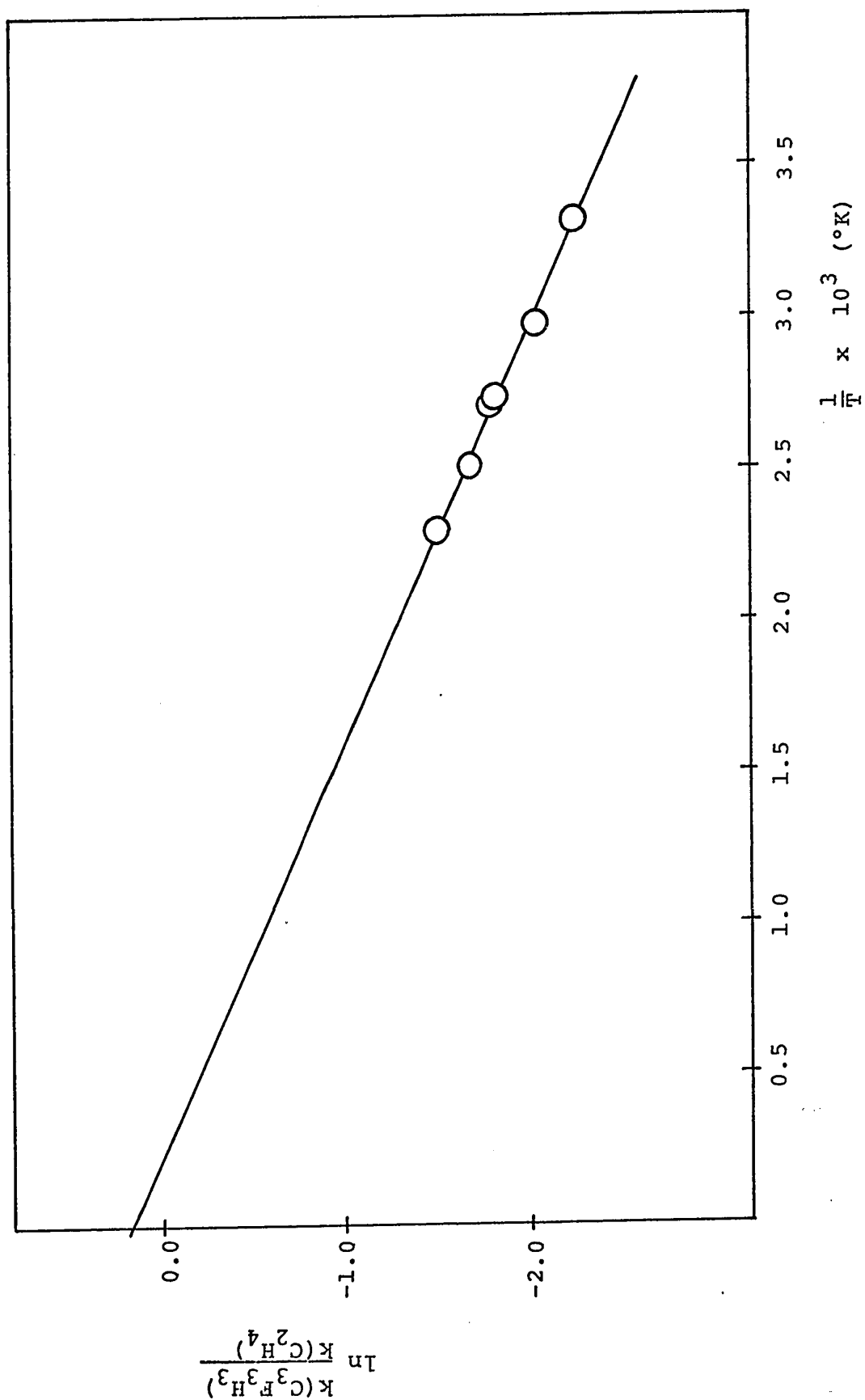


Figure 28: Addition of  $\text{S}(^3\text{P})$  Atoms to 3,3,3-trifluoropropene and Ethylene.  
Arrhenius plot.

thus calculated are  $E(C_3F_3H_3) - E(C_2H_4) = 1.46 \pm 0.16$  kcal mole<sup>-1</sup> and  $A(C_3F_3H_3)/A(C_2H_4) = 1.18$  within a factor of 1.28.

### Acetylene - Propene System

Table XXIX gives the yields of propene episulfide and the relative addition rates for acetylene and propene at different temperatures, obtained from the photolysis of a mixture of 21 torr COS, 920 torr CO<sub>2</sub>, 5.4 torr C<sub>3</sub>H<sub>6</sub> and 67.5 torr C<sub>2</sub>H<sub>2</sub>. In the light of the relative reaction rate measured in Chapter V for  $k(S + C_3H_6S)/k(S + C_3H_6)$  it would seem that the propene concentration in this system is not sufficiently high to scavenge all the S(<sup>3</sup>P) atoms and thus prevent the depletion of propene episulfide. Thus the measured value of  $A_0 = 133$  is probably too low. When acetylene is added to the system the extent of sulfur atom attack on the episulfide is lessened, making the measured value of A high with respect to  $A_0$ . Therefore, the relative rate  $k(S + C_2H_2)/k(S + C_3H_6)$  would be too low. This is borne out by the fact that the relative rate for  $k(S + C_2H_2)/k(S + C_2H_4)$  at room temperature calculated from the data in Table XXIX is 0.20, which is low compared with the value of 0.35 previously measured. Due to its lower activation energy the abstraction reaction becomes negligible, compared with addition to the substrates, as the temperature is increased. Thus at the higher temperatures the points in



TABLE XXIX

ADDITION OF  $S(^3P)$  ATOMS TO ACETYLENE AND PROPYLENE<sup>a</sup>  
 $C_3H_6S^b$  FORMATION AS A FUNCTION OF TEMPERATURE FOR  $[C_3H_6]/[C_2H_2] = 0.080$

Exposure Time (Minutes)	$\frac{1}{T^\circ K} \times 10^3$	CO	$\frac{C_3H_6S^e}{CO}$	$\frac{A_O - A^c}{A}$	$\frac{k_{C_2H_2}^d}{k_{C_3H_6}}$	$\ln \frac{k_{C_2H_2}}{k_{C_3H_6}}$
120	3.322	1.90	97	0.37	0.030	-3.51
140	2.994	2.45	81	0.64	0.051	-2.98
145	2.762	2.77	70	0.90	0.072	-2.63
135	2.532	2.91	54	1.46	0.117	-2.15
145	2.353	3.33	50	1.66	0.133	-2.02

a.  $P(COS) = 21.0$ ;  $P(CO_2) = 920$ ;  $P(C_3H_6) = 5.4$  torr;  $P(C_2H_2) = 67.5$  torr

b. Propylene - episulfide

c.  $A_O = \frac{C_3H_6S}{CO}$  in the absence of  $C_2H_2 = 133$

$A = \frac{C_3H_6S}{CO}$  in the presence of  $C_2H_2$

d.  $\frac{A_O - A}{A} \times 0.080$

e. Arbitrary units

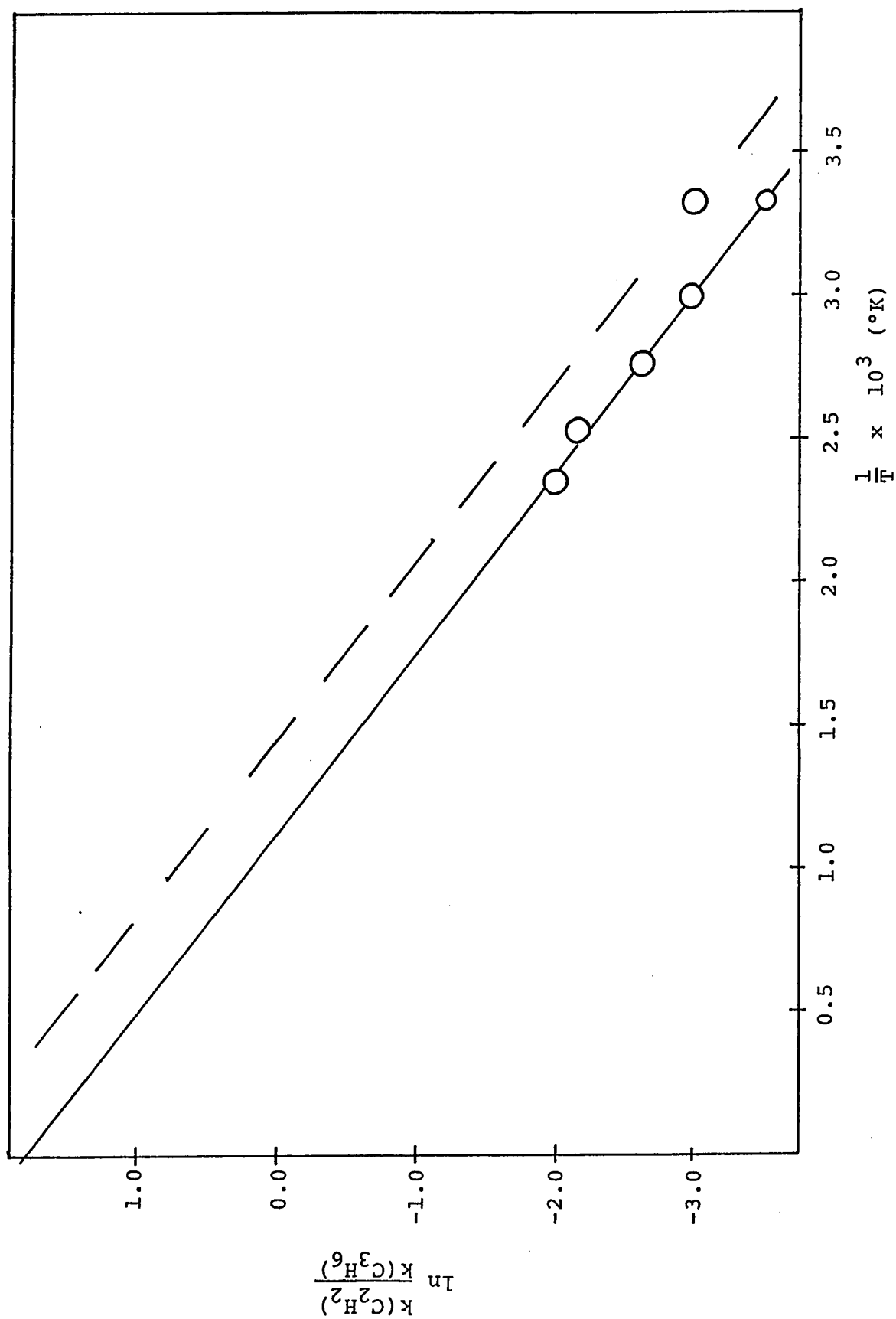


Figure 29: Addition of  $S(^3P)$  Atoms to Acetylene and Propylene.  
Arrhenius plot.

Fig. 29 are too low by a slightly larger margin than the point taken at room temperature. This would have the effect of making the measured activation energy difference slightly smaller than the true one. The measured value for the relative pre-exponential factor for acetylene, however, will be considerably lower than the true value. The values as measured are  $E(C_2H_2) - E(C_3H_6) = 3.17 \pm 0.40$  kcal mole<sup>-1</sup> and  $A(C_2H_2)/A(C_3H_6) = 6.02$  within a factor of 1.76. Thus  $E(C_2H_2) - E(C_2H_4) = 2.03$  kcal mole<sup>-1</sup> and  $A(C_2H_2)/A(C_2H_4) \geq 6.02$ . If it is assumed that the previously measured value of  $k(C_2H_2)/k(C_2H_4) = 0.35$  at 27°C is correct, the dotted line can be drawn in Fig. 29. through this point with a slope equal to that of the measured line. This corrected line leads to a value of  $A(C_2H_2)/A(C_2H_4) = 10.3$ . Since the Arrhenius parameters for methylacetylene were measured using the same value of  $A_0 = 133$ , either value of the A-factor is valid for comparative purposes.

#### Methylacetylene - Propene System

As in the previous system, the relative Arrhenius parameters were determined by measuring the propene epoxide yield as a function of temperature assuming the yield to be 133 G.L.C. peak area units per  $\mu$ mole CO (about 40% scavenging) in the absence of methylacetylene. The photolysis mixture consisted of 22.1 torr COS, 915 torr CO<sub>2</sub>, 10.4 torr C<sub>3</sub>H<sub>6</sub> and 11.6 torr C<sub>3</sub>H<sub>4</sub>. Table XXX gives

TABLE XXX

ADDITION OF  $S(^3P)$  ATOMS TO METHYLACETYLENE AND PROPYLENE<sup>a</sup> $C_3H_6$ <sup>b</sup> FORMATION AS A FUNCTION OF TEMPERATURE FOR  $[C_3H_6]/[C_3H_4] = 0.897$ 

Exposure Time (minutes)	$\frac{1}{T^{\circ}K} \times 10^3$	CO	$\frac{C_3H_6S^e}{CO}$	$\frac{A_O - A^c}{A}$	$\frac{k_{C_3H_4}^d}{k_{C_3H_6}}$	$\frac{k_{C_3H_4}}{\ln k_{C_3H_6}}$
135	3.322	1.55	106	0.25	0.22	-1.51
150	2.967	2.06	97	0.37	0.33	-1.11
150	2.747	2.26	94	0.41	0.37	-0.99
138	2.538	2.25	85	0.56	0.50	-0.69
140	2.336	2.82	79	0.68	0.61	-0.49

a.  $P(COS) = 22.1$ ;  $P(CO_2) = 915$ ;  $P(C_3H_6) = 10.4$ ;  $P(C_3H_4) = 11.6$  torr

b. Propylene - episulfide

c.  $A_O = \frac{C_3H_6S}{CO}$  in the absence of  $C_3H_4 = 133$  $A = \frac{C_3H_6S}{CO}$  in the presence of  $C_3H_4$ d.  $\frac{A_O - A}{A} \times 0.897$ 

e. Arbitrary units

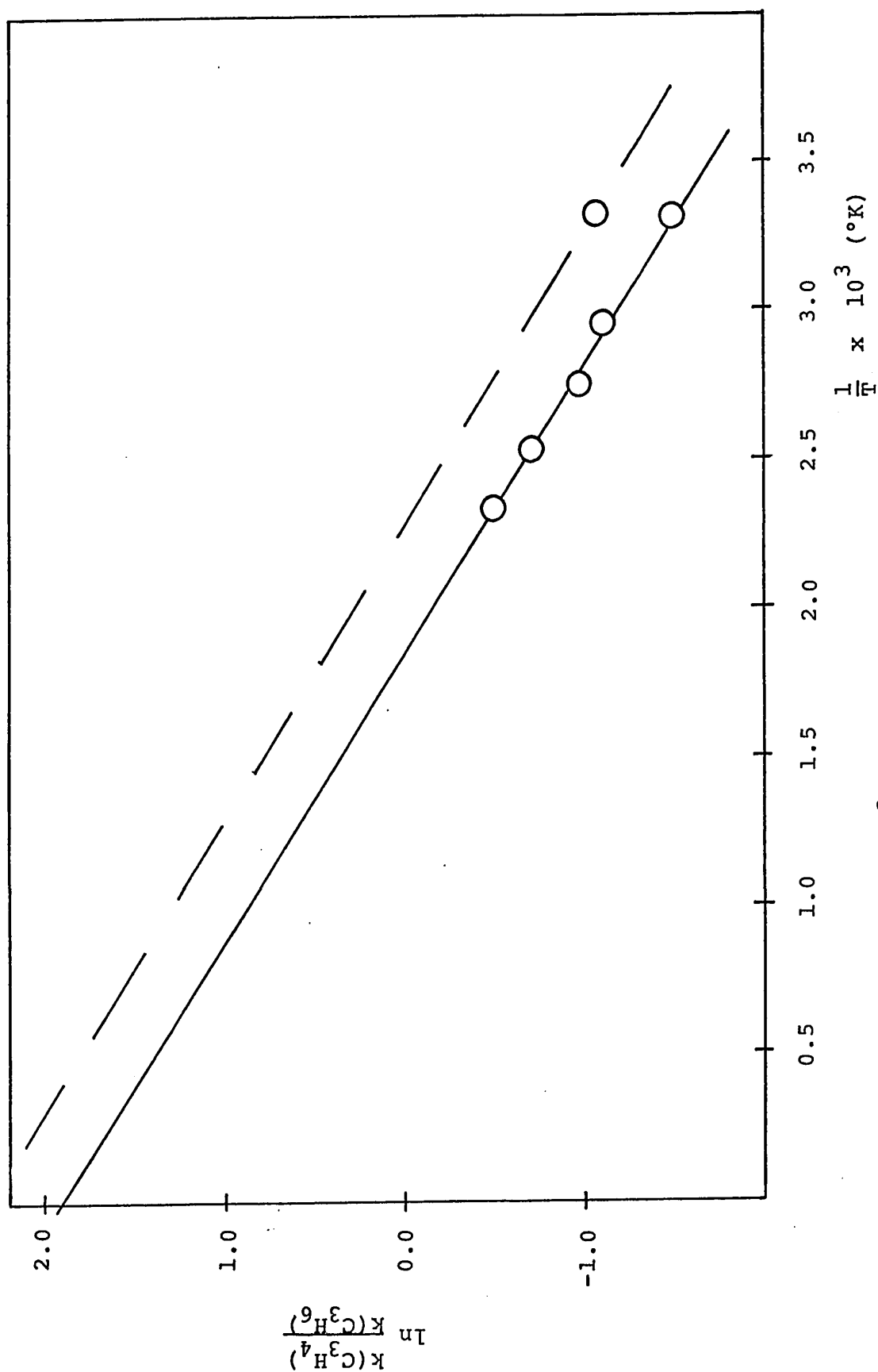


Figure 30: Addition of S(<sup>3</sup>P) Atoms to Methylacetylene and Propylene.

Arrhenius plot.

the relevant data. The slope and intercept of the corresponding Arrhenius plot in Fig. 30 were calculated by the method of least mean squares and yielded the following parameters:  $E(C_3H_4) - E(C_3H_6) = 2.03 \pm 0.27 \text{ kcal mole}^{-1}$  and  $A(C_3H_4)/A(C_3H_6) = 6.61$  within a factor of 1.50. Thus relative to ethylene we get  $E(C_3H_4) - E(C_2H_4) = 0.89 \text{ kcal mole}^{-1}$  and  $A(C_3H_4)/A(C_2H_4) = 6.61$ . In this system, with a pressure of 10.4 torr  $C_3H_6$  the secondary reaction of sulfur atoms with propene episulfide is probably negligible; however since the value of  $A_0 = 133$  is too low, the relative rate constants at each temperature will be too low and consequently so will the A-factor. The measured activation energy difference is probably correct. If the relative rate which was previously measured i.e.  $k(C_3H_4)/k(C_2H_4) = 2.30$  at room temperature is taken to be correct and the dotted line in Fig. 30 is drawn through it with a slope equal to the measured line we get a relative A-factor of  $A(C_3H_4)/A(C_2H_4) = 10.2$ . This value will be very close to the time value.

#### Dimethylacetylene - Cyclopentene System

The Arrhenius parameters for  $S(^3P)$  addition to dimethylacetylene were measured relative to those for cyclopentene by measuring the yields of the episulfide of the latter compound as a function of temperature in a photolysis mixture consisting of 26.6 torr COS, 912 torr

TABLE XXXI

ADDITION OF  $S(^3P)$  ATOMS TO DIMETHYLACETYLENE AND CYCLOPENTENE<sup>a</sup> $C_5H_8$ <sup>b</sup> FORMATION AS A FUNCTION OF TEMPERATURE FOR  $[C_5H_8]/[C_4H_6] = 2.16$ 

Exposure Time (minutes)	$\frac{1}{T^\circ K} \times 10^3$	CO	$\frac{C_5H_8S^e}{CO}$	$\frac{A - A^c}{A}$	$\frac{k_{C_4H_6}^d}{k_{C_5H_8}}$	$\frac{k_{C_4H_6}}{\ln k_{C_5H_8}}$
160	3.278	1.41	164	0.494	1.067	0.058
160	2.985	1.54	163	0.503	1.086	0.086
173	2.735	2.04	153	0.601	1.298	0.262
155	2.544	1.83	144	0.701	1.514	0.412
150	2.370	2.35	147	0.667	1.440	0.364

a.  $P(COS) = 26.6$ ;  $P(CO_2) = 912$ ;  $P(C_5H_8) = 14.9$ ;  $P(C_4H_6) = 6.9$  torr

b. Cyclopentene - episulfide

c.  $A_O = \frac{C_5H_8S}{CO}$  in the absence of  $C_4H_6 = 245$  $A = \frac{C_5H_8S}{CO}$  in the presence of  $C_4H_6$ d.  $\frac{A_O - A}{A} \times 2.16$ 

e. Arbitrary units

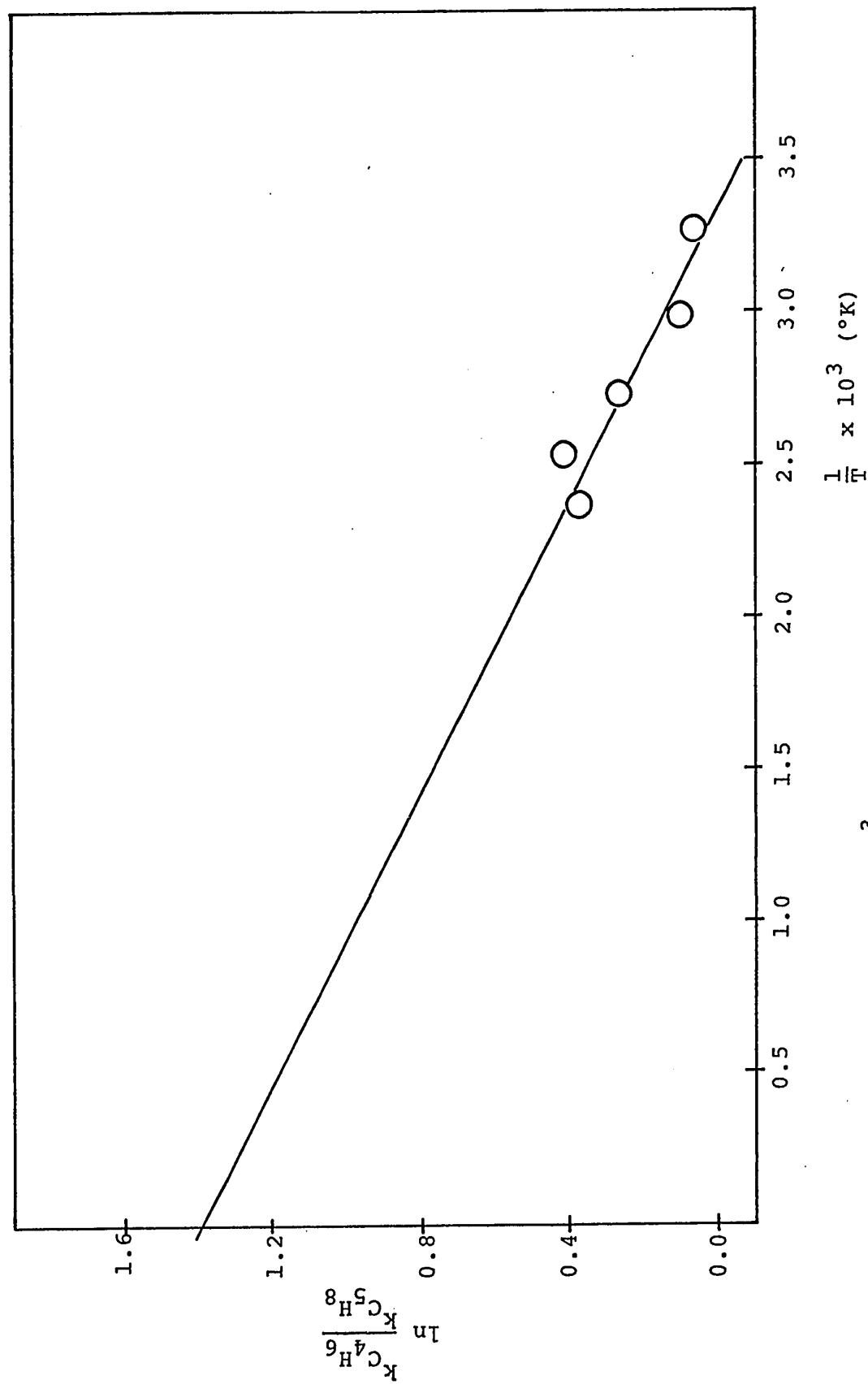


Figure 31: Addition of  $S(^3P)$  Atoms to Dimethylacetylene and Cyclopentene.  
Arrhenius plot.



CO<sub>2</sub>, 14.9 torr C<sub>5</sub>H<sub>8</sub> and 6.9 torr C<sub>4</sub>H<sub>6</sub>. Table XXXI gives the yields and relative reaction rates at each temperature. The corresponding Arrhenius plot is shown in Fig. 31 along with the slope and intercept obtained by the method of least mean squares. The resulting parameters are as follows:  $E(C_4H_6) - E(C_5H_8) = 0.83 \pm 0.40 \text{ kcal mole}^{-1}$  and  $A(C_4H_6)/A(C_5H_8) = 4.03$  within a factor of 1.82. Therefore, relative to ethylene, one gets  $E(C_4H_6) - E(C_2H_4) = -1.32 \text{ kcal mole}^{-1}$  and  $A(C_4H_6)/A(C_2H_4) = 2.70$ .

### Discussion

The relative rates and Arrhenius parameters for S(<sup>3</sup>P) addition to the three classes of substrates olefinic hydrocarbons, halogenated olefins and acetylenes are summarized in Table XXXII. Comparison of the second and third columns in the table demonstrates the generally excellent agreement between independently measured values of the relative rates. The increase in reactivity, upon successive methylation of the double bond, clearly reveals the electrophilic nature of S(<sup>3</sup>P) atoms in their addition reactions with olefins. Similarly, substitution of a halogen atom for hydrogen in ethylene causes a drastic decrease in reactivity, indicating a pronounced correlation between the reactivity and the electron density of the double bond. This electrophilic trend in the reactions of ground state sulfur atoms is not surprising in view of the

TABLE XXXII

RELATIVE RATES AND ARRHENIUS PARAMETERS FOR S(<sup>3</sup>P) ADDITIONS

	$k/k_{\text{Eth}}^a$	$k/k_{\text{Eth}}^b$	$E_{\text{Eth}} - E$	$A/A_{\text{Eth}}$
$\text{CH}_2=\text{CH}_2$	1.0	1.0	0.0	1.0
$\text{CH}_3-\text{CH}=\text{CH}_2$	6.8	6.7	1.14	1.0
cis $\text{CH}_3-\text{CH}=\text{CH}-\text{CH}_3^c$	18	17	2.09	0.53
trans $\text{CH}_3-\text{CH}=\text{CH}-\text{CH}_3^c$	23	18	2.01	0.65
$\text{CH}_3\cdot\text{CH}_2-\text{CH}=\text{CH}_2^c$	11	-	-	-
$(\text{CH}_3)_2\text{C}=\text{CH}_2$	54	50	2.36	0.97
$(\text{CH}_3)_2\text{C}=\text{CH}(\text{CH}_3)$	88	77	3.01	0.51
$(\text{CH}_3)_2\text{C}=\text{C}(\text{CH}_3)_2$	131	135	3.36	0.50
$\text{CH}_2=\text{CH}-\text{CH}=\text{CH}_2$	77	72	2.04	2.4
$\text{CH}_3\text{CH}_2\text{C}(\text{CH}_3)=\text{CH}_2^c$	63	87	2.83	0.78
$\text{CH}_3\text{CH}_2\text{CH}_2=\text{CH}_2^c$	11	13	1.72	0.75
$\text{C}-\text{C}_5\text{H}_8^c$	21	24	2.15	0.67
$\text{CH}_2=\text{CHF}^d$	-	0.42	-0.73	1.40
cis $\text{CHF}=\text{CHF}$	-	0.018	-2.71	1.66
trans $\text{CHF}=\text{CHF}$	-	0.043	-2.62	3.36
$\text{CF}_2=\text{CH}_2^d$	-	0.10	-1.7	1.9
$\text{CF}_2=\text{CFH}^d$	-	0.07	-2.0	2.1
$\text{CF}_2=\text{CF}_2$	-	0.14	-1.38	1.35
$\text{CH}_3\text{CF}=\text{CH}_2$	2.6	-	-	-
$\text{CF}_3\text{CH}=\text{CH}_2$	-	0.104	-1.46	1.18
$\text{CF}_3(\text{CH}_3)\text{C}=\text{CH}_2$	1.2	-	-	-
$\text{CF}_3\text{CF}_2-\text{CH}=\text{CH}_2$	0.094	-	-	-
$\text{SiF}_3-\text{CH}=\text{CH}_2$	0.4	-	-	-
$\text{CH}_2=\text{CHCl}$	1.4	1.4	-0.52	3.4
trans $\text{CHCl}=\text{CHCl}$	>4.6	-	-	-

TABLE XXXII (continued)

	$k/k_{\text{Eth}}^{\text{a}}$	$k/k_{\text{Eth}}^{\text{b}}$	$E_{\text{Eth}} - E$	$A/A_{\text{Eth}}$
$\text{CH}\equiv\text{CH}$	0.35		-2.03	6.2
$\text{CH}_3-\text{C}\equiv\text{CH}$	2.3		-0.89	6.2
$\text{CH}_3-\text{C}\equiv\text{C}-\text{CH}_3$	29	24	1.32	2.7

a. Measured at 27°C

b. Calculated from Arrhenius parameters

c. Taken from Ref. (60)

d. Taken from Ref. (59)

relative addition rates for the other group VI atoms, O and Se, shown in Table I. On the Pauling scale, the electronegativities of O, S and Se are 3.5, 2.5 and 2.4 respectively (63).

Since the factors affecting the electron density distribution are different in all three classes of substrates measured, it seems best to discuss each class separately. Furthermore, since the relative rates of addition are determined by two independently contributing factors, the activation energy and the A-factor, these parameters will be discussed separately for each class of compound.

#### A) Activation Energy

##### i) Olefinic Hydrocarbons

The existence of an activation energy for radical additions to unsaturated compounds implies an initial repulsion between the two species as they approach along the reaction co-ordinate. This treatment, which was first proposed by Evans (64) and later adopted by Szwarc (65) to explain the reactivities of methyl radicals with aromatic compounds and olefins is shown diagrammatically in Fig. 32. As the reacting species come closer together, various electronic rearrangements take place within the molecule which enable crossover to

an attractive surface to take place at points A, B, C, etc.  
The height of this barrier then constitutes the activation

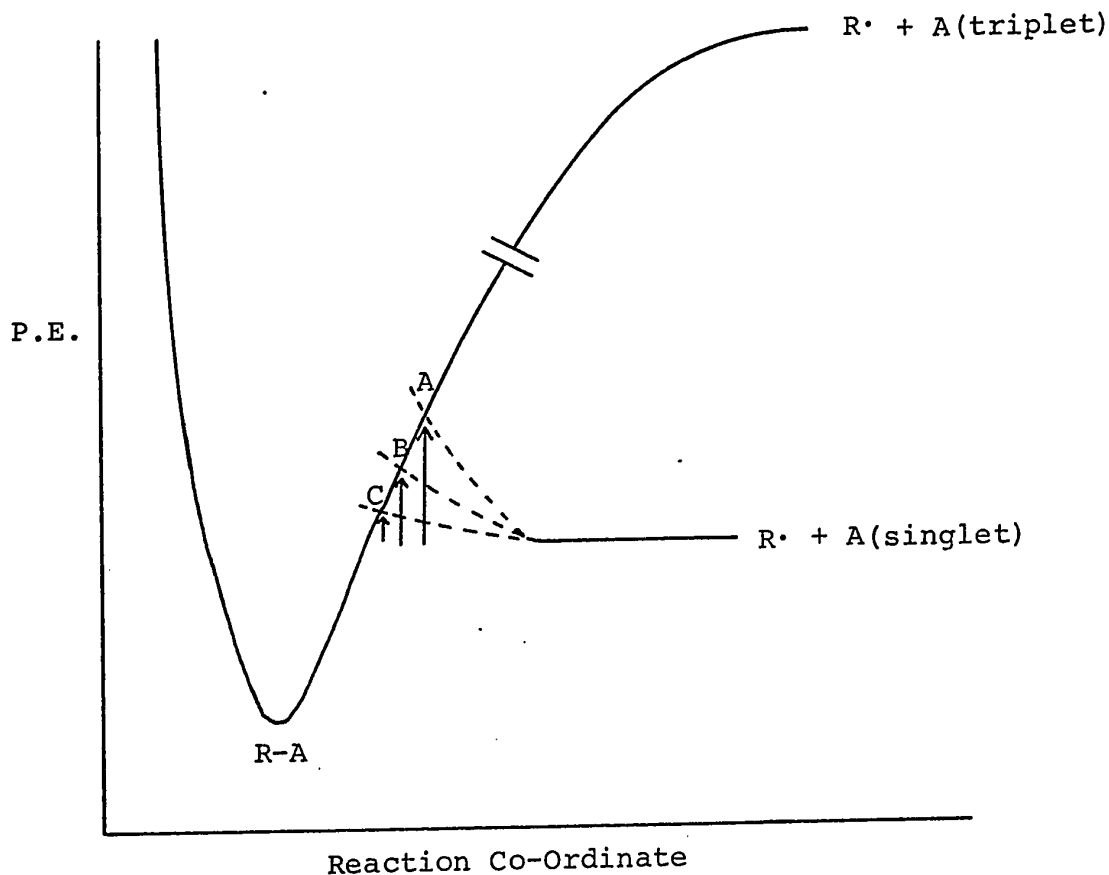


Figure 32

energy. Assuming for the moment, that the dissociation energy of the newly formed bond remains the same for a series of substrates and therefore, leaving the depth and contour of the attractive surface invariant in Fig. 32, we can see how the activation energy is affected by substituents which influence the charge distribution and polarization in the transition state by the change in the slope of the repulsive

curve. This effect, however, will only be present when the attacking free radical is electrophilic or nucleophilic in character. Methyl or ethyl substituents, by means of their electron-donating inductive effect increase the electron density in the double bond, thus increasing its polarizability, and thereby lowering the activation energy for addition of electrophilic reagents. Table XXXIII gives the activation energies for the addition to olefins relative to ethylene for some electrophilic reagents, along with those for methyl radicals, the latter being a typical member of the "free radical" type reagents which include  $\cdot\text{C}_2\text{H}_5$ ,  $\cdot\text{CCl}_3$ ,  $:\text{CH}_2^{(1)}$ ,  $:\text{CH}_2^{(3)}$  and H atoms. The activation energies of the electrophilic reagents all undergo a substantial decrease upon substitution of a methyl group in sharp contrast to those for  $\cdot\text{CH}_3$  addition. A linear correlation between activation energy and ionization potential, the latter being a rough measure of polarizability in the substrate molecule, is therefore anticipated for the electrophilic reagents and Fig. 33 shows such a plot for the addition of  $\text{S}^{(3\text{P})}$  atoms. This relationship also holds true for the other electrophilic reagents  $\text{O}^{(3\text{P})}$  (10),  $\text{Se}^{(3\text{P})}$  (14) and  $\text{CF}_3$  (29). In the case of Se atom addition, the relationship is not linear, but the activation energy nevertheless decreases monotonously with the ionization potential.

TABLE XXXIII  
RELATIVE ACTIVATION ENERGIES<sup>a</sup> FOR ADDITIONS TO HYDROCARBON OLEFINS

	O( <sup>3</sup> P) <sup>b</sup>	S( <sup>3</sup> P)	Se( <sup>3</sup> P) <sup>c</sup>	C <sub>2</sub> O( <sup>3</sup> Σ) <sup>d</sup>	CF <sub>3</sub> <sup>e</sup>	CH <sub>3</sub> <sup>f</sup>
Ethylene	0.0	0.0	0.0	0.0	0.0	0.0
Propene	-	1.14	0.47	1.2	0.41	-0.03
1-butene	1.2	-	0.56	1.8	-	-
cis-2-butene	-	2.09	1.60	1.7	1.10	-
trans-2-butene	-	2.01	2.22	2.3	1.11	-
Isobutene	2.1	2.36	1.80	2.8	1.17	0.26
2-methyl-2-butene	2.5	3.01	-	4.0	-	-
2,3-dimethyl-2-butene	2.6	3.36	-	4.4	1.60	-
1,3-butadiene	1.8	2.04	1.93	2.9	1.43	2.12
Cyclopentene	2.0	2.15	-	-	0.15	-

a) E<sub>eth</sub>-E;      b) Ref. 10;      c) Ref. 14;

d) Ref. 21;      e) Ref. 29, 28;      f) Ref. 26

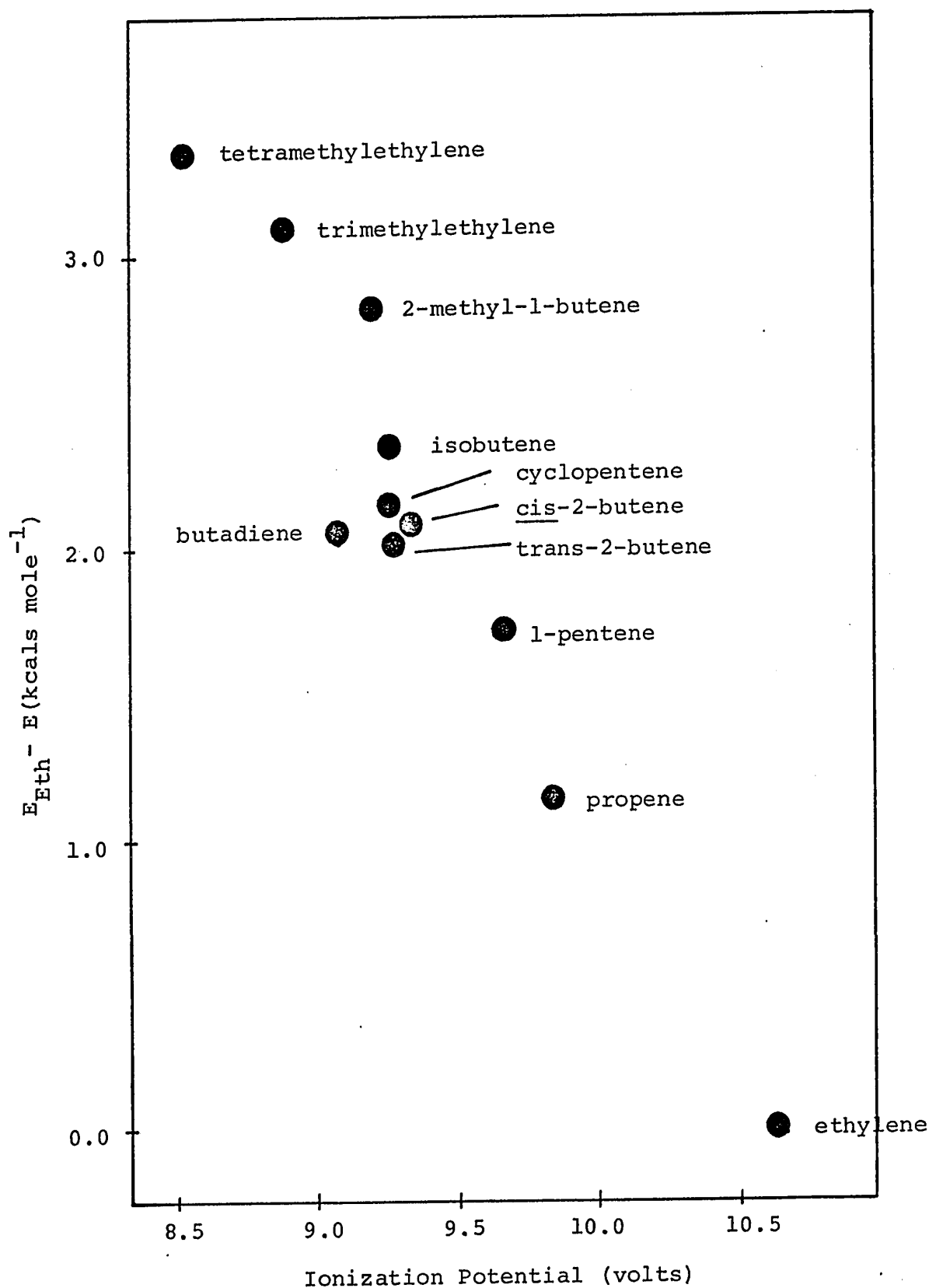


Figure 33: Plot of Ionization Potentials versus Activation Differences for  $S(3p)$  Addition to Olefins. Ionization Potentials taken from References 66, 67, 68.



The second effect responsible for the variations in activation energies is the mesomeric effect, which includes resonance and hyperconjugation originated by Mulliken and co-workers (69). This effect plays the predominant role in determining the activation energy for "free radical" type addition reactions, and must also be operative, though to a lesser extent, in additions of electrophilic reagents. Also, its influence on the additions of monoradicals should be much greater than on those of diradicals, since in the monoradical reaction the mesomeric effect should contribute significantly to the stabilization of the adduct radical.

Resonance involves the rearrangement of the electron pairs in an unsaturated molecule and only occurs in conjugated molecules or in molecules containing non-bonding electron pairs. Thus in Table XXXIII, the only molecule exhibiting this phenomenon is 1,3-butadiene. Each of the two  $\pi$ -bonds in butadiene is stabilized relative to the  $\pi$ -bond in ethylene by delocalization. When a monoradical adds to a conjugated molecule, the resultant adduct radical is resonance-stabilized by delocalization of the unpaired electron. The stabilization energy in this adduct radical relative to the corresponding ethylenic adduct is greater than that of butadiene relative to ethylene. The net effect of resonance therefore, is to decrease the bond-energy of the  $\pi$ -bond to be broken, thus

causing a decrease in the activation energy of the addition reaction. This effect can be seen in Table XXXIII for the case of methyl radical addition and it is a common feature of all "free radical" type reagents that their relative addition rate is very much higher for 1,3-butadiene than for the monoolefins, as shown in Table I in the Introduction.

The addition rates of monoradicals such as  $\text{Ph.CO.O.O.}$  (70),  $\text{CCl}_3$  (71),  $\text{CH}_3$  (72),  $\text{CF}_3$  (27) and  $\text{C}_2\text{H}_5$  (25) to aromatic compounds increase rapidly with the size of the molecule and consequently with the extent of conjugation. This marked increase is due predominantly to the resonance effect - the greater the extent of delocalization energy, the lower the activation energy. These molecules show approximately the same variations in reactivity for strongly electrophilic monoradicals like  $\text{CF}_3$  as for the "free radical" types, since the electron density is the same in all compounds. Szwarc (27) has shown that the "intrinsic selectivity" of the  $\text{CF}_3$  radical relative to that of  $\cdot\text{CH}_3$  - that is, the slope of the  $\log k(\text{CF}_3)/n$  versus  $\log k(\text{CH}_3)/n$  plot, where  $k$  represents the rate constant for addition to a series of unsubstituted aromatics and  $n$  is the number of reactive sites in a given molecule - is 0.8. In the additions of these radicals to monoolefins, as Table I indicates, the selectivity is markedly reversed; this is clear evidence that in additions of electrophilic

reagents, the inductive effect heavily outweighs the mesomeric effect in its influence on the activation energy.

Hyperconjugation occurs in a molecule when there is overlap between a p-or  $\Pi$ -orbital, occupied or otherwise, and the C-H  $\sigma$ -bond of an adjacent carbon atom. For overlap to occur the C-H bond must be approximately parallel to the p-or  $\Pi$ -orbital; thus, in a monoolefin, hyperconjugation can only occur with allylic hydrogens. Therefore the amount of hyperconjugation increases as the number of methyl groups substituted on the double bond increases. For additions of monoradicals to olefins, hyperconjugation has the same effect on the reactivity as resonance, i.e. through delocalization of the  $\Pi$ -electrons, the  $\Pi$ -bond is strengthened relative to ethylene. Also, on the resulting adduct radical, the unpaired electron is delocalized, causing stabilization. Thus hyperconjugation in trans-2-butene is analogous with the resonance effect in 1,3-butadiene, although the delocalization is not as pronounced. The influence of hyperconjugation in lowering the activation energy of monoradical additions is most strongly felt in isobutene where the unpaired electron in the adduct radical is located on the substituted carbon atom and can thus be delocalized over three carbon atoms. The same delocalization occurs in the adduct radical arising from addition to trimethylethylene and tetramethylethylene; however, in these cases the hyperconjugative delocalization in the substrate

molecule extends over 5 and 6 carbon atoms respectively, so that more energy is required to disrupt the  $\Pi$ -bond. For monoradical additions to monoolefins, therefore, the activation energy is lowest for isobutene, while that for trimethylethylene is somewhat lower than that for tetramethylethylene. For the same reason the reactivity of propene is greater than that of the 2-butenes. This effect is seen in Table I, especially in the relative rates of addition of H atoms, where the effect of steric hindrance is negligible, and contrasts with the trend in the corresponding relative rates of electrophilic reagents where the reverse order is observed.

Considering now the addition of diradicals to olefins, two different cases arise - addition by formation of two bonds simultaneously, and addition to form a diradical. In the former case the net effect of resonance or hyperconjugation will be to strengthen the  $\Pi$ -bond in the olefin relative to ethylene thus raising the activation energy, since there is no unpaired electron in the primary adduct. Where formation of an open diradical occurs, in which case the reaction is non-stereospecific, the unpaired electrons may be delocalized by the mesomeric effect resulting in a lower activation energy. The mesomeric effect affords therefore a possible explanation for the different trends in reactivity of singlet and triplet states of the same species. Table XXXIV shows a

TABLE XXXIV

## RELATIVE REACTIVITIES OF SINGLET AND TRIPLET SPECIES WITH OLEFINS

	$1_{CH_2}^c$ (24°C)	$3_{CH_2}^c$ (24°C)	$1_{C_2O}^d$ (30.5°C)	$3_{C_2O}^d$ (25°)	$3_{Cae}$	$3_{Cbe}$
Ethylene	1.0	1.0	1.0	1.0	-	-
Propene	1.31	1.0	1.2	6.1	1.0	1.0
1-butene	1.65	1.6	-	7.0	-	-
cis-2-butene	1.44	0.94	1.9	10.1	3.0	1.25
trans-2-butene	1.46	0.89	-	11.4	6.4	0.13
Isobutene	1.85	2.9	-	58	6.0	0.75
2-methyl-2-butene	2.16	1.8	-	100	-	-
2,3-dimethyl-2-butene	2.09	2.7	2.1	250	-	-
1,3-butadiene	3.20	19	2.4	210	0.2	2.5

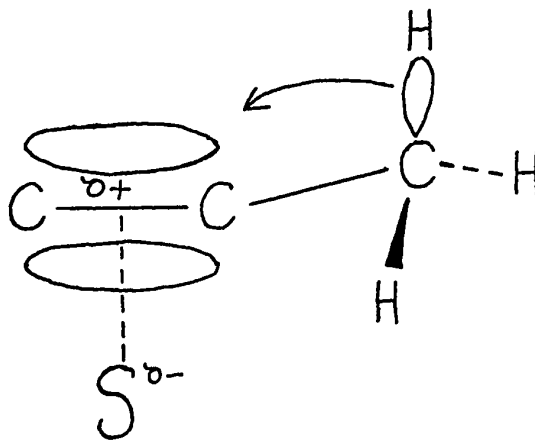
a) stereospecific; b) nonstereospecific; c) Ref. 16;

d) Ref. 21 e) Ref. 73

comparison of these reactivities for  $\text{CH}_2$ ,  $\text{C}_2\text{O}$  and C atoms.  $^3\text{CH}_2$  is known to form a diradical on addition to ethylene (74), while the singlet species probably forms a bond simultaneously with both carbon atoms of the olefin. For the addition of  $^3\text{CH}_2$ ,  $k(2\text{-butene}) < k(\text{propene})$ , while the opposite is true for  $^1\text{CH}_2$ . Also,  $^3\text{CH}_2$  reacts more slowly with trimethylethylene and tetramethylethylene than with isobutene, while again the reverse order holds for  $^1\text{CH}_2$ . Finally, for  $^3\text{CH}_2$   $k(\text{butadiene})/k(\text{ethylene}) \approx 19$ , while for  $^1\text{CH}_2$  the ratio is  $< 4$ . Carbon atoms add to olefins in two steps, the first stereospecific and the second non-stereospecific (73). For the addition of the first olefin to a carbon atom,  $k(\text{butadiene})/k(\text{propylene}) = 0.2$  while for the non-stereospecific addition the same ratio is 2.5. Also for the addition of  $^3\text{C}_2\text{O}$ ,  $k(\text{butadiene})/k(\text{ethylene})$  is 210, while for  $^1\text{C}_2\text{O}$  it is 2.4. It is unlikely that the changes in reactivity are due to the pre-exponential factor, as the same variations in A-factor would be expected in both the singlet and the triplet case. Kryzanowski and Cvetanovic (16) have attributed the lower selectivity of singlet methylene, as compared with the triplet, to its excess energy; this may well be true but it does not explain the reversals in the order of reactivity of certain olefins,  $\text{S}(^1\text{D})$  atoms have been shown to be less selective than  $\text{S}(^3\text{P})$  atoms (60) but their relative rate of addition to butadiene is not known. For the more

electrophilic divalent reagents, however, the effect of resonance and hyperconjugation in stabilizing the primary adduct is outweighed by its effect on the initial  $\Pi$ -complex so that, from the relative rates, it is not possible to distinguish between a one-step and a two-step addition. A knowledge of the relative rates of addition to aromatic hydrocarbons, where the electron density remains constant throughout the series might be helpful in this regard.

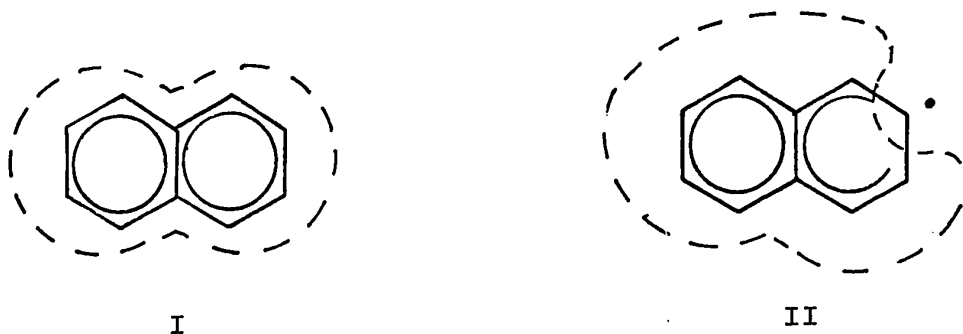
The mesomeric effect increases the polarizability of the olefin in the  $\Pi$ -complex and thus enhances the inductive effect in lowering the activation energy for the addition, as shown in the following diagram for the propylene-sulfur  $\Pi$ -complex.



Through hyperconjugation, the partial positive charge on the double bond is delocalized, thus lowering the energy of the  $\Pi$ -complex. A similar explanation can be invoked to explain the low activation energy for addition of  $S(^3P)$  atoms to butadiene as compared with ethylene.

The inductive effect of the vinyl group in butadiene cannot be operative since it is opposed by that of the other vinyl group. Thus the low activation energy must be due to the delocalization of the partial positive charge in the transition state through resonance interactions.

Coulson et al (75, 76) have established the resonance and hyperconjugation effects on a semi-quantitative basis by calculating the Atom Localization Energy from M.O. theory for a specific carbon atom in a molecule. This is the energy necessary to localize 2, 1 or 0 electrons on the carbon atom, depending on whether the attacking species is a cation, free radical or anion. Thus it is the difference in resonance energy between the unperturbed molecule and a hypothetical structure as, for example, in free radical addition to carbon 2 in naphthalene:

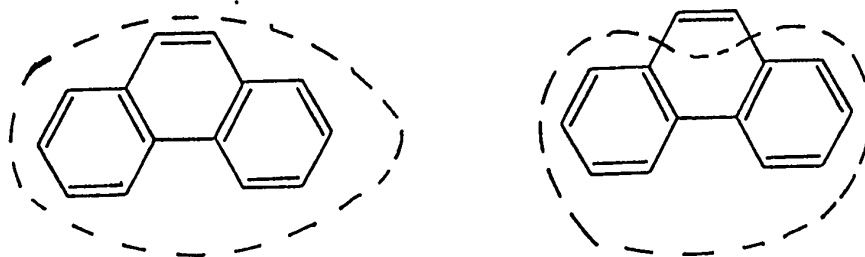


$$\text{A.L.E.} = \text{R.E. (I)} - \text{R.E. (II)}$$

The dotted line encloses the resonating framework. Bond Localization Energy has been defined (77) as the energy required to localize two electrons in a particular bond



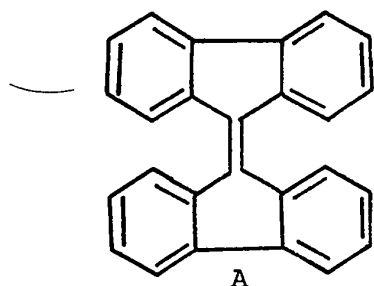
apart from the resonating framework of the molecule, as for example, in the  $C_9 - C_{10}$  bond in phenanthrene:



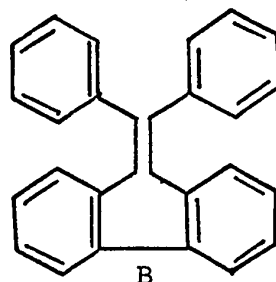
$$B.L.E. = R.E.(\text{Phenanthrene}) - 2 R.E.(\text{Benzene})$$

Coulson (76) has calculated the Localization Energies for the most reactive carbon in a series of unsubstituted aromatic compounds and on comparing them with the methyl affinities of these compounds, as measured by Szwarc (23, 24, 78), found an excellent linear relationship between L.E. and  $\log k/n$ , where  $k$  is the methyl affinity and  $n$  is the number of reactive sites in the molecule. The activation energies have not been measured and the above relationship implies a constant pre-exponential factor in the aromatic series. A similar correlation has been found to hold for the relative addition rates to aromatic compounds of  $\cdot C_2H_5$  (25),  $CCl_3$  (71), Styryl (78) and  $\cdot CF_3$  (27) radicals. Since the bond lengths are all equal in these compounds the localization energies are of the form  $C\beta$  where  $\beta$ , the overlap integral is constant

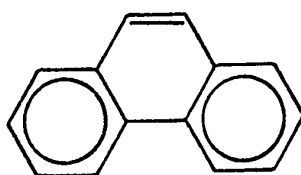
and C is calculated. Szwarc (79) has measured the methyl affinities with aromatically substituted olefins where the double bonds are either longer or shorter than normal or the p-orbitals are twisted so that the overlap integral  $\beta$  is a variable. These methyl affinities show a dramatic dependence on the extent of overlap and, consequently, on the magnitude of the localization energy as shown in the examples below:



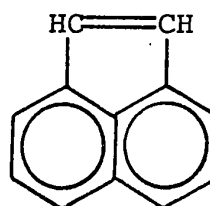
$$k_{\text{rel}} = 15$$



$$k_{\text{rel}} = 1,370$$



$$k_{\text{rel}} = 27$$



$$k_{\text{rel}} = 1,030$$

In compound B the bottom half of the molecule is twisted from the plane of the top half, decreasing the overlap and thus the localization energy, relative to A where the double bond is not twisted. In C, the double bond has a normal bond length while in D the bond is stretched.

$\log (k/n)$  for these radicals is also linearly related to the spectroscopically observed singlet-triplet excitation energy of the aromatic molecule (78), this parameter being, like the localization energy, a relative measure of the strength of the  $\pi$ -bond to be broken.

To understand better the relations discussed above it is desirable to consider the details of the addition reaction in terms of the energy-distance diagram originally proposed by Evans and Polanyi (87) and shown below:

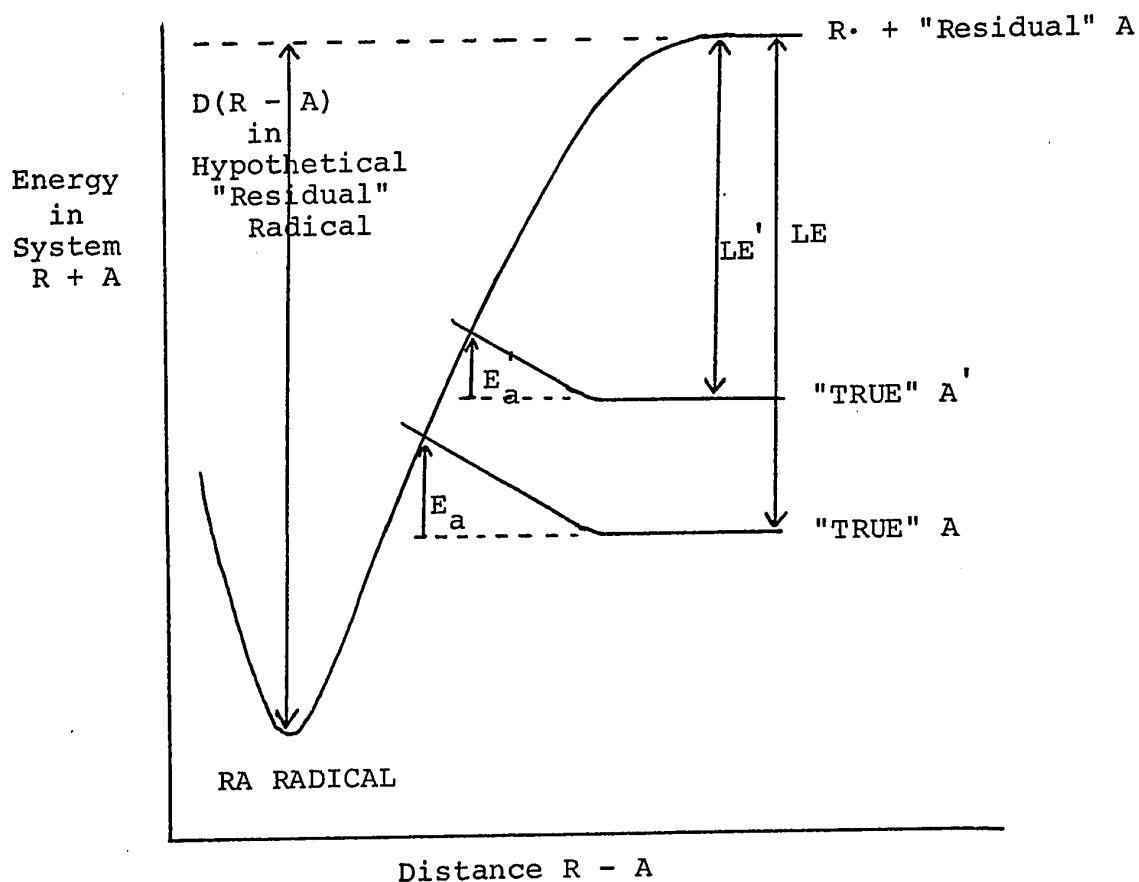


Fig. 34

The "Residual" A is the aromatic molecule in the hypothetical state where one electron is localized on a carbon atom and isolated from the rest of the resonating system. Thus the strength of the R-A bond in the 'residual' radical RA will be the same for each molecule A of the series, and the attractive curve in the diagram will remain identical for a given radical R. If we assume that the only molecular property which varies through the series is the localization energy, it is clear from the diagram that the activation energy is linearly related to the localization energy. In reality, the relationship is only approximate however, due to the effect of the bond strength of the newly formed bond on the activation energy, an aspect which will be considered later.

Turning now to the monoolefins, Szwarc and Binks (80) have calculated the atom localization energies for a series of terminal olefins and found a linear relationship between these and  $\log k$  for methyl addition to the terminal carbon atom. The lack of correlation with non-terminal olefins was attributed to steric hindrance occurring whenever a methyl group was substituted on the reacting carbon atom, so that  $\log k$  was no longer proportional to the activation energy. This steric effect was later confirmed by Feld and Szwarc (26) when the Arrhenius parameters were measured. A similar relationship was found by Jennings and Cvetanovic (33) for the addition of

H atoms to olefins, steric hindrance being unlikely in this instance. An independent calculation of atom localization energies for a series of olefins carried out by Sato and Cvetanovic (81) revealed no correlation between these localization energies and the reactivities with either 'free radical' type reagents or electrophilic reagents. The variations in localization energy in the monoolefin series are caused by hyperconjugation and considerable approximations are required in the calculation; this may explain the difference in the findings of Szwarc et al and Cvetanovic et al.

No relationship exists between localization energy and activation energy for addition of electrophilic reagents to olefins, such as  $\text{CF}_3$  (28) or  $\text{O}(^3\text{P})$  (81). The same is true for  $\text{S}(^3\text{P})$  atoms, indicating that the  $\pi$ -electron density plays the major role in determining the activation energy for these reagents. Calculations by J. B. Flannery (82) have afforded another series of localization energies for olefins, which are different from either those of Szwarc or Cvetanovic. The activation energies for  $\text{S}(^3\text{P})$  addition to olefins observe a linear relationship with Flannery's Atom Localization Energies (59); however the relationship is reversed, i.e. the higher the localization energy, the lower the activation energy, so that the correlation is meaningless. Walton and Tedder (83) have proposed the equation

$$E = AL + BQ$$

where  $E$  is activation energy for monoradical addition,  $L$  is atom localization energy and  $Q$  is charge density. Thus, for aromatic compounds  $Q$  is constant and a linear relationship is observed between  $E$  and  $L$  even for electrophilic radicals like  $\cdot\text{CF}_3$ . For non-aromatic olefins, on the other hand, a linear relationship between  $E$  and  $L$  will only exist when the adding radical is non-electrophilic. It is unlikely that the above equation holds for diradical additions; further experimental data is needed, however, such as activation energies for diradical additions to aromatic compounds or for addition of non-electrophilic diradicals such as  $^3(\text{CH}_2)$  to olefins.

Cvetanovic and Sato (81) have calculated the Bond Localization Energies for a series of olefins. The B.L.E. increases for each methyl group substituted on ethylene; thus the trend in activation energies for addition of  $\text{S}(^3\text{P})$  atoms is opposite to that anticipated on the basis of the B.L.E. The dependence of activation energy on B.L.E. for electrophilic reagents therefore is minimal.

Another parameter, often used in reactivity correlations, is the Maximum Free Valence ( $F$ ), originated by Coulson (77) and is a measure of the free valence of the least substituted carbon atom. For olefins it can be calculated from the equation  $F = 4.732 - \Sigma p$  where  $\Sigma p$  is the sum of bond orders of all the bonds from the atom under consideration. For a series of aromatic compounds the free valence is linearly related to the localization energy and excellent correlations have been observed between free

valence and  $\log k/n$  for additions of "free radical" type reagents such as  $\cdot\text{CCl}_3$  (71),  $\text{Ph. COOO}$  (70),  $\text{CH}_3$  and  $\text{C}_2\text{H}_5$  (25) to these substrates. For olefins, on the other hand, the free valence and localization energy are not linearly related. The free valence may be looked upon as a measure of the ease with which an incipient bond may be formed and therefore is concerned with the initial stages of the reaction prior to the formation of the transition-state complex (84). The atom localization energy, on the other hand, represents an idealized condition which approximates the later stages of the reaction, subsequent to the formation of the transition state complex. Thus, in either case, at best only approximate correlations may be expected. It has been suggested by Burkitt, Coulson and Longuet-Higgins (75) that the atom localization energies rather than the maximum free valences are the more reliable measure of the reactivity of unsaturated compounds toward free radicals. This suggestion appears to be borne out by experiment, for example in the addition of H atoms (33) and  $\cdot\text{CH}_3$  radicals (30), (85) to olefins, where no linear correlation is found between  $\log k$  and free valence. Sato and Cvetanovic (81) found a roughly linear correlation between these parameters for an addition of  $\cdot\text{CCl}_3$ ,  $\text{CH}_3$ , and  $\text{C}_2\text{H}_5$  to olefins but this seems to be a fortuitous result, as later experiments by Szwarc (80) showed that the low relative rate for  $\alpha\beta$  substituted ethylenes was due to steric hindrance and not to an increase in activation

energy.

No linear correlation exists between the free valences and the activation energies for electrophilic additions to olefins, again supporting the argument that the polar interactions outweigh all other factors.

Cvetanovic (89) found good correlations between both the excitation energies and the bond orders of a series of monoolefins, and the logarithms of the relative addition rate constants of the electrophilic reagents,  $O(^3P)$ ,  $CBr_2$ ,  $Br^+$  and Peracetic acid. The corresponding plots for the activation energies of  $S(^3P)$  atom addition are given in Figs. 35 and 36. The excitation energy, calculated from M.O. theory, is the difference between the energy of the ground state and the average of the singlet and triplet excited states (86). Fig. 35 shows that butadiene does not fit the plot, so that the relationship is not universal and may be fortuitous for one class of compounds. The reasonably linear plot for the bond orders versus activation energies may also be trivial in that, while substitution of alkyl groups on ethylene decreases the bond order of the double bond, they also happen to increase the reactivity towards electrophiles by their inductive effect. Cvetanovic, however, has interpreted these linear relationships as evidence that the rate determining step in the addition of electrophilic diradicals is an interaction with the double bond as a whole rather than with a specific carbon atom.



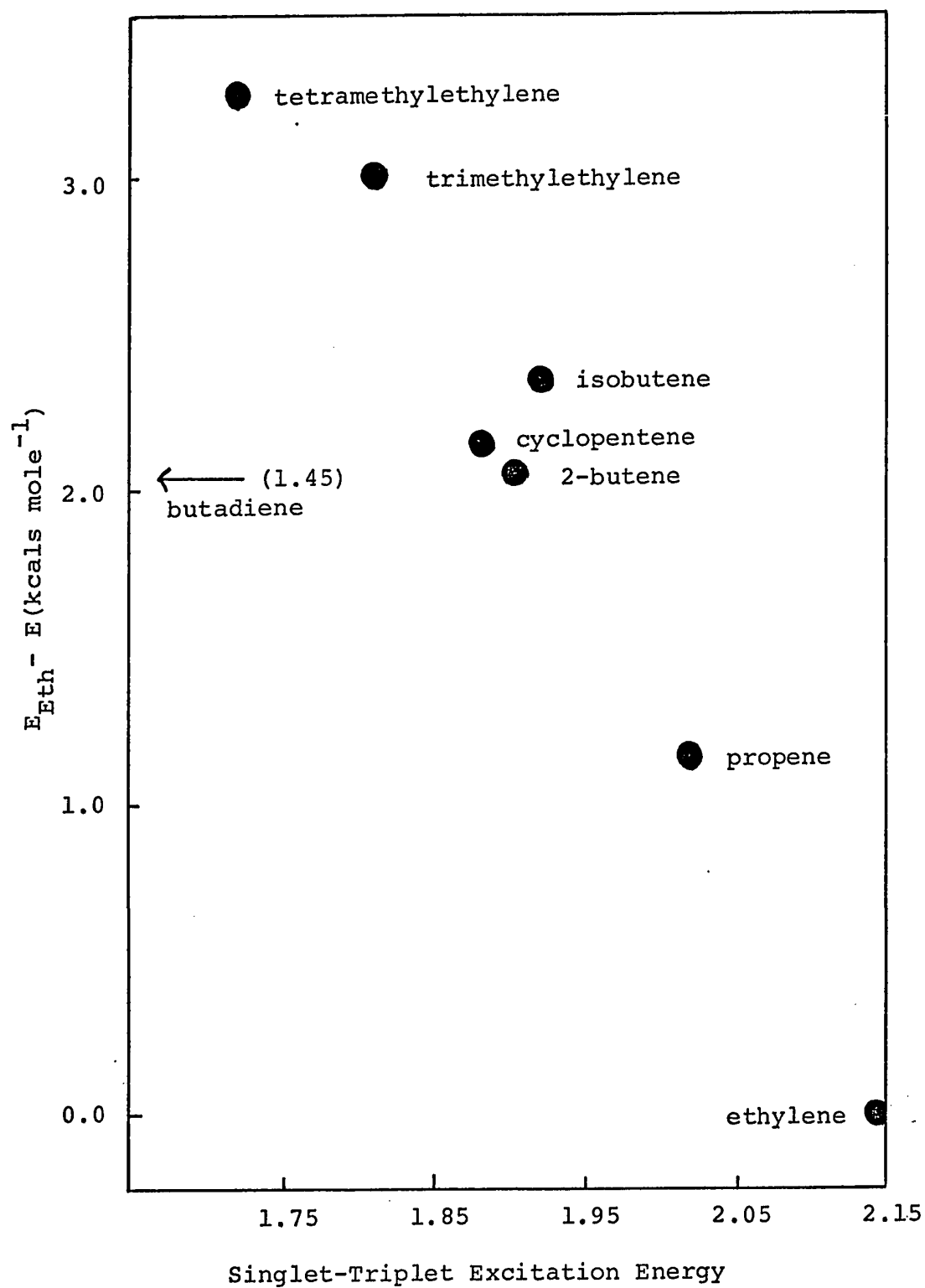


Figure 35: Plot of Activation Energies for  $\text{S}(^3\text{P})$  Atom Addition to Olefins against Excitation Energies (Reference 81).

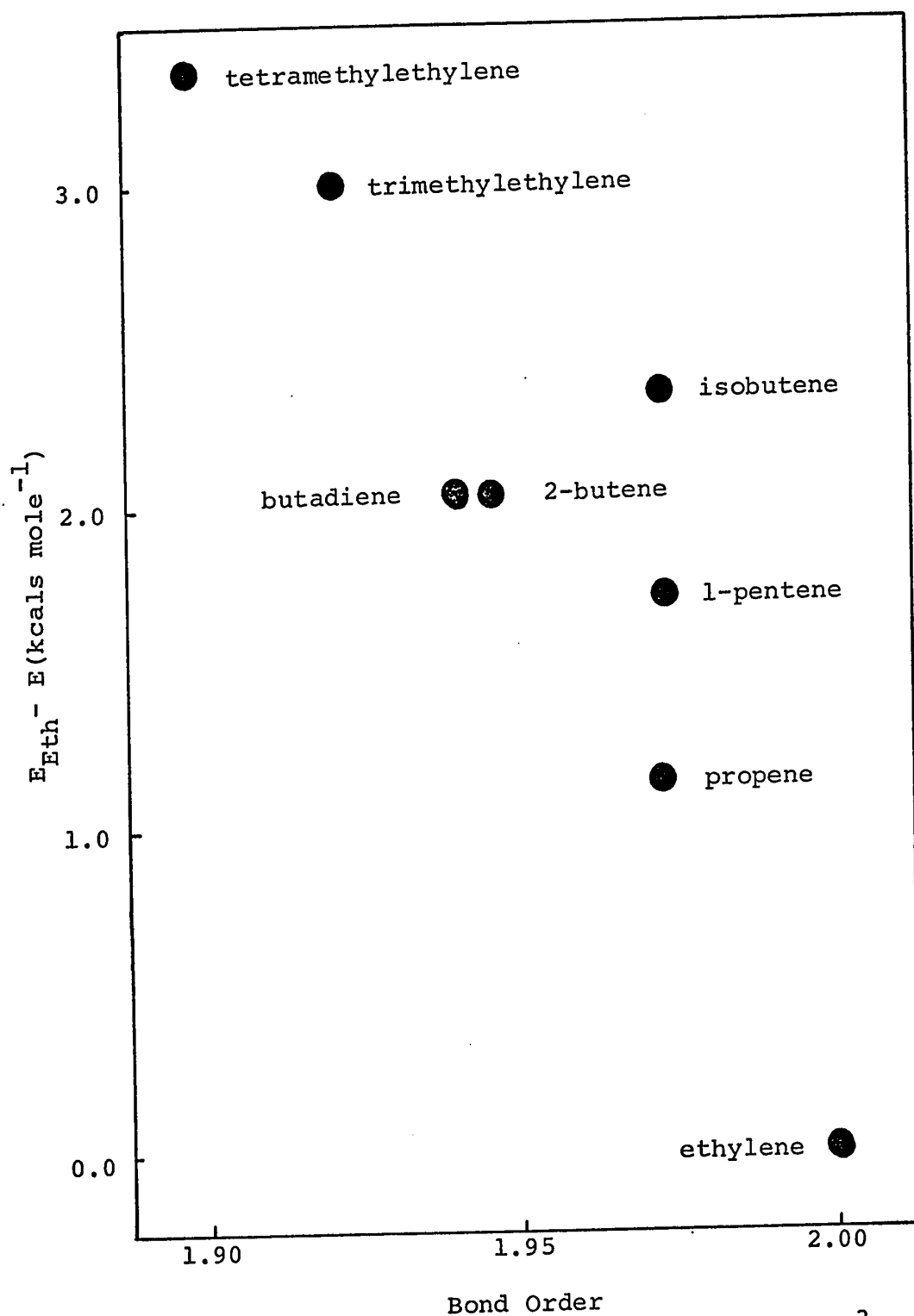
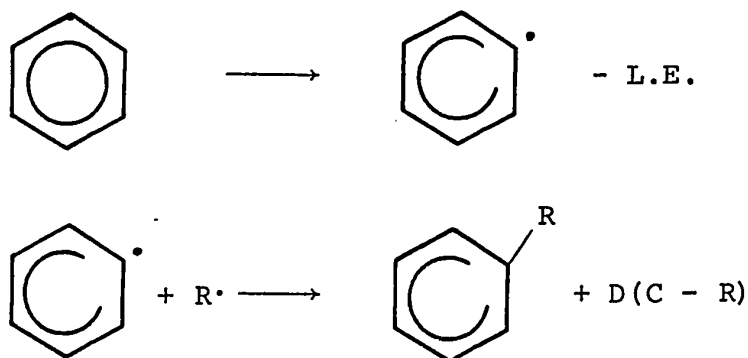


Figure 36: Plot of Activation Energies for  $S(^3P)$  Addition to Olefins against Bond Orders. Bond Orders taken from Reference 81.

The third factor which should influence the activation energy of addition reactions is the bond strength of the newly formed bond or bonds. For example, the addition of a free radical to an aromatic compound can be visualized as taking place in two hypothetical steps, as follows



where L.E. and  $\text{D}(\text{C} - \text{R})$  are the localization energy and  $\sigma$ -bond dissociation energy, respectively. Therefore  $-\Delta\text{H} = \text{D}(\text{C} - \text{R}) - \text{L.E.}$  Evans et al (64) have shown that the heat of reaction for an addition reaction is related to the activation energy, so that  $E_a = \text{D}(\text{C} - \text{R}) - \text{L.E.} + \text{const.}$  Szwarc (78) has shown that for  $\cdot\text{CH}_3$  additions to a series of aromatic compounds the activation energy (as represented by  $\log k$ ) is linearly related to the localization energy, indicating that the former is hardly affected by the dissociation energy of the newly formed bond. As further confirmation of this viewpoint, Szwarc found that the intrinsic reactivity of the methyl radical with respect to these additions is equal to that of the ethyl radical, although the strengths of the newly formed bonds are different in the two cases. Thus, unlike a hydrogen abstraction

reaction where the driving force of the process comes from the energy of the C-H bond which is formed, the strength of the newly formed bond in the addition reaction is of minor importance.

It seems likely that the same holds true in the case of  $S(^3P)$  additions. Thermolytic studies of episulfides (61) indicate that the C-S bond strength decreases as methyl groups are substituted on the ring while the activation energy for sulfur addition to olefins also decreases as methyl groups are substituted.

#### ii) Halogenated Olefins

From the data summarized in Table XXXII a pronounced decrease is evident in the relative rates of addition to fluoroethylenes as F is successively substituted for H. Clark, Murrell and Tedder (88) have discussed the inductive and mesomeric effects of halogen atoms and conclude that a halogen atom has an electron-attracting effect ( $-I_\sigma$ ) on  $\sigma$ -electrons, an electron repelling effect ( $+I_\pi$ ) on  $\pi$ -electrons and an electron-donating ( $+M$ ) mesomeric effect. In the case of fluorinated olefins where the fluorine atom is attached to a saturated carbon atom, only the  $-I_\sigma$  effect is operative, thus leading to a reduction in electron density at the double bond, the effect of which falls off rapidly as the distance from the substituted carbon increases. In the case of  $\alpha$ -substituted olefins, the combined effects of

the  $-I_\sigma$ ,  $+I_\pi$  and  $+M$  effects will lead to a reduction in the electron density of the substituted carbon atom but to an increase in electron density at the carbon atom which is at the nonfluorinated end of the double bond.

These trends are clearly evident from the data in Table XXXV, which summarizes the reactivities of halogenated olefins with various electrophiles relative to the analogous hydrocarbon olefin.

The relative rates of addition of the different radicals are quite similar especially those of  $O(^3P)$  and  $S(^3P)$ . Consider first the olefins having a fluorine atom substituted at a saturated carbon; these suffer the greatest deactivation relative to the hydrocarbon since the  $-I_\sigma$  effect is the only one operative. Table XXXV shows that the relative addition rates of both  $S(^3P)$  and  $O(^3P)$  atoms to 3,3,3-trifluoropropene and 2-(trifluoromethyl)-propene are in good agreement. The  $-I_\sigma$  effect of a perfluoroethyl group is about the same as that of perfluoromethyl as evidenced by the equal rates of addition of S atoms to 3,3-4,4,4-pentafluoro-1-butene and 3,3,3-trifluoropropene due to the decreasing influence of the inductive effect with increasing distance. This falling-off of the inductive effect is again shown by the  $O(^3P)$  additions; the relative rate of addition to 3-fluoropropene is 0.21 whereas for 4-fluoro-1-butene it is 0.57. The rate of  $S(^3P)$  addition to vinyltrifluorosilane is about four times as high as that to 3,3,3-trifluoropropene due to the fact that the

TABLE XXXV  
RELATIVE RATES<sup>a</sup> FOR ADDITION TO HALOGENATED OLEFINS

Olefin	S( <sup>3</sup> P) (27°C)	O( <sup>3</sup> P) (23°C)	CF <sub>3</sub> <sup>e</sup> (65°C)	Br <sup>f</sup> (40°C)	Se( <sup>3</sup> P) (29°C)	O <sub>3</sub> <sup>g</sup> (25°C)
CH <sub>2</sub> =CHF	0.42		0.095	0.014		
cis CFH=CFH	0.018					
trans CFH=CFH	0.043					
CF <sub>2</sub> =CH <sub>2</sub>	0.10					
CF <sub>2</sub> =CFH	0.07					
CF <sub>2</sub> =CF <sub>2</sub>	0.14	1.10 <sup>b</sup>	0.12			
CH <sub>3</sub> CF=CH <sub>2</sub>	0.38	0.50 <sup>c</sup>				
CF <sub>3</sub> CH=CH <sub>2</sub>	0.015	0.011 <sup>c</sup>				
CH <sub>3</sub> (CF <sub>3</sub> )C=CH <sub>2</sub>	0.023	0.018 <sup>c</sup>				
CF <sub>3</sub> CF <sub>2</sub> -CH=CH <sub>2</sub>	0.008					
SiF <sub>3</sub> -CH=CH <sub>2</sub>	0.06					
CH <sub>2</sub> F-CH=CH <sub>2</sub>	-	0.21 <sup>c</sup>				
CH <sub>2</sub> FCH <sub>2</sub> -CH=CH <sub>2</sub>	-	0.57 <sup>c</sup>				
CH <sub>3</sub> -CF=CH <sub>2</sub>	-	0.50 <sup>c</sup>				
CH <sub>3</sub> -CH=CF <sub>2</sub>	-	0.45 <sup>c</sup>				
CH <sub>3</sub> CH <sub>2</sub> CF=CF <sub>2</sub>	-	0.93 <sup>c</sup>				
CF <sub>3</sub> -CF=CF <sub>2</sub>	-	0.006 <sup>b</sup>				

TABLE XXXV (continued)

Olefin	S( <sup>3</sup> P) (27°C)	O( <sup>3</sup> P) (23°C)	CF <sub>3</sub> <sup>e</sup> (65°C)	Br <sup>f</sup> (40°C)	Se( <sup>3</sup> P) (29°C)	O <sub>3</sub> <sup>g</sup> (25°C)
CH <sub>2</sub> =CHCl	1.4	-	0.51	0.30	1.3 <sup>h</sup>	0.47
CH <sub>2</sub> =CHBr	-	-	-	0.68	-	-
cis CClH=CClH	-	-	0.018	-	-	0.0014
trans CClH=CClH	-	-	0.04	-	-	0.024
CCl <sub>2</sub> =CH <sub>2</sub>	-	-	1.0	-	-	0.0009
CCl <sub>2</sub> =CClH	-	-	-	-	-	0.0001
CCl <sub>2</sub> =CCl <sub>2</sub>	-	-	0.003	-	-	0.00004
CF <sub>2</sub> =CCl <sub>2</sub>	-	0.7 <sup>d</sup>	0.033	-	-	-
CClF=CF <sub>2</sub>	-	0.53 <sup>d</sup>	-	-	-	-

a) k(olefin)/k(hydrocarbon); b) Ref. 12; c) Ref. 11;

d) Ref. 13; e) Ref. 29, 28; f) Ref. 90;

g) Ref. 91; h) Ref. 14.

TABLE XXXVI  
E-E<sub>Eth</sub> (kcal mole<sup>-1</sup>) FOR ADDITIONS TO HALOGENATED OLEFINS

	S( <sup>3</sup> P)	Se( <sup>3</sup> P) <sup>a</sup>	CF <sub>3</sub> <sup>b</sup>	O( <sup>3</sup> P)	Br <sup>e</sup>
CH <sub>2</sub> =CHF	0.73	-	1.33	-	1.7
CH <sub>2</sub> =CHCl	0.52	-0.37	0.51	-	-0.83
CH <sub>2</sub> =CHBr	-	-	-	-	-0.44
CH <sub>2</sub> =CCl <sub>2</sub>	-	--	-0.4	-	-
cis CHCl=CHCl	-	-	1.9	-	-
trans CHCl=CHCl	-	-	1.1	-	-
CCl <sub>2</sub> =CCl <sub>2</sub>	-	--	3.2	-	-
CF <sub>2</sub> =CCl <sub>2</sub>	-	--	0.7	-0.2 <sup>c</sup>	-
CF <sub>2</sub> =CH <sub>2</sub>	1.7	-	-	-	-
CF <sub>2</sub> =CF <sub>2</sub>	1.4	-	0.5	-0.9 <sup>d</sup>	-
CClF=CF <sub>2</sub>	-	-	-	1.1 <sup>c</sup>	-
CF <sub>3</sub> -CF=CF <sub>2</sub>	-	-	-	0.7 <sup>d</sup>	-

a) Ref. 14;    b) Ref. 29, 28;    c) Ref. 13;    d) Ref. 12;    e) Ref. 90.



silicon atom is less electronegative than carbon.

Turning to the olefins having fluorine attached to the unsaturated carbon atom, substitution of one fluorine atom for a vinylic hydrogen decreases the addition rate of  $S(^3P)$  by a factor of 0.4 as in vinyl fluoride and 2-fluoropropene. A similar substitution decreases the addition rate of  $O(^3P)$  by a factor of 0.5. Both for  $S(^3P)$  and  $O(^3P)$  addition the addition rate does not decrease steadily upon successive substitutions of fluorine atoms for vinylic hydrogens, but goes through a minimum; thus cis and trans-1,2-difluoroethylene are the least reactive towards sulfur atoms, while, next to vinyl fluoride, tetrafluoroethylene is the most reactive of all the fluorinated ethylenes. From the activation energies for  $S(^3P)$  addition, it seems that the combined ( $+I_\pi$  and  $+M$ ) effect is stronger for 1,1-difluoroethylene than for the 1,2-difluoroethylenes and that the combination of these electron repelling effects exceeds the  $-I_o$  effect of both the third and fourth substituted fluorine atom. A similar trend is exhibited by the reactivities of fluorinated olefins toward both  $O(^3P)$  and  $CF_3$ . As can be seen in Table XXXV, the reactivities, relative to the analogous hydrocarbon, of mono-, di-, tri-, and tetrafluorinated olefins with  $O(^3P)$  are 0.50, 0.45, 0.93 and 1.1 again showing a minimum for the gem-difluorinated olefin; also  $CF_3 - CF = CF_2$  is 0.63 times as reactive as  $CF_3 - CH = CH_2$ , thus fitting in the same series. In the

case of  $\text{CF}_3$  addition also,  $\text{C}_2\text{F}_4$  is more reactive than  $\text{C}_2\text{H}_3\text{F}$ . One is forced to conclude that substitution of two fluorine atoms on a doubly bonded carbon atom activates the carbon atom on the other end of the double bond with respect to electrophilic addition.

In accord with the above electronic interpretation of the variations in activation energy is the observation that the activation energy difference between  $\text{CF}_3 - \text{CH} = \text{CH}_2$  and  $\text{CH}_3 - \text{CH} = \text{CH}_2$  is  $2.6 \text{ kcal mole}^{-1}$  ( $\beta$ -substitution) while between  $\text{CFH} = \text{CF}_2$  and  $\text{CH}_2 = \text{CH}_2$  ( $\alpha$ -substitution) it is lower,  $2.0 \text{ kcal mole}^{-1}$ , although in the former case the fluorines are further removed from the double bond. This is a further illustration of the compensating effect of the  $+M$  and  $+I_\pi$  effect in the  $\alpha$ -substituted olefin. The interpretation is supported further by the relative rate of  $\text{S}(^3\text{P})$  addition to  $\text{CF}_3(\text{CH}_3)\text{C} = \text{CH}_2$ , where the deactivation relative to the corresponding hydrocarbon is the same as that for  $\text{CF}_3 - \text{CH} = \text{CH}_2$ .

In the unsymmetrically substituted ethylenes the electron density on each carbon atom is different. Tedder and Walton (31) have measured the Arrhenius parameters for  $\text{CCl}_3$  addition to each of the two carbons of a series of fluorinated ethylenes and found that the charge density, calculated from Hückel theory, correctly predicted the orientation of  $\text{CCl}_3$  addition, but did not correlate with the magnitude of the activation energy. The sum of the

charge densities on both carbons increased steadily with successive fluorination; it is thus probable that in the calculations of charge densities, no account was taken of the  $-I_o$  effect. It is of interest to note the identical trend in the activation energies of  $\text{CCl}_3$  and  $\text{S}(^3\text{P})$  additions in the fluorinated ethylene series; in Table XXXVII the average of the two activation energies of  $\text{CCl}_3$  addition to each fluorinated olefin is computed and compared with the activation energy of  $\text{S}(^3\text{P})$  addition. Both show the decrease in  $E_a$  when the fourth fluorine is substituted. By appropriately adjusting the Hückel parameters,  $\alpha$  and  $\beta$ , Flannery (82) has calculated the localization energies for the series of fluorinated ethylenes so that he obtained a linear relationship between the difference in localization energies ( $\text{LE}(1) - \text{LE}(2)$ ) and the difference in activation energies of  $\text{CCl}_3$  addition ( $E_1 - E_2$ ) to carbon atoms (1) and (2) for each of the olefins. By taking the differences instead of the absolute values, the symmetrical olefins were eliminated from the plot. Fig. 37 shows a plot of  $\frac{\text{LE}(1) + \text{LE}(2)}{2}$ , taken from Flannery's values for the localization energies, against the activation energies for  $\text{S}(^3\text{P})$  addition to a series of olefins. A reasonably linear plot is obtained with the notable exception of  $\text{C}_2\text{F}_4$  and possibly  $\text{CFH} = \text{CFH}$ , the localization energy of which is not available. The approximate correlation between the activation energy of  $\text{S}(^3\text{P})$  addition and the average localization energy

TABLE XXXVII

COMPARISON OF ACTIVATION ENERGIES FOR  $\text{CCl}_3$  AND  $\text{S}(\text{}^3\text{P})$  ADDITIONS TO FLUOROETHYLENES

	C(1)	C(2)	$\text{CCl}_3$ <sup>a</sup>	Average	E-E <sub>Eth</sub>	E-E <sub>Eth</sub>
$\text{CH}_2=\text{CH}_2$	3.2	3.2		3.2	0	0
$\text{CH}_2=\text{CHF}$	3.3	5.4		4.4	1.2	0.73
$\text{CH}_2=\text{CF}_2$	4.6	8.3		6.5	3.3	1.7
$\text{CHF}=\text{CF}_2$	6.1	7.1		6.6	3.4	2.0
$\text{CF}_2=\text{CF}_2$	6.1	6.1		6.1	2.9	1.4

a) Ref. 31.

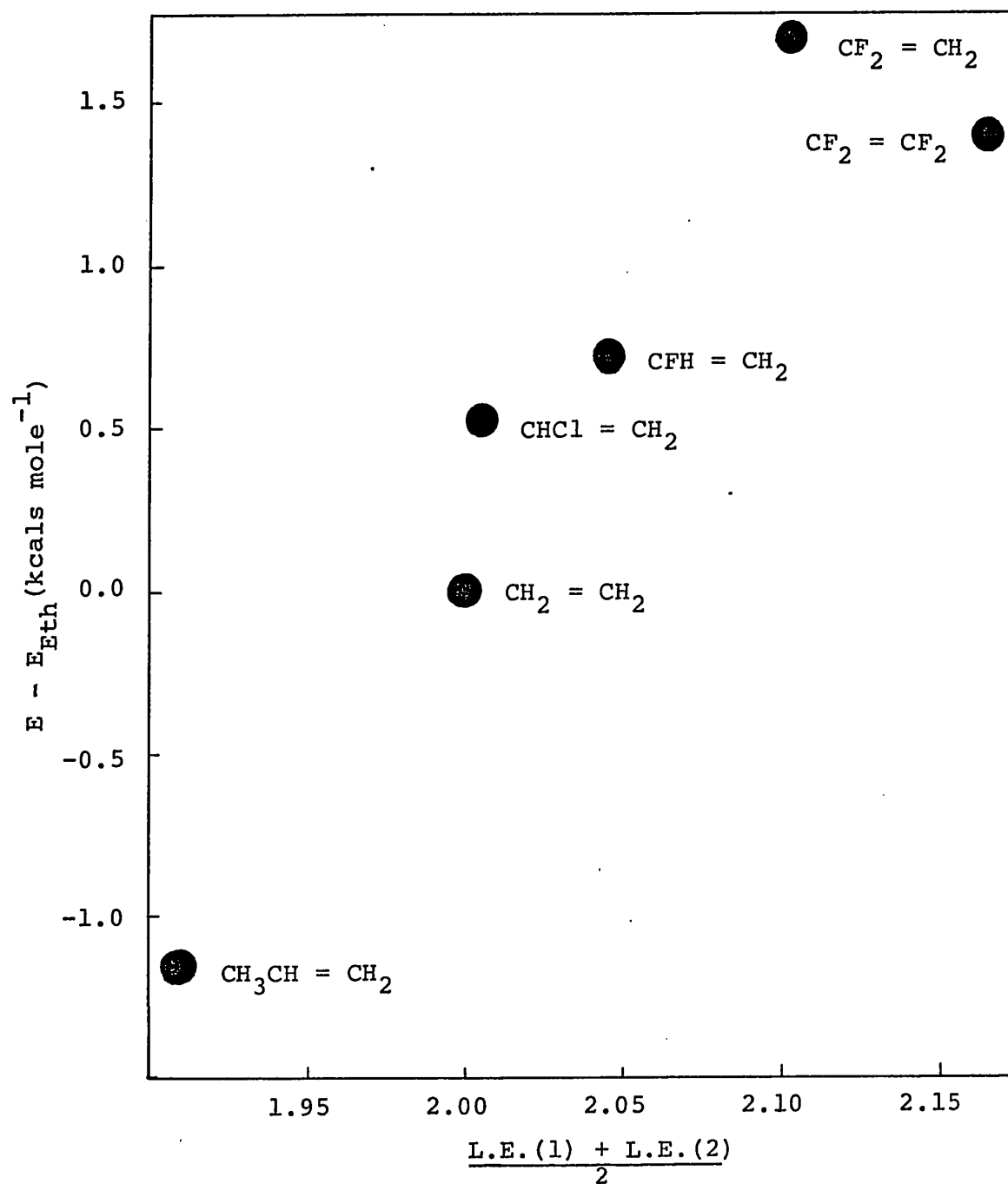
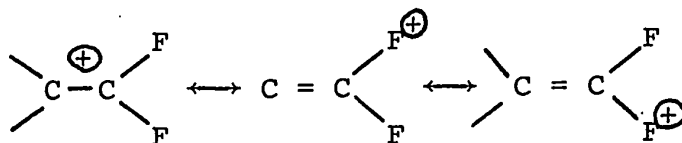


Figure 37: Plot of Average Atom Localization Energies of Both Carbon Atoms versus Activation Energies for  $S(^3P)$  Addition to Olefins. Localization Energies Taken from Reference 82.

is suggestive of a transition state structure which involves partial bonding of the sulfur atom to both carbon atoms; in such a structure each carbon atom would retain partial free radical character. The large deviation of  $C_2F_4$  in the plot suggests an anomalously strong  $+I_\pi$  or a low  $-I_\sigma$  effect, so that the Hückel parameters chosen for the series do not fit this molecule. The approximate nature of their calculations must also be emphasized.

From Fig. 38, it is clear that no linear correlation exists between the activation energies for  $S(^3P)$  addition to the fluorinated ethylenes and their ionization potentials. The latter decrease monotonously upon successive substitution of F atoms. This trend has been ascribed to resonance stabilization of the molecular ion by the following structures (92)



Thus, with respect to the ionization potential, the  $+I_\pi$  and  $+M$  effect outweighs the  $-I_\sigma$  effect resulting in a lower ionization potential for the fluorinated ethylenes than for ethylene. Clearly, then, the magnitude of the activation energy for  $S(^3P)$  addition is not dependent solely on the electron availability in the substrate and is not influenced by the mesomeric effect to as great an extent as the ionization potential. For the mono-substituted ethylenes,

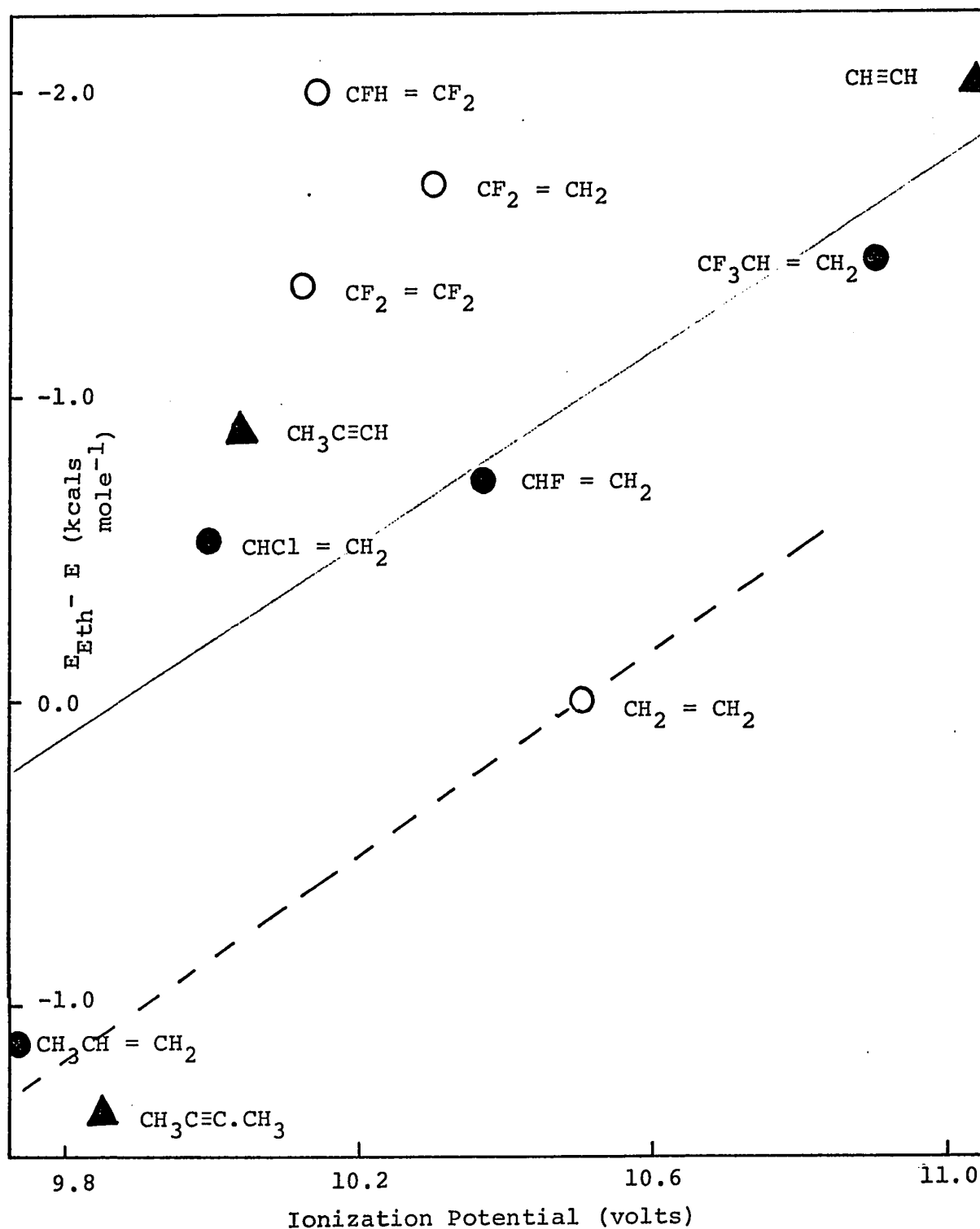


Figure 38: Plot of Activation Energies for  $\text{S}(^3\text{P})$  Atom Addition to Halogenated Alkenes and Alkynes against Ionization Potential. (I.P. taken from References 66, 92 and 29). Dashed line represents slope in Figure 33.

vinyl chloride, vinyl fluoride and vinyl trifluoromethane an approximately linear relationship exists as shown in Fig. 38, the line having a slope equal to that of the hydrocarbon olefins, but displaced toward higher activation energy by about  $1.2 \text{ kcal mole}^{-1}$ . Owen Pearson and Szwarc (29) reported a linear relation between the activation energy for  $\text{CF}_3$  addition to, and the ionization potential of the following four series of substrates, substituted benzenes, acetylenes, monoolefins and diolefins. All four lines had similar slopes but different intercepts. This change in activation energy among different classes of compounds with the same ionization potential would seem to indicate either a greater stabilization of the "transition state" for electron removal, than of the transition state for radical addition, by the mesomeric effect, as mentioned above, or a marked difference in exothermicities between the different classes of compounds since the activation energy for an addition reaction is related inversely to the total enthalpy change (64).

Table XXXV also summarizes the published relative rate constants for radical addition to chlorinated ethylenes. The reactivity of  $\text{O}_3$  decreases rapidly with successive substitution of Cl, thus demonstrating an electrophilic tendency. There is a marked difference in reactivity between the three isomeric dichloro-ethylenes, with 1,1-dichloro ethylene being the least reactive in contrast with both



$\text{CF}_3$  and  $\text{S}(^3\text{P})$  where the gem-substituted compound is the most reactive.  $\text{O}_3$ , behaves as a 1,3 dipolar addend and its mode of addition is probably more complicated than the other radicals (91), with steric hindrance playing a major role. To make a valid comparison between various radical additions, the activation energies must be known; all of the activation energy data available on addition to halogenated ethylenes are summarized in Table XXXVI relative to ethylene. They demonstrate once again that the effect of halogenation on reactivity toward electrophiles is a complex one, as can be seen from the following features: (i) The activation energy for addition to vinyl halides seems to decrease in the order  $\text{F} > \text{Cl} > \text{Br}$  for all reagents, although for the fourth row elements Br and Se,  $E_a$  for vinyl chloride is less than that for ethylene while the opposite holds true for S and  $\text{CF}_3$ . (ii) Geminal substitution of two chlorine atoms activates the unsubstituted carbon atom with respect to  $\text{CF}_3$  and  $\text{O}(^3\text{P})$  addition e.g. for  $\text{O}(^3\text{P})$  addition, as one of the fluorine atoms is replaced by a chlorine atom the activation energy increases by  $2 \text{ kcal mole}^{-1}$ , but replacement of the second fluorine on the same carbon atom by a chlorine atom decreases the activation energy by  $1.3 \text{ kcal mole}^{-1}$ . (iii) The activation energy for  $\text{CF}_3$  addition reaches a maximum for chlorinated ethylenes with  $\text{CCl}_2 = \text{CCl}_2$  while the activation energy for addition to  $\text{C}_2\text{F}_4$  is the lowest of all the fluorinated ethylenes.

iii) Acetylenes

The known activation energies for atomic and free radical additions to alkynes are summarized in Table XXXVIII. For each of the reagents, which are all electrophiles, the activation energy of addition to acetylene is about 1.5 - 2.0 kcal mole<sup>-1</sup> higher than to ethylene. This result is not unexpected and is due to the electrophilic tendencies and relatively high acidity of acetylene which is also manifested in its well-known ability to form acetylide salts. Methylation of the triple bond increases the electron availability to adding electrophiles by the +I<sub>σ</sub> inductive effect thereby decreasing the activation energy of addition. Substitution of two trifluoromethyl groups lowers the activation energy of addition, as shown by the results of Br addition, though to a lesser extent than two methyl groups, while a similar substitution in the ethylene molecule causes deactivation. Unlike butene-2 the perfluorobutyne-2 molecule is linear with respect to the four carbon atoms and has a shorter C-C σ-bond than the analogous olefin. This allows overlap between the cylindrically symmetrical π-electrons and the filled p-orbitals of the fluorine atoms so that the +I<sub>π</sub> and +M effects are operative and outweigh the -I<sub>σ</sub> effect, resulting in a lower activation energy for electrophilic addition.

Owen, Pearson and Szwarc (29) found an approximately linear relationship between the activation energy of CF<sub>3</sub>

TABLE XXXVIII

## ACTIVATION ENERGIES AND RELATIVE RATES FOR ADDITIONS TO ACETYLENES

	$\overline{(E-E_{\text{Eth}})}$				$\overline{k/k_{\text{C}_2\text{H}_2} (27^\circ\text{C})}$			
	$\text{S}(^3\text{P})$	$\text{CF}_3^{\text{a}}$	$\text{O}(^3\text{P})^{\text{b}}$	$\text{O}_3^{\text{c}}$	$\text{Br}^{\text{d}}$	$\text{C}_2\text{O}(^3\Sigma)^{\text{e}}$	$\text{S}(^3\text{P})$	$(\text{O}^3\text{P})^{\text{b}}$
$\text{CH}\equiv\text{CH}$	2.0	1.9	1.7	6.1	1.57	0.34	0.35	0.21
$\text{CH}_3-\text{C}\equiv\text{CH}$	0.9	1.3	-	-	-	-	2.3	-
$\text{CH}_3-\text{C}\equiv\text{C}-\text{CH}_3$	-1.3	1.1	-	-	-2.17	8.9	29	-
$\text{CF}_3-\text{C}\equiv\text{C}-\text{CF}_3$	-	-	-	-	-0.48	-	-	-

a) Ref. 29

b) Ref. 12, 93

c) Ref. 101

d) Ref. 90

e) Ref. 21

addition to and the ionization potentials of a series of four alkynes. The line had the same slope as the corresponding line representing the monoolefins, although it was displaced from it to higher activation energies. A similar plot for  $S(^3P)$  addition, shown in Fig. 38, reveals a direct relationship between  $E_a$  and ionization potential, though, in as far as can be determined from three points, not a linear one.

## B) A-Factors

### i) Olefins

Table XXXIX summarizes the available data on Arrhenius pre-exponential factors relative to ethylene taken as 1.0. In general the numbers are accurate within a factor of 1.3. With the exception of 1,3-butadiene, the relative A-factors for olefins fall in the range 0.1 to 3.5, the vast majority being less than unity.

Considering first the hydrocarbons, there is no obvious direct correlation between the A-factor and the structure of the olefin. For  $O(^3P)$  additions, the A-factors are approximately unity within experimental error, while those for both  $S(^3P)$  and  $C_2O(X^3\Sigma)$  tend to decrease with successive methyl substitution. The A-factors for  $Se(^3P)$ , on the other hand, tend to increase with methylation. A decrease in the A-factor is due to steric

TABLE XXXIX  
RELATIVE A-FACTORS FOR ADDITION OF ATOMS AND RADICALS TO OLEFINS AND ACETYLENES

	$O(^3P)^a$	$S(^3P)$	$Se(^3P)^d$	$C_2O(^3\Sigma)^e$	$CF_3^f$	$CCl_3^h$	$CH_3^i$
Ethylene	1.0	1.0	1.0	1.0	1.0	0.9	1.0
Propene	1.0	1.0	1.2	0.9	0.63 <sup>g</sup>	-	0.65
1-Butene	0.74	0.75	-	0.4	-	-	-
<u>cis</u> -2-butene	-	0.53	1.8	0.6	0.17	-	-
<u>trans</u> -2-butene	-	0.65	1.6	0.2	0.17	-	-
Isobutene	0.67	0.97	2.2	0.5	0.61 <sup>g</sup>	-	0.67
Trimethylethylene	1.18	0.51	-	0.1	-	-	-
Tetramethylethylene	1.25	0.50	-	0.2	0.12	-	-
Cyclopentene	1.0	0.67	-	-	0.50	-	-
1,3-butadiene	1.14	2.4	4.9	1.5	1.17 <sup>g</sup>	-	2.14
$CH_2=CHF$	-	1.4	-	-	0.65 <sup>g</sup>	0.8	-
$CH_2=CHCl$	-	3.4	0.72	-	1.0 <sup>g</sup>	-	-
<u>cis</u> - $CFH=CHF$	-	1.7	-	-	-	-	-
<u>trans</u> $CFH=CFH$	-	3.7	-	-	-	-	-
$CF_2=CH_2$	-	1.9	-	-	-	1.0	-
$CF_2=CFH$	-	2.1	-	-	-	6.3	-
$CF_2=CF_2$	0.23 <sup>b</sup>	1.4	-	-	0.21	32	-

TABLE XXXIX (continued)

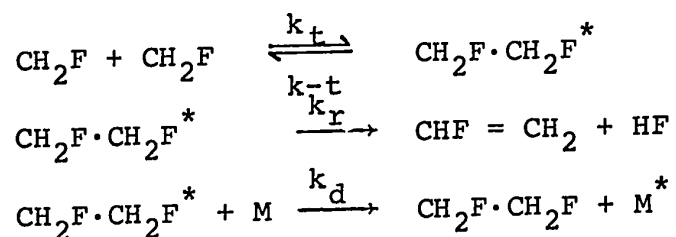
	$O(^3P)^a$	$S(^3P)$	$Se(^3P)^d$	$C_2O(^3\Sigma)^e$	$CF_3^f$	$CCl_3^h$	$CH_3^i$
$CF_3 \cdot CH=CH_2$	-	1.2	-	-	-	-	-
$CF_3 \cdot CF=CF_2$	0.11 <sup>b</sup>	-	-	-	-	-	-
cis $CHCl=CHCl$	-	-	-	-	0.25	-	-
trans $CHCl=CHCl$	-	-	-	-	0.17	-	-
$CCl_2=CH_2$	-	-	-	-	0.91	-	-
$CCl_2=CCl_2$	-	-	-	-	0.33	-	-
$CFCl=CF_2$	3.4 <sup>c</sup>	-	-	-	-	-	-
$CCl_2=CF_2$	0.5 <sup>c</sup>	-	-	-	0.17	-	-
$CH \equiv CH$	3.7 <sup>b,k</sup>	6.2	-	-	3.3	-	3.0 <sup>j</sup>
$CH_3-C \equiv CH$	-	6.2	-	-	3.1	-	-
$CH_3-C \equiv C-CH_3$	-	2.7	-	-	1.2	-	-

- a) Ref. 10;    b) Ref. 12;    c) Ref. 13;    d) Ref. 14;    e) Ref. 21;  
 f) Ref. 29;    g) Ref. 28;    h) Ref. 31;    i) Ref. 28;    j) Ref. 102;  
 k) Ref. 93.

hindrance and it has been proposed that the absence of such an effect in the reactions of  $O(^3P)$  with olefins indicates a very loosely bound transition state (10). This line of reasoning would imply a tighter transition state for both  $S(^3P)$  and  $C_2O(X^3\Sigma)$  additions, which is not surprising in view of their larger size compared with the oxygen atom, but does not explain the increasing trend in Se atom additions. Thus the effect of the successive substitution of the olefin on the A-factor must be at least two-fold, comprising two opposing factors. In the case of the  $O(^3P)$  additions these two factors cancel each other while for  $S(^3P)$  and  $C_2O(X^3\Sigma)$  the steric effect predominates, and the opposite holds for Se additions.

In the case of  $S(^3P)$  additions to the halogenated olefins, as seen in Table XXXIX, all the A-factors are greater than that for ethylene indicating a predominance of the enhancing effect. The addition of  $S(^3P)$  to ethylene to form ethylene episulfide is exothermic by 58 kcal (59). If this excess energy is not "syphoned" off from the incipient C-S bonds and equipartitioned among the other degrees of freedom in the molecule, the complex can dissociate to the initial reactants. Substitution of a fluorine or a chlorine atom for a hydrogen increases the number of effective oscillators, in the RRK sense, in the molecule due to the lower vibrational frequencies of the halogen atoms. The efficiency of F or Cl atoms

in partitioning the excess energy and thereby increasing the lifetime of a 'hot' adduct, has been clearly demonstrated by Benson and Haugen (113) who applied the classical RRK theory of unimolecular reactions to the decomposition of "hot" fluoroethanes. Their system is described by the following reactions:



By application of the classical RRK equation to the rate constants  $k_{-t}$  and  $k_r$ , and assuming  $k_d = 0.2Z$  where  $Z$  is the collision frequency, the ratios  $k_d/k_{-t}$  and  $k_d/k_r$  were calculated for a series of fluorinated ethanes. The relative elimination rate constants for the series agreed well with the experimental values, when it was assumed that substitution of an F atoms for an H atom increased the number of effective oscillators in the molecule by 1.5.

It can similarly be shown that for the addition of  $\text{S}(^3\text{P})$  to fluorinated or chlorinated ethylenes, the excess energy of  $\sim 60 \text{ kcal mole}^{-1}$  would be more rapidly removed from the newly formed C-S bonds and distributed among the other degrees of freedom in the episulfide molecule than for the addition to ethylene. The cause of this lies with the lower vibrational frequencies



associated with the C-F bonds compared with C-H bonds. As a result of the lower vibrational frequencies, the standard entropies of fluorinated compound are higher than the hydrocarbon analogues. As the ethylene molecule with  $sp^2$  hybridization changes to the  $sp^3$  configuration of the epoxide the C-F or C-H bending modes are "tightened"; this increase in frequency can be better accommodated by the C-F bonds than by C-H so that the decrease in entropy in going from reactants to transition state is less for the fluorinated molecule.

The high A-factor for vinyl chloride supports the above argument; Cl is a more effective 'oscillator' than F due to its lower vibrational frequencies. Also, the minimum relative rate constant for trans-dichloroethylene indicates a minimum A-factor of 10, assuming the activation energy to be the same as that for vinyl chloride. The higher A-factors for both trans-2-butene and trans-difluoroethylene than the corresponding cis isomers are likely due to a greater steric hindrance in the approach to the latter olefins.

The relative A-factors for  $O(^3P)$  addition to  $C_2F_4$ ,  $C_2Cl_3F$  and  $CCl_2 = CCF_2$  respectively are 0.23, 3.4 and 0.5; replacement of one F atom by a Cl increases the A-factor by more effective partitioning of the excess energy, while substitution of a second Cl atom causes steric inhibition of the reaction. Szwarc (29) has

postulated that the initial step in both  $O(^3P)$  and  $CF_3$  additions to olefins is the formation of a  $\sigma$ -complex, i.e. an attack on a single carbon atom attached to the double bond. Thus, for symmetrical olefins, the relative A-factor was divided by two since either carbon atom can be involved. These adjusted A-factors were then taken to indicate that the steric hindrance was the only factor affecting the entropy of activation. Thus, in the case of  $CF_3$  addition, substitution of one methyl group on a carbon atom lowers the A-factor by a factor of  $\sim 5$  while substitution of two methyl groups lowers it by a factor of  $\sim 8$ . On the other hand the values for propylene, isobutene and vinyl fluoride are considered by Szwarc et al to be one half that of ethylene, there being only one active carbon atom in these molecules as opposed to two in ethylene. This interpretation, based only on steric hindrance does not explain the A-factors for  $CF_3$  addition to the chlorinated ethylenes, where vinyl chloride and gem-dichloro ethylene have an A-factor equal to that of ethylene and tetrachloroethylene has a higher A-factor than the 1,2-dichloro compound or their 1,1-dichloro-2,2-difluoroethylene although the fluorine atom is smaller than Cl. Szwarc has proposed that the steric hindrance is effected through the inhibition of the rotation of the  $CF_3$  group about the incipient C-C bond in the transition state resulting in a lower entropy. Thus the constancy

of the A-factors for  $O(^3P)$  additions to hydrocarbon olefins is rationalized by the spherical symmetry of the oxygen atom and its consequent lack of a rotational degree of freedom and is therefore consistent with the formation of a  $\sigma$ -complex in the transition state for  $O(^3P)$  addition. The low A-factors measured by Heicklen and Saunders (12) (Table XXXIX) for the reaction of  $O(^3P)$  with the fluorinated olefins do not support this view however, although it is possible that a different transition state is involved in these reactions.

The theory that the A-factors are dependent on the number of 'effective oscillators' in the entire molecule and not just on the immediate environment of the carbon atom attacked gains considerable support from the results of Tedder and Walton on the addition of  $CCl_3$  radicals to the fluorinated ethylenes (Table XXXIX). These authors found that the A-factors for addition to each carbon in an unsymmetrically substituted molecule were identical, and furthermore they increased with the extent of fluorination. Owen, Pearson and Szwarc (114) have compared the relative A-factors for  $CF_3$  addition to olefins measured both in the liquid and gas phases and found that compared with A-factors for abstraction from 2,3-dimethylbutane, the A-factors for addition were consistently higher in the liquid phase. Thus the more effective equipartitioning of excess energy occurring in the liquid phase was reflected in the A-factor.

Finally, the consistently higher A-factors for addition of both mono- and diradicals to butadiene relative to ethylene are most likely a consequence of the greater effective collision diameter of this molecule due to the extended  $\pi$ -orbitals.

ii) Acetylenes

Table XXXIX includes the available data on the A-factors of radical additions to acetylenes. These are consistently higher than those for ethylene. The explanation of Owen et al (29) for the relative A-factors of  $\text{CF}_3$  addition seems to apply to all the systems studied and is based on the symmetry of the acetylene molecule.

The effect of symmetry on the entropy of activation for addition to acetylene relative to ethylene may be interpreted in terms of either of two approaches. In the language of the transition state theory, the expression for the A-factor includes the products of all the partition functions of reactants in the denominator, and of products in the numerator. Hence, in the case of ethylene, the denominator includes the partition function of rotation of the molecule around its  $\text{C}=\text{C}$  axis while, in the case of acetylene, this term disappears due to the linearity of the molecule, thus making the A-factor for acetylene higher. In the case of additions to methyl acetylene or dimethyl acetylene, while each of these molecules has a rotational degree of freedom about the  $\text{C}\equiv\text{C}$  axis,

nevertheless the moment of inertia increases considerably upon the addition of an atom or radical thus increasing the corresponding partition function in the numerator. This, in conjunction with the contribution of the internal free rotation of one methyl group with respect to the  $C\equiv C$  axis, a mode of motion which becomes operative in the transition state, being meaningless in the parent molecule, leads to the fairly high A-factor for methyl-acetylene. The decreased A-factor for dimethyl acetylene can be accounted for by steric hindrance as in the 2-butenes. In fact, the trend in the A-factors for the three acetylenes is very similar to that for the corresponding olefins, ethylene, propylene and the 2-butenes.

In the language of the collision theory, since the initial interaction of an electrophilic reagent is with the  $\Pi$ -bond, the cylindrical symmetry in the acetylene molecule as opposed to the planar ethylene molecule could be expected to result in a larger effective collision diameter.

#### C) The Transition State for $S(^3P)$ Addition to Olefins

First of all, the absolute rate constant of  $S(^3P)$  addition to ethylene will be considered. Table XL summarizes the available data on rate constants and Arrhenius parameters for additions of Group VI atoms to ethylene.

TABLE XL

RATE CONSTANTS AND ARRHENIUS PARAMETERS FOR GROUP VI ATOM ADDITIONS TO ETHYLENE

	$k(25^\circ\text{C})$	$A(\text{M}^{-1} \text{sec}^{-1})$	$E(\text{kcal mole}^{-1})$	$k_{\text{C}_3\text{H}_6}/k_{\text{C}_2\text{H}_4}$
$\text{O}_2(^3\text{P})$	$5.7 \times 10^8$ (a) $3 \times 10^8$ (b)	$7 \times 10^9$ (a)	1.5 (a)	5.8 (b)
$\text{S}_3(^3\text{P})$	$7 \times 10^8$ (c) $1.7 \times 10^6$ (d)	$4 \times 10^9$ (h)	1.0 (i) 4.7 (j)	6.8
$\text{Se}_4(^3\text{P})$	$1 \times 10^8$ (e)	$1.1 \times 10^{10}$ (e)	2.8 (e)	3.5 (f)
$\text{Te}_5(^3\text{P})$	$2 \times 10^7$ (g)	-	-	2

a) Ref. 96; b) Ref. 10; c) Ref. 97; d) Ref. 98; e) Ref. 99;  
 f) Ref. 14; g) Ref. 15; h) Calculated in text; i) Calculated from (c); j) Calculated from (d).

Considering first the activation energy of addition of  $O(^3P)$  to  $C_2H_4$ , a value of  $1.6 \text{ kcal mole}^{-1}$  has been measured by Elias and Schiff (94) and a value of  $1.5 \text{ kcal mole}^{-1}$  by Westenberg and de Haas (93) and independently by Smith (95). If we accept this value, along with the activation energy differences for the series of olefins reported by Cvetanovic (10), then the activation energy for  $O(^3P)$  addition to tetramethylethylene is  $-1.1 \text{ kcal mole}^{-1}$ . With the exception of propene and 1-butene, the activation energies for  $O(^3P)$  atom addition to all the olefins studied by Cvetanovic are negative.

Callear and Tyerman (14) plotted the activation energies of Se addition to a series of olefins against the ionization potential of the olefins and found that the activation energy falls rapidly with I.P. becoming negative at an ionization potential of 9.15 ev. This prediction has not been confirmed, however, since no activation energies were measured for olefins with an ionization potential as low as 9.15 ev. These authors derived an empirical equation which predicts that the activation energy for Se addition to olefin is dependent on the percentage ionization of the olefin in the transition state, and has a maximum value of  $3.4 \text{ kcal mole}^{-1}$  for zero ionization.

A reasonable value for the activation energy of  $S(^3P)$  atom addition to ethylene can be arrived at by estimating the A-factor. This can be done by estimating

the standard entropy of the activated complex and applying the transition state equation for a bimolecular gas phase reaction (100)

$$A = \frac{e^2 kT}{h} (RT) e^{+\Delta S_p^\ddagger / R} \text{ M}^{-1} \text{ sec}^{-1}$$

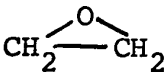
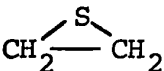
$$= 1.12 \times 10^{15} e^{\Delta S_p^\ddagger / R} \text{ M}^{-1} \text{ sec}^{-1}$$

where  $\Delta S_p^\ddagger = S^\circ(\ddagger) - S^\circ(\text{C}_2\text{H}_4) - S^\circ(\text{S})$  gibbs/mole and  $S^\circ(\ddagger)$  denotes the standard entropy of the activated complex at an ideal gas pressure of one atmosphere and a temperature of 298°K. W. B. de More in a similar calculation (101) for the addition of  $\text{O}_3$  to  $\text{C}_2\text{H}_4$  and  $\text{C}_2\text{H}_2$ , approximated the value of  $S^\circ(\ddagger)$  by taking the standard entropy of the analogous hydrocarbon. Table XLI gives the calculated A-factor for both  $\text{O}(^3\text{P})$  and  $\text{S}(^3\text{P})$  addition to ethylene, by assuming two kinds of activated complex, an open diradical and a three-membered ring approximated by  $\text{CH}_3\text{CH}_2\text{O}\cdot$  and ethylene oxide respectively. The standard entropies of  $\text{C}_2\text{H}_2$ ,  $\text{O}$ ,  $\text{S}$ ,  $\text{CH}_3\text{CH}_2\text{O}\cdot$  and  $\overline{\text{CH}_3\text{CH}_2\text{O}}$  respectively are 52.45, 38.47, 40.09, 68.7 and 58.1 gibbs/mole (103). The standard entropies for sulfur-containing compounds and radicals are approximately 4 gibbs/mole higher than the oxygen-containing analogues (103) so that for  $\text{CH}_3\text{-CH}_2\text{S}\cdot$  and ethylene episulfide, we may take 73 and 62 gibbs/mole, respectively.

The true A-factor would be expected to lie between the two extreme values calculated in Table XLI. Such is the case for oxygen atom addition where the



TABLE XLI

Activated Complex	$S^{\circ}(\ddagger)$ gibbs/mole	$A(M^{-1}, \text{Sec}^{-1})$
$\cdot\text{CH}_2\text{CH}_2\text{O}\cdot$	68.7	$10^{10.2}$
	58.1	$10^{7.9}$
$\cdot\text{CH}_3\text{CH}_2\text{S}\cdot$	73	$10^{10.8}$
	62	$10^{8.4}$

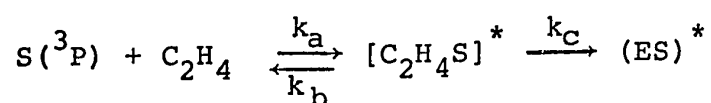
measured value of  $10^{9.8}$  lies close to that calculated for the open biradical structure. In contrast to the  $O(^3P)$  atom case, the addition of  $S(^3P)$  atoms is stereospecific; thus we would expect a somewhat tighter transition state with partial bonding to both carbon atoms. Taking the mean of the two values in Table XLI we get an A-factor for  $S(^3P)$  addition, of  $10^{9.6}$ . Of the two values quoted in Table XL for the rate constant of sulfur addition, the value of  $7 \times 10^8 \text{ M}^{-1} \text{ sec}^{-1}$  seems the most reasonable, by comparison with the  $E_a$  rate constants of the other Group VI atoms. Therefore,  $e^{\frac{-E_a}{RT}} = 10^{(8.8 - 9.6)}$  so that the activation energy for sulfur addition to ethylene is  $\sim 1$  kcal. This value fits well with the values of O and Se atoms and is consistent with the trend in selectivities of the four Group VI atoms, i.e. the greater the selectivity the lower the activation energy, as can be seen in Table XL.

To restate the foregoing, if the A-factor for addition of  $S(^3P)$  to ethylene is the same as for addition of  $O(^3P)$  or  $Se(^3P)$  atoms and if we accept the value of  $k(S + C_2H_4) = 7 \times 10^8 \text{ M}^{-1} \text{ sec}^{-1}$ , then the activation energy for  $S(^3P)$  addition to ethylene is about 1 kcal.

This is a strong indication that the activation energy for  $S(^3P)$  addition to the higher olefins is negative. If the activation energy for addition to tetramethylethylene were not negative, then ethylene would have an  $E_a$  not less than  $3.36 \text{ kcal mole}^{-1}$ . Assuming  $k(S + C_2H_4) = 7 \times 10^8 \text{ M}^{-1}$

$\text{sec}^{-1}$ , the A-factor is  $2 \times 10^{11} \text{ M}^{-1} \text{ sec}^{-1}$ . This is an impossibly high value, since reactions are known (see Chapter IV) that have an A-factor 8.4 times as high as that for  $\text{S}(^3\text{P}) + \text{ethylene}$ , and this would exceed the gas collision frequency. It is possible, though, that the lower value of  $1.7 \times 10^6$  for the rate constant is correct, in which case the activation energy for  $\text{S}(^3\text{P})$  addition to ethylene would have an upper limit of  $5.4 \text{ kcal mole}^{-1}$  and would be equal to  $4.7 \text{ kcal mole}^{-1}$ , if we assume an A-factor of  $10^{9.6} \text{ M}^{-1} \text{ sec}^{-1}$ .

The potential-energy barrier for any elementary process cannot be negative; therefore, a "negative" activation energy must indicate some complexity of the process. Shimomura, Tolle, Smid and Szwarc (104) have reported negative activation energies for the propagation step in the polymerization of polystyryl anions. They suggest three possible explanations for this phenomenon, two of which involve solvation of the ions. The third possibility is applicable to the present study and has been invoked by de More (101) to explain the anomalously high activation energy and A-factor for  $\text{O}_3$  addition to acetylene as compared with the same addition to acetylene. The mechanism can be applied to the  $\text{S}(^3\text{P}) + \text{C}_2\text{H}_4$  reaction as follows:



A fast reversible reaction produces minute amounts of a sulfur-ethylene complex and is followed by a rate-determining unimolecular rearrangement, having rate constant  $k_c$ , to form an excited episulfide molecule. Assuming a steady-state concentration of the sulfur-ethylene complex,

$$\begin{aligned}\frac{d(ES)}{dt} &= k_c [C_2H_4, S]_{ss} \\ &= \frac{k_c}{k_b + k_c} (C_2H_4) (S)\end{aligned}$$

$$k_{eff} = \frac{k_c}{k_b + k_c} k_a$$

The unimolecular step becomes rate determining when  $k_b \gg k_c$ , so that

$$k_{eff} = \frac{k_a k_c}{k_b} = \frac{A_a A_c}{A_b} e^{-[E_a + E_c - E_b]/RT}$$

The activation energy becomes negative when  $E_b > E_a + E_c$ , or when the exothermicity of the complex forming reaction exceeds the activation energy for the unimolecular rearrangement, i.e.  $-\Delta H_a = E_b - E_a > E_c$ . The reaction path is illustrated in the diagram below.

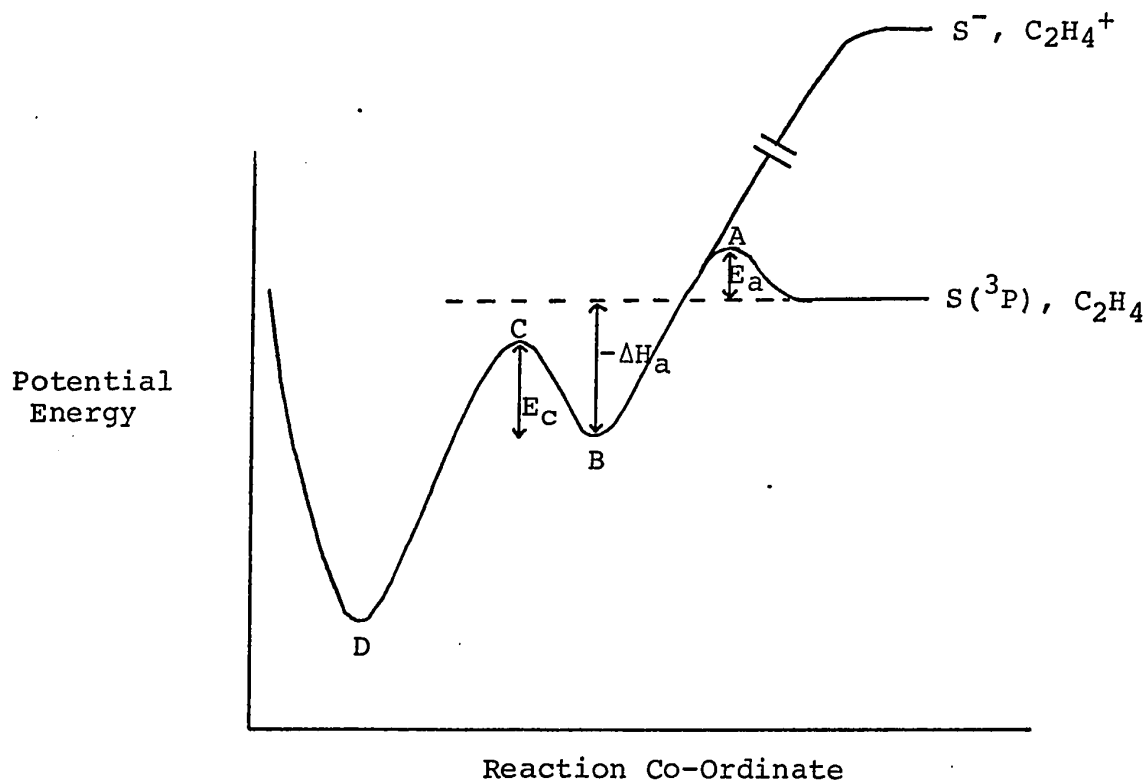


Figure 39

The complex which lies at the potential energy minimum at B represents a  $\Pi$ -complex, while that at D is a  $\sigma$ -complex, so that Fig. 39 is similar to that suggested by Cvetanovic (89). The major difference between the two descriptions is that, while Cvetanovic believed the crossing of the potential energy barrier at A to be the rate-determining step, it is proposed here that the crossing at C is rate-determining, so that the transition state lies at C and not A. Whenever the potential energy

at C is higher than that of the  $S(^3P) + C_2H_4$  at infinite separation, as represented by the dotted line, the activation energy for the addition will be positive.

The present description of the reaction path affords a much more logical explanation for the relationship between the activation energy and the ionization potential of the olefin. According to Cvetanovic (89), the activation energy for addition is  $E_a$  (Fig. 39) and decreases with decreasing ionization potential of the olefin due to a lowering of the crossover point of the repulsive and attractive surfaces. In the present description the activation energy is  $E_c + \Delta H_a$  ( $\Delta H_a$  being negative), so that the activation energy is determined by the depth of the potential well at B, particularly if  $E_c$  remains approximately constant as it should (27). The depth of the potential well at B which represents the stability of the  $\Pi$ -complex, is, in turn, dependent on the ionization potential of the olefin and the electron affinity of the attacking atom or radical.

There are two further objections to Cvetanovic's representation, as raised by Stefani and Szwarc (27). Firstly, there is no valid reason to expect a high potential energy barrier in  $\Pi$ -complex formation. If the potential energy barrier at A existed, it would be due to repulsion between the  $\Pi$ -electrons of the olefin and the free electrons on the oxygen or sulfur atom, and this repulsion

would be expected to increase as the electron density of the double bond increases leading to an increase in the activation energy for addition with successive methylation. This is contrary to experimental observations. Also, methyl radicals react eleven times more rapidly with  $C_2F_4$  than with  $C_2H_4$  due to the lower electron density in the fluorinated molecule and consequently lower repulsion: in this case the repulsion is not balanced by attractive forces since no  $\Pi$ -complex is formed. It is unlikely that the range of any repulsive forces would be larger than the range of attractive forces resulting from the charge-transfer interaction.

Secondly, if such a barrier does exist, then it is superfluous to consider a lower hump separating the  $\Pi$ - and  $\sigma$ -complexes. The system would acquire the necessary excess of energy in passing the first hump, and conceptually the second hump would only be of significance if a mechanism existed to dissipate the internal energy of the complex before it reached the  $\sigma$ -complex stage. In a radical or free atom addition, it is unlikely that such a mechanism exists.

The diagram in Fig. 39, can therefore be revised by setting  $E_a = 0$ , so that the reaction path is represented by the following diagram, with the dotted line representing an olefin having a negative activation energy for  $S(^3P)$

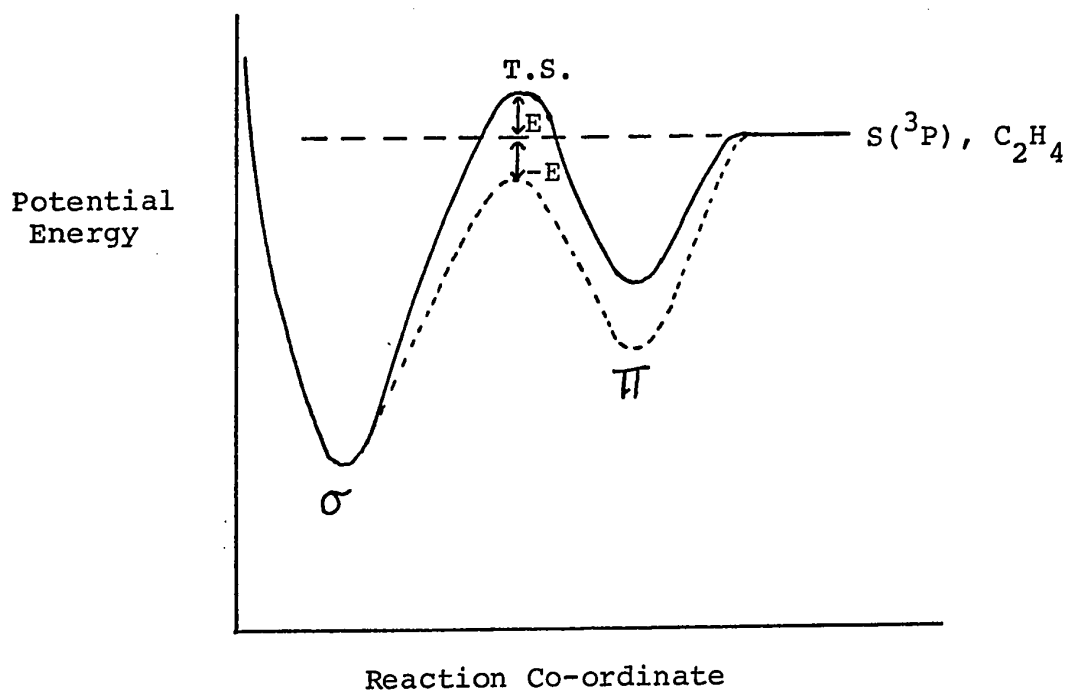
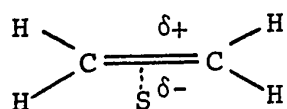


Figure 40

or  $O(^3P)$  addition. The  $\Pi$ -complex in Fig. 40 has the following structure:



in which the sulfur is not attached to either carbon atom of the double bond. The greater the polarity of the  $\Pi$ -complex, the lower will be the energy of the transition state.

According to the proposed reaction course as shown in Fig. 40, the transition state lies at the hump between the  $\Pi$ - and  $\sigma$ -complex and therefore resembles a  $\sigma$ -complex. Cvetanovic (89) reasoned that the transition

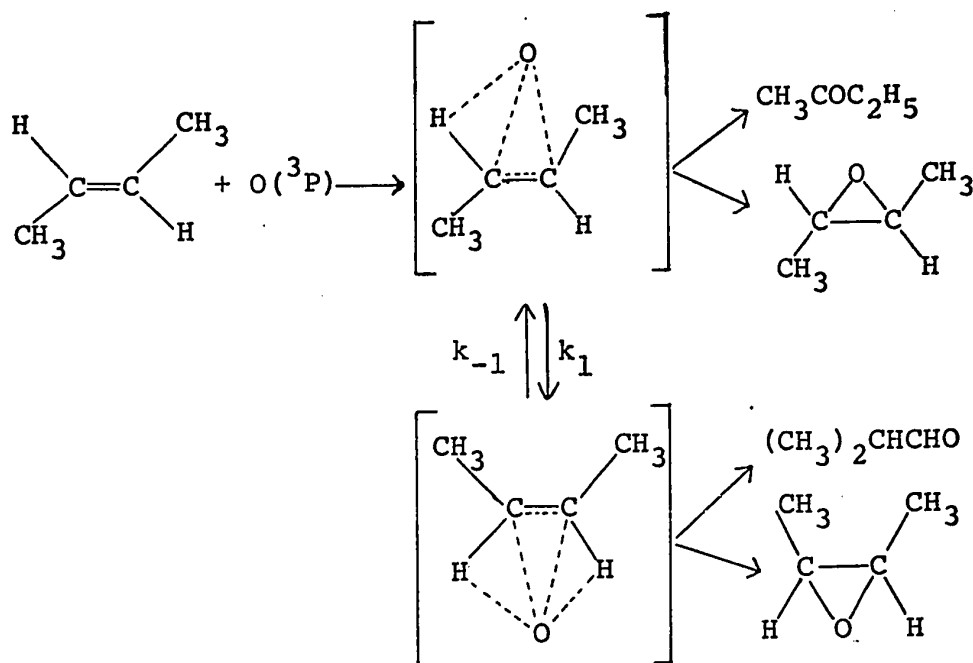


state for  $O(^3P)$  addition had to resemble a  $\Pi$ -complex and that consequently there had to be an energy barrier prior to the  $\Pi$ -complex stage. His reasoning was based on the following experimental observations; the rates of  $O$  atom addition to propylene and 1-butene were equal as were the rates of addition to 2-butene and 2-pentene, indicating that a methyl group and an ethyl group both had the same effect on reactivity; however, in the case of 2-pentene the oxygen atom addition took place exclusively at the double bonded carbon atom to which the methyl group was attached. If the same factors governed the over-all reactivity and the orientation, about equal addition to the two doubly bonded carbon atoms in 2-pentene would be expected. Therefore the transition state responsible for the observed activation energies must occur early in the reaction i.e. before the oxygen atom becomes oriented on one specific carbon. This reasoning is compatible with the reaction path illustrated in Fig. 40, if, in the  $\sigma$ -complex, the oxygen atom is bound to both carbon atoms, and the intramolecular rearrangements to form carbonyl compounds occur at a later stage. The  $\sigma$ -complex visualized by Cvetanovic was a triplet oxydimethylene biradical with some Zwitterion character, so that the oxygen atom had become attached to a specific carbon atom in the transition state. This biradical structure was invoked in order to explain the lack of stereospecificity of  $O(^3P)$  additions

to internal olefins. However, the non-stereospecificity of the addition is still feasible with the oxygen atom partially bonded to both carbon atoms, if the partial bonds are weak enough. While the bonding in the ( $S(^3P)$ ,  $C_2H_4$ )  $\sigma$ -complex is probably stronger than that in oxygen, nevertheless the reaction is not 100% stereospecific.

The results of the addition of  $CF_3$  radicals to benzene and some of its derivatives (105,106) suggest that a C-C bond is being formed in the transition state. These radicals, being highly electrophilic, probably form a  $\Pi$ -complex in the early stage of the reaction as their activation energies for addition to substituted benzenes are linearly related to the ionization potentials (29). Also Szwarc et al (27) found that the log of the relative rate constants per reactive centre for  $CF_3$  addition to aromatic compounds was linearly related to the localization energies. This means that for this electrophilic radical the transition state resembles a  $\sigma$ -complex.

If, then, the transition state for oxygen or sulfur atom addition is not a biradical and is a  $\sigma$ -complex, the question arises as to its detailed structure. In a recent study on the low temperature addition of  $O(^3P)$  atoms to cis and trans-2-butene (107) and to 2-methyl-2-pentene (108), Scheer and Klein have proposed the following scheme to account for the experimental observations.



In the reaction with *trans*-2-butene at 77°K, 2-butanone and *trans*-2,3-epoxybutane constituted over 90% of the products. The % yield of these products decreased with increasing temperature but their ratio remained constant at all temperatures, as did the ratio of *cis*-epoxybutane to isobutyraldehyde, regardless of whether the starting olefin was *cis* or *trans*. This implied two precursor states, one leading to *trans*-epoxybutane and 2-butanone and the other to *cis*-epoxybutane and isobutyraldehyde. The proposed structure of these transition states, in which the oxygen atom is weakly bonded to both carbon atoms and to any hydrogen atoms on the same side of the molecule, is based on the observation that in the *cis* isomer the methyl group migrates while in the *trans* isomer a hydrogen atom migrates. The difference in  $E_a$  for  $k_1$  and  $k_{-1}$  is 370 cal mole<sup>-1</sup>.

The uncoupled electrons are not localized on the oxygen or carbon atoms.

At 77°K, the addition to trans-2-butene was highly stereospecific, the total epoxide yield consisting of 94% trans and 6% cis. The degree of stereospecificity decreased as the temperature was raised, indicating a considerable energy barrier to rotation. The two isomeric transition states are not in equilibrium since the ratio of epoxides is different for the two starting olefins. The high dependence of their rate of interconversion on temperature suggests that this takes place before any appreciable enthalpy is released; thus, the partially formed C-O bonds in the transition state are very weak resulting in a structure very much looser than that of the final epoxide.

The cyclic structure for this addition reaction is further supported by the A-factors for addition to acetylene and ethylene. The ratio of  $A_{C_2H_2}/A_{C_2H_4} \sim 4$  can be explained by the difference in standard entropy between a cyclic structure for the transition state of  $O + C_2H_4$  and a linear one for  $O + C_2H_2$  (93).

The features of  $S(^3P)$  addition to olefins are similar to those reported by Scheer and Klein for  $O(^3P)$  addition. Although the additions of both  $S(^1D)$  and  $S(^3P)$  atoms are equally stereospecific, the degree of stereospecificity is different for the addition to the cis and

trans isomer, as in the case of  $O(^3P)$  atoms. Thus, at room temperature, cis and trans-2-butene retain their configuration in the episulfide product, respectively, to the extent of 87% and 98% ( 8 ). For cis and trans 1,2-dichloro-ethylenes retention is 80% and 90% respectively, ( 7 ) while for trans and cis 1,2-difluoro-ethylene the configuration is retained to the extent of 80% and >98% respectively (59 ). In the case of trans-difluoroethylene at least, the degree of stereospecificity is temperature dependent, as shown by the data in Table XXVI.

The current hypotheses of stereospecificity of addition of divalent species to olefins have evolved from methylene chemistry where it has been shown that the lowest singlet state of methylene adds stereospecifically while the ground state triplet does not. Three schools of thought on the subject exist and may be summarized as follows.

1) The concept put forward by Skell and Woodworth (109) proposes that singlet species add across double bonds with simultaneous formation of two bonds. With triplet additions, the primary adduct is believed to be trimethylene triplet, in order to conserve spin. Cvetanovic et al (74) have reported convincing evidence obtained in an isotopic labeling study that in the addition of triplet methylene, a biradical is indeed formed having little or no interaction between the terminal carbon atoms.

2) De More and Benson (110) have suggested that both

singlet and triplet methylene addition give rise to a short-lived biradical intermediate and that the degree of stereospecificity is determined largely by the relative rates of rotation versus ring closures rather than by the spin state of the reagent. These authors calculated an activation energy barrier to ring closure of about 10 kcal, so that the more energetic singlet methylene would lead to more rapid closure.

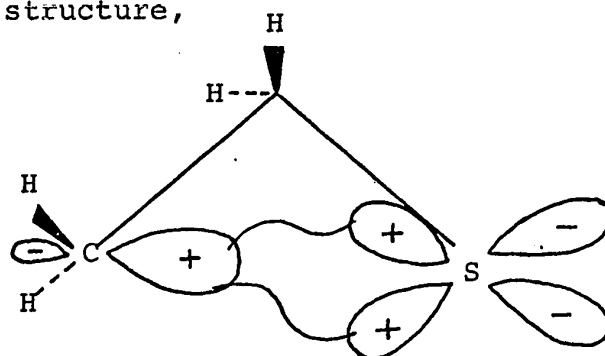
3) The results of extended Hückel calculations, reported by Hoffman (111), have revealed the existence of a singlet trimethylene intermediate, having in the ground electronic configuration, a C-C-C angle of  $125^\circ$  and trigonal terminal methylene groups coplanar with the carbon skeleton. This excited state has an energy barrier to internal rotation of about 10 kcal and the most facile mode of reaction is closure to cyclopropane via a conrotatory motion of the terminal methylene groups, the activation energy for which is about 1 kcal. The potential surface for the excited configuration, however, consists of a broad minimum indicating an excited state in which there are no barriers to rotation about the C-C bonds. The lowest singlet state of methylene,  $^1A_1$ , has the ground electronic configuration and, since it correlates with the ground configuration of trimethylene, adds to an ethylene molecule to form a cyclopropane-like structure resulting in a stereospecific reaction. On the other hand, the triplet methylene

species ( $^3B_1$ ) and the upper singlet ( $^1B_1$ ) have an excited electronic configuration and on addition to ethylene will pass through the "floppy" biradical in which free rotation takes place about the C-C bonds. The major contribution of Hoffman's study is that the stereospecificity of methylene additions to olefins can be rationalized in terms of the orbital occupancy or electronic configuration alone without recourse to spin arguments or energetic considerations.

The hypothesis of Skell and Woodworth is clearly inadequate to explain the stereospecificity of  $S(^1D)$  and  $S(^3P)$  atoms. Since the excess energy of  $26 \text{ kcal mole}^{-1}$  contained by  $S(^1D)$  atoms does not alter the stereospecificity the argument of de More and Benson is difficult to assess. Both the  $S(^3P)$  and  $S(^1S)$  atoms have the same orbital occupancy i.e. one electron in each of two degenerate p-orbitals, thus, following the arguments of Hoffman they might be expected to go through the same intermediate and perhaps correlate with a ground electronic configuration of thiodimethylene as in the case of  $CH_2(^1A_1)$ . This intermediate could have a structure somewhat similar to the excited state described by Hoffman.

Recently, Lown et al (61) have investigated the thermolysis of some episulfides and have concluded that the reaction, which is first order below  $250^\circ\text{C}$ , proceeds via a long-lived excited state of the episulfide molecule. The proposed intermediate,  $\Pi$ -thiacyclopropane has the

following structure,



and is analogous to the excited cyclopropane described by Hoffman, with the important difference that the terminal methylene group is not in the plane of the CCS skeleton but has a configuration intermediate between the planar structure and the original configuration in the olefin molecule; hence if ring closure is effected by conrotation of the terminal carbon and the sulfur atom, the stereochemistry of the reactant molecule is preserved. This structure is not unreasonable for a sulfur containing species, and is made possible by hybridization of the filled and half-filled p-orbitals of the sulfur atom to form two equivalent hybrid orbitals which can interact with the p-orbital of the carbon atom. This species has been proposed also as an intermediate in the addition of  $S(^3P)$  atoms to olefins and thus corresponds to the  $\sigma$ -complex in Fig. 40.

The transition state for  $S(^3P)$  addition to ethylene may be envisioned therefore as having a structure which is intermediate between  $\Pi$ -thiacyclopropane and the ethylene-sulfur  $\Pi$ -complex, and having considerable polar character,



the negative charge being on the sulfur. The complete reaction path is shown in Fig. 41 below. Rotation about

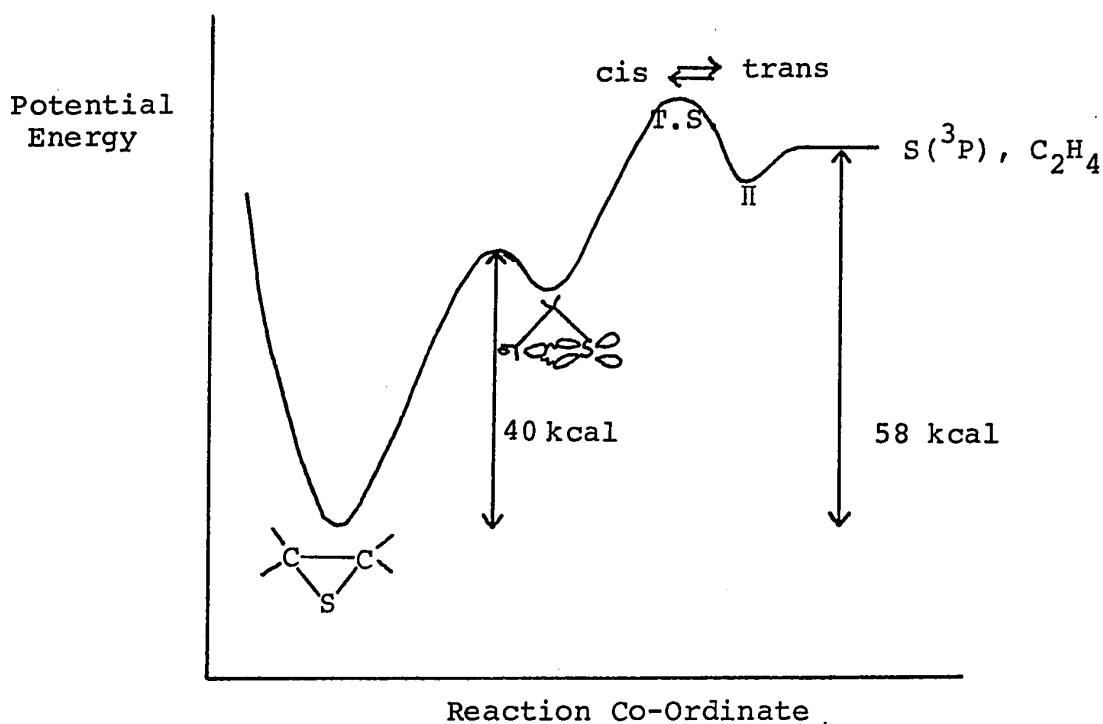


Figure 41

the C-C bond can probably take place in the activated complex with an activation energy of several kcal mole<sup>-1</sup>, although the cis and trans isomers are not in equilibrium at normal temperatures. At relatively high pressures then, the activated complex will rapidly pass through the intermediate thiacyclopropane and undergo collisional deactivation to the ground state ethylene episulfide. At low pressures, the vibrational energy of the II-thiacyclopropane will not be removed as rapidly and the complex can alternate

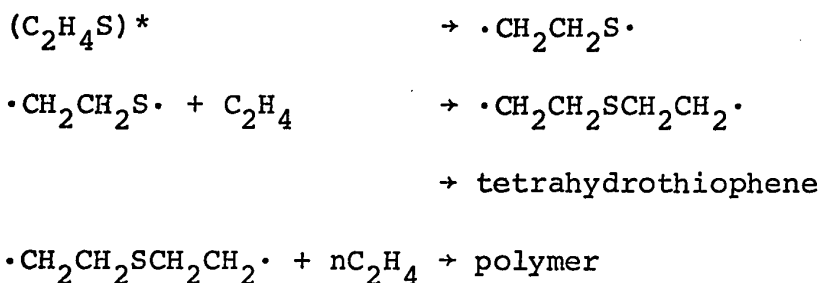
between a vibrationally excited  $\Pi$ -thiacyclopropane, the transition state and the separated reactants, so that a mixture of cis and trans episulfides and olefins can result. A recent study by Schmidt and Lee (112) has shown that such is the case with cis-2-butene. These authors photolyzed a mixture of COS and cis-2-butene at about 1 torr pressure and found that the cis-2-butene isomerized to the trans isomer with a quantum yield of 230. The proposed chain carrier was the  $S(^3P)$  atom.

Further evidence for the proposed transition state is given in the following two chapters.

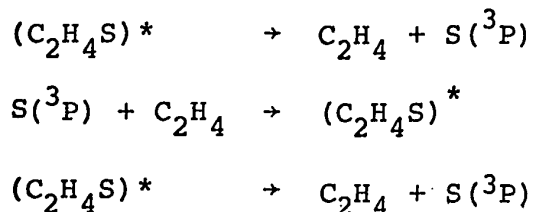
## CHAPTER IV

INVESTIGATION OF  $S(^3P)$  - OLEFIN SYSTEMS AT LOW PRESSURESA) Preliminary Experiments

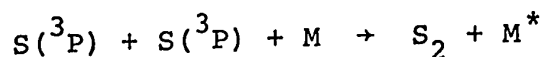
The addition of ground state sulfur atoms to ethylene is exothermic by  $58.5 \text{ kcal mole}^{-1}$ . Due to the relatively low number of degrees of freedom in the newly-formed 'hot' episulfide molecule, it is probably a fairly short-lived species, and would therefore be expected, at low pressures, to undergo unimolecular fragmentation, or rearrangement to the thiodimethylene biradical which could then undergo polymerization, as follows:



In the case of fragmentation, the following chain reaction (112) might obtain:



terminated by the reaction



Such reactions of a hot episulfide molecule should be manifested in a lower ethylene episulfide to CO ratio, as the pressure in the system decreases.

In order to investigate this effect, a gas mixture was made up of COS, CO<sub>2</sub> and C<sub>2</sub>H<sub>4</sub> and photolyzed at different total pressures. The ratio of these three components to each other was chosen such that there was sufficient CO<sub>2</sub> present to deactivate all the S(<sup>1</sup>D) atoms to the ground state, and sufficient C<sub>2</sub>H<sub>4</sub> to prevent the abstraction reaction of S(<sup>3</sup>P) atoms with COS. In order to vary the pressure, therefore, aliquots were taken of a mixture of 30 torr COS, 940 torr CO<sub>2</sub> and 40 torr C<sub>2</sub>H<sub>4</sub> measured in the photolysis cell.

The results of the preliminary study are shown in Table XLII and the ratio of EES/CO is plotted against total pressure in Fig. 42. It is clear from Fig. 42 that there is a marked decrease in the EES/CO ratio with pressure, but the decrease is not smooth and other factors must be involved. For example, in runs #428 and #429, the total pressure is the same, yet the yields of episulfide per μmole CO are very different; this must be due to the difference in irradiation time, indicating some secondary reaction whereby EES is removed from the system. Also,

TABLE XLII

PHOTOLYSIS OF COS-CO<sub>2</sub>-C<sub>2</sub>H<sub>4</sub><sup>a</sup>; VARIATION OF EES/CO WITH PRESSURE AND TIME

Run	Pressure (torr)	μ CO	μ EES	EES CO	Time (mins)
430	1,010	1.66	0.809	0.49	45
435	700	0.79	0.360	0.46	20
431	440	2.65	0.824	0.31	145
434	300	2.42	0.515	0.21	190
428	165	1.14	0.232	0.20	120
429	165 <sup>b</sup>	2.44	0.280	0.11	240
432	111 <sup>b</sup>	1.40	0.434	0.31	240
433	40 <sup>b</sup>	1.06	0.147	0.14	720

a) Aliquots taken of [940 torr CO<sub>2</sub>; 30 torr COS; 40 torr C<sub>2</sub>H<sub>4</sub>].

b) Reaction vessel was 1-litre bulb ∴ total amount of gas greater.

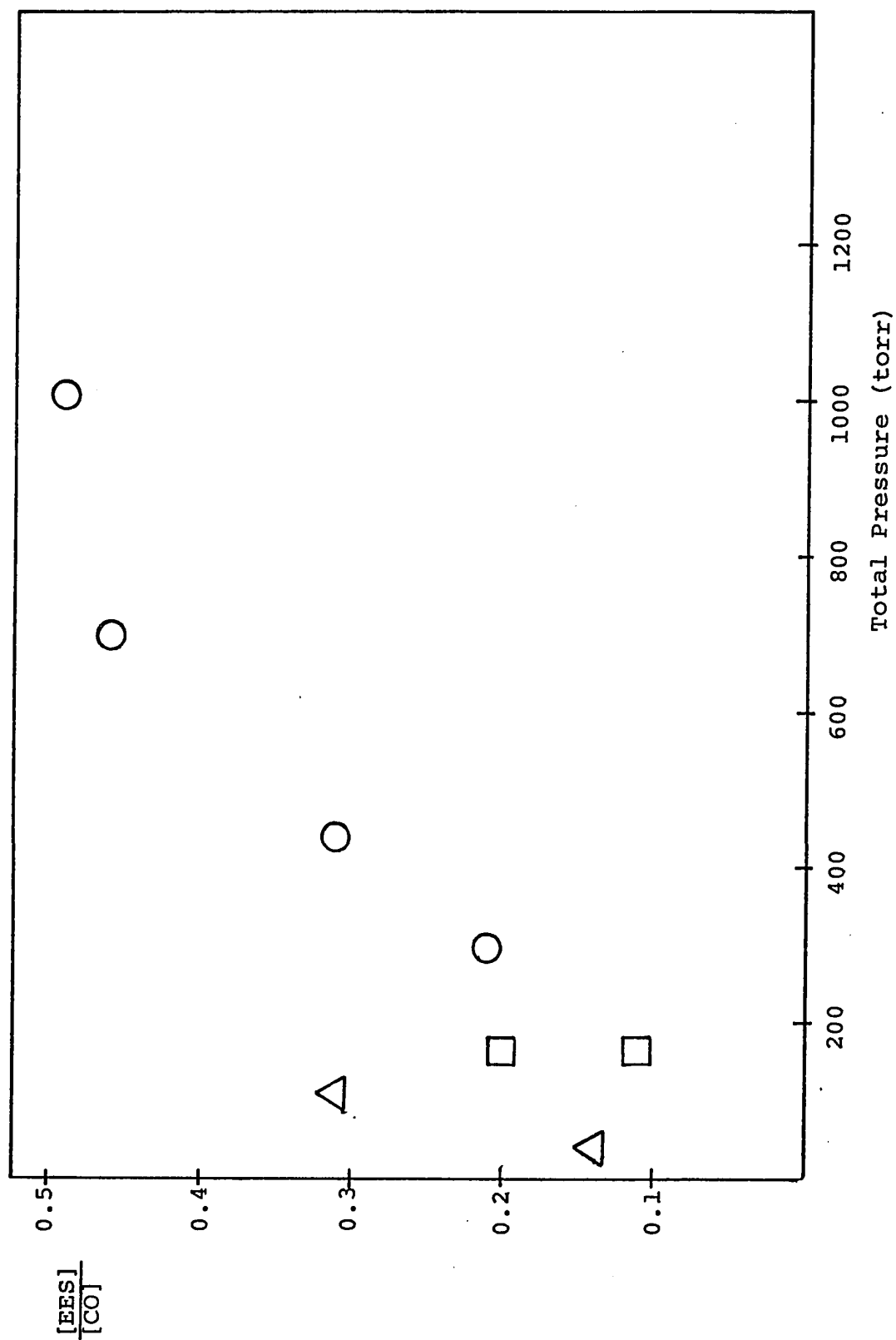


Figure 42: Variation of  $\frac{[EES]}{[CO]}$  with total pressure

O - quartz cell (250 ml);  $\Delta$  - 1-litre bulb;  $\square$  different irradiation times (Runs 428, 429)

runs #432 and #433 were carried out in a one-litre bulb, fitted with a quartz window, and give an anomalously high EES/CO ratio. Since the amount of ethylene in the 1-litre bulb was about 5 times as large as that contained in the quartz cell, it seems that ethylene is effective in preventing the reaction by which EES is removed.

In order to observe the pressure independent depletion of EES, a series of runs was carried out at constant pressure; these are summarized in Table XLIII and Fig. 43 shows the corresponding plot of EES yield against CO yield, the latter quantity increasing linearly with irradiation time. The two most likely routes for the time-dependent disappearance of EES are via (a) secondary photolysis of the ethylene episulfide and (b) reaction of EES with  $S(^3P)$  atoms, since either of these would result in a steady-state concentration of the episulfide. In order to check out the first possibility the light source was varied as indicated in Table XLIII. Ethylene episulfide starts to absorb weakly at about  $3700\text{\AA}$ , with a weak maximum around  $2500\text{\AA}$  and an intense maximum just below  $2200\text{\AA}$  (115). COS has a maximum absorption at  $2290\text{\AA}$  (2). By using a Cadmium resonance lamp instead of the Hg-arc, the effective wavelength was changed from about  $2490\text{\AA}$  to  $2288\text{\AA}$ , yet this had no effect on the steady-state yield of episulfide, as shown in Fig. 43. Similarly, insertion of a 7910 filter, cutting off light below c.  $2200\text{\AA}$  had no effect.

TABLE XLIII  
 PHOTOLYSIS OF COS-CO<sub>2</sub>-C<sub>2</sub>H<sub>4</sub><sup>a</sup>; VARIATION OF  $\mu$  EES WITH  $\mu$  CO AT CONSTANT PRESSURE

Run	Conditions	$\mu$ CO	$\mu$ EES	Total Pressure (torr)
438	Hg-arc; 7910 filter	1.62	0.088	124
439	Cd-Res. Lamp; 7910 filter	2.20	0.088	124
440	Cd-Lamp; No filter	0.77	0.066	124
441	10 torr COS added	1.21	0.085	134
442	10 torr COS added	2.07	0.085	134
443	10 torr COS added	0.48	0.033	134
444	10 torr COS added	5.03	0.085	134
446	5.5 torr C <sub>2</sub> H <sub>4</sub> added	5.78	0.62	139.5
447	5.0 torr C <sub>2</sub> H <sub>4</sub> added	5.16	0.83	144.5
448	5.0 torr C <sub>2</sub> H <sub>4</sub> added	5.56	1.06	149.5

a) Ratio of CO<sub>2</sub>:COS:C<sub>2</sub>H<sub>4</sub> initially = 940:30:40.



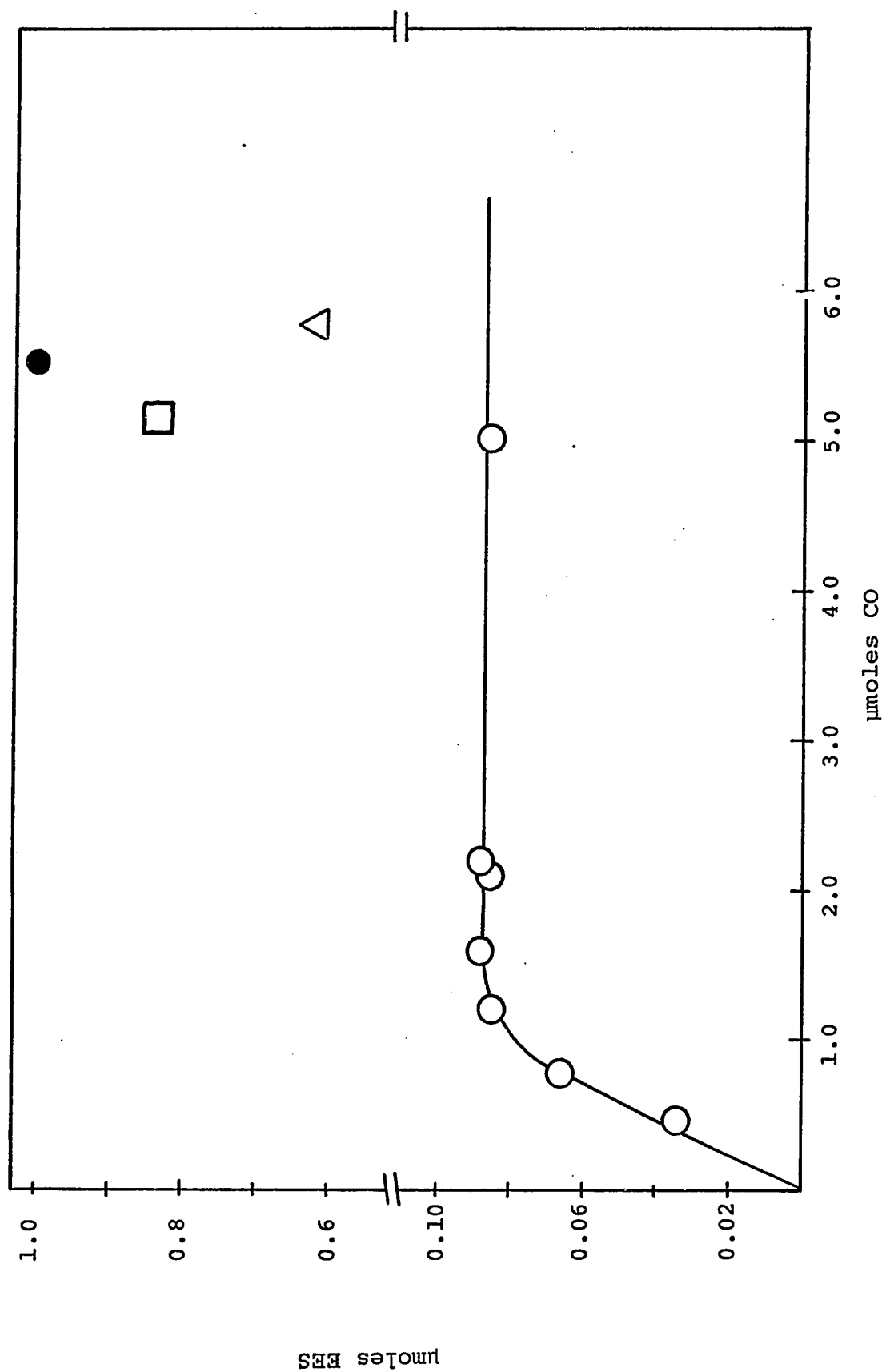
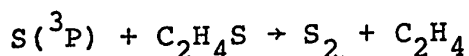


Figure 43: Variation of  $\mu\text{moles EES}$  with  $\mu\text{moles CO}$   
 O - 5 torr  $\text{C}_2\text{H}_4$ ;  $\Delta$  Run 447;  $\square$  Run 446;  $\bullet$  Run 448 (Table XLIII)

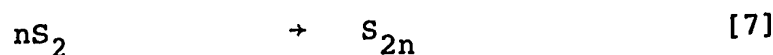
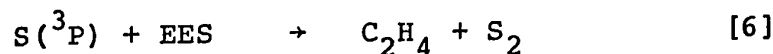
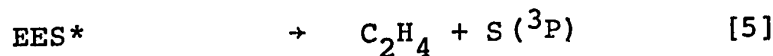
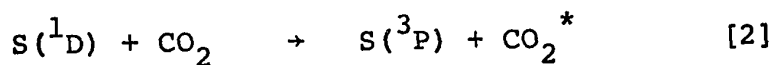
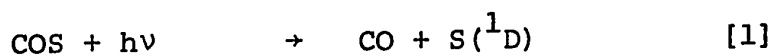
The pressure of COS in the system was then increased by 10 torr, again leaving the steady-state yield of ethylene episulfide unchanged. Thus possibility (a) was ruled out.

The partial pressure of  $C_2H_4$  in the system was then increased, resulting in an increase in the steady-state concentration of EES. Therefore, the constancy of the EES yield is due to competition for  $S(^3P)$  atoms between  $C_2H_4$  and EES. The reaction of  $S(^3P)$  atoms with EES may be tentatively assumed to be an abstraction reaction, as follows:



#### B) Steady-State Treatment

The system can be described by the following scheme:



The proposal of reaction [5] for the unimolecular

fragmentation of 'hot' episulfide, rather than a polymerization reaction via the thiodimethylene biradical is supported by recent results of Lee et al (112).

These authors photolyzed a mixture of COS and cis-2-butene at about 1 torr pressure and reported the isomerization of the cis-2-butene to the trans isomer with a quantum yield of 300. The proposed chain carrier was  $S(^3P)$ .

Assuming a steady state concentration of both EES and EES\* in the above scheme and following the usual treatment we get:

$$\frac{d[EES]}{dt} = k_4 [EES^*] [M] - k_6 [S] [EES] = 0$$

$$\therefore [EES^*] = \frac{k_6 [S] [EES]}{k_4 [M]} \quad (i)$$

$$\frac{d[EES^*]}{dt} = k_3 [S] [C_2H_4] - k_4 [EES^*] [M] - k_5 [EES^*] = 0$$

$$[EES^*] = \frac{k_3 [S] [C_2H_4]}{k_4 [M] + k_5} \quad (ii)$$

Combining (i) and (ii)

$$\frac{k_6 [S] [EES]}{k_4 [M]} = \frac{k_3 [S] [C_2H_4]}{k_4 [M] + k_5}$$

$$\therefore \frac{[C_2H_4]}{[EES]} = \frac{k_6}{k_3} \left( 1 + \frac{k_5}{k_4 [M]} \right)$$

A plot of  $[C_2H_4]/[EES]$  against  $\frac{1}{[M]}$ , where  $[M]$  is the total pressure in the system and  $[EES]$  is the steady state concentration, should give a straight line with an intercept equal to  $k_6/k_3$  and a slope equal to  $k_6k_5/k_3k_4$ . The results of a study of the variation of  $[C_2H_4]/[EES]$  with pressure are shown in Table XLIV and plotted in Fig. 44. The ethylene pressure was measured in a standard volume and the runs were carried out in three different volumes, a quartz cell (volume  $\sim 200$  ml), a 1-litre bulb and a 3-litre bulb. Each of these three volumes was accurately calibrated against the standard volume, which in turn was calibrated against the gas buret. The G.L.C. peak area for EES was also calibrated against the gas buret. Thus, the  $C_2H_4$  pressure, the total pressure and the steady-state pressure of EES could be calculated in either of the three reaction vessels. The precise volumes of the reaction vessels were 2,997 ml, 1,106 ml and 250.0 ml.

A least mean squares treatment of the line in Fig. 44 gave the following values for the slope and intercept for a 95% confidence level:

$$\text{Intercept} = k_6/k_3 = 139 \pm 24$$

$$\text{Slope} = k_6/k_3 \cdot k_5/k_4 = (10.0 \pm 0.66) \times 10^3 \text{ torr.}$$

$$\begin{aligned} \text{Therefore } k_5/k_4 &= 72 \text{ torr} \\ &= 3.85 \times 10^{-3} \text{ moles/litre} \end{aligned}$$

Reactions [5] and [6] will now be discussed separately.

TABLE XLIV

PHOTOLYSIS OF COS-CO<sub>2</sub>-C<sub>2</sub>H<sub>4</sub><sup>a</sup>; VARIATION OF  $\frac{[C_2H_4]}{[EES]}$  WITH TOTAL PRESSURE

Run	Pressure <sup>b</sup> (torr)	P(C <sub>2</sub> H <sub>4</sub> ) <sup>c</sup>	μ CO	μ EES	P(EES) <sup>d</sup>	$\frac{[C_2H_4]}{[EES]}$	$\frac{10^3}{P}$
1a	29.6 <sup>f</sup>	25.4	9.63	0.607	0.0583	436	33.9
3a	130.9 <sup>e</sup>	24.7	13.0	1.21	0.116	213	7.64
4a	48.9 <sup>f</sup>	24.3	9.1	0.743	0.0714	340	20.4
8a	68.6 <sup>f</sup>	25.2	34.2	0.912	0.0876	288	14.6
9a	303.8 <sup>e</sup>	24.9	26.3	1.48	0.142	175	3.29
437	40 <sup>f</sup>	9.0	10.2	0.235	0.0226	398	25.0
13a	11.3 <sup>g</sup>	25.3	27.5	0.254	0.0244	1,037	88.5
452	934 <sup>e</sup>	12.4	8.6	0.765	0.0735	169	1.07

a) P(CO<sub>2</sub>):P(COS):P(C<sub>2</sub>H<sub>4</sub>) ≈ 5:1.5:1

b) Pressure in reaction vessel

c) Pressure in standard volume

d) Calculated pressure in standard volume

e) Quartz cell

f) 1-litre bulb

g) 3-litre bulb

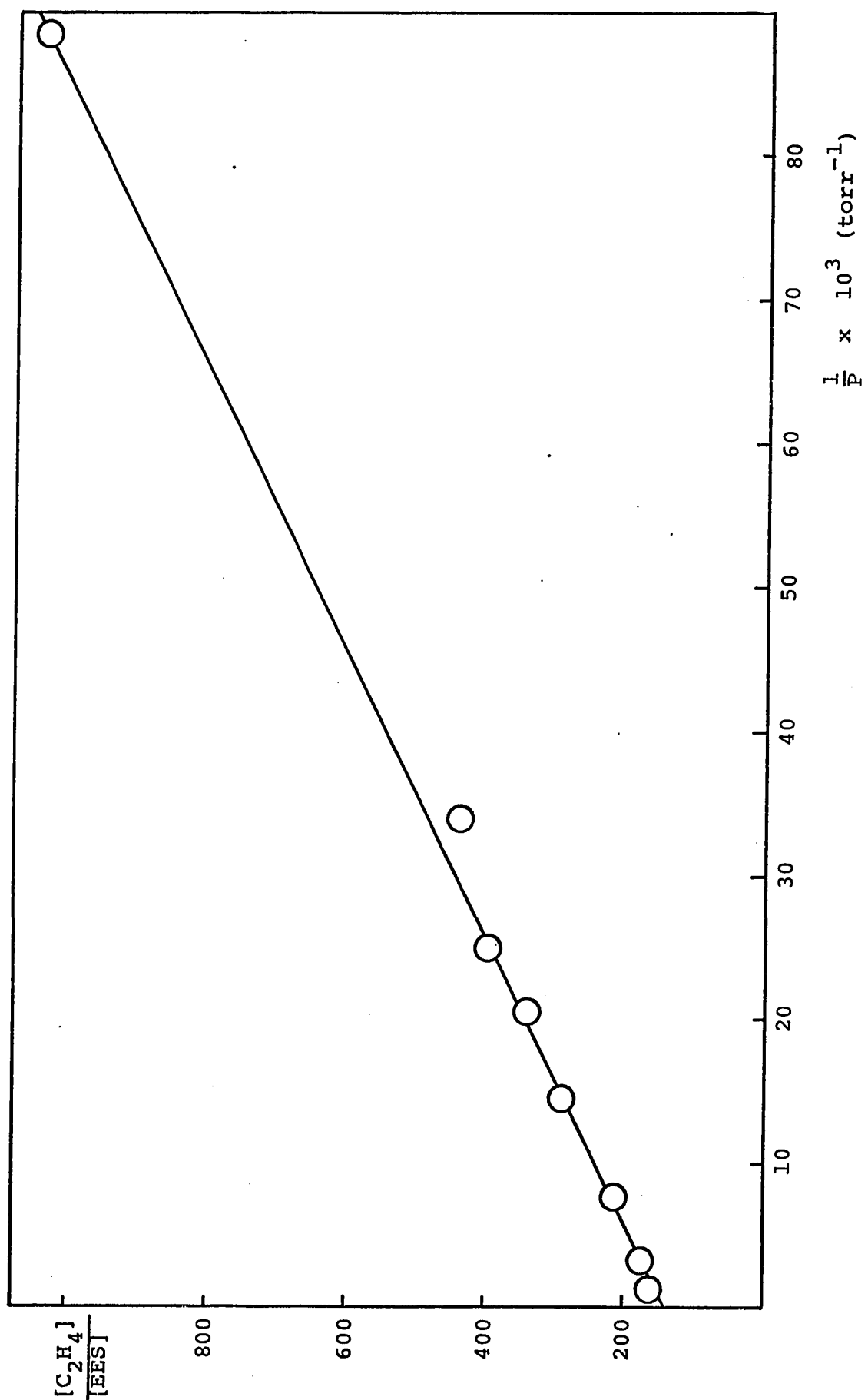


Figure 44: Plot of  $\frac{[C_2H_4]}{[EES]}$  versus  $\frac{1}{P}$

L.M.S. Intercept = 139; Slope = 10,000

C) Fragmentation of 'Hot' Episulfides

If we assume a collision efficiency ( $\lambda$ ) of unity for reaction [4] we can calculate an upper limit for the unimolecular rate constant  $k_5$ .

The collision frequency is given by the following expression (103):

$$Z = N \left( \frac{8\pi kT}{\mu} \right)^{1/2} \sigma^2 \text{ cc. mole}^{-1} \text{ sec}^{-1}.$$

If we assume an average collision diameter for the quenching gas, most of which is  $\text{CO}_2$ , of  $5.0\text{\AA}$ , then

$$Z = 2.4 \times 10^{14} \text{ cc. mole}^{-1} \text{ sec}^{-1}$$

$$\therefore k_5 \leq 2.4 \times 10^{14} \times 3.85 \times 10^{-6} \text{ sec}^{-1}$$

$$\leq 9.2 \times 10^8 \text{ sec}^{-1}$$

Although an upper limit, this value is probably very close to the correct value since the 'hot' episulfide only requires the removal of a few  $\text{kcal mole}^{-1}$  of energy in order to prevent it from returning along the same reaction path by which it was formed. Thus one or two collisions with an efficient deactivator such as  $\text{CO}_2$  should be sufficient.

An approximate value for  $k_5$  can be arrived at by means of the classical RRK equation

$$k_5 = A \left( \frac{E - E^*}{E} \right)^{n-1}$$

Following the treatment by Strausz et al (61) of the

thermal decomposition of ethylene episulfide we can set  $n = 5$ , as the best value for the number of effective oscillators. Fig.45 shows the proposed reaction surface and the approximate energies of the intermediate. The reaction co-ordinate may be assumed to be the distance between the sulfur atoms and the centre of the C-C bond. Thus the activation energy for decomposition to  $S(^3P)$  and  $C_2H_4$  is about  $61 \text{ kcal mole}^{-1}$  so that

$$\begin{aligned} k_5 &= A \left( \frac{nRT}{61} \right)^{n-1} \\ &= A \left( \frac{3.0}{61} \right)^4 \\ &= A \times 5.7 \times 10^{-6} \end{aligned}$$

The A-factor for the decomposition would be expected to be quite high and is probably greater than  $10^{13}$ . The decomposition of  $C_2H_6^*$  has an A-factor of  $10^{17.5}$  (116) while the A-factor for  $C_2F_4H_2^*$  fragmentation was taken by Benson and Haugen (113) to be  $10^{17} \text{ sec}^{-1}$ . If we arbitrarily assign a value of  $10^{14} \text{ sec}^{-1}$  to the A-factor for  $C_2H_4S^*$  decomposition, then

$$k_5 = 5.7 \times 10^8 \text{ sec}^{-1}$$

This value, then, agrees with the experimentally determined one if we assume  $\lambda = 0.62$  for the collision efficiency, so that the 'hot' episulfide requires an average of 1.6 collisions to produce stabilization. The



approximate lifetime of EES\* is therefore about  $2 \times 10^{-9}$  sec.

The thermal decomposition of ethylene episulfide (61) occurs via a different reaction path so that the two unimolecular rate constants cannot be compared. The difference in the two reactions is illustrated in Fig. 45 where the thermally activated molecule (below  $250^\circ\text{C}$ )

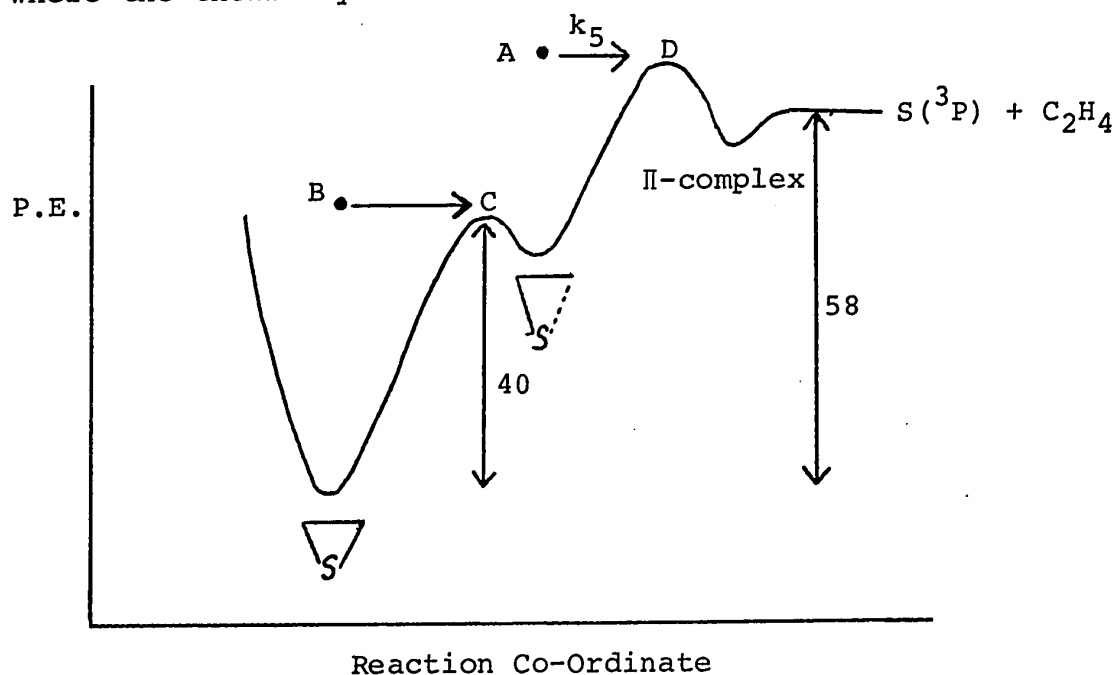


Figure 45

is represented by B, and the high pressure rate determining step for its decomposition is the crossing of the energy barrier at C, with an A-factor of  $10^{12.9} \text{ sec}^{-1}$ . The chemically excited molecule resulting from addition of  $\text{S}(^3\text{P})$  to ethylene is represented at A and its unimolecular fragmentation occurs by crossing the barrier at D,

presumably with a much higher A-factor than in the thermal case.

Using the relative rate  $k_5/k_4 = 72$  torr, it can be shown that even at a total pressure of 1,000 - 1,100 torr, the pressure range at which the Arrhenius parameters were measured (cf. Chapter III) reaction [5] occurs to a small extent. If there is a sufficiently high concentration of  $C_2H_4$  in the system to eliminate reaction [6], then, assuming a steady state concentration of EES\* we get

$$\frac{d(EES^*)}{dt} = k_3 [S] [C_2H_4] - k_4 [M] [EES^*] - k_5 [EES^*] = 0$$

$$\therefore k_3 [S] [C_2H_4] = k_4 [EES^*] [M + 72] \quad (iii)$$

$$R(EES) = k_4 [M] [EES^*] \quad (iv)$$

From (iii) and (iv)

$$k_3 [S] [C_2H_4] = R(EES) \frac{M + 72}{M}$$

At a pressure of 1,100 torr:

$$k_3 [S] [C_2H_4] = R(EES) (1.065)$$

Thus, about 6% of the newly-formed episulfide is lost by fragmentation. Accordingly, the relative rate value of 6.8 for  $S(^3P)$  addition to propylene will be 6% too high, which is hardly outside the experimental error.

### S(<sup>3</sup>P) + C<sub>3</sub>H<sub>6</sub> System

Due to the larger number of degrees of freedom in the propylene episulfide molecule, the newly formed hot species should be quite long-lived. Assuming the number of effective oscillators in propylene episulfide (PES) to be 9, and applying the RRK equation, one gets a unimolecular fragmentation rate constant of about  $5 \times 10^5 \text{ sec}^{-1}$  for PES\*. Thus, for a fixed C<sub>3</sub>H<sub>6</sub> concentration, the steady state concentration of PES would only decrease to half its limiting high pressure value, at a pressure of about 0.1 torr. It is not feasible to study the present system at such low pressures, however the data in Table XLV show that down to a pressure as low as 12 torr the C<sub>3</sub>H<sub>6</sub>/PES ratio remains the same.

### D) The Reaction of S(<sup>3</sup>P) Atoms with Episulfides

#### Results

### S(<sup>3</sup>P) + C<sub>2</sub>H<sub>4</sub>S System

The products of the reaction of S(<sup>3</sup>P) atoms with ethylene episulfide have been tentatively proposed to be S<sub>2</sub> and ethylene (Reaction [6]). The steady state treatment of the mechanism yielded the relationship

$$[C_2H_4] = [EES] \left[ \frac{k_6}{k_3} \left( 1 + \frac{k_5}{k_4} [M] \right) \right] \text{ where } [EES] \text{ is the limiting}$$

TABLE XLV

PHOTOLYSIS<sup>d</sup> OF COS-C<sub>3</sub>H<sub>6</sub>-CO<sub>2</sub>;  $\frac{C_3H_6}{PES}$  AS A FUNCTION OF PRESSURE

Run	Pressure in Standard Volume (torr)	Pressure in Reaction Vessel	Time (Mins)	$\mu$ CO	$\mu$ PES	$\frac{P(C_3H_6)}{P(PES)}$
11a	COS = 39 CO <sub>2</sub> = 140 C <sub>3</sub> H <sub>6</sub> = 7.9	32.8 <sup>a</sup>	645	33.8	2.05	40.1
12a	COS = 39 CO <sub>2</sub> = 142 C <sub>3</sub> H <sub>6</sub> = 8.7	12.3 <sup>b</sup>	840	20.8	2.48	36.6
470	COS = 40 CO <sub>2</sub> = 1,160 C <sub>3</sub> H <sub>6</sub> = 8.2	942 <sup>c</sup>	400	29.5	2.24	38.1

a) 1-litre bulb

b) 3-litre bulb

c) Quartz cell

d) Cd-Resonance lamp with 7910 filter

ethylene episulfide pressure with respect to irradiation time. Thus a plot of  $[C_2H_4]$  against  $[EES]$  at constant pressure should yield a straight line through the origin. Fig. 46, plotted from the data in Table XLVI shows such a line, the slope of which is 170. This result is in good agreement with that obtained from the data in Table XLIV.

Table XLVII shows the results of a study of the variation of the relative rate  $k_6/k_3$  with temperature. The total pressure in the system was 946 torr at room temperature; thus, from the steady state equation,  $k_6/k_3 = [C_2H_4]/[EES] \div 1.076$  at room temperature, where  $[EES]$  is the steady state pressure of EES in the system. At temperatures above  $27^\circ C$ , however, the value of  $k_5/k_4$  is not known. ( $k_5$  varies with temperature as  $e^{-\frac{1}{T}}$ ;  $k_4 = \lambda Z$  and  $Z$ , the collision frequency varies as  $T^{\frac{1}{2}}$ , but the dependence of the collision efficiency,  $\lambda$ , on temperature is unknown.) In the Arrhenius plot, therefore, which is shown in Fig. 47,  $k_6/k_3$  is taken to be  $[C_2H_4]/[EES]$  so that the relative Arrhenius parameters calculated are not precise. The A-factor for abstraction relative to addition may be high by about 7%. A least mean squares treatment of the data in Table XLVII for a 95% confidence level yielded for the relative Arrhenius parameters:  $E_3 - E_6 = 1.84 \pm 0.20 \text{ kcal mole}^{-1}$  and  $A_6/A_3 = 8.3$  within a factor of 1.3.

TABLE XLVI

PHOTOLYSIS<sup>a</sup> OF COS-CO<sub>2</sub>-C<sub>2</sub>H<sub>4</sub><sup>b</sup>; STEADY-STATE EES PRESSURE AS A FUNCTION OF P(C<sub>2</sub>H<sub>4</sub>)

Run	P(C <sub>2</sub> H <sub>4</sub> )	Irradiation Time (mins)	μ CO	μ EES	P(EES) (torr)
451	4.8	26	8.99	0.368	0.0275
452	9.8	26	8.63	0.765	0.0573
453	15.6	26	7.53	1.19	0.0891
454	21.2	32	8.33	1.64	0.123

a) Cd-Resonance lamp with 7910 cut-off filter

b) P(COS) = 24 torr; P(CO<sub>2</sub>) = 900 torr

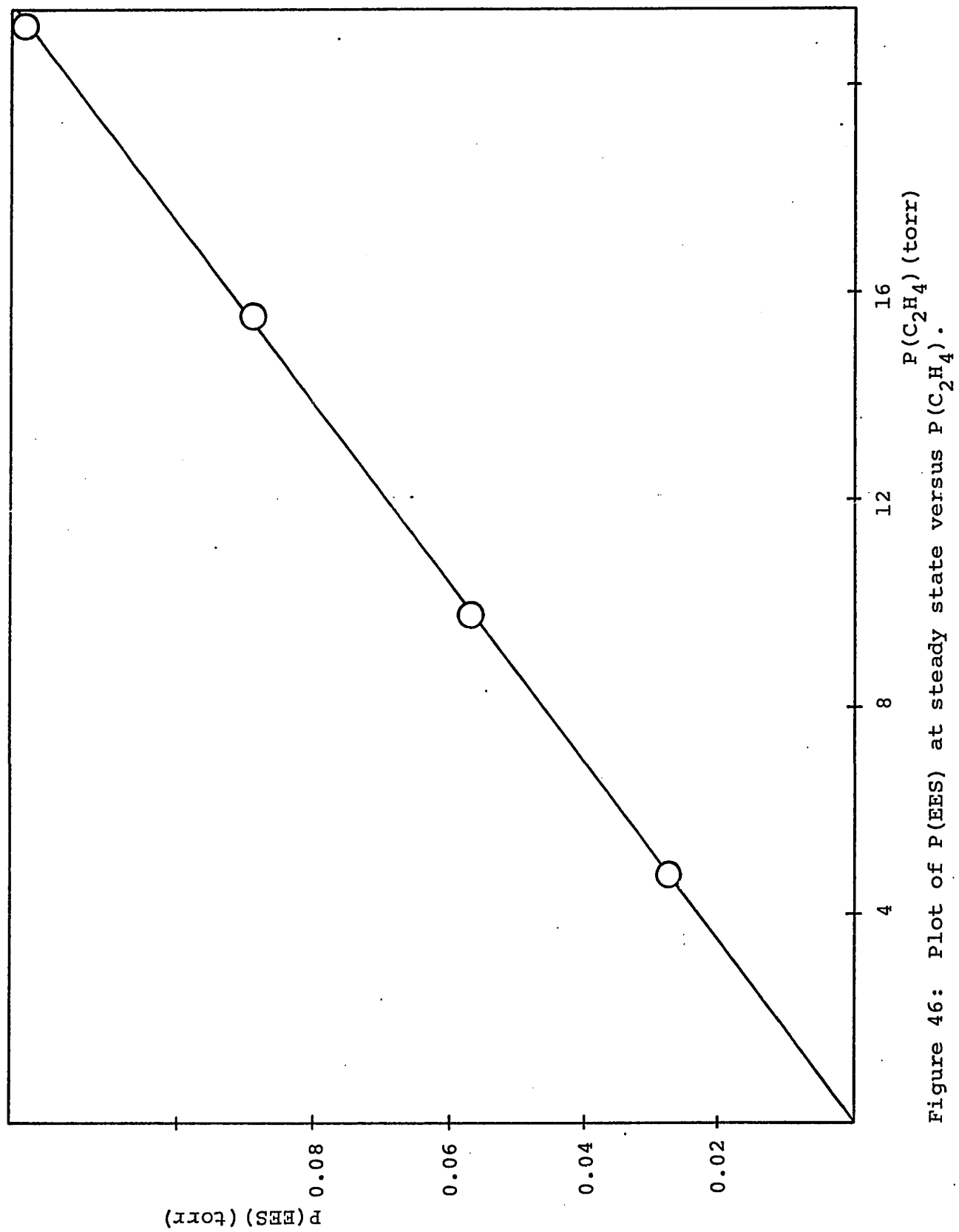


Figure 46: Plot of  $P(\text{EES})$  at steady state versus  $P(\text{C}_2\text{H}_4)$ .

TABLE XLVII  
 $\frac{k_3}{k_6}$  AS A FUNCTION OF TEMPERATURE  
 VARIATION OF  $\frac{k_3}{k_6}$

Run	$P(C_2H_4)$ torr	$\frac{1}{T} \times 10^3$	$\mu$ CO	$\mu$ EES	$\frac{k_3}{k_6} \times 100$ b	$\ln \frac{k_3}{k_6} \times 100$ a
467	25.7	3.259	35.3	1.60	0.599	-0.512
468	25.5	2.368	30.5	3.57	1.35	0.300
469	25.1	2.703	26.2	2.43	0.928	-0.075
461	25.4	2.398	51.1	3.56	1.35	0.300
457	24.4	2.954	18.3	1.93	0.758	-0.277
460	25.7	2.747	20.3	2.67	0.996	-0.004
464	25.0	2.941	46.0	2.03	0.780	-0.248
454	26.9	3.289	8.33	1.64	0.587	-0.533

a)  $P(CO_2) = 35$  torr;  $P(CO_2) = 900$  torr

b)  $\frac{P(EES)}{P(C_2H_4)}$



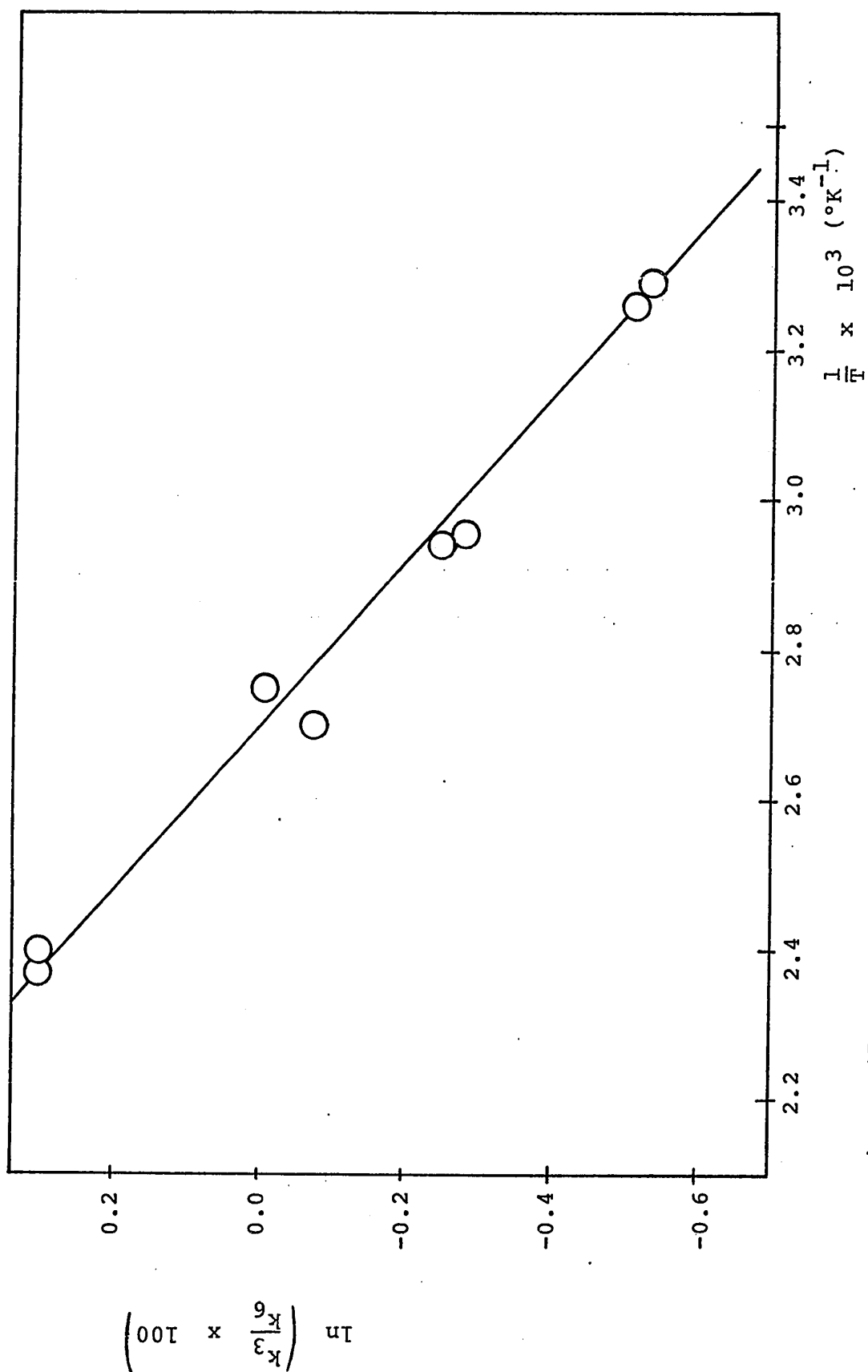
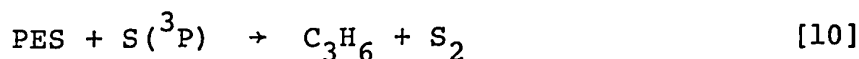


Figure 47: Arrhenius plot for  $k_3/k_6$ .

### S(<sup>3</sup>P) - C<sub>3</sub>H<sub>6</sub> - C<sub>3</sub>H<sub>6</sub>S System

In this system, the competing reactions are [9] and [10], since all the newly formed episulfide molecules are collisionally stabilized.



$k_{10}/k_9$  is given by  $[\text{C}_3\text{H}_6]/[\text{PES}]$ , where  $[\text{PES}]$  is the steady state pressure of propylene episulfide. From Table XLV it is seen that  $k_{10}/k_9 = 38$  at 27°C. Table XLVIII shows the variation of  $k_{10}/k_9$  with temperature and the corresponding Arrhenius plot is given in Fig. 48. A least mean squares treatment of the data, for a 95% confidence level yielded the following values for the relative Arrhenius parameters:  $E_9 - E_{10} = 0.93 \pm 0.17$  kcal mole<sup>-1</sup> and  $A_{10}/A_9 = 8.4$  within a factor of 1.28.

### Discussion

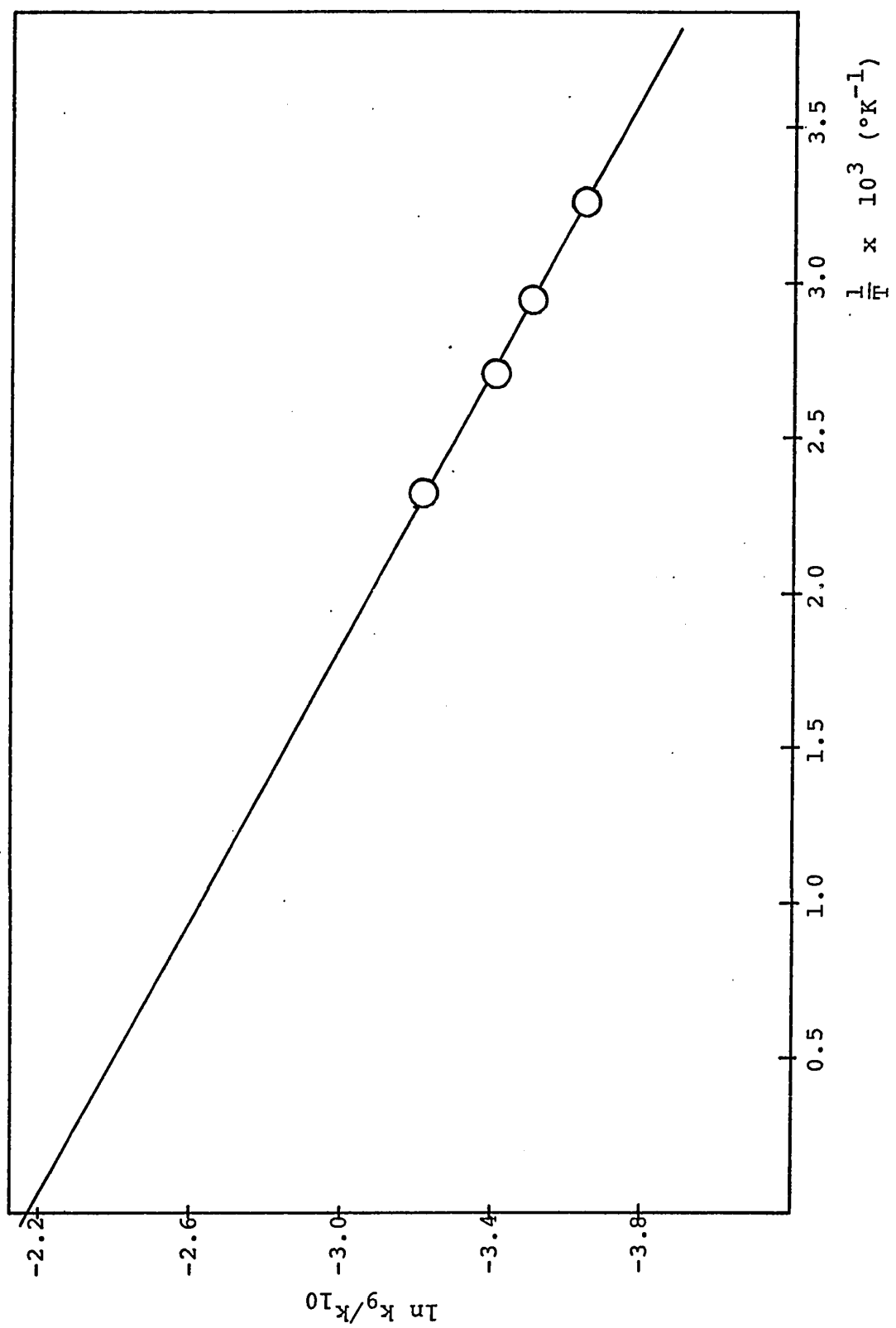
The products of reaction [6] cannot be detected in the present system; thus, there is as yet no conclusive evidence that the proposed reaction [6] correctly describes the process by which ethylene episulfide is removed. It is desirable therefore to examine any other possibilities which might exist.

TABLE XLVIII

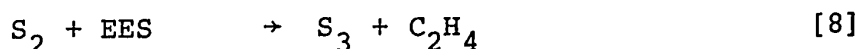
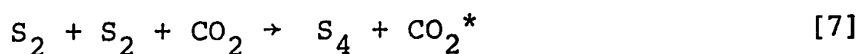
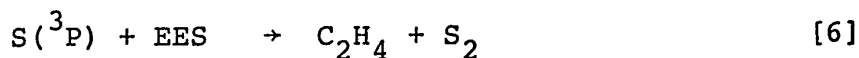
VARIATION OF  $k_9/k_{10}$  AS A FUNCTION OF TEMPERATURE<sup>a</sup>

Run	$P(C_2H_4)$ torr	$\frac{1}{T} \times 10^3$	$\mu$ CO	$\mu$ PES	$\frac{k_9}{k_{10}}$ <sup>b</sup>	$\ln \frac{k_9}{k_{10}}$
470	8.2	3.265	29.5	2.20	0.0257	-3.650
471	7.6	2.328	69.1	3.18	0.0401	-3.219
472	8.2	2.710	43.6	2.81	0.0329	-3.411
473	8.1	2.950	38.6	2.52	0.0299	-3.507

a)  $P(COS) = 40$  torr;  $P(CO_2) = 904$  torrb)  $\frac{P(PES)}{P(C_3H_6)}$

Figure 48: Arrhenius Plot for  $k_9/k_{10}$

For example the  $S_2$ , formed in reaction [6] might be capable of abstracting a sulfur atom from an episulfide molecule. The system would then be described by the following scheme, assuming, for the present purposes, that all the initially formed episulfide undergoes collisional deactivation:



At long irradiation times, we can assume a steady state concentration of both  $S_2$  and EES. Thus,

$$\frac{d(EES)}{dt} = k_3[S][C_2H_4] - k_6[S][EES] - k_8[S_2][EES] = 0$$

$$\frac{d[S_2]}{dt} = k_6[EES][S] - k_7[S_2]^2[CO_2] - k_8[S_2][EES] = 0$$

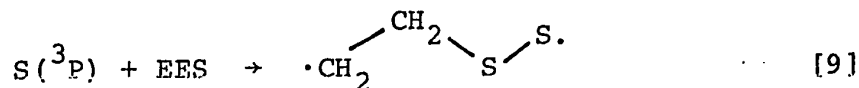
$$\therefore k_8[S_2][EES] = k_6[EES][S] - k_7[S_2]^2[CO_2]$$

$$\therefore k_3[C_2H_4] = 2k_6[EES] - k_7 \frac{[S_2]^2[CO_2]}{[S]} \quad (iii)$$

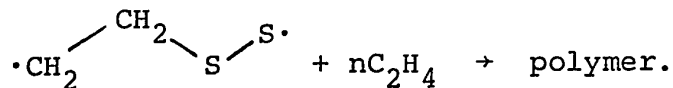
From equation (iii), a plot of [EES] against  $[C_2H_4]$  would not give a straight line, since  $[S_2]^2/[S]$  is a function of the other variables,  $[C_2H_4]$  and [EES]. No curvature is apparent, however, in the plot in Fig. 46 indicating that the above mechanism is unlikely. It is

possible that the last term in equation (iii) is negligibly small, in which case the quoted value of  $k_6/k_3$  is high by a factor of 2. Furthermore,  $S_3$ ,  $S_4$  and  $S_5$  may abstract sulfur from ethylene episulfide, so that  $k_6/k_3$  would be high by a factor of 3, 4 or 5 respectively. It is most likely though that all the  $S_2$  disappears via reaction [7]. The second order rate constant for reaction [7] has been reported as  $5.3 \times 10^9 \text{ M}^{-1} \text{ sec}^{-1}$  (117), at a pressure of 600 torr  $\text{CO}_2$ . Besides reaction [7] we could have recombination of  $S_2 + S_3$ ,  $S_2 + S_4$ ,  $S_2 + S_5$ , etc. This would increase the last term in equation (iii).

Another possibility is the reaction



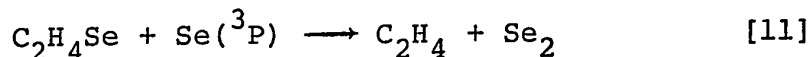
followed by



It was observed that after each run, the decrease in ethylene was greater than could be accounted for by the ethylene episulfide formed. Also the reaction vessel was coated with a faintly yellow deposit, which however could well have been pure sulfur. In order to distinguish between reactions [6] and [9], a run was carried out in which a gas mixture consisting of 100 torr COS, 1,145 torr  $\text{CO}_2$  and 12 torr  $\text{C}_2\text{H}_4\text{S}$  was photolyzed using a medium pressure mercury arc and 7910 cut-off filter. The products were

13.3  $\mu\text{moles}$  CO and 11.8  $\mu\text{moles}$   $\text{C}_2\text{H}_4$ . Presumably, the only reactions of  $\text{S}(^3\text{P})$  atoms were with  $\text{C}_2\text{H}_4\text{S}$ . A blank run was then carried out, in which 12 torr  $\text{C}_2\text{H}_4\text{S}$  was photolyzed for the same duration. The yield of  $\text{C}_2\text{H}_4$  was 8.2  $\mu\text{moles}$ . Thus, in the first run, at least 3.6  $\mu\text{moles}$  of  $\text{C}_2\text{H}_4$  were produced by reaction [6]. The quantum yield of  $\text{C}_2\text{H}_4$  in the photolysis of  $\text{C}_2\text{H}_4\text{S}$  is pressure dependent, being 2 at low pressures (115), so that the  $\text{C}_2\text{H}_4$  produced in the first run, especially in the presence of 100 torr COS, was probably exceedingly small. Thus, the major reaction of  $\text{S}(^3\text{P})$  with ethylene episulfide is via reaction [6].

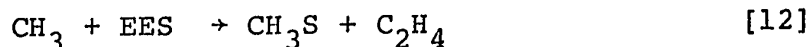
Callear and Tyerman (99) have observed the analogous reaction [11] in the selenium-ethylene system:

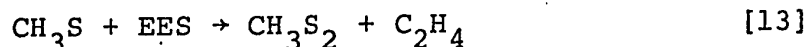


This reaction is exothermic by 35  $\text{kcal mole}^{-1}$  and is about 100 times faster than the addition of selenium to ethylene. At higher temperatures the reaction became negligible indicating a very low activation energy.

If one accepts the value of  $7 \times 10^8 \text{ M}^{-1} \text{ sec}^{-1}$  for  $k_3$  (15), then  $k_6 = 9.8 \times 10^{10} \text{ M}^{-1} \text{ sec}^{-1}$  at  $27^\circ\text{C}$ . This value of  $k_6$  requires an upper limit for  $E_6$  of  $\sim 0.5 \text{ kcal mole}^{-1}$ . The alternate value of  $k_3 = 1.76 \times 10^6 \text{ M}^{-1} \text{ sec}^{-1}$  reported by Lown et al (98) leads to an upper limit for  $E_6$  of  $2.8 \text{ kcal mole}^{-1}$ . The low activation energy is not surprising in view of the fact that reaction [6] is exothermic by  $42.5 \text{ kcal mole}^{-1}$ .

Recently Jakubowski (118) has measured the activation energies for the following two reactions:





The activation energies measured were  $E_{12} = 7.7$  kcal mole<sup>-1</sup> and  $E_{13} = 3.1$  kcal mole<sup>-1</sup>.  $D(\text{S} - \text{S})$  and  $D(\text{CH}_3\text{S} - \text{SCH}_3)$  are about 101 and 73 kcal mole<sup>-1</sup> respectively; if  $D(\text{CH}_3\text{S} - \text{S}\cdot)$  is taken as intermediate between these two values, then the exothermicity is about 29 kcal mole<sup>-1</sup>. These results therefore support the extremely low activation energy for reaction [6].

Turning now to the propylene system, the value obtained for  $E_9 - E_{10}$  was 0.93.  $E_3 - E_9$  has been measured to be 1.14 kcal mole<sup>-1</sup> (Chapter III), and  $E_3 - E_6 = 1.84$  kcal mole<sup>-1</sup>. Therefore  $E_6 - E_{10} = 0.23$  kcal mole<sup>-1</sup>.  $A_6/A_{10}$  is equal to unity. The 0.23 kcals difference between the activation energy for abstraction of S atoms from propylene episulfide and ethylene episulfide indicate that the exothermicity of  $\text{S}(^3\text{P})$  addition to propylene is slightly less than that for addition to ethylene. In accordance with this observation, the activation energy for thermal decomposition of PES was found to be slightly less than that for EES (98).

The high A-factors for both reactions [6] and [10] indicate a very loose transition state for the reaction, one which is probably non-cyclic. From the estimated A-factor for reaction [3],  $A_6$  must be about  $10^{14}$  cc mole<sup>-1</sup> sec<sup>-1</sup>.

Therefore

$$10^{14} = e^2 \frac{kT}{h} (RT) e^{\frac{\Delta S^\ddagger}{R}}$$

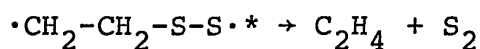
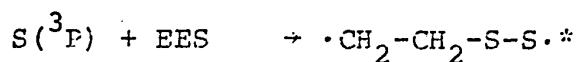


$$= (1.12 \times 10^{18}) e^{\frac{\Delta S^\ddagger}{R}}$$

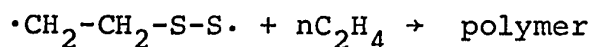
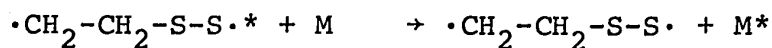
$$\therefore \Delta S^\ddagger \approx -19 \text{ gibbs/mole}$$

$$\text{Now, } \Delta S^\ddagger = S^\ddagger_0 - S^\circ_0(\text{S}^3\text{P}) - S^\circ_0(\text{EES})$$

Assuming  $S^\circ(\text{S}^3\text{P}) = 40$  gibbs/mole (103) and  $S^\circ(\text{EES}) = 62$  gibbs/mole (Chapter III), then  $S_0 \approx 83$ , where  $S^\ddagger_0$  is the standard entropy of the transition state at 297°K. The standard entropy of  $\text{CH}_3\text{CH}_2\text{-O-O}\cdot$  is 74 gibbs/mole and substitution of S for O increases the entropy by about 3 - 4 gibbs/mole. Therefore the structure of the transition state must closely resemble the diradical  $\cdot\text{CH}_2\text{-CH}_2\text{-S-S}\cdot$ . The reaction may occur in two distinct steps as follows:



In support of this proposal, it was observed that following each run, the amount of ethylene in the system had decreased below that which could be accounted for by the yield of EES. Thus the following reactions may occur:



It should be possible to gain further information concerning the transition state of the abstraction reaction

by observing the extent of stereospecificity in the reaction of  $S(^3P)$  with cis or trans-2-butene - episulfide.

ADDITION OF S(<sup>3</sup>P) ATOMS TO DEUTERIO-ETHYLENESRESULTS

The secondary deuterium isotope effects for S(<sup>3</sup>P) addition to C<sub>2</sub>D<sub>4</sub>, ethylene-1,1-d<sub>2</sub>, cis-ethylene-1,2-d<sub>2</sub> and trans-ethylene-1,2-d<sub>2</sub> were measured by competition between equal pressures of each of these and C<sub>2</sub>H<sub>4</sub> for S(<sup>3</sup>P) atoms produced by the in situ photolysis of COS in the presence of a large excess of CO<sub>2</sub>. Conversions were kept down to about 3 μmoles of episulfide so that no secondary reactions occurred between the episulfide and the sulfur atoms. The episulfides were separated from the reaction mixture by distillation through five traps at -140°C, and from other contaminants such as CS<sub>2</sub> by gas chromatography. The binary mixture of episulfides was then analyzed by mass spectrometry and the relative amounts of each episulfide calculated from calibrated mass spectra. The isotope effect was then obtained from the equation:

$$\frac{k_D}{k_H} = \frac{C_2D_4S}{C_2H_4S} \times \frac{P(C_2H_4)}{P(C_2D_4)}$$

in the case of C<sub>2</sub>D<sub>4</sub>.

The isotope effects were measured over a 120°C temperature range. The data for each deuterated compound are presented below.

Ethylene-d<sub>4</sub>1) Calibration of Mass Spectra

A sample of C<sub>2</sub>D<sub>4</sub>S was prepared and eight recordings were made of the m/e values 59, 60 and 64 on an MS10 Mass Spectrometer. From the average values of the ratios of these peak heights the following peak height ratios were obtained:

$$\frac{64}{59} = 78; \quad \frac{64}{60} = 5.1$$

A mass spectrum of C<sub>2</sub>H<sub>4</sub>S showed no peak at m/e = 64. Four samples were then made up consisting of carefully measured mixtures of C<sub>2</sub>H<sub>4</sub>S and C<sub>2</sub>D<sub>4</sub>S. For each sample, eight recordings were made on the mass spectrometer of the 59, 60 and 64 peaks. The peak heights were measured and the fraction of each peak which was due to a given episulfide was calculated, thus the "corrected" 64/59 and 64/60 ratios were obtained. (i.e. the part of the 59 and 60 peaks due to C<sub>2</sub>D<sub>4</sub>S were subtracted so that the "corrected" peak ratio is a measure of the episulfide ratio.) The peak height ratios were then calculated corresponding to equimolar mixtures of C<sub>2</sub>D<sub>4</sub>S and C<sub>2</sub>H<sub>4</sub>S as given in Table XLIXa.

2) Photolysis Runs

A gas mixture was made up consisting of the following:

TABLE XLIXa

CALIBRATIONS OF BINARY EPISULFIDE MIXTURES

Sample	$\mu\text{mC}_2\text{D}_4\text{S}$	$\mu\text{mC}_2\text{H}_4\text{S}$	$\frac{\text{C}_2\text{D}_4\text{S}}{\text{C}_2\text{H}_4\text{S}}$	$\left(\frac{64}{59}\right)^a$	$\left(\frac{64}{60}\right)^a$
1	1.63	1.94	0.840	1.100	0.913
2	1.63	1.96	0.831	1.100	0.897
3	1.60	1.94	0.825	1.110	0.926
4	1.93	1.61	1.199	1.092	0.907
Average	-	-	-	1.100	0.911

a) "Corrected" value, corresponding to 1:1 ratio of episulfide.

TABLE XLIXb

ISOTOPE EFFECTS AS A FUNCTION OF TEMPERATURE FOR  $\text{C}_2\text{D}_4$

Run	T (°C)	$\frac{64}{59}$	$\frac{\text{C}_2\text{D}_4\text{S}^a}{\text{C}_2\text{H}_4\text{S}}$	$\frac{64}{60}$	$\frac{\text{C}_2\text{D}_4\text{S}^b}{\text{C}_2\text{H}_4\text{S}}$	$\frac{k_D^c}{k_H}$
1	29°	1.211	1.101	1.037	1.138	1.154
2	29°	1.246	1.133	1.050	1.153	-
3	29°	1.212	1.102	0.994	1.091	1.130
4	96°	1.178	1.071	1.057	1.160	1.150
5	157°	1.201	1.092	1.024	1.124	1.142
Average	-	-	-	-	-	1.144

a) Calculated from 64/59 ratio.

b) Calculated from 64/60 ratio.

c) Average of  $\frac{\text{C}_2\text{D}_4\text{S}}{\text{C}_2\text{H}_4\text{S}}$  x 1.031

$$P(\text{COS}) = 20 \text{ torr}$$

$$P(\text{CO}_2) = 940 \text{ torr}$$

Olefin pressures read on cathatometer:

$$P(\text{C}_2\text{H}_4) = 34.7 \text{ torr}$$

$$P(\text{C}_2\text{D}_4) = 33.6 \text{ torr}$$

$$\frac{P(\text{C}_2\text{H}_4)}{P(\text{C}_2\text{D}_4)} = 1.033$$

Each olefin was then transferred to gas buret and re-measured.

$$\text{From Gas-Buret Readings: } \frac{P(\text{C}_2\text{H}_4)}{P(\text{C}_2\text{D}_4)} = 1.031$$

The mixture was then photolyzed at different temperatures as recorded in Table XLIXb. The mass spectrum for the 59, 60 and 64 peaks of the episulfide product was scanned eight times, the average 64/59 and 64/60 peaks were then "corrected" and divided by the calibration factor to give the ratios  $\text{C}_2\text{D}_4\text{S}/\text{C}_2\text{H}_4\text{S}$ .

#### Ethylene-1,1-d<sub>2</sub>

The procedure was the same as in the previous case except that the mass spectral peaks at  $m/e = 62$  and  $m/e = 60$  were the only ones measured. From the spectrum of  $\text{C}_2\text{D}_2\text{H}_2\text{S}$ ,  $62/60 = 2.4$ . Using these ratios it was possible to "correct" the peak ratios due to the mixtures of episulfides. The calibrations are given in Table La and

the results in Table Lb. The photolysis mixture consisted of the following partial pressures:

$$P(\text{COS}) = 23 \text{ torr}$$

$$P(\text{CO}_2) = 920 \text{ torr}$$

$$P(\text{CD}_2\text{CH}_2) = 31.09 \text{ torr}$$

$$P(\text{C}_2\text{H}_4) = 30.33 \text{ torr}$$

$$\frac{P(\text{CD}_2\text{CH}_2)}{P(\text{C}_2\text{H}_4)} = 1.025$$

$$\text{From Gas Buret } \frac{P(\text{CD}_2\text{CH}_2)}{P(\text{C}_2\text{H}_4)} = 1.016$$

$$\text{Average } \frac{P(\text{CD}_2\text{CH}_2)}{P(\text{C}_2\text{H}_4)} = 1.021$$

cis-ethylene-1,2-d<sub>2</sub>

The mass spectrum of this compound gave an m/e ratio of 62/60 = 2.2. The calibration results of the episulfide mixtures are given in Table LIa and the results for  $k_D/k_H$  in Table LIb. The photolysis mixture consisted of the following partial pressures:

$$P(\text{COS}) = 24 \text{ torr}$$

$$P(\text{CO}_2) = 920 \text{ torr}$$

$$P(\text{C}_2\text{H}_4) = 32.2 \text{ torr}$$

$$P(\text{CDHCDH}) = 32.7 \text{ torr}$$

$$\therefore \frac{P(\text{CDHCDH})}{P(\text{C}_2\text{H}_4)} = 1.015$$

TABLE La

CALIBRATION OF BINARY EPISULFIDE MIXTURES

Sample	$\mu$ moles $\text{CH}_2\text{CD}_2\text{S}$	$\mu$ moles $\text{C}_2\text{H}_4\text{S}$	$\frac{\text{C}_2\text{H}_4\text{S}}{\text{CH}_2\text{CD}_2\text{S}}$	$\frac{60^a}{62}$
1	1.78	1.80	1.011	1.042
2	1.55	2.02	1.303	1.044
3	2.08	1.58	0.760	1.017
Average	-	-	-	1.034

- a) "Corrected" ratio corresponding to 1:1 ratio of episulfides;  
Each value is an average of 8 recordings.

TABLE Lb

ISOTOPE EFFECTS AS A FUNCTION OF TEMPERATURE FOR  $\text{CD}_2\text{CH}_2$ 

Run	T (°C)	$\frac{60^a}{62}$	$\frac{k_D^b}{k_H}$
1	28°	0.955	1.062
2	98°	0.945	1.073
3	158°	0.955	1.062
4	29°	0.945	1.073
Average	-	-	1.07

- a) "Corrected" ratio

$$b) \frac{k_D}{k_H} = 1 / \left[ \frac{\left( \frac{60}{62} \right)}{1.034} \times 1.021 \right]$$



TABLE LIa

CALIBRATION OF BINARY EPISULFIDE MIXTURES

Sample	$\mu\text{moles}$ CDHCDH	$\mu\text{moles}$ $\text{C}_2\text{H}_4\text{S}$	$\frac{\text{C}_2\text{H}_4\text{S}}{\text{CDHCDHS}}$	$\frac{60^a}{62}$
1	1.89	1.81	0.958	1.118
2	1.66	2.08	1.253	1.097
3	2.17	1.66	0.765	1.098
Average	-	-	-	1.104

a) "Corrected" ratio corresponding to 1:1 episulfide ratio

TABLE LIb

ISOTOPE EFFECTS AS A FUNCTION OF TEMPERATURE FOR CIS-CDHCDH

Run	T (°C)	$\frac{60^a}{62}$	$\frac{k_D^b}{k_H}$
1	27°	1.059	1.028
2	93°	1.059	1.028
3	155°	1.036	1.051
4	28°	1.036	1.050
Average	-	-	1.04

a) "Corrected ratio"

$$b) \frac{k_D}{k_H} = 1 / \left[ \frac{\left( \frac{60}{62} \right)}{1.104} \times 1.014 \right]$$

$$\text{From Gas Buret } \frac{P(\text{CDHCDH})}{P(\text{C}_2\text{H}_4)} = 1.014$$

$$\text{Average } \frac{P(\text{CDHCDH})}{P(\text{C}_2\text{H}_4)} = 1.014$$

trans-ethylene-1,2-d<sub>2</sub>

The spectrum of a sample of trans ethylene episulfide -d<sub>2</sub> gives a ratio of m/e peak heights, 62/60 = 2.22. That of C<sub>2</sub>H<sub>4</sub>S gives 60/62 = 21.9. From these values the 62/60 ratios due to the episulfide mixtures were corrected. The calibrations of the mixtures are recorded in Table LIIa and the isotope effects in Table LIIb. The photolysis mixture consisted of the following partial pressures:

$$P(\text{COS}) = 41 \text{ torr}$$

$$P(\text{CO}_2) = 1,243 \text{ torr}$$

$$P(\text{C}_2\text{H}_4) = 103.39 \text{ torr}$$

$$P(\text{trans CDHCDH}) = 104.41 \text{ torr}$$

$$\frac{P(\text{trans CDHCDH})}{P(\text{C}_2\text{H}_4)} = 1.010$$

The secondary isotope effects together with probably errors are summarized in Table LIII.

TABLE LI IaCALIBRATION OF BINARY EPISULFIDE MIXTURES

Sample	$\mu\text{moles}$ $\text{C}_2\text{H}_4\text{S}$	$\mu\text{moles}$ $\text{trans-C}_2\text{D}_2\text{H}_2\text{S}$	$\frac{62^a}{60}$
1	2.02	1.65	1.007
2	1.83	2.04	0.982
3	2.02	1.74	1.053
Average	-	-	1.014

a) Corrected ratio for 1:1 episulfide ratio

TABLE LI IbISOTOPE EFFECTS AS A FUNCTION OF TEMPERATURE FORTRANS-CDHCDH

Run	T(°C)	$\frac{62^a}{60}$	$\frac{k_D^b}{k_H}$
1	27°	1.139	1.112
2	28°	1.235	1.205
3	152°	1.218	1.190
4	97°	1.013	0.989
Average	-	-	1.12

a) Corrected ratio

$$b) \frac{k_D}{k_H} = \left( \frac{62}{60} \right) \div 1.014 \times 1.01$$

TABLE LIII

SECONDARY ISOTOPE EFFECTS FOR ADDITION OF  
S(<sup>3</sup>P) TO ETHYLENE

Olefin	$\frac{k_D}{k_H}$
C <sub>2</sub> D <sub>4</sub>	1.14 ± 0.02
CD <sub>2</sub> CH <sub>2</sub>	1.07 ± 0.02
cis CDHCDH	1.04 ± 0.02
trans CDHCDH	1.12 ± 0.08

TABLE LIV

SECONDARY ISOTOPE EFFECTS FOR ADDITION OF ATOMS AND

RADICALS TO OLEFINS

Olefin	Atom or Radical				Epoxidation <sup>d</sup>
	S	H <sup>a</sup>	CH <sub>3</sub> <sup>b</sup>	CF <sub>3</sub> <sup>b</sup>	
C <sub>2</sub> D <sub>4</sub>	1.14	-	1.05	1.07	-
C <sub>3</sub> D <sub>6</sub>	-	1.08	1.17	1.09	-
φCD·CH <sub>2</sub>	-	-	1.09 <sup>c</sup>	1.10	-
trans stilbene	-	-	-	-	1.11

a) Reference 51

c) Reference 50

b) Reference 52

d) Reference 49

## DISCUSSION

As predicted by the Streitweiser model for the secondary  $\alpha$ -deuterium isotope effect (36), the results show an inverse isotope effect for the addition of  $S(^3P)$  to ethylene. The  $k_D/k_H$  values measured cannot by themselves indicate whether in the transition state the sulfur atom is partially bonded to both carbon atoms or to just one of them. In either case the isotope effect for ethylene- $d_2$  would be expected to equal one half of the effect for ethylene- $d_4$ . Within experimental error the rate ratios for ethylene-1,1- $d_2$  and cis-ethylene-1,2- $d_2$  are half that for ethylene- $d_4$ . The anomalously high value for trans-ethylene- $d_2$  was found to be reproducible and is difficult to explain unless the deuterated sample was impure.

It is interesting to compare the present results with those of other atomic and radical additions to olefins, which are summarized in Table LIV. In the addition of H atoms,  $CF_3$  and  $CH_3$  radicals to olefins only one of the carbon atoms (the least substituted one) undergoes a hybridization change from  $sp^2$  to  $sp^3$ ; the change in the free energy of activation for the addition of these species to  $=CH_2$  and  $=CD_2$  is roughly half that for the addition of  $S(^3P)$  atoms to  $C_2H_4$  and  $C_2D_4$ . The suggestion is strong, therefore, that bonding occurs simultaneously between the sulfur atom and both carbon atoms in the transition state.

The most striking feature of the present results

however is the constancy of  $k_D/k_H$  over a 120° temperature range. This is the first study of the temperature dependence of the secondary isotope effect in the gas phase, and is over a much wider temperature range than previous studies in solution. According to Streitwieser's simplified equation (see Introduction)

$$\frac{k_D}{k_H} = b \cdot \exp\left\{\frac{-0.187}{T} (\omega_{H_i} - \omega_{H_i}^\ddagger)\right\}$$

thus the cause for the secondary isotope effect in this case lies in the pre-exponential factor  $b$ , which is equal to  $\kappa_D/\kappa_H \cdot (m_H^\ddagger/m_D^\ddagger)^{1/2}$  where  $\kappa$  is the transmission coefficient and  $m^\ddagger$  is the effective mass along the reaction co-ordinate. This factor will be discussed later on, but for the moment it is clear that it would be a futile exercise to discuss the magnitude of the isotope effect in terms of the vibrational frequency changes incurred in going from the trigonal configuration at a carbon atom to a tetrahedral one as Szwarc (50) and Seltzer (54,55) have done, and to derive, by comparison of the calculated effect with the experimental one, the extent to which C-S bond formation has occurred in the transition state.

Unfortunately there are not sufficient temperature data to permit the calculation of the enthalpy of activation difference,  $\Delta\Delta H^\ddagger$ , and the entropy of activation difference,  $\Delta\Delta S^\ddagger$ , by fitting the data to the equation

$$\ln \frac{k_D}{k_H} = \frac{\Delta H_H^\ddagger - \Delta H_D^\ddagger}{RT} - \frac{\Delta S_H^\ddagger - \Delta S_D^\ddagger}{R}$$

by the method of least squares, but it is clear nevertheless that the effect is due predominantly if not entirely to the entropy of activation difference. Thus for  $S(^3P)$  addition to  $C_2D_4$

$$\Delta S_D^\ddagger - \Delta S_H^\ddagger \approx 0.26 \text{ gibbs/mole}$$

$$\sim 0.065 \text{ gibbs/mole per deuterium atom}$$

Several examples are reported in the literature where  $SN_1$  solvolysis reactions in 'water-poor' solvents such as ethanol-water, showed a secondary  $\beta$ -effect which was due to both  $\Delta\Delta H^\ddagger$  and  $\Delta\Delta S^\ddagger$  differences. Shiner (119) studied the temperature dependence of  $k_H/k_D$  for solvolysis of  $\beta$ -deuterated 2,3-dimethyl-2-chlorobutane in an ethanol water solvent and found a difference in experimental energy of activation of 580 cal/mole which was balanced by a very large entropy of activation difference, so that  $\Delta\Delta F^\ddagger$  was reduced to a reasonable 100 - 150 cal/mole. In a 'water rich' solvent on the other hand, Lewis and Boozer (120) found a very small  $E_a$  difference and no entropy of activation difference in the  $SN_1$  acetolysis of  $\beta$ -deuterated compounds. The explanation offered was that in the transition state, hyperconjugative charge dispersal is more effective in the deuterated compound, (see Introduction) hence there is less solvation and consequently a higher energy of activation; with the non-deuterated compound more solvation occurs resulting in a lower energy of activation and a greater entropy of activation due to the 'solvent sorting' required in a

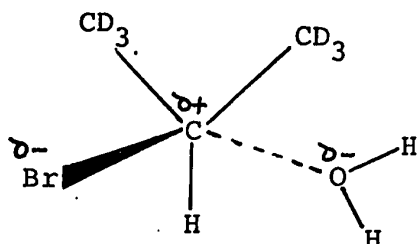
'water-poor' solvent.

The first report of a temperature independent isotope effect was by Leffek et al (121), who measured the  $\beta$ -effect on water solvolysis of isopropyl sulfonates and bromide. At 50°C,  $\Delta\Delta F^\ddagger/n = 46, 47$  and  $29$  cal/mole, respectively, for the tosylate, methanesulfonate and bromide, of which 45, 50 and 30 cal/mole were due to  $T\Delta\Delta S^\ddagger$ . In a later paper Leffek and MacLean (122) measured an inverse  $\alpha$ -effect of 0.88 for the Menschutkin reactions between methyl and methyl- $d_3$  iodide and a series of tertiary amines in solvent benzene. Over a 40°C temperature range the  $\alpha$ -isotope effect for reaction between methyl iodide and 2-picoline was temperature independent and it was found that  $\Delta S_D^\ddagger - \Delta S_H^\ddagger = +0.083$  gibbs/mole per deuterium atom.

In both these instances the mechanism was  $SN_2$  and Leffek and MacLean proposed that the lack of an enthalpy of activation difference between the normal and deuterated molecules was due to a cancellation of two opposing vibrational effects and the entropy of activation arose from an inhibition of the internal rotation of the methyl group in the transition state. This inhibition would be greater in the case of the non-deuterated molecule, resulting in an inverse effect. Hakka et al (123) found a temperature dependence for  $k_H/k_D$  for hydrolysis of t-butyl-chloride - an  $SN_1$  reaction - such that  $\Delta\Delta F^\ddagger = \Delta\Delta H^\ddagger$  and suggested that it may be possible to differentiate between an  $SN_1$  and



SN2 mechanism depending on whether  $\Delta\Delta F^\ddagger = \Delta\Delta H^\ddagger$  or  $\Delta\Delta F^\ddagger = -T\Delta\Delta S^\ddagger$ ; in their opinion two opposing effects occur in an SN2 situation, e.g. in the hydrolysis of isopropyl bromide.

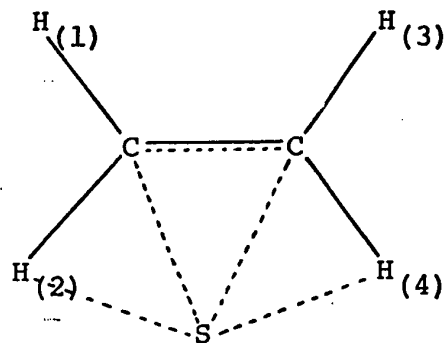


Strong C-O interaction increases the torsional force constants about the C-C bond while electronic changes, associated with bonding to both Br and O provide for a decrease in the "high" frequencies such as stretching. A recent study of the temperature dependence of an SN2  $\alpha$ -effect by Jackson and Leffek (124) is in agreement with the proposal of Hakka et al.

In order to investigate the theoretical causes of temperature independent isotope effects, Wolfsberg and Stern (47) have carried out 'exact' calculations of the isotopic rate ratio equation for a model system assuming certain force constant changes in going to the transition state. They concluded that it is possible to obtain large temperature-independent isotope effects if some "small" force constants in the reactant (e.g. those corresponding to torsions) become larger in the transition state while some "large" force constants (e.g. those corresponding to stretches) in the reactant become smaller in the transition state. From their model, they also

found the important result that the pre-exponential term reached its "high temperature limit" at room temperature. ( $v_H^\ddagger/v_D^\ddagger$  is not temperature independent, but is a "varying" function of temperature so that the value obtained from the intercept of an Arrhenius plot of  $k_H/k_D$  depends on the temperature range in which  $k_H/k_D$  was measured;  $v_H^\ddagger/v_D^\ddagger$  is the "high temperature limit" of  $k_H/k_D$  measured at  $\sim 1000^\circ\text{K}$ .)

The results of the temperature study of  $k_D/k_H$  for  $S(^3P)$  addition to deuterated ethylenes seem to be very similar to the theoretical results of Wolfsberg and Stern. There is no enthalpy of activation difference between the deuterated and normal ethylenes and no curvature in the Arrhenius plot. Thus, either there are no zero-point energy differences or there is a fortuitous cancellation of opposing charges in the C-H bonds. The latter seems to be the more likely particularly since it is fairly well established (34) that C-D has a higher inductive effect than C-H and therefore a lower activation energy would be expected for  $S(^3P)$  addition to  $C_2D_4$  unless there is an opposing effect. The occurrence of two opposing charges in the C-H vibrational frequencies is evident if we postulate a transition state similar to that proposed by Scheer and Klein (107) for the addition of  $O(^3P)$  atoms to the 2-butenes, as follows:



The sulfur atom approaches in the plane of the ethylene molecule and partial bonds are formed between it and the carbon atoms and the two hydrogen atoms  $H_{(2)}$  and  $H_{(4)}$ . This results in a decrease of the frequencies of the stretching modes of the  $CH_{(2)}$  and  $CH_{(4)}$  atoms, as is observed in hydrogen-bonded complexes in general. At the same time, the configuration of the carbon atoms has changed (partly) from  $sp^2$  to  $sp^3$  resulting in an increase in the frequency of the  $H_{(1)}$  and  $H_{(3)}$  bending modes. Although there are, no doubt, other force constant changes such as the C-C stretching, etc. it is very possible that the net frequency change is zero. The frequency changes should also cancel in any of the dideutero-ethylenes, since the sulfur atoms will approach each side approximately 50% of the time.

Having cancelled the effects due to zero-point energy differences, we must now rationalize the observed isotope effect. Streitweiser (36) assumed that  $m_H^\ddagger/m_D^\ddagger$  and  $\kappa_H/\kappa_D$  were approximately unity in the acetolysis of cyclopentyl tosylate; it is unlikely that this is so in the case of sulfur atom addition to ethylene. The

important motions along the reaction co-ordinate are the approach of the sulfur atom and its increasing interaction with 2 carbon atoms and 2 hydrogen atoms, and the out-of-plane bending of 2 hydrogen atoms. Thus since the hydrogens are involved to a very great extent, changing their mass from 4 to 8 compared with 32 for sulfur should certainly affect the 'effective mass' along the reaction co-ordinate. In Streitweiser's paper, the leaving group was a heavy tosylate group. If  $m_H^\ddagger/m_D^\ddagger$  is non-zero, it must be less than unity, however, so that it would not give an inverse isotope effect.

It was shown in Chapter IV that in the  $S(^3P) + \text{ethylene}$  system at c. 1,000 torr, approximately 6% of the newly-formed activated ethylene episulfide decomposes unimolecularly. It is likely that a 'hot' deuterated episulfide molecule would decompose less rapidly, resulting in an observed inverse isotope effect for the addition of sulfur atoms to ethylene. Deuterium atoms should be more efficient than protium atoms in partitioning the excess energy in the activated molecule, because of their lower frequencies. The isotope effect may thus be pressure dependent, and would thus require further study. Rabinowitch et al have reported very high secondary isotope effects for chemically activated systems (125) which were also pressure dependent. However, even if all of the 'hot'

$C_2D_4S$  is stabilized this would only account for an isotope effect of ~6% instead of the 14% observed. The effect might be a consequence of the smaller steric requirements of the deuterated molecule.

## CHAPTER VI

SUMMARY AND CONCLUSIONS

Relative rates and Arrhenius parameters have been measured for the addition of  $S(^3P)$  atoms to a series of hydrocarbon olefins, halogenated olefins and acetylenes. The ground state sulfur atoms were produced by the  $CO_2$ -induced collisional deactivation of  $S(^1D)$  atoms resulting from the photolysis of COS and by mercury-photosensitization of COS.

The relative addition rates to the hydrocarbon olefins increase with successive methylation of the double bonded carbon atoms indicating that triplet sulfur atoms are electrophilic in character. The increase in reactivity is due mainly to a decrease in activation energy while the pre-exponential factors decrease very slightly with the amount of alkyl substitution. The latter effect is ascribed to steric hindrance.

The electrophilic character of  $S(^3P)$  atoms is further evidenced by their lower addition rates to halogenated olefins compared with the hydrocarbon analogues. Again this is caused by an increase in activation energy upon substitution of a fluorine or chlorine atom for a hydrogen. In the series of fluorinated ethylenes the activation energy for sulfur atom addition increases to a

maximum for the di-substituted compounds and decreases again for tri- and tetrafluoroethylene. This behaviour is ascribed to the opposing inductive effects of the  $\sigma$ - and p-electrons of the fluorine atoms; the electron-repelling effect of the p-electrons predominates in the more substituted compounds. In the case of olefins where a fluorine atom is substituted at a  $\beta$  or  $\gamma$  position relative to the double bond, the electron-withdrawing effect of the  $\sigma$ -electrons alone is operative and the activation energy increases consistently with the number of fluorine atoms. The pre-exponential factors for sulfur atom addition to the halogenated olefins are higher by a factor of 2 to 3 than those for the analogous hydrocarbons. This is ascribed to the greater effectiveness of halogenated compounds in equipartitioning the excess energy in the newly-formed adduct.

Ground state sulfur atoms add to alkynes with a higher activation energy and a higher A-factor than to the corresponding alkenes. The higher activation energy arises from the greater electron-demanding properties of the triple bond while the higher A-factor is due to the cylindrical symmetry of the  $\Pi$ -electrons and consequent larger effective collision diameter.

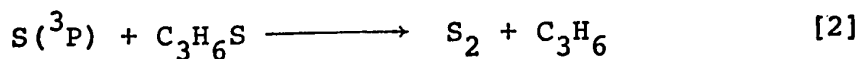
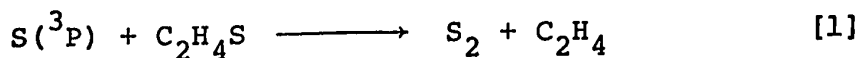
The activation energies for addition to hydrocarbon alkenes and alkynes were found to decrease with the ionization potentials in an approximately linear fashion

while for the halogenated alkenes no such correlation exists. For olefins containing a  $=CH_2$  group the activation energy for sulfur atom addition increased linearly with the average atom localization energy of the two doubly-bonded carbon atoms. This suggests partial bonding of the sulfur atom to both carbon atoms in the transition state.

A detailed reaction path is proposed for the addition reaction of  $S(^3P)$  with  $C_2H_4$ , which is consistent with the observed stereospecificity of the reaction, the dependence of activation energy on electron availability in a series of olefins and the apparently low activation energy for the addition reaction.

The addition of  $S(^3P)$  atoms to ethylene and propylene have been investigated at low pressures. In the ethylene reaction, the "hot" episulfide undergoes unimolecular fragmentation to a sulfur atom and ethylene with a rate constant  $k < 9.2 \times 10^8 \text{ sec}^{-1}$ . About 90% of the episulfide is collisionally stabilized at a total pressure of 500 torr. No fragmentation of the propylene episulfide was observed at total pressures as low as 12 torr.

Arrhenius parameters relative to those for  $S(^3P)$  addition to ethylene were measured for the following reactions of episulfides:





Both reactions have a pre-exponential factor 8.3 times as high as that for addition of  $S(^3P)$  to ethylene while  $E_1$  and  $E_2$  were respectively 1.84 and 2.07 kcal mole<sup>-1</sup> lower than  $E_{(S(^3P) + C_2H_4)}$ .

The secondary  $\alpha$ -deuterium isotope effect was measured for addition of  $S(^3P)$  atoms to  $C_2D_4$ ,  $CD_2=CH_2$ , cis-CDH=CDH and trans-CDH=CDH over a temperature range from 27°C to 150°C. The  $k_D/k_H$  ratio for each of the deuterioethylenes was constant over the temperature range and the results are consistent with a transition state in which the sulfur atom is partially bonded to both carbon atoms and two hydrogen atoms.

## BIBLIOGRAPHY

- (1) Circular of the National Bureau of Standards, No. 467, (1949).
- (2) H. E. Gunning and O. P. Strausz, Adv. in Photochem., 4, 143, (1966).
- (3) K. S. Sidhu, I. G. Csizmadia, O. P. Strausz and H. E. Gunning, JACS, 88, 2417, (1966).
- (4) R. K. Gosavi, O. P. Strausz and H. E. Gunning, private communication.
- (5) A. R. Knight, O. P. Strausz and H. E. Gunning, JACS, 85, 2349, (1963).
- (6) H. A. Wiebe, A. R. Knight, O. P. Strausz and H. E. Gunning, JACS, 87, 1443, (1965).
- (7) E. M. Lown, E. L. Dedio, O. P. Strausz and H. E. Gunning, JACS, 89, 1056, (1967).
- (8) K. S. Sidhu, E. M. Lown, O. P. Strausz and H. E. Gunning, JACS, 88, 254, (1966).
- (9) O. P. Strausz, J. Font, E. L. Dedio, P. Kebarle and H. E. Gunning, JACS, 89, 4805, (1967).
- (10) R. J. Cvetanovic, Adv. in Photochem., 1, 115, (1963).
- (11) S. J. Moss and K. R. Jennings, Trans. Farad. Soc., 65, 415, (1969).
- (12) D. Saunders and J. Heicklen, J. Phys. Chem., 70, 1950, (1966).
- (13) W. J. R. Tyerman, Trans. Farad. Soc., 65, 163, (1969).

- (14) A. B. Cailear and W. J. R. Tyerman, *Trans. Farad. Soc.*, 62, 2760, (1966).
- (15) J. Connor, G. Greig, and O. P. Strausz, *JACS*, in press.
- (16) S. Kryzanowski and R. J. Cvetanovic, *Can. J. Chem.*, 45, 665, (1967).
- (17) P. S. Skell and A. Y. Yarner, *JACS*, 78, 5430, (1956).
- (18) G. L. Closs and J. J. Coyle, *JACS*, 87, 4270, (1965).
- (19) Yi-Noo Tang and F. S. Rowland, *JACS*, 89, 6420, (1967).
- (20) C. Willis and K. D. Bayes, *JACS*, 88, 3203, (1966).
- (21) D. G. Williamson and K. D. Bayes, *JACS*, 90, 1957, (1968).
- (22) M. Szwarc, *J. Polymer Sci.*, 16, 367, (1955).
- (23) A. Rembaum and M. Szwarc, *JACS*, 77, 4468, (1955).
- (24) F. Leavitt, M. Levy, M. Szwarc and V. Stannett, *JACS*, 77, 5493, (1955).
- (25) J. Smid and M. Szwarc, *JACS*, 78, 3322, (1956).
- (26) M. Feld and M. Szwarc, *JACS*, 82, 3791, (1960).
- (27) A. P. Stefani and M. Szwarc, *JACS*, 84, 3661, (1962).
- (28) J. M. Pearson and M. Szwarc, *Trans. Farad. Soc.*, 60, 553, (1964).
- (29) G. E. Owen, J. M. Pearson and M. Szwarc, *Trans. Farad. Soc.*, 61, 1722, (1965).
- (30) R. J. Cvetanovic and R. S. Irwin, *J. Chem. Phys.*, 46, 1694, (1967).
- (31) J. M. Tedder and J. C. Walton, *Trans. Farad. Soc.*, 62, 1859, (1966).

- (32) R. J. Cvetanovic and L. C. Doyle, J. Chem. Phys., 50, 4705, (1969).
- (33) K. R. Jennings and R. J. Cvetanovic, J. Chem. Phys., 35, 1233, (1961).
- (34) E. A. Haleir, Progr. in Phys. Org. Chem., 1, 109, (1963).
- (35) A. Streitweiser and R. C. Fahey, Chem. and Ind., 1417, (1957).
- (36) A. Streitweiser, R. H. Jagow, A. C. Fahey and S. Suzuki, JACS, 80, 2326, (1958).
- (37) V. J. Shiner, Tetrahedron, 14, 243, (1959).
- (38) V. J. Shiner, JACS, 78, 2653 (1956).
- (39) E. S. Lewis and G. M. Coppinger, JACS, 76, 4495, (1954).
- (40) V. J. Shiner and C. J. Verbanic, JACS, 79, 373, (1957).
- (41) K. T. Leffek, J. A. Llewellyn and R. E. Robertson, JACS, 82, 6315, (1960).
- (42) L. S. Bartell, Tetrahedron, 17, 177, (1962).
- (43) H. C. Brown, M. E. Azzaro, J. G. Koelling and G. J. McDonald, JACS, 88, 2520, (1966).
- (44) J. Bigeleison, J. Chem. Phys., 17, 425, (1949).
- (45) J. H. Schachtschneider and R. G. Snyder, Spectrochim. Acta., 19, 117, (1963).
- (46) M. Wolfsberg and M. Stern, Pure Appl. Chem., 8, 225, (1964).

- (47) M. Wolfsberg and M. Stern, Pure Appl. Chem., 8, 325, (1964).
- (48) S. Seltzer and S. G. Mylonakis, JACS, 89, 6584, (1967).
- (49) D. B. Denney and N. Tunkel, Chem. and Ind., 1383, (1959).
- (50) M. Matsuoka and M. Szwarc, JACS, 83, 1260, (1961).
- (51) M. Takahasi and R. J. Cvetanovic, Can. J. Chem., 40, 1037, (1962).
- (52) M. Feld, A. P. Stefani and M. Szwarc, JACS, 84, 4451, (1962).
- (53) J. W. Simons and B. S. Rabinowitch, JACS, 85, 1023, (1963).
- (54) S. Seltzer, JACS, 83, 1861, (1961).
- (55) A. A. Zavitsas and S. Seltzer, JACS, 86, 3836, (1964).
- (56) A. R. Knight, O. P. Strausz, S. M. Malm and H. E. Gunning, JACS, 86, 4243, (1964).
- (57) E. L. Dedio, Ph. D. Thesis, University of Alberta, (1967).
- (58) S. Searles and E. F. Lutz, JACS, 80, 3168, (1958).
- (59) H. A. Wiebe, Ph. D. Thesis, University of Alberta, (1968).
- (60) E. M. Lown, Ph. D. Thesis, University of Alberta, (1966).
- (61) E. M. Lown, H. S. Sandhu, H. E. Gunning and O. P. Strausz, JACS, 90, 7164, (1968).

- (62) E. M. Lown, private communication.
- (63) L. Pauling, "The Nature of the Chemical Bond",  
Cornell University Press, (1960).
- (64) M. G. Evans, J. Gergely and E. C. Seaman, J. Polymer  
Sci., 3, 866, (1948).
- (65) R. P. Buckley and M. Szwarc, JACS, 78, 5696, (1956).
- (66) J. Collin and F. P. Lossing, JACS, 81, 2064, (1959).
- (67) K. Watanabe, J. Chem. Phys., 26, 542, (1957).
- (68) R. E. Honig, J. Chem. Phys., 16, 105, (1948).
- (69) R. S. Mulliken, C. A. Rieke and W. G. Brown, JACS,  
63, 41, (1941).
- (70) J. R. Dunn, W. A. Waters and I. M. Roitt, JCS, 580,  
(1954).
- (71) E. C. Kooyman and E. Fahrenhost, Trans. Farad. Soc.,  
49, 58, (1953).
- (72) M. Levy and M. Szwarc, JACS, 77, 1949, (1955).
- (73) P. S. Skell and R. R. Engel, JACS, 87, 4663, (1965).
- (74) R. J. Cvetanovic, H. E. Avery and R. S. Irwin, J.  
Chem. Phys., 46, 1993, (1967).
- (75) F. H. Burkitt, C. A. Coulson and H. C. Longuet-  
Higgins, Trans. Farad. Soc., 47, 553, (1951).
- (76) C. A. Coulson, JCS, 1435, (1955).
- (77) C. A. Coulson, Research, 4, 307, (1951).
- (78) M. Szwarc, J. Phys. Chem., 61, 40, (1957).
- (79) M. Szwarc and F. Leavitt, JACS, 78, 3590, (1956).
- (80) J. H. Binks and M. Szwarc, J. Chem. Phys., 30, 1494,  
(1959).

- (81) S. Sato and R. J. Cvetanovic, JACS, 81, 3223, (1959).
- (82) J. P. Flannery, J. Phys. Chem., 70, 3707, (1966).
- (83) J. C. Walton and J. M. Tedder, Progr. in Reaction Kinetics, 4, 55, (1967).
- (84) R. D. Brown, JCS Quart. Revs., 6, 63, (1952).
- (85) J. H. Binks and M. Szwarc, Proc. Roy. Soc., 226, (1958).
- (86) J. R. Platt, J. Chem. Phys., 18, 1168, (1950).
- (87) M. G. Evans and M. Polanyi, Trans. Farad. Soc., 34, 11, (1938).
- (88) D. T. Clark, J. N. Murrell and J. M. Tedder, JCS, 1250, (1963).
- (89) R. J. Cvetanovic, Can. J. Chem., 38, 1678, (1960).
- (90) P. I. Abel, Trans. Farad. Soc., 60, 2214, (1964).
- (91) D. G. Williamson and R. J. Cvetanovic, JACS, 90, 4248, (1968).
- (92) R. Bralsford, P. V. Harris and W. C. Price, Proc. Roy. Soc., A258, 459, (1960).
- (93) A. A. Westenberg and N. de Haas, J. Phys. Chem., 73, 1181, (1969).
- (94) L. Elias and H. I. Schiff, Can. J. Chem., 38, 1657, (1960).
- (95) I. W. M. Smith, private communication to W. J. R. Tyerman, Ref. 13.
- (96) L. Elias, J. Chem. Phys., 38, 989, (1963).
- (97) R. J. Donovan, private communication.

- (98) E. M. Lown, O. P. Strausz and H. E. Gunning, to be published.
- (99) A. B. Callear and W. J. R. Tyerman, Trans. Farad. Soc., 62, 371, (1966).
- (100) S. Glasstone, K. J. Laidler and H. Eyring, "The Theory of Rate Processes", McGraw-Hill, 199, (1941).
- (101) W. B. de More, Int. J. Chem. Kinetics, 1, 209, (1969).
- (102) M. Gazith and M. Szwarc, JACS, 79, 3339, (1957).
- (103) J. G. Calvert and J. N. Pitts, "Photochemistry", Wiley & Sons, (1966).
- (104) K. Shimomura, K. J. Tolle, J. Smid and M. Szwarc, JACS, 89, 796, (1967).
- (105) S. W. Charles and E. Whittle, Trans. Farad. Soc., 56, 794, (1960).
- (106) S. W. Charles, J. T. Pearson and E. Whittle, Trans. Farad. Soc., 57, 1356, (1961).
- (107) M. D. Scheer and R. Klein, J. Phys. Chem., 73, 597, (1969).
- (108) R. Klein and M. D. Scheer, J. Phys. Chem., 73, 1598, (1969).
- (109) P. S. Skell and R. C. Woodworth, JACS, 78, 4496, (1956).
- (110) W. B. de More and S. W. Benson, Adv. in Photochem., 2, 219, (1964).
- (111) R. Hoffmann, JACS, 90, 1475, (1968).
- (112) M. W. Schmidt and E. K. C. Lee, J. Chem. Phys., 51, 2024, (1969).



- (113) S. W. Benson and G. Haugen, J. Phys. Chem., 69, 3898, (1965).
- (114) G. E. Owen, J. M. Pearson and M. Szwarc, Trans. Farad. Soc., 60, 564, (1964).
- (115) K. S. Sidhu, Ph. D. Thesis, University of Alberta, (1965).
- (116) S. W. Benson, Adv. in Photochem., 2, 6, (1964).
- (117) P. Fowles, M. de Sorgo, A. J. Yarwood, O. P. Strausz and H. E. Gunning, JACS, 89, 1352, (1967).
- (118) E. N. Jakubowski, private communication.
- (119) V. J. Shiner, JACS, 76, 1603, (1954).
- (120) E. S. Lewis and C. E. Boozer, JACS, 76, 791, (1954).
- (121) K. T. Leffek, R. E. Robertson and S. E. Sugamori, Can. J. Chem., 39, 1989, (1961).
- (122) K. T. Leffek and J. W. MacLean, Can. J. Chem., 43, 40, (1961).
- (123) L. Hakka, A. Queen and R. E. Robertson, JACS, 87, 161, (1965).
- (124) G. E. Jackson and K. T. Leffek, Can. J. Chem., 47, 1537, (1969).
- (125) J. W. Simons, D. W. Stetser and B. S. Rabinowitch, JACS, 84, 1758, (1962); R. B. Rabinowitch and J. H. Current, Can. J. Chem., 40, 557, (1962); B. S. Rabinowitch, D. W. Stetser and F. W. Schneider, Can. J. Chem., 39, 2609, (1961).
- (126) J. T. Herron and R. E. Huie, J. Phys. Chem., 72, 2538, (1968).

APPENDIXMass Spectral Data1. 2-Trifluoromethyl-propene Episulfide

<u>m/e</u>	<u>Rel. Int.</u>	<u>m/e</u>	<u>Rel. Int.</u>
27	8.8	69	13.3
28	38.5	71	9.5
32	11.9	73	42.5
38	55.3	77	9.7
39	29.0	89	12.4
41	30.1	91	6.6
43	6.4	95	5.3
44	13.7	107	9.3
45	100	109	6.6
46	25.2	121	6.4
47	14.2	122	15.0
57	6.6	123	2.4
58	8.8	142	60.6
59	17.5	143	3.8
65	6.0		

2. 2-Fluoro-propene Episulfide

<u>m/e</u>	<u>Rel. Int.</u>	<u>m/e</u>	<u>Rel. Int.</u>
26	3.4	57	12.8
27	9.3	58	7.7
28	5.2	59	94.4
31	4.9	60	10.2
32	5.1	63	6.9
33	17.9	71	24.1
38	4.4	72	15.2
39	26.4	77	7.0
44	4.7	92	88.3
45	100	93	3.8
46	35.7	94	4.0
47	26.5		

3. 3,3-4,4,4-Pentafluoro-butene-1 Episulfide

<u>m/e</u>	<u>Rel. Int.</u>	<u>m/e</u>	<u>Rel. Int.</u>
26	9.5	58	21.0
27	34.1	59	100
28	27.7	60	4.0
31	10.7	61	4.0
32	9.1	63	9.1
33	3.6	69	19.5
39	14.9	75	7.3
44	10.4	77	32.9
45	94.5	83	4.9
46	9.1	89	3.0
47	4.6	95	4.3
50	4.9	107	4.9
51	21.3	109	45.1
53	5.2	113	3.6
54	8.2	178	78.0
57	10.7	180	3.6

-----